NORTH CAROLINA STATE UNIVERSITY | AT RALEIGH

SCHOOL OF ENGINEERING

DEPARTMENT OF ENGINEERING SCIENCE AND MECHANICS
Box 5130, Zip 27607

October 29, 1974

(NASA-CR-141549) [METHOD OF CHARACTERISTICS CALCULATIONS AND COMPUTER CODE FOR MATERIALS WITH ARBITRARY EQUATIONS OF STATE AND USING ORTHOGONAL POLYNOMIAL LEAST SQUARE SURFACE FITS] Final Report (North Carolina State

N75-15329

Unclas
G3/61 04939

Dr. Robert G. Thompson
Technical Representative of the
Contracting Officer (TRCO)
Mail Stop 230
NASA-Langley Research Center
Hampton, Virginia 23665

RE: Final Report, NASA Research Grant NGL 34-002-084

Dear Bob:

How are you?

I am enclosing two (2) copies of the Final Report of the above Research Grant. Three (3) additional copies have been forwarded directly to:

NASA Scientific and Technical
Information Facility
Post Office Box 33
College Park, Maryland 20740

This report is subdivided into three sections as follows:

Section I Journal Papers and Technical Reports of Research Projects directly related to and partially supported by the research grant.

I.1. "Stress Waves Resulting from Hypervelocity Impact," AIAA paper No. 69-355, Presented at the 1969 AIAA Hypervelocity Impact Conference in Cincinnati, Ohio (Authored by R. Madden and T. S. Chang) Results from a numerical scheme based on the method of characteristics are presented for the axially symmetric, hypervelocity impact of similar materials. The analysis is restricted to the early stages of the impact of a right circular cylinder on a halfspace. The resulting rarefaction and shock waves produced by the impact are considered as discrete wavefronts which divide the impacted zone into regions. Numerical diffusion is then controlled by requiring that the values of the dependent variables at a given point in the impacted zone to depend on only the calculated values at earlier times at points in the same region as the point in question. The numerical results give accurate representations of the stress wave profiles (i.e., rarefaction and shock waves) which should be useful as inputs for a later stage elastoplastic analysis and/or spallation analysis. The effects of "numerical diffusion" on the calculated pressure and flow fields when the rarefaction wave is not considered as discrete is investigated and the "diffused" results are compared with the more exact analysis.

I.2. "Nonlinear Waves in a Rate-Sensitive, Elastoplastic Material," International Journal of Engineering Science, Volume 10, pp. 353-367, 1972. (Authored by E. E. Burniston and T. S. Chang).
Two classes of closed form solutions of one-dimensional, nonlinear waves in a rate-sensitive, elastoplastic material are reported. One class of these solutions is self-similar and the other class consists of constant speed propagations. Applications of these solutions to unsteady motions behind propagating discontinuities are also considered.

I.3. "Curved Characteristics Behind Blast Waves," The Physics of Fluids, Volume 15, pp. 502-504, 1972. (Authored by O. Laporte and T. S. Chang)
Exact solutions, expressed in closed form in terms of elementary functions, are presented for the three sets of curved characteristics behind a self-similar, strong blast wave.

I.4. "On Dispersion and Characteristic Motions of Temperature-Rate Dependent Materials," National Aeronautics and Space Administration Report CR-1795, 1971.
A general three-dimensional theory of a thermomechanical material which can be a metallic or polymeric medium, or a structured composite, is developed using the modern techniques of axiomatic continuum mechanics and the laws of thermodynamics. One-dimensional linear spatial gradient temperature-rate dependent theories are presented for both thermoviscoelastic and thermoelastic materials. The characteristic motions are considered and it is shown that, due to the presence of temperature-rate effects, thermal propagation speeds have finite values. A comprehensive study of the dispersion relations is presented and illustrated graphically for typical values of the material constants. Analytical expressions are obtained for both high and low frequency responses. It is demonstrated that the characteristic speeds coincide with the high frequency asymptotic phase velocities in both cases. Physical and numerical limitations on the material constants are obtained for stable wave propagations. A class of self-similar solutions is obtained for the temperature-rate dependent thermoelastic medium using the theory of continuous group of transformations.

I.5. "Comments on Application of Singular Eigenfunction Expansions to the Propagation of Periodic Disturbances in a Radiating Grey Gas," The Physics of Fluids, Volume 16, pp. 159-160, 1973. (Authored by T. S. Chang, K. H. Kim and M. N. Osizik)
Recently, we have been extending our analysis of sound propagation

in dissociative, radiative media to include the effects of scattering. It is of interest to note that the set of pertinent integrodifferential equations can also be solved exactly using the singular eigenfunction expansion technique.

Section II Computer Programs and Numerical Results of Hypervelocity Impact Calculations

II.1. Method of Characteristics Calculations and the Computer Code Using Orthogonal Polynomial Least Square Surface Fits.
Very recently, we have developed a new numerical scheme using the method of characteristics to calculate the flow properties and pressures behind decaying shock waves for materials under hypervelocity impact. This procedure is quite different from our earlier methods (see paper I.1). We are now able to replace the time-consuming double interpolation subroutines used in paper I.1 by a technique based on Orthogonal Polynomial Least Square Surface Fits. Typical calculated results are given and in Tables 1-19. These results are compared with the double-interpolation results. The complete computer program is also included.

II.2. Method of Characteristics Calculations and the Computer Code for Materials with Arbitrary Equations of State.
As reported in our earlier status reports, we have developed a numerical code capable of calculating flow properties and pressures behind decaying shock waves for materials under hypervelocity impact with arbitrary equations of state. For comparison purposes, we have made some sample calculations using the new code for impact conditions similar to those reported in I.1. These results are quite encouraging and are displayed graphically in Figures 1-3. A listing of the numerical code is also attached.

Section III Fundamental Research on Equations of State and Non-Equilibrium Statistical Mechanics Generated by the Research Grant.

Materials under hypervelocity impact experience extreme changes of stresses, strains, and thermodynamic states. We have looked into some basic research areas related to (1) the non-equilibrium statistical mechanical aspects of heat transfer with discontinuous velocity boundary conditions, and (2) the fundamental understanding of the equations of state, phase transitions, and critical phenomena of materials under extreme thermodynamic environments. Our research efforts along these directions are found in the following research papers:

III.1. "Elementary Solutions of Coupled Model Equations in the Kinetic Theory of Gases," International Journal of Engineering Science, Volume 12, pp. 441-470, 1974. (Authors: J. T. Kriese, T. S. Chang, and C. E. Siewert.)

The method of elementary solutions is employed to solve two coupled integrodifferential equations sufficient for determining temperature - density effects in a linearized BGK model in the kinetic theory of gases. Full-range completeness and orthogonality theorems are proved for the developed normal modes and the infinite-medium Green's function is constructed as an illustration of the full-range formalism. The appropriate homogeneous matrix Riemann problem is discussed, and half-range completeness and orthogonality theorems are proved for a certain subset of the normal modes. The required existence and uniqueness theorems relevant to the **H** matrix, basic to the half-range analysis, are proved, and an accurate and efficient computational method is discussed. The half-space temperature-slip problem is solved analytically, and a highly accurate value of the temperature-slip coefficient is reported.

III.2. "Tricritical Points in Multicomponent Fluid Mixtures," Physical Review, Volume A9, pp. 2573-2578, 1974. (Authors: A. Hankey, T. S. Chang, and H. E. Stanley)
In view of experimental considerations, we give a model-independent argument that the novel tricritical points in multicomponent fluid mixtures, where three phases simultaneously become critical, are points on the boundary of a single two-dimensional surface of critical points. This result is corroborated by the Landau model suggested by Griffiths. The relationship between these tricritical points and the complex "higher-order" critical points proposed to exist in certain magnetic systems is elucidated.

III.3. "Generalized Scaling Hypothesis in Multicomponent Systems. I. Classification of Critical Points by Order and Scaling at Tricritical Points," Physical Review, Volume B8, pp. 346-364. (Authored by T. S. Chang, A. Hankey, and H. E. Stanley.)
The goal of this work is to provide an analysis of spaces of critical points for multicomponent systems. First, we propose the geometric concept of order $\mathcal{O}$ for critical points; we distinguish it from a previous definition of a "multicritical" point. Specifically, we may define the intersection of space of critical points of order $\mathcal{O}$ to be a space of critical points of order $(\mathcal{O} + 1)$. Ordinary critical points are defined to be of order $\mathcal{O} = 2$, so that the tricritical points introduced by Griffiths are of order $\mathcal{O} = 3$. We discuss more general examples of critical spaces of order $\mathcal{O} = 3$ which are known for a wide variety of systems; we also propose several examples of models of magnetic systems showing critical points of order $\mathcal{O} = 4$ - i.e., systems having intersecting lines of tricritical points. The analysis of critical and coexistence spaces also provides a new form of the Gibbs phase rule suitable for complex magnetic models. Next we define - for the critical points of order $\mathcal{O}$ of which examples have been given - special directions in terms of which to make a scaling hypothesis. We give the hypothesis for simple systems and then for tricritical points, and then, in a subsequent paper, part II, the special directions are used to make a scaling hypothesis at spaces of critical points of any order. Certain predictions (e.g., scaling laws and "single-power"

scaling functions) follow in a simple and straightforward fashion. We consider the scaling hypothesis at a critical space of order O in terms of a group of transformations. We can define a set of invariants of the group. It is possible, for $O \geq 3$, to make a second scaling hypothesis for the space of order $O - 1$ using certain of these invariants as independent variables. This is advantageous because certain "double-power" scaling functions then follow directly; these predict that for $O = 3$, experimental data collapse from a volume onto a line. This prediction is to be contrasted with ordinary scaling function, which predict that data collapse by only a single dimension (e.g., from a volume onto a surface or from a surface onto a line).

III.4. "Double-Power Scaling Functions Near Tricritical Points," Physical Review, Volume B7, pp. 4263-4266, 1973. (Authored by T. S. Chang, A. Hankey, and H. E. Stanley.)
We introduce invariants of the scaling equation about the tricritical point. Using these invariants, a modified version of the scaling hypothesis about the three critical lines meeting at the tricritical point is presented. From it we demonstrate that the thermodynamic equation of state near a tricritical point and near a critical line may be expressed as double-power scaling functions. These imply that experimental data should collapse from a volume onto a line (i.e., by two dimensions). This behavior is in contrast to ordinary "single-power" scaling functions, which predict data collapsing from a volume onto a surface or from a surface onto a line (i.e., by one dimension).

In conclusion, we have obtained much information pertaining to the behavior materials under impact, particularly hypervelocity impact. Two useful numerical des have been developed for calculations of axisymmetric hypervelocity impact for terials with rather general equations of state. Fundamental research in the eas of critical equations of state and non-equilibrium statistical mechanics and at transfer have also been considered.

With best wishes, I am

Very sincerely yours,

Tom

Tien Sun Chang
Professor

C:mlm

closures

: NASA Scientific and Technical
Information Facility (3 copies)

I.1. "Stress Waves Resulting from Hypervelocity Impact"

I.2. "Nonlinear Waves in a Rate-Sensitive, Elastoplastic Material"

I.3. "Curved Characteristics Behind Blast Waves"

I.4. "On Dispersion and Characteristic Motions of Temperature-Rate Dependent Materials"
NASA Report - copies not enclosed

I.5. "Comments on Application of Singular Eigenfunction Expansions to the Propagation of Periodic Disturbances in a Radiating Grey Gas"

PAPERS INTENTIONALLY OMITTED

II.1. Method of Characteristics Calculations and the Computer Code Using Orthogonal Polynomial Least Square Surface Fits

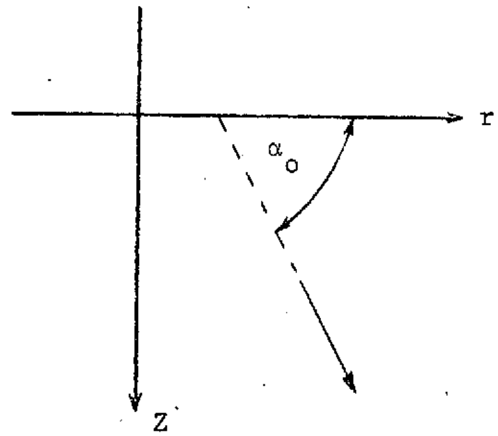

List of Symbols

t = time (μsec)

r = radial coordinate (cm)

Z = axial coordinate (cm)

U = radial velocity (cm/μsec)

V = axial velocity (cm/μsec)

ρ = mass density (gm/cm^3)

e = internal energy per unit mass (megabar cm^3/gm)

a = sound speed (cm/μsec)

P = pressure (megabars)

cos α_o = direction cosine of normal with respect to r axis

sin α_o = direction cosine of normal with respect to Z axis

Table 1. Flow properties in Projectile Shock at t = 1.18 μsec after impact of a 2.5-cm-diameter projectile at 0.76 cm/μsec on an aluminum half-space based on (1) Double Interpolation and (2) Othogonal Polynomials Least Square Surface Fit with Double Interpolation after t = 1.1 μsec.

(1)					(2)				
Z	r	P	U	V	Z	r	P	U	V
ρ	e	a	cos α_o	sin α_o	ρ	e	a	cos α_o	sin α_o
-0.3532	0.0	1.0869	0.0	0.3800	-0.3532	0.0	1.0869	0.0	0.3800
4.2103	0.0722	1.0038	0.0	1.0000	4.2103	0.0722	1.0038	0.0	1.0000
-0.3532	0.2500	1.0869	0.0	0.3800	-0.3532	0.2500	1.0869	0.0	0.3800
4.2103	0.0722	1.0038	0.0	1.0000	4.2103	0.0722	1.0038	0.0	1.0000
-0.3521	0.5012	1.0412	0.0025	0.3910	-0.3509	0.5009	0.9911	0.0017	0.4033
4.1738	0.0681	0.9934	-0.0068	1.0000	4.1325	0.0636	0.9820	-0.0049	1.0000
-0.3312	0.7611	0.8591	0.0209	0.4372	-0.3312	0.7630	0.7891	0.0106	0.4554
4.0185	0.0521	0.9500	-0.0648	0.9976	3.9533	0.0463	0.9318	-0.0348	0.9991
-0.2120	1.0183	0.4162	0.0124	0.5679	-0.2117	1.0177	0.4090	0.0116	0.5704
3.5399	0.0183	0.8122	-0.0667	0.9968	3.5303	0.0178	0.8094	-0.0613	0.9972

Table 2. Flow properties in Target Shock at t = 1.18 μsec after impact of a 2.5-cm-diameter projectile at 0.76 cm/μsec on an aluminum half-space based on (1) Double Interpolation and (2) Orthogonal Polynomials Least Square Surface Fit with Double Interpolation after t = 1.1 μsec.

(1)					(2)				
Z	r	P	U	V	Z	r	P	U	V
ρ	e	a	cos α_o	sin α_o	ρ	e	a	cos α_o	sin α_o
1.2500	0.0	1.0869	0.0	0.3800	1.2500	0.0	1.0869	0.0	0.3800
4.2103	0.0722	1.0038	0.0	1.0000	4.2103	0.0722	1.0038	0.0	1.0000
1.2500	0.2500	1.0869	0.0	0.3800	1.2500	0.2500	1.0869	0.0	0.3800
4.2103	0.0722	1.0038	0.0	1.0000	4.2103	0.0722	1.0038	0.0	1.0000
1.2500	0.5007	1.0686	0.0029	0.3756	1.2497	0.5007	1.0685	0.0029	0.3756
4.1957	0.0750	0.9997	0.0078	1.0000	4.1957	0.0705	0.9997	0.0078	1.0000
1.2398	0.7544	0.9647	0.0058	0.3501	1.2398	0.7544	0.9647	0.0058	0.3501
4.1106	0.0613	0.9758	0.0165	0.9998	4.1106	0.0613	0.9758	0.0165	0.9998
1.2143	1.0281	0.8382	0.0192	0.3169	1.2143	1.0281	0.8382	0.0192	0.3169
3.9996	0.0503	0.9446	0.0605	0.9979	3.9996	0.0503	0.9446	0.0605	0.9979
1.1235	1.3139	0.5624	0.0302	0.2368	1.1236	1.3139	0.5679	0.0304	0.2384
3.7190	0.0285	0.8649	0.1265	0.9910	3.7252	0.0290	0.8666	0.1265	0.9910
0.7683	1.7372	0.1558	0.0540	0.0691	0.7678	1.7377	0.1546	0.0528	0.0694
3.1170	0.0038	0.6776	0.6152	0.7870	3.1144	0.0037	0.6768	0.6050	0.7948
0.5808	1.8634	0.0670	0.0330	0.0263	0.5807	1.8634	0.0664	0.0327	0.0261
2.9088	0.0008	0.6045	0.7817	0.6227	2.9071	0.0008	0.6039	0.7816	0.6227
0.3716	1.9378	0.0	0.0	0.0	0.3716	1.9377	0.0	0.0	0.0
2.7000	0.0	0.5277	0.9289	0.3690	2.7000	0.0	0.5277	0.9289	0.3690

Table 3. Flow properties in Rarefaction at t = 1.18 μsec after impact of a 2.5-cm-diameter projectile at 0.76 cm/μsec on an aluminum half-space based on (1) Double Interpolation and (2) Orthogonal Polynomials Least Square Surface Fit with Double Interpolation after t = 1.1 μsec.

(1)				(2)			
Z	r	$\cos \alpha_o$	$\sin \alpha_o$	Z	r	$\cos \alpha_o$	$\sin \alpha_o$
1.2500	0.3781	0.6768	-0.7362	1.2500	0.3781	0.6768	-0.7362
1.1356	0.2852	0.5801	-0.8145	1.1355	0.2852	0.5801	-0.8145
1.0210	0.2132	0.4834	-0.8754	1.0210	0.2132	0.4834	-0.8754
0.9065	0.1577	0.3867	-0.9222	0.9065	0.1577	0.3867	-0.9222
0.7920	0.1165	0.2901	-0.9570	0.7920	0.1165	0.2901	-0.9570
0.6774	0.0879	0.1934	-0.9811	0.6774	0.0879	0.1934	-0.9811
0.5629	0.0711	0.0967	-0.9953	0.5629	0.0711	0.0967	-0.9953
0.4484	0.0656	-0.0000	-1.0000	0.4484	0.0656	-0.0000	-1.0000
0.3339	0.0711	-0.0967	-0.9953	0.3339	0.0711	-0.0967	-0.9953
0.2194	0.0879	-0.1934	-0.9811	0.2194	0.0879	-0.1934	-0.9811
0.1048	0.1165	-0.2901	-0.9570	0.1048	0.1165	-0.2901	-0.9570
-0.0097	0.1577	-0.3867	-0.9222	-0.0097	0.1577	-0.3867	-0.9222
-0.1242	0.2132	-0.4834	-0.8754	-0.1242	0.2132	-0.4834	-0.8754
-0.2387	0.2852	-0.5801	-0.8145	-0.2387	0.2852	-0.5801	-0.8145
-0.3532	0.3781	-0.6768	-0.7362	-0.3532	0.3781	-0.6768	-0.7362

Table 4. Flow properties in Interior Region at t = 1.18 μsec after impact of a 2.5-cm-diameter projectile at 0.76 cm/μsec on an aluminum half-space based on (1) Double Interpolation and (2) Orthogonal Polynomial Least Square Surfact Fit with Double Interpolation after t = 1.1 μsec at Z = -0.25 cm.

Z = - 0.25 cm	r	P	U	V	ρ	e	a
(1)	0.0	1.0869	0.0	0.3800	4.2103	0.0722	1.0038
	0.2500	1.0869	0.0	0.3800	4.2103	0.0722	1.0038
	0.5000	0.9289	0.0167	0.4159	4.050	0.0622	0.9654
	0.7500	0.6891	0.0558	0.3987	3.8200	0.0422	0.9012
	1.0000	0.0	0.0	0.0	2.7000	0.0	0.5277
	1.2500	0.0	0.0	0.0	2.7000	0.0	0.5277
	1.5000	0.0	0.0	0.0	2.7000	0.0	0.5277
	1.7500	0.0	0.0	0.0	2.7000	0.0	0.5277
	2.0000	0.0	0.0	0.0	2.7000	0.0	0.5277
(2)	0.0	1.0869	0.0	0.3800	4.2103	0.0722	1.0038
	0.2500	1.0869	0.0	0.3800	4.2103	0.0722	1.0038
	0.5000	0.6710	-0.1555	0.4333	3.7854	0.0425	0.8946
	0.7500	2.2439	-0.0865	0.9374	5.2602	0.1201	1.2174
	1.0000	0.0	0.0	0.0	2.7000	0.0	0.5277
	1.2500	0.0	0.0	0.0	2.7000	0.0	0.5277
	1.5000	0.0	0.0	0.0	2.7000	0.0	0.5277
	1.7500	0.0	0.0	0.0	2.7000	0.0	0.5277
	2.0000	0.0	0.0	0.0	2.7000	0.0	0.5277

Table 5. Flow properties in Interior Region at t = 1.18 μsec after impact of a 2.5-cm-diameter projectile at 0.76 cm/μsec on an aluminum half-space based on (1) Double Interpolation and (2) Orthogonal Polynomial Least Square Surface Fit with Double Interpolation after t = 1.1 μsec at Z = 0.0 cm.

Z = 0.0 cm	r	P	U	V	ρ	e	a
(1)	0.0	1.0869	0.0	0.3800	4.2103	0.0722	1.0038
	0.2500	0.9644	0.0130	0.3829	4.0861	0.0646	0.9743
	0.5000	0.6875	0.0985	0.4466	3.7705	0.0478	0.8972
	0.7500	0.4822	0.2065	0.5931	3.5022	0.0348	0.8269
	1.0000	0.1931	0.2829	0.7128	3.0774	0.0132	0.6916
	1.2500	0.0	0.6160	0.3904	2.7000	0.0	0.5277
	1.5000	0.0	0.1923	-0.0971	2.7000	0.0	0.5277
	1.7500	0.0	0.1103	-0.1452	2.7000	0.0	0.5277
	2.0000	0.0	0.0303	-0.0074	2.7000	0.0	0.5277
(2)	0.0	1.0869	0.0	0.3800	4.2103	0.0722	1.0038
	0.2500	0.4956	-0.1726	0.3333	3.5563	0.0318	0.8347
	0.5000	0.5533	0.0033	0.4539	3.6020	0.0395	0.8537
	0.7500	0.7227	0.2308	0.6779	3.8156	0.0497	0.9081
	1.0000	0.0112	0.3021	0.6287	2.6397	0.0053	0.5362
	1.2500	0.0	0.3460	0.4024	2.7000	0.0	0.5277
	1.5000	0.0	0.2988	-0.1707	2.7000	0.0	0.5277
	1.7500	0.0	0.0076	-0.0333	2.7000	0.0	0.5277
	2.000	0.0	1.0304	0.0920	2.7000	0.0	0.5277

Table 6. Flow properties in Interior Region at t = 1.18 μsec after impact of a 2.5-cm-diameter projectile at 0.76 cm/μsec on an aluminum half-space based on (1) Double Interpolation and (2) Orthogonal Polynomial Least Square Surface Fit with Double Interpolation after t = 1.1 μsec at Z = 0.25 cm.

Z = 0.25 cm	r	P	U	V	ρ	e	a
(1)	0.0	1.0869	0.0	0.3800	4.2103	0.0722	1.0038
	0.2500	0.9018	0.0414	0.3889	4.0190	0.0608	0.9582
	0.5000	0.6611	0.1029	0.3898	3.7383	0.0461	0.8890
	0.7500	0.5468	0.1589	0.4410	3.5875	0.0393	0.8504
	1.0000	0.4078	0.2552	0.5698	3.3982	0.0296	0.7973
	1.2500	0.2713	0.3356	0.2505	3.1741	0.0216	0.7328
	1.5000	0.1800	0.2782	-0.0038	3.0497	0.0126	0.6831
	1.7500	0.1452	0.1345	-0.0307	3.0979	0.0032	0.6704
	2.0000	0.0	0.0	0.0	2.7000	0.0	0.5277
(2)	0.0	1.0869	0.0	0.3800	4.2103	0.0722	1.0038
	0.2500	0.9041	0.0405	0.4685	4.0212	0.0610	0.9588
	0.5000	0.6238	0.1083	0.3428	3.6922	0.0436	0.8770
	0.7500	0.4999	0.1591	0.4221	3.5219	0.0365	0.8332
	1.0000	0.4384	0.1553	0.5946	3.4452	0.0314	0.8102
	1.2500	0.3310	0.3414	0.2448	3.2767	0.0250	0.7629
	1.5000	0.1820	0.2935	0.0031	3.0507	0.0130	0.6841
	1.7500	0.1509	0.1379	-0.0592	3.1113	0.0033	0.6746
	2.0000	0.0	0.0	0.0	2.7000	0.0	0.5277

Table 7. Flow properties in Interior Region at t = 1.18 μsec after impact of a 2.5-cm-diameter projectile at 0.76 cm/μsec on an aluminum half-space based on (1) Double Interpolation and (2) Orthogonal Polynomial Least Square Surface Fit with Double Interpolation after t = 1.1 μsec at Z = 0.50 cm.

Z = 0.50 cm	r	P	U	V	ρ	e	a
(1)	0.0	1.0869	0.0	0.3800	4.2103	0.0722	1.0038
	0.2500	0.9285	0.0338	0.3758	4.0475	0.0625	0.9651
	0.5000	0.7314	0.0768	0.3523	3.8244	0.0504	0.9106
	0.7500	0.6101	0.1090	0.3385	3.6714	0.0432	0.8723
	1.0000	0.5674	0.1441	0.3850	3.6154	0.0406	0.8577
	1.2500	0.3240	0.2039	0.1874	3.2650	0.0246	0.7595
	1.5000	0.2336	0.1796	0.0690	3.2048	0.0115	0.7206
	1.7500	0.1461	0.0865	0.0345	3.1018	0.0031	0.6713
	2.0000	0.0	0.0	0.0	2.7000	0.0	0.5277
(2)	0.0	1.0869	0.0	0.3800	4.2103	0.0722	1.0038
	0.2500	0.9477	0.0025	0.4235	4.0676	0.0637	0.9700
	0.5000	0.7109	0.0920	0.3266	3.8004	0.0491	0.9045
	0.7500	0.5934	0.0993	0.3379	3.6493	0.0422	0.8666
	1.0000	0.5876	0.1442	0.3938	3.6421	0.0418	0.8647
	1.2500	0.3056	0.2154	0.1785	3.2283	0.0241	0.7501
	1.5000	0.2380	0.1708	0.0771	3.2140	0.0117	0.7232
	1.7500	0.1611	0.1319	0.0292	3.1346	0.0036	0.6820
	2.000	0.0	0.0	0.0	2.7000	0.0	0.5277

Table 8. Flow properties in Interior Region at $t = 1.18$ μsec after impact of a 2.5-cm-diameter projectile at 0.76 cm/μsec on an aluminum half-space based on (1) Double Interpolation and (2) Orthogonal Polynomial Least Square Surface Fit with Double Interpolation after $t = 1.1$ μsec at $Z = 0.75$ cm.

Z = 0.75 cm	r	P	U	V	ρ	e	a
(1)	0.0	1.0869	0.0	0.3800	4.2103	0.0722	1.0038
	0.2500	1.0006	0.0200	0.3730	4.1231	0.0669	0.9832
	0.5000	0.8307	0.0490	0.3472	3.9397	0.0565	0.9391
	0.7500	0.7051	0.0710	0.3163	3.7917	0.0489	0.9026
	1.0000	0.6166	0.0937	0.3127	3.6908	0.0423	0.8752
	1.2500	0.4242	0.1292	0.1985	3.4661	0.0263	0.8077
	1.5000	0.3014	0.1187	0.1145	3.3803	0.0108	0.7624
	1.7500	0.0	0.0	0.0	2.7000	0.0	0.5277
	2.0000	0.0	0.0	0.0	2.7000	0.0	0.5277
(2)	0.0	1.0869	0.0	0.3800	4.2103	0.0722	1.0038
	0.2500	0.9148	-0.0201	0.4072	4.0334	0.0615	0.9616
	0.5000	0.8167	0.0542	0.3333	3.9244	0.0556	0.9352
	0.7500	0.6996	0.0658	0.3149	3.7846	0.0486	0.9009
	1.0000	0.5993	0.0982	0.3095	3.6667	0.0414	0.8693
	1.2500	0.4229	0.1272	0.1785	3.4620	0.0265	0.8070
	1.5000	0.3248	0.1134	0.1264	3.4247	0.0115	0.7744
	1.7500	0.0	0.0	0.0	2.7000	0.0	0.5277
	2.0000	0.0	0.0	0.0	2.7000	0.0	0.5277

Table 9. Flow properties in Interior Region at t = 1.18 μsec after impact of a 2.5-cm-diameter projectile at 0.76 cm/μsec on an aluminum half-space based on (1) Double Interpolation and (2) Orthogonal Polynomial Least Square Surface Fit with Double Interpolation after t = 1.1 μsec at Z = 1.00 cm.

Z = 1.00 cm	r	P	U	V	ρ	e	a
(1)	0.0	1.0869	0.0	0.3800	4.2103	0.0722	1.0038
	0.2500	1.0869	0.0	0.3800	4.2103	0.0722	1.0038
	0.5000	0.9551	0.0239	0.3569	4.0754	0.0642	0.9719
	0.7500	0.8458	0.0404	0.3263	3.9658	0.0562	0.9438
	1.0000	0.7492	0.0545	0.3053	3.8760	0.0477	0.9180
	1.2500	0.5566	0.0703	0.2330	3.6866	0.0306	0.8607
	1.5000	0.0	0.0	0.0	2.7000	0.0	0.5277
	1.7500	0.0	0.0	0.0	2.7000	0.0	0.5277
	2.0000	0.0	0.0	0.0	2.7000	0.0	0.5277
(2)	0.0	1.0869	0.0	0.3800	4.2103	0.0722	1.0038
	0.2500	1.0869	0.0	0.3800	4.2103	0.0722	1.0038
	0.5000	0.9137	0.0337	0.3572	4.0315	0.0616	0.9613
	0.7500	0.8233	0.0460	0.3269	3.9397	0.0549	0.9376
	1.0000	0.7430	0.0646	0.3254	3.8604	0.0465	0.9137
	1.2500	0.5142	0.0880	0.2854	3.6369	0.0275	0.8463
	1.5000	0.0	0.0	0.0	2.7000	0.0	0.5277
	1.7500	0.0	0.0	0.0	2.7000	0.0	0.5277
	2.0000	0.0	0.0	0.0	2.7000	0.0	0.5277

Table 10. Flow properties in Interior Region at t = 1.18 μsec after impact of a 2.5-cm-diameter projectile at 0.76 cm/μsec on an aluminum half-space based on (1) Double Interpolation and (2) Orthogonal Polynomial Least Square Surface Fit with Double Interpolation after t = 1.1 μsec at Z = 1.25 cm.

Z = 1.25 cm	r	P	U	V	ρ	e	a
(1)	0.0	1.0869	0.0	0.3800	4.2103	0.0722	1.0038
	0.2500	1.0869	0.0	0.3800	4.2103	0.0722	1.0038
	0.5000	0.0	0.0	0.0	2.7000	0.0	0.5277
	0.7500	0.0	0.0	0.0	2.7000	0.0	0.5277
	1.0000	0.0	0.0	0.0	2.7000	0.0	0.5277
	1.2500	0.0	0.0	0.0	2.7000	0.0	0.5277
	1.5000	0.0	0.0	0.0	2.7000	0.0	0.5277
	1.7500	0.0	0.0	0.0	2.7000	0.0	0.5277
	2.0000	0.0	0.0	0.0	2.7000	0.0	0.5277
(2)	0.0	1.0869	0.0	0.3800	4.2103	0.0722	1.0038
	0.2500	1.0869	0.0	0.3800	4.2103	0.0722	1.0038
	0.5000	0.0	0.0	0.0	2.7000	0.0	0.5277
	0.7500	0.0	0.0	0.0	2.7000	0.0	0.5277
	1.0000	0.0	0.0	0.0	2.7000	0.0	0.5277
	1.2500	0.0	0.0	0.0	2.7000	0.0	0.5277
	1.5000	0.0	0.0	0.0	2.7000	0.0	0.5277
	1.7500	0.0	0.0	0.0	2.7000	0.0	0.5277
	2.0000	0.0	0.0	0.0	2.7000	0.0	0.5277

Table 11. Flow properties in Projectile Shock at t = 1.25 μsec after impact of a 2.5-cm-diameter projectile 0.76 cm/μsec on an aluminum half-space based on (1) Double Interpolation and (2) Orthogonal Polynomials Least Square Surface Fit with Double Interpolation after t = 1.1 μsec.

(1)					(2)				
Z ρ	r e	P a	U cos α_o	V sin α_o	Z ρ	r e	P a	U cos α_o	V sin α_o
-0.3742 4.2103	0.0 0.0722	1.0869 1.0038	0.0 0.0	0.3800 1.0000	-0.3742 4.2103	0.0 0.0722	1.0869 1.0038	0.0 0.0	0.3800 1.0000
-0.3742 4.2103	0.2500 0.0722	1.0869 1.0038	0.0 0.0	0.3800 1.0000	-0.3742 4.2103	0.2500 0.0722	1.0869 1.0038	0.0 0.0	0.3800 1.0000
-0.3713 4.1460	0.5018 0.0650	1.0071 0.9857	0.0029 -0.0079	0.3993 0.9999	-0.3684 4.0789	0.5014 0.0581	0.9280 0.9670	0.0019 -0.0057	0.4191 1.0000
-0.3468 3.9954	0.7660 0.0501	0.8343 0.9436	0.0217 -0.0685	0.4438 0.9973	-0.3437 3.8844	0.7655 0.0405	0.7182 0.9123	0.0104 -0.0366	0.4750 0.9990
-0.2153 3.5195	1.0232 0.0173	0.4007 0.8060	0.0144 -0.0775	0.5731 0.9958	-0.2140 3.4869	1.0213 0.0157	0.3767 0.7961	0.0113 -0.0636	0.5816 0.9970

Table 12. Flow properties in Target Shock at t = 1.25 μsec after impact of a 2.5-cm-diameter projectile at 0.76 cm/μsec or an aluminum half-space based on (1) Double Interpolation and (2) Orthogonal Polynomials Least Square Surface Fit with Double Interpolation after t = 1.1 μsec.

(1)					(2)				
Z ρ	r e	P a	U $\cos\alpha_o$	V $\sin\alpha_o$	Z ρ	r e	P a	U $\cos\alpha_o$	V $\sin\alpha_o$
1.3242 4.2103	0.0 0.0722	1.0869 1.0038	0.0 0.0	0.3800 1.0000	1.3242 4.2103	0.0 0.0722	1.0869 1.0038	0.0 0.0	0.3800 1.0000
1.3242 4.2103	0.2500 0.0722	1.0869 1.0038	0.0 0.0	0.3800 1.0000	1.3242 4.2103	0.2500 0.0722	1.0869 1.0038	0.0 0.0	0.3800 1.0000
1.3233 4.1863	0.5015 0.0695	1.0568 0.9970	0.0039 0.0105	0.3724 0.9999	1.3232 4.2848	0.5014 0.0693	1.0550 0.9966	0.0034 0.0092	0.3723 1.0000
1.3110 4.0991	0.7558 0.0601	0.9511 0.9726	0.0066 0.0190	0.3467 0.9998	1.3109 4.0986	0.7558 0.0600	0.9506 0.9725	0.0066 0.0190	0.3465 0.9998
1.2823 3.9830	1.0325 0.0490	0.8208 0.9401	0.0203 0.0650	0.3122 0.9976	1.2823 3.9859	1.0325 0.0492	0.8240 0.9409	0.0204 0.0649	0.3130 0.9976
1.1836 3.7041	1.3220 0.0276	0.5493 0.8654	0.0312 0.1328	0.2325 0.9901	1.1840 3.7174	1.3224 0.0284	0.5610 0.8645	0.0332 0.1390	0.2359 0.9892
0.8044 3.1120	1.7655 0.0037	0.1534 0.6759	0.0550 0.6341	0.0669 0.7718	0.8039 3.0997	1.7655 0.0035	0.1475 0.6717	0.0512 0.6098	0.0664 0.7910
0.6060 2.9000	1.8958 0.0007	0.0637 0.6013	0.0318 0.7876	0.0248 0.6152	0.6060 2.8955	1.8957 0.0007	0.0621 0.5997	0.0310 0.7875	0.0242 0.6152
0.3853 2.7000	1.9721 0.0	0.0 0.5277	0.0 0.9354	0.0 0.3522	0.3853 2.7000	1.9722 0.0	0.0 0.5277	0.0 0.9354	0.0 0.3524

Table 13. Flow properties in Rarefaction at t = 1.25 μsec after impact of a 2.5-cm-diameter projectile at 0.76 cm/μsec on an aluminum half-space based on (1) Double Interpolation and (2) Orthogonal Polynomials Least Square Surface Fit with Double Interpolation after t = 1.1 μsec.

(1)				(2)			
Z	r	cos α_o	sin α_o	Z	r	cos α_o	sin α_o
1.3242	0.3263	0.6768	-0.7362	1.3242	0.3263	0.6768	-0.7362
1.2029	0.2280	0.5801	-0.8145	1.2029	0.2280	0.5801	-0.8145
1.0816	0.1517	0.4834	-0.8754	1.0816	0.1517	0.4834	-0.8754
0.9602	0.0929	0.3867	-0.9222	0.9602	0.0929	0.3867	-0.9222
0.8389	0.0493	0.2901	-0.9570	0.8389	0.0493	0.2901	-0.9570
0.7176	0.0190	0.1934	-0.9811	0.7176	0.0190	0.1934	-0.9811
0.5963	0.0012	0.0967	-0.9953	0.5963	0.0012	0.0967	-0.9953
0.4750	-0.0047	0.0000	-1.0000	0.4750	-0.0047	0.0000	-1.0000
0.3537	0.0012	-0.0967	-0.9953	0.3537	0.0012	-0.0967	-0.9953
0.2324	0.0190	-0.1934	-0.9811	0.2324	0.0190	-0.1934	-0.9811
0.1111	0.0493	-0.2901	-0.9570	0.1111	0.0493	-0.2901	-0.9570
-0.0102	0.0929	-0.3867	-0.9222	-0.0102	0.0929	-0.3867	-0.9222
-0.1316	0.1517	-0.4834	-0.8754	-0.1316	0.1517	-0.4834	-0.8754
-0.2529	0.2280	-0.5801	-0.8145	-0.2529	0.2280	-0.5801	-0.8145
-0.3742	0.3263	-0.6768	-0.7362	-0.3742	0.3263	-0.6768	-0.7362

Table 14. Flow properties in Interior Region at t = 1.11 μsec after impact of a 2.5-cm-diameter projectile at 0.76 cm/μsec on an aluminum half-space based on (1) Double Interpolation and (2) Orthogonal Polynomials Least Square Surface Fit with Double Interpolation afte t = 1.1 μsec at Z = -0.25 cm.

Z = - 0.25cm	r	P	U	V	ρ	e	a
(1)	0.0	1.0869	0.0	0.3800	4.2103	0.0722	1.0038
	0.2500	1.0869	0.0	0.3800	4.2103	0.0722	1.0038
	0.5000	1.0000	0.0011	0.3947	4.1232	0.0668	0.9832
	0.7500	0.9432	0.0686	0.4380	4.1035	0.0579	0.9715
	1.0000	0.0	0.0	0.0	2.70000	0.0	0.5277
	1.2500	0.0	0.0	0.0	2.7000	0.0	0.5277
	1.5000	0.0	0.0	0.0	2.7000	0.0	0.5277
	1.7500	0.0	0.0	0.0	2.7000	0.0	0.5277
	2.0000	0.0	0.0	0.0	2.7000	0.0	0.5277
(2)	0.0	1.0869	0.0	0.3800	4.2103	0.0722	1.0038
	0.2500	1.0869	0.0	0.3800	4.2103	0.0722	1.0038
	0.5000	0.9865	-0.0923	0.4746	4.1090	0.0660	0.9798
	0.7500	1.6829	0.0102	0.7228	4.7963	0.0979	1.1264
	1.0000	0.0	0.0	0.0	2.7000	0.0	0.5277
	1.2500	0.0	0.0	0.0	2.7000	0.0	0.5277
	1.5000	0.0	0.0	0.0	2.7000	0.0	0.5277
	1.7500	0.0	0.0	0.0	2.7000	0.0	0.5277
	2.0000	0.0	0.0	0.0	2.7000	0.0	0.5277

Table 15. Flow properties in Interior Region at t = 1.11 μsec after impact of a 2.5-cm-diameter projectile at 0.76 cm/μsec on an aluminum half-space based on (1) Double Interpolation and (2) Orthogonal Polynomials Least Square Surface Fit with Double Interpolation after t = 1.1 μsec at Z = 0.0 cm.

Z = 0.0 cm	r	P	U	V	ρ	e	a
(1)	0.0	1.0869	0.0	0.38000	4.2103	0.0722	1.0038
	0.2500	1.0869	0.0	0.3800	4.2103	0.0722	1.0038
	0.5000	0.7294	0.0887	0.4327	3.8222	0.0503	0.9100
	0.7500	0.5505	0.1836	0.5982	3.5915	0.0396	0.8517
	1.0000	0.1969	0.2836	0.7136	3.0808	0.0137	0.6937
	1.2500	0.0	0.6041	0.3687	2.7000	0.0	0.5277
	1.5000	0.0	0.2022	-0.1010	2.7000	0.0	0.5277
	1.7500	0.0	0.1250	-0.1445	2.7000	0.0	0.5277
	2.0000	0.0	0.0672	0.0310	2.7000	0.0	0.5277
(2)	0.0	1.0869	0.0	0.3800	4.2103	0.0722	1.0038
	0.2500	1.0869	0.0	0.3800	4.2103	0.0722	1.0038
	0.5000	0.6684	0.0649	0.4247	3.7487	0.0464	0.8914
	0.7500	0.5433	0.2089	0.5837	3.5837	0.0390	0.8493
	1.0000	0.1233	0.2851	0.6878	2.9268	0.0100	0.6429
	1.2500	0.0	0.5798	0.3784	2.7000	0.0	0.5277
	1.5000	0.0	0.2384	-0.1266	2.7000	0.0	0.5277
	1.7500	0.0	0.0790	-0.1272	2.7000	0.0	0.5277
	2.0000	0.0	0.7397	0.1453	2.7000	0.0	0.5277

Table 16. Flow properties in Interior Region at t = 1.11 μsec after impact of a 2.5-cm-diameter projectile at 0.76 cm/μsec on an aluminum half space based on (1) Double Interpolation and (2) Orthogonal Polynomials Least Square Surface Fit with Double Interpolation after t = 1.1 μsec at Z = 0.25 cm.

Z = 0.25cm	r	P	U	V	ρ	e	a
(1)	0.0	1.0869	0.0	0.3800	4.2103	0.0722	1.0038
	0.2500	0.9839	0.0272	0.3851	4.1059	0.0659	0.9791
	0.5000	0.7084	0.0902	0.3852	3.7971	0.0489	0.9037
	0.7500	0.5403	0.1560	0.4163	3.5790	0.0388	0.8481
	1.0000	0.4323	0.2422	0.5445	3.4320	0.0315	0.8073
	1.2500	0.2618	0.3301	0.2324	3.1521	0.0215	0.7274
	1.5000	0.1760	0.2720	0.0015	3.0472	0.0120	0.6809
	1.7500	0.1315	0.1172	-0.0253	3.0716	0.0025	0.6606
	2.0000	0.0	0.0	0.0	2.7000	0.0	0.5277
(2)	0.0	1.0869	0.0	0.3800	4.2103	0.0722	1.0038
	0.2500	0.9982	0.0263	0.4170	4.1207	0.0668	0.9826
	0.5000	0.6946	0.0922	0.3700	3.7806	0.0480	0.8995
	0.7500	0.5285	0.1555	0.4120	3.5626	0.0381	0.8439
	1.0000	0.4507	0.2414	0.5557	3.4600	0.0325	0.8148
	1.2500	0.2818	0.3320	0.2294	3.1875	0.0226	0.7380
	1.5000	0.1784	0.2771	0.0039	3.0516	0.0122	0.6825
	1.7500	0.1331	0.1192	-0.0361	3.0754	0.0025	0.6618
	2.0000	0.0	0.0	0.0	2.7000	0.0	0.5277

Table 17. Flow properties in Interior Region at t = 1.11 μsec after impact of a 2.5-cm-diameter projectile at 0.76 cm/μsec on an aluminum half space based on (1) Double Interpolation and (2) Orthogonal Polynomials Least Square Surface Fit with Double Interpolation after t = 1.1 μsec at Z = 2.50 cm.

Z = 0.50 cm	r	P	U	V	ρ	e	a
(1)	0.0	1.0869	0.0	0.3800	4.2103	0.0722	1.0038
	0.2500	1.0058	0.0224	0.3776	4.1284	0.0672	0.9845
	0.5000	0.7873	0.0644	0.3560	3.8904	0.0538	0.9270
	0.7500	0.6405	0.1002	0.3370	3.7108	0.0450	0.8823
	1.0000	0.5742	0.1362	0.3663	3.6236	0.0410	0.8600
	1.2500	0.3283	0.1942	0.1842	3.2750	0.0246	0.7618
	1.5000	0.2347	0.1758	0.0773	3.2145	0.0110	0.7219
	1.7500	0.1343	0.0741	0.0354	3.0770	0.0026	0.6626
	2.0000	0.0	0.0	0.0	2.7000	0.0	0.5277
(2)	0.0	1.0869	0.0	0.3800	4.2103	0.0722	1.0038
	0.2500	1.0122	0.0136	0.3928	4.1350	0.0676	0.9860
	0.5000	0.7791	0.0687	0.3477	3.8810	0.0533	0.9246
	0.7500	0.6353	0.0971	0.3368	3.7042	0.0447	0.8806
	1.0000	0.5763	0.1374	0.3665	3.6261	0.0412	0.8607
	1.2500	0.3191	0.1977	0.1809	3.2574	0.0243	0.7572
	1.5000	0.2371	0.1742	0.0802	3.2194	0.0111	0.7233
	1.7500	0.1428	0.0846	0.0336	3.0931	0.0028	0.6679
	2.0000	0.0	0.0	0.0	2.7000	0.0	0.5277

Table 18. Flow properties in Interior Region at t = 1.1 μsec after impact of a 2.5-cm-diameter projectile at 0.76 cm/μsec on an aluminum half space based on (1) Double Interpolation and (2) Orthogonal Polynomials Least Square Surface Fit with Double Interpolation after t = 1.1 μsec at Z = 0.75 cm.

Z = 0.75 cm	r	P	U	V	ρ	e	a
(1)	0.0	1.0869	0.0	0.3800	4.2103	0.0722	1.0038
	0.2500	1.0575	0.0069	0.3782	4.1810	0.0704	0.9969
	0.5000	0.8898	0.0374	0.3551	4.0054	0.0601	0.9550
	0.7500	0.7535	0.0622	0.3208	3.8501	0.0518	0.9171
	1.0000	0.6515	0.0859	0.3099	3.7372	0.0442	0.8867
	1.2500	0.4555	0.1199	0.2073	3.5178	0.0276	0.8208
	1.5000	0.3195	0.1068	0,1168	3.4168	0.0112	0.7720
	1.7500	0.0	0.0	0.0	2.7000	0.0	0.5277
	2.0000	0.0	0.0	0.0	2.7000	0.0	0.5277
(2)	0.0	1.0869	0.0	0.3800	4.2103	0.0722	1.0038
	0.2500	0.9930	-0.0229	0.3930	4.1156	0.0664	0.9814
	0.5000	0.8864	0.0404	0.3514	4.1108	0.0599	0.9541
	0.7500	0.7504	0.0603	0.3195	3.8462	0.0517	0.9162
	1.0000	0.6505	0.0868	0.3100	3.7355	0.0442	0.8864
	1.2500	0.4552	0.1210	0.2011	3.5168	0.0277	0.8263
	1.5000	0.3313	0.1054	0.1197	3.4382	0.0116	0.7778
	1.7500	0.0	0.0	0.0	2.7000	0.0	0.5277
	2.0000	0.0	0.0	0.0	2.7000	0.0	0.5277

Table 19. Flow properties in Interior Region at t = 1.1 μsec after impact of a 2.5-cm-diameter projectile at 0.76 cm/μsec on an aluminum half space based on (1) Double Interpolation and (2) Orthogonal Polynomials Least Square Surface Fit with Double Interpolation after t = 1.1 μsec at Z = 1.00 cm.

Z = 1.00 cm	r	P	U	V	ρ	e	a
(1)	0.0	1.0869	0.0	0.3800	4.2103	0.0722	1.0038
	0.2500	1.0869	0.0	0.3800	4.2103	0.0722	1.0038
	0.5000	1.0119	0.0131	0.3673	4.1346	0.0676	0.9860
	0.7500	0.8990	0.0297	0.3359	4.0258	0.0593	0.9581
	1.0000	0.7910	0.0414	0.3143	3.9271	0.0499	0.9302
	1.2500	0.6043	0.0512	0.2428	3.7526	0.0330	0.8773
	1.5000	0.0	0.0	0.0	2.7000	0.0	0.5277
	1.7500	0.0	0.0	0.0	2.7000	0.0	0.5277
	2.0000	0.0	0.0	0.0	2.7000	0.0	0.5277
(2)	0.0	1.0869	0.0	0.3800	4.2103	0.0722	1.0038
	0.2500	1.0869	0.0	0.3800	4.2103	0.0722	1.0038
	0.5000	1.0110	0.0122	0.3680	4.1335	0.0676	0.9857
	0.7500	0.8941	0.0332	0.3364	4.0203	0.0590	0.9568
	1.0000	0.7734	0.0489	0.3178	3.9067	0.0488	0.9252
	1.2500	0.6046	0.0551	0.2587	3.7552	0.0328	0.8776
	1.5000	0.0	0.0	0.0	2.7000	0.0	0.5277
	1.7500	0.0	0.0	0.0	2.7000	0.0	0.5277
	2.0000	0.0	0.0	0.0	2.7000	0.0	0.5277

```
      COMMON CASEID(14),ITS1,ITS2,ITS3,ITS4,ITI1,ITI2,ITI3,ITI4,EPS1,EPS
     12,EPS3,EPS4,EPS5,EPS6,EPI1,EPI2,EPI3,EPI4,EPI5,EPI6,EPI7,VP,AR,LEN
     1GTH,APR,BPR,BIGAPR,BIGBPR,ESTAR,ALPHA,BETA,RHOSTR,EPRS,RHOS
      COMMON XMESH(20,20,6),XMESH2(20,20,6),Z(20),R(20),SURF(15,8),SURF2
     1(15,8),TAB(15,14,2),TAB2(15,14,2),SPART(15,2,2),RARF(15,11),RARF2(
     115,4),RPART(15,2)
C
C
      COMMON ZO,RO,PO,UO,VO,LO,MO,RHOO,EO,AO,UBARO,VBARO
C
      COMMON NP,NT,NR,NI,NDEL,ISUB
C
      COMMON ZMIN,ZMAX,RMIN,RMAX,RADIUS,GZ,GR,DELTA,H
      COMMON DIRCOS
      COMMON TIME
      COMMON IRARF
      COMMON KSTOP
      COMMON TPSI
      COMMON KKK
C
C
      REAL LO,MO,LENGTH,MU,KO
      DOUBLE PRECISION PHI(20,20,6)
      KR=7
      EPS=.0000001
      KSTOP=0
1     FORMAT (1H1)
      CALL DVCHK(KEY)
      KICK=0
      IF (KEY.EQ.1) GO TO 9980
C
      DO 2 K=1,6
      DO 2 J=1,20
      DO 2 I=1,20
      XMESH(I,J,K)=0.
      XMESH2(I,J,K)=0.
```

```
2      CONTINUE
C      KRW=0
       NUZON=0
C
C
       WRITE (3,4)
C
C          DATA INPUT SECTION
C
4      FORMAT (52H1HYPERVELOCITY IMPACT METHOD OF CHARACTERISTICS CODE///
     1)
C        ID AND FX. PT. CONSTANTS
C
       READ (1,8) CASEID,ITS1,ITS2,ITS3,ITS4,ITI1,ITI2,ITI3,ITI4,NDEL
8      FORMAT (13A6,A2/9I3)
       IRARF=ITI2
C
C        FL. PT. CONSTANTS
C
       READ (1,15) EPS1,EPS2,EPS3,EPS4,EPS5,EPS6,EPI1,EPI2,EPI3,EPI4,EPI5
     1,EPI6,EPI7
       READ (1,14) NP,NT,NR
14     FORMAT (3I3)
       READ (1,15) APR,BPR,BIGAPR,BIGBPR,ESTAR,ALPHA,BETA,RHOSTR,EPRS,REF
     1L
       READ (1,15) ZMIN,ZMAX,RMIN,RMAX,GR,GZ,DELTA,VP,LENGTH,RADIUS,HSTAR
15     FORMAT (6E12.8)
       READ (1,15) RST
       IF (RST.GT.0.) GO TO 16
       REWIND 5
C      DO 1529 JTP=1,200
       READ (5)TIME
C      IF(ABS(RST+TIME).LT..001) GO TO 1530
C      READ(5)BLOB
C1529  CONTINUE
1530   CONTINUE
```

```
C     KRW=1
      READ (5)(((XMESH(I,J,K),I=1,20),J=1,20),K=1,6),(Z(I),I=1,20),(R(I)
     1,I=1,20),((SURF(I,J),I=1,15),J=1,8),(((TAB(I,J,K),I=1,15),J=1,14),
     1K=1,2),((RARF(I,J),I=1,15),J=1,11),TIME,ZMIN,ZMAX,RMIN,RMAX,GR,GZ,
     1AR
      DO 1500 J=1,20
      DO 1500 I=1,20
      DO 1500 K=1,6
 1500 XMESH2(I,J,K)=XMESH(I,J,K)
      DO 1501 I=1,15
      DO 1501 J=1,8
 1501 SURF2(I,J)=SURF(I,J)
      WRITE (3,145) TIME
      CALL SOUT
      CALL PRINT(XMESH2,Z,R,1)
      KREFL=0
   16 CONTINUE
      WRITE (3,10) CASEID,ITS1,ITS2,ITS3,ITS4,ITI1,ITI2,ITI3,ITI4,NDEL
   10 FORMAT (1X13A6,A2//17H SHOCK ITERATIONS6X,4I4//20H INTERIOR ITERAT
     1IONS3X,4I4//7H NDEL =,I4///)
      WRITE (3,18) EPS1,EPS2,EPS3,EPS4,EPS5,EPS6,EPI1,EPI2,EPI3,EPI4,EPI
     15,EPI6,EPI7,ZMIN,ZMAX,RMIN,RMAX,DELTA,VP,LENGTH,RADIUS,APR,BPR,BIG
     1APR,BIGBPR,ESTAR,ALPHA,BETA,RHOSTR,EPRS,REFL
   18 FORMAT (///38H ERROR CRITERIA FOR SHOCK COMPUTATIONS//5X8HDELTA Z1
     18X8HDELTA R18X9HDELTA RHO7X7HDELTA E9X7HDELTA P9X7HDELTA U/6E16.6/
     1//41H ERROR CRITERIA FOR INTERIOR COMPUTATIONS//5X8HDELTA ZI8X8HDE
     1LTA RI8X7HDELTA P9X7HDELTA U9X7HDELTA V9X9HDELTA RHO7X7HDELTA E/7E
     116.6///5X4HZMIN12X4HZMAX12X4HRMIN12X4HRMAX12X5HDELTA11X2HVP14X6HLE
     1NGTH10X6HRADIUS/8E16.6///5X2HA'14X2HB'14X6HBIG A'10X6HBIG B'10X2HE
     1*14X5HALPHA11X4HBETA12X4HRHO*/8E16.6//5X3HE'S13X4HREFL/2E16.6///)
      IF (RST.LT.0.) GO TO 140
C
C         STORE RHO* IN ALL XMESH
C
      DO 22 J=1,20
      DO 22 I=1,20
```

```
22    XMESH(I,J,4)=RHOSTR
40    FORMAT (5E12.8)
C
C       PROJECTILE SHOCK
C
      CALL EQOS1(PRHO,PPP,PVV,PEE,TEE,TRHO,KICK)
      IF (KICK.EQ.2200) GO TO 9980
      DO 230 N=1,NP
      TAB(N,1,1)=(PRHO*PVV-RHOSTR*VP)*HSTAR/(PRHO-RHOSTR)
      EE=N-1
      FNP=NP
      TAB(N,2,1)=RMIN+EE*(RADIUS-RMIN)/FNP
      TAB(N,3,1)=PPP
      TAB(N,4,1)=0.0
      TAB(N,5,1)=PVV
      TAB(N,6,1)=PRHO
      TAB(N,7,1)=PEE
      TAB(N,9,1)=0.0
      TAB(N,10,1)=1.0
230   CONTINUE
C
C       TARGET SHOCK
C
      M=0
      DO 240 N=1,NT
      EE=N-1
      FNT=NT-4
      TAB(N,2,2)=RMIN+EE*(RADIUS-RMIN)/FNT
      TAB(N,7,2)=TEE
      TAB(N,6,2)=TRHO
      TAB(N,3,2)=PPP
      IF (TAB(N,2,2).GT.RADIUS) GO TO 250
      TAB(N,1,2)=TRHO*PVV*HSTAR/(TRHO-RHOSTR)
      TAB(N,4,2)=0.0
      TAB(N,5,2)=PVV
      TAB(N,9,2)=0.0
```

```
      TAB(N,10,2)=1.0
      GO TO 240
250   EF=M
      TAB(N,9,2)=SIN(.5236+EF*.2618)
      TAB(N,10,2)=COS(.5236+EF*.2618)
      TAB(N,4,2)=PVV*TAB(N,9,2)
      TAB(N,5,2)=PVV*TAB(N,10,2)
      TAB(N,1,2)=TAB(1,1,2)*TAB(N,10,2)
      TAB(N,2,2)=RADIUS+TAB(1,1,2)*TAB(N,9,2)
      M=M+1
240   CONTINUE
C
C       RAREFACTION
C
      CALL EQOS2(PPP,PRHO,PEE)
      EE=NR-1
      ADEL=(TAB(1,1,2)-TAB(1,1,1))/EE
      RARF(1,1)=TAB(1,1,2)
      DO 205 N=2,NR
      RARF(N,1)=RARF(N-1,1)-ADEL
205   CONTINUE
      DO 210 N=1,NR
      RARF(N,10)=(RARF(N,1)/HSTAR-.5*VP)/AR
      RARF(N,9)=-SQRT(1.-RARF(N,10)**2)
      RARF(N,2)=RADIUS+HSTAR*AR*RARF(N,9)
210   CONTINUE
      DO 220 N=1,NR
      RARF(N,3)=TAB(1,3,1)
      RARF(N,4)=0.
      RARF(N,5)=TAB(1,5,1)
      RARF(N,6)=TAB(1,6,1)
      RARF(N,7)=TAB(1,7,1)
220   CONTINUE
C       REGION INTERIOR TO SHOCKS
      I=-ZMIN/GZ+1.2
      J=0
```

```
260   J=J+1
      XMESH(I,J,1)=PPP
      XMESH(I,J,3)=PVV
      XMESH(I,J,4)=PRHO
      XMESH(I,J,5)=PEE
      EE=(J-1)
      IF ((EE*GR-RADIUS).LT.-EPS) GO TO 260
      XMESH(I,J,1)=0.
      XMESH(I,J,4)=RHOSTR
      XMESH(I,J,5)=0.
C
C       FREE SURFACE
C
      DO 50 I=1,NP
      SURF(I,1)=-LENGTH+VP*HSTAR
      SURF(I,2)=TAB(I,2,1)
      SURF(I,3)=0.
      SURF(I,4)=0.
      SURF(I,5)=VP
      SURF(I,6)=RHOSTR
      SURF(I,7)=0.
      SURF(I,8)=SQRT(BIGAPR/RHOSTR)
50    CONTINUE
      DO 51 I=1,NP
      DO 51 J=1,8
51    SURF2(I,J)=SURF(I,J)
      IF (NUZON.EQ.0) GO TO 5001
5000  GR=GR*2.
      GZ=GZ*2.
      ZMAX=ZMAX*2.-ZMIN
      RMAX=RMAX*2.
      NUZON=1
      WRITE (3,5003)
5003  FORMAT (7H REZONE///)
5001  CONTINUE
C
```

```
C
      DO 55 I=1,20
      EE=I-1
      Z(I)=ZMIN+EE*GZ
      R(I)=RMIN+EE*GR
55    CONTINUE
      IF (NUZON.EQ.0) GO TO 5101
      DO 5100 I=1,10
      DO 5100 J=1,10
      DO 5100 K=1,6
      L=2*I-1
      M=2*J-1
      XMESH(I,J,K)=XMESH(L,M,K)
5100  CONTINUE
      GO TO 157
5101  CONTINUE
C
C         COMPUTE A FOR 2 SHOCKS AND MESH
C
      DO 86 K=1,3
      GO TO (57,59,61),K
57    NN=NP
      JJ=1
      GO TO 63
59    NN=NT
      JJ=1
      GO TO 63
61    NN=20
      JJ=20
63    DO 84 N=1,NN
      DO 82 J=1,JJ
      GO TO (65,65,68),K
65    P=TAB(N,3,K)
      RHO=TAB(N,6,K)
      E=TAB(N,7,K)
      GO TO 70
```

```
68    P=XMESH(J,N,1)
      RHO=XMESH(J,N,4)
      E=XMESH(J,N,5)
70    CONTINUE
      CALL EQOS3(RHO,AA,E,P)
      GO TO (76,76,78),K
76    TAB(N,8,K)=AA
      GO TO 82
78    XMESH(J,N,6)=AA
82    CONTINUE
84    CONTINUE
86    CONTINUE
      KICK=86
      CALL DVCHK(KQ)
      IF (KQ.EQ.1) GO TO 9980
C
C         STORE A FOR RAREFACTION
C
      DO 90 I=1,NR
90    RARF(I,8)=AR
C
C         COMPLETE SHOCK TABLES
C
      DO 99 K=1,2
      GO TO (92,94),K
92    NN=NP
      GO TO 95
94    NN=NT
      US=0.
95    DO 97 N=1,NN
      GO TO (93,96),K
93    CONTINUE
      US=VP*TAB(N,10,1)
96    CONTINUE
      TAB(N,11,K)=TAB(N,9,K)*TAB(N,4,K)+TAB(N,10,K)*TAB(N,5,K)
      TAB(N,12,K)=TAB(N,9,K)*TAB(N,5,K)-TAB(N,10,K)*TAB(N,4,K)
```

```
      TAB(N,13,K)=((TAB(N,6,K)*ABS(TAB(N,11,K)))/(TAB(N,6,K)-RHOSTR)-US)
     1*(-1.)**K
      TAB(N,14,K)=1.
97    CONTINUE
99    CONTINUE
C
C
C          STORE ALL XMESH IN XMESH2
C
130   DO 135 K=1,6
      DO 135 J=1,20
      DO 135 I=1,20
      XMESH2(I,J,K)=XMESH(I,J,K)
135   CONTINUE
      TIME=HSTAR
      WRITE (3,145) TIME
      CALL SOUT
C     CALL PRINT(XMESH2,Z,R,1)
      CALL PRINT(XMESH2,Z,R,1,PHI,NMAX,MMAX)
C
      KREFL=0
139   IF (KREFL.NE.0) GO TO 143
C          ENTRY FOR TIME STEP
C
140   READ (1,142) H
142   FORMAT (E12.8)
143   CONTINUE
      TIME=TIME+H
      WRITE (3,145) TIME
145   FORMAT (1H1///6H TIME=,E15.8///)
      WRITE (3,999) KR
999   FORMAT (5X,4H KR=,I5)
C
C
C          ADVANCE SHOCK POINTS
C
```

```
      DO 159 N=1,NP
      IF (TAB(N,14,1).LT.0.) GO TO 156
      IF ((TAB(N,1,1)-SURF(N,1)).GT.EPS) GO TO 154
156   TAB2(N,1,1)=TAB(N,1,1)
      TAB2(N,2,1)=TAB(N,2,1)
      TAB(N,14,1)=-1.
      GO TO 159
154   TAB2(N,1,1)=TAB(N,1,1)+TAB(N,13,1)*H*TAB(N,10,1)-VP*TAB(N,9,1)*TAB
     1(N,10,1)*H
150   TAB2(N,2,1)=TAB(N,2,1)+TAB(N,13,1)*H*TAB(N,9,1)-VP*TAB(N,9,1)**2*H
159   CONTINUE
      DO 155 N=1,NT
      TAB2(N,1,2)=TAB(N,1,2)+TAB(N,13,2)*H*TAB(N,10,2)
155   TAB2(N,2,2)=TAB(N,2,2)+TAB(N,13,2)*H*TAB(N,9,2)
      DO 158 M=1,NT
      IF (TAB2(M,1,2).GT.ZMAX) GO TO 5000
      IF (TAB2(M,2,2).GT.RMAX) GO TO 5000
158   CONTINUE
157   NUZON=0
C          ADVANCE RAREFACTION
C
      IF (RARF(1,2).LT.0.)IRARF=1
      IF (IRARF.EQ.1) GO TO 516
      ENR=NR-1
      ADEL=(TAB2(1,1,2)-TAB2(1,1,1))/ENR
      RARF2(1,1)=TAB2(1,1,2)
      DO 510 N=2,NR
      RARF2(N,1)=RARF2(N-1,1)-ADEL
510   CONTINUE
      DO 515 N=1,NR
      RARF2(N,3)=(RARF2(N,1)/TIME-.5*VP)/AR
      RARF2(N,4)=-SQRT(1.-RARF2(N,3)**2)
      RARF2(N,2)=RADIUS+TIME*AR*RARF2(N,4)
515   CONTINUE
516   CONTINUE
      CALL SHOCK
```

```
C
C
      IF (ITS3.EQ.1) GO TO 569
C         SHOCK COMPUTATIONS COMPLETED
C         COMPUTE PARTICLE CURVES
C
      TMP=.5*VP*H
      DO 520 N=1,NP
      SPART(N,1,1)=TAB(N,1,1)+TAB(N,5,1)*H
520   SPART(N,2,1)=TAB(N,2,1)+TAB(N,4,1)*H
      DO 525 N=1,NT
      SPART(N,1,2)=TAB(N,1,2)+TAB(N,5,2)*H
525   SPART(N,2,2)=TAB(N,2,2)+TAB(N,4,2)*H
      IF (IRARF.EQ.1) GO TO 531
      DO 530 N=1,NR
      RPART(N,1)=RARF(N,1)+TMP
530   RPART(N,2)=RARF(N,2)
531   CONTINUE
C
C
568   CALL SOUT2
569   CONTINUE
C       ADVANCE PROJECTILE REAR SURFACE
      DO 5300 I=1,NP
      DO 5300 J=1,8
5300  SURF2(I,J)=SURF(I,J)
      KICK=568
      CALL DVCHK(KQ)
      IF (KQ.EQ.1) GO TO 9980
C
C         START INTERIOR REGION COMPUTATIONS
C
C     CALL INTER
      CALL INTER(PHI,NMAX,MMAX)
C
C         INTERIOR REGION COMPUTATIONS COMPLETED
```

```
C
C     CALL PRINT(XMESH2,Z,R,2)
      CALL PRINT(XMESH2,Z,R,2,PHI,NMAX,MMAX)
570   CONTINUE
C
C         INITIALIZE FOR NEXT TIME STEP
C
      DO 920 K=1,6
      DO 920 J=1,20
      DO 920 I=1,20
      XMESH(I,J,K)=XMESH2(I,J,K)
920   CONTINUE
      DO 930 J=1,13
      DO 930 I=1,NP
      TAB(I,J,1)=TAB2(I,J,1)
930   CONTINUE
      DO 940 J=1,13
      DO 940 I=1,NT
      TAB(I,J,2)=TAB2(I,J,2)
940   CONTINUE
      IF (IRARF.EQ.1) GO TO 951
      DO 950 I=1,NR
      RARF(I,1)=RARF2(I,1)
      RARF(I,2)=RARF2(I,2)
950   CONTINUE
951   CONTINUE
      DO 960 I=1,NP
      DO 959 J=1,5
      SURF(I,J)=SURF2(I,J)
959   CONTINUE
960   CONTINUE
777   IF (KREFL.EQ.0) GO TO 980
      KREFL=0
      H=H1
      GO TO 143
980   CONTINUE
```

```
      CALL DVCHK(KICK)
      IF (KICK.EQ.2) GO TO 140
      WRITE (3,970)
970   FORMAT (28HODIVIDE CHECK AT END OF CASE/1H1)
      CALL EXIT
C
C         DIVIDE CHECK
C
9980  WRITE (3,9985) KICK
9985  FORMAT (32HODIVIDE CHECK NEAR STATEMENT NO.,I5/1H1)
      RETURN
      DEBUG SUBCHK
      END
      SUBROUTINE DBLTRP(ZX,RX,ANS)
C
C         1ST ORDER DOUBLE INTERPOLATION THAT CONSIDERS
C         LINES OF DISCONTINUITY IF IN CONSIDERED REGION
C
      COMMON CASEID(14),ITS1,ITS2,ITS3,ITS4,ITI1,ITI2,ITI3,ITI4,EPS1,EPS
     12,EPS3,EPS4,EPS5,EPS6,EPI1,EPI2,EPI3,EPI4,EPI5,EPI6,EPI7,VP,AR,LEN
     1GTH,APR,BPR,BIGAPR,BIGBPR,ESTAR,ALPHA,BETA,RHOSTR,EPRS,RHOS
      COMMON XMESH(20,20,6),XMESH2(20,20,6),Z(20),R(20),SURF(15,8),SURF2
     1(15,8),TAB(15,14,2),TAB2(15,14,2),SPART(15,2,2),RARF(15,11),RARF2(
     115,4),RPART(15,2)
C
C
      COMMON ZO,RO,PO,UO,VO,LO,MO,RHOO,EO,AO,UBARO,VBARO
C
      COMMON NP,NT,NR,NI,NDEL,ISUB
C
      COMMON ZMIN,ZMAX,RMIN,RMAX,RADIUS,GZ,GR,DELTA,H
      COMMON DIRCOS
      COMMON TIME
      COMMON IRARF
      COMMON KSTOP
      COMMON TPSI
```

```
      COMMON KKK
      REAL LO,MO,LENGTH,MU,KO
C
      DIMENSION ANS(6),ANS1(2,8),ANS2(2,8),ZI(4),RI(4),IK(4)
      CALL DVCHK(KEY)
      IF (KEY.EQ.2) GO TO 4
      NO=0
      GO TO 940
C
C         FIND SUBSCRIPTS FOR GRID
C
4     I1=(ZX-ZMIN)/GZ+1.000001
      I2=I1+1
      J1=(RX-RMIN)/GR+1.000001
      J2=J1+1
      NN=NP
      IF (ITS3.EQ.1) GO TO 3
      DO 1 K=1,2
      IF (K.EQ.2)NN=NT
      DO 1 I=1,NN
      ALF=SQRT((TAB(I,1,K)-ZX)**2+(TAB(I,2,K)-RX)**2)
      IF (ALF.GT.EPS1) GO TO 1
      ANS(1)=TAB(I,3,K)
      ANS(2)=TAB(I,4,K)
      ANS(3)=TAB(I,5,K)
      ANS(4)=TAB(I,6,K)
      ANS(5)=TAB(I,7,K)
      ANS(6)=TAB(I,8,K)
      RETURN
1     CONTINUE
      IF (IRARF.EQ.1) GO TO 3
      DO 2 I=1,NR
      ALF=SQRT((RARF(I,1)-ZX)**2+(RARF(I,2)-RX)**2)
      IF (ALF.GT.EPI1) GO TO 2
      ANS(1)=RARF(I,3)
      ANS(2)=RARF(I,4)
```

```
      ANS(3)=RARF(I,5)
      ANS(4)=RARF(I,6)
      ANS(5)=RARF(I,7)
      ANS(6)=RARF(I,8)
      RETURN
2     CONTINUE
3     CONTINUE
C
C
      ZXX=ZX+.01
      RXX=RX+.01
C
C         I LOOP FOR UPPER AND LOWER Z GRID LINES
C
      DO 800 I=1,2
      IF (ITS3.EQ.1) GO TO 14
      IF (I.EQ.2) GO TO 8
      II=I1
      GO TO 12
8     II=I2
12    M=COMP(ZX,RX,Z(II),R(J1))
      IF (M.EQ.1) GO TO 13
      MCOM=1
      GO TO 20
13    M=COMP(ZX,RX,Z(II),R(J2))
      IF (M.EQ.1) GO TO 14
      MCOM=2
      GO TO 20
C
C         GET 6 VALUES ON GRID LINES
C
14    DO 15 K=1,6
      ANS1(I,K+2)=XMESH(II,J1,K)+(XMESH(II,J2,K)-XMESH(II,J1,K))*(RX-R(J
     11))/(R(J2)-R(J1))
15    CONTINUE
      CALL DVCHK(NO)
```

```
      IF (NO.EQ.2) GO TO 17
      NO=15
      GO TO 940
17    ANS1(I,1)=Z(II)
      ANS1(I,2)=RX
      GO TO 800
C
C
20    ZZ=Z(II)
      RR=RX
      M=COMP(ZX,RX,ZZ,RR)
      IF (M.EQ.1) GO TO 300
C
C
      DO 25 K=1,2
      KATCH=0
      GO TO (21,22),K
21    NN=NP
      GO TO 23
22    NN=NT
23    JJJ=NN-1
      DO 24 M=1,JJJ
      IF (M.EQ.JJJ) GO TO 210
      IF (RX.GT.TAB(M+1,2,K).OR.RX.LT.TAB(M,2,K)) GO TO 24
210   ZI(K)=TAB(M+1,1,K)+(TAB(M,1,K)-TAB(M+1,1,K))*(RX-TAB(M+1,2,K))/(TA
     1B(M,2,K)-TAB(M+1,2,K))
      NO=210
      CALL DVCHK(KQ)
      IF (KQ.EQ.1) GO TO 940
      IF (I.EQ.2) GO TO 211
      IF (KATCH.EQ.1) GO TO 212
      KATCH=1
      GO TO 213
212   IF ((ZX-ZI(K)).GT.(ZX-ZM)) GO TO 24
      IF (ZI(K).GT.ZX) GO TO 24
213   ZM=ZI(K)
```

```
      IF (K.EQ.2) GO TO 215
      NPS=M
      GO TO 24
215   NTS=M
      GO TO 24
211   CONTINUE
      IF (KATCH.EQ.1) GO TO 26
      KATCH=1
      GO TO 213
26    IF ((ZI(K)-ZX).GT.(ZM-ZX)) GO TO 24
      IF (ZI(K).LT.ZX) GO TO 24
      GO TO 213
24    CONTINUE
      ZI(K)=ZM
      IF (KATCH.NE.0) GO TO 25
      ZI(K)=ZMAX+1.
25    CONTINUE
      IF (IRARF.EQ.1)ZI(3)=ZMAX+1.
      IF (IRARF.EQ.1) GO TO 2504
      KATCH=0
      JJJ=NR-1
      DO 27 M=1,JJJ
      ZI(3)=RARF(M+1,1)+(RARF(M,1)-RARF(M+1,1))*(RX-RARF(M+1,2))/(RARF(M
     1,2)-RARF(M+1,2))
      NO=25
      CALL DVCHK(KQ)
      IF (KQ.EQ.1) GO TO 940
      IF (ABS(ZI(3)-ZX).GT.1.E-5) GO TO 279
      DO 2799 LN=1,6
      LNN=LN+2
      ANS(LN)=RARF(1,LNN)
2799  CONTINUE
      GO TO 820
279   CONTINUE
      IF (I.EQ.2) GO TO 28
      IF (ZI(3).GT.ZX) GO TO 27
```

```
      IF (KATCH.EQ.1) GO TO 280
      KATCH=1
      GO TO 281
280   IF ((ZX-ZI(3)).GT.(ZX-ZM)) GO TO 27
281   ZM=ZI(3)
      MR=M
      GO TO 27
28    IF (ZI(3).LT.ZX) GO TO 27
      IF (KATCH.EQ.1) GO TO 282
      KATCH=1
      GO TO 281
282   IF ((ZI(3)-ZX).GT.(ZM-ZX)) GO TO 27
      GO TO 281
27    CONTINUE
      ZI(3)=ZM
2504  CONTINUE
      KATCH=0
      K=4
      JJJ=NP-1
      DO 2700 M=1,JJJ
      IF (M.EQ.JJJ) GO TO 2710
      IF (RX.GT.SURF(M+1,2).OR.RX.LT.SURF(M,2)) GO TO 2700
2710  ZI(4)=SURF(M+1,1)+(SURF(M,1)-SURF(M+1,1))*(RX-SURF(M+1,2))/(SURF(M
     1,2)-SURF(M+1,2))
      IF (KQ.EQ.1) GO TO 940
      CALL DVCHK(KQ)
      NO=2710
      IF (I.EQ.2) GO TO 2711
      IF (KATCH.EQ.1) GO TO 2712
      KATCH=1
      GO TO 2713
2712  IF ((ZX-ZI(K)).GT.(ZX-ZM)) GO TO 2700
2713  ZM=ZI(4)
      MS=M
      GO TO 2700
2711  CONTINUE
```

```
      IF (KATCH.EQ.1) GO TO 2726
      KATCH=1
      GO TO 2713
 2726 IF ((ZI(K)-ZX).GT.(ZM-ZX)) GO TO 2700
      GO TO 2713
 2700 CONTINUE
      ZI(4)=ZM
      IF (KATCH.NE.0) GO TO 2701
      ZI(4)=ZMAX+1.
 2701 CONTINUE
      RI(1)=RX
      RI(2)=RX
      RI(3)=RX
      RI(4)=RX
C         FIND INTERSECTION TO USE
C
 30   KEY=0
      IF (I.EQ.2) GO TO 50
C
C         UPPER GRID LINE
C
      DO 40 KK=1,4
      IF (Z(II).GT.ZI(KK)) GO TO 40
      IF (ABS(ZI(KK)-ZX).LT.1.E-5) GO TO 35
      IF (ZI(KK).GT.ZX) GO TO 40
      IF (KEY.EQ.0) GO TO 35
      IF (ZI(KK).LE.ZI(KEEP)) GO TO 40
      KEEP=KK
      GO TO 40
 35   KEEP=KK
      KEY=1
 40   CONTINUE
      GO TO 65
C
C         LOWER GRID LINE
C
```

```
50    DO 60 KK=1,4
      IF (Z(II).LT.ZI(KK)) GO TO 60
      IF (ABS(ZI(KK)-ZX).LT.1.E-5) GO TO 55
      IF (ZI(KK).LT.ZX) GO TO 60
      IF (KEY.EQ.0) GO TO 55
      IF (ZI(KK).GE.ZI(KEEP)) GO TO 60
      KEEP=KK
      GO TO 60
55    KEEP=KK
      KEY=1
60    CONTINUE
C
65    IF (KEY.NE.0) GO TO 70
      WRITE (6,67) ZX,RX,I,(ZI(KEY),KEY=1,4),(RI(KEY),KEY=1,4)
67    FORMAT (34H0ERROR NEAR STATEMENT 65 IN DBLTRP/1X3HZX=,E15.8,4X3HRX
     1=,E15.8,4X2HI=,I3/1X3HZI=,4E20.8/1X3HRI=,4E20.8/1H1)
      XYZ=-2.
      ZYX=SQRT(XYZ)
      CALL EXIT
C
C         FIND 6 VALUES ON SELECTED DISCONTINUITY
C
70    IF (KEEP.EQ.3) GO TO 80
      IF (KEEP.EQ.4) GO TO 81
      IF (KEEP.EQ.2) GO TO 71
      N=NPS
      GO TO 72
71    N=NTS
72    CONTINUE
      ZY=ZI(KEEP)
      RY=RX
      DO 75 K=3,8
      ANS1(I,K)=TAB(N,K,KEEP)+(TAB(N+1,K,KEEP)-TAB(N,K,KEEP))*SQRT(((RY-
     1TAB(N,2,KEEP))**2+(ZY-TAB(N,1,KEEP))**2)/((TAB(N+1,2,KEEP)-TAB(N,2
     1,KEEP))**2+(TAB(N+1,1,KEEP)-TAB(N,1,KEEP))**2))
      NO=75
```

```
      CALL DVCHK(KQ)
      IF (KQ.EQ.1) GO TO 940
 75   CONTINUE
      GO TO 90
 80   N=MR
      ZY=ZI(3)
      RY=RX
      DO 85 K=3,8
      ANS1(I,K)=RARF(N,K)+(RARF(N+1,K)-RARF(N,K))*SQRT(((RY-RARF(N,2))**
     12+(ZY-RARF(N,1))**2)/((RARF(N+1,2)-RARF(N,2))**2+(RARF(N+1,1)-RARF
     1(N,1))**2))
      NO=85
      CALL DVCHK(KQ)
      IF (KQ.EQ.1) GO TO 940
 85   CONTINUE
      GO TO 90
 81   N=MS
      ZY=ZI(4)
      RY=RX
      DO 86 K=3,8
      ANS1(I,K)=SURF(N,K)+(SURF(N+1,K)-SURF(N,K))*SQRT(((RY-SURF(N,2))**
     12+(ZY-SURF(N,1))**2)/((SURF(N+1,2)-SURF(N,2))**2+(SURF(N+1,1)-SURF
     1(N,1))**2))
 86   CONTINUE
 90   CALL DVCHK(NO)
      IF (NO.EQ.2) GO TO 92
      NO=90
      GO TO 940
 92   ANS1(I,1)=ZY
      ANS1(I,2)=RY
      GO TO 800
C
C         FIND INTERSECTIONS OF 3 DISCONTINUITIES AND Z GRID LINE
C
 300  CONTINUE
      KATCHP=0
```

```
      KATCHR=0
      KATCHT=0
      KATCHS=0
      DO 310 K=1,2
      KATCH=0
      GO TO (303,301),K
303   NN=NP
      GO TO 302
301   NN=NT
302   JJJ=NN-1
      DO 309 M=1,JJJ
      IF ((TAB(M,1,K)-TAB(M+1,1,K)).GT.1.E-6) GO TO 3030
      GO TO 309
3030  RI(K)=TAB(M+1,2,K)+(TAB(M,2,K)-TAB(M+1,2,K))*(Z(II)-TAB(M+1,1,K))/
     1(TAB(M,1,K)-TAB(M+1,1,K))
      CALL DVCHK(NO)
      IF (NO.EQ.2) GO TO 3031
      NO=3030
      GO TO 940
3031  CONTINUE
      IF (M.EQ.JJJ) GO TO 3022
      IF (RI(K).GT.TAB(M+1,2,K).OR.RI(K).LT.TAB(M,2,K)) GO TO 309
3022  IF (MCOM.EQ.2) GO TO 305
      IF (KATCH.EQ.1) GO TO 304
      KATCH=1
      GO TO 3050
304   IF ((RX-RI(K)).GT.(RX-RM)) GO TO 309
3050  RM=RI(K)
      IF (K.EQ.2) GO TO 3040
      MPS=M
      KATCHP=1
      GO TO 309
3040  MTS=M
      KATCHT=1
      GO TO 309
305   CONTINUE
```

```
      IF (KATCH.EQ.1) GO TO 306
      KATCH=1
      GO TO 3050
  306 IF ((RI(K)-RX).GT.(RM-RX)) GO TO 309
      GO TO 3050
  309 CONTINUE
      RI(K)=RM
      IF (KATCH.NE.0) GO TO 310
      RI(K)=RMAX+1.
  310 CONTINUE
      K=3
      IF (IRARF.EQ.1)RI(3)=RMAX+1.
      IF (IRARF.EQ.1) GO TO 315
      JJJ=NR-1
      KATCH=0
      DO 312 M=1,JJJ
      RI(3)=RARF(M+1,2)+(RARF(M,2)-RARF(M+1,2))*(Z(II)-RARF(M+1,2))/(RAR
     1F(M,1)-RARF(M+1,1))
      NO=3122
      CALL DVCHK(KQ)
      IF (KQ.EQ.1) GO TO 940
      IF (M.EQ.JJJ.OR.M.EQ.1) GO TO 3122
      IF (RI(K).GT.RARF(M+1,2).OR.RI(K).LT.RARF(M,2)) GO TO 312
 3122 IF (MCOM.EQ.2) GO TO 316
      IF (KATCH.EQ.1) GO TO 317
      KATCH=1
      GO TO 3051
  317 IF ((RX-RI(K)).GT.(RX-RM)) GO TO 312
 3051 RM=RI(K)
      MR=M
      KATCHR=1
      GO TO 312
  316 CONTINUE
      IF (KATCH.EQ.1) GO TO 318
      KATCH=1
      GO TO 3051
```

```
318   IF ((RI(K)-RX).GT.(RM-RX)) GO TO 312
      GO TO 3051
312   CONTINUE
      RI(K)=RM
      IF (KATCH.NE.0) GO TO 315
      RI(K)=RMAX+1.
315   CONTINUE
      KATCH=0
      JJJ=NP-1
      DO 3150 M=1,JJJ
      IF ((SURF(M,1)-SURF(M+1,1)).GT.1.E-6) GO TO 3130
      GO TO 3150
3130  RI(4)=SURF(M+1,2)+(SURF(M,2)-SURF(M+1,2))*(Z(II)-SURF(M+1,1))/(SUR
     1F(M,1)-SURF(M+1,1))
      NO=3130
      CALL DVCHK(KQ)
      IF (KQ.EQ.1) GO TO 940
      IF (M.EQ.JJJ) GO TO 3123
      IF (RI(4).GT.SURF(M+1,2).OR.RI(4).LT.SURF(M,2)) GO TO 3150
3123  IF (MCOM.EQ.2) GO TO 3105
      IF (KATCH.EQ.1) GO TO 3104
      KATCH=1
      GO TO 3109
3104  IF ((RX-RI(4)).GT.(RX-RM)) GO TO 3150
3109  RM=RI(4)
      MS=M
      KATCHS=1
      GO TO 3150
3105  IF (KATCH.EQ.1) GO TO 3106
      KATCH=1
      GO TO 3109
3106  IF ((RI(4)-RX).GT.(RM-RX)) GO TO 3150
      GO TO 3109
3150  CONTINUE
      RI(4)=RM
      IF (KATCH.NE.0) GO TO 3107
```

```
      RI(4)=RMAX+1.
3107  CONTINUE
      IF (KATCHP+KATCHT+KATCHR+KATCHS.EQ.0) GO TO 485
      ZI(1)=Z(II)
      ZI(2)=Z(II)
      ZI(3)=Z(II)
      ZI(4)=Z(II)
C          J LOOP FOR LEFT AND RIGHT R GRID LINES
C
      DO 700 J=1,2
      IF (J.EQ.2) GO TO 350
C
C          LEFT R GRID LINE
C
      JJ=J1
      KEY=0
      DO 340 N=1,4
      IF (R(J1).GT.RI(N)) GO TO 340
      IF (RI(N).GT.RX) GO TO 340
      IF (KEY.EQ.1) GO TO 330
      KEY=1
      KEEP=N
      GO TO 340
C
C          FIND CLOSEST
C
330   DIF1=RX-RI(KEEP)
      DIF2=RX-RI(N)
      IF (DIF1.LE.DIF2) GO TO 340
      KEEP=N
340   CONTINUE
      GO TO 375
C
C          RIGHT R GRID LINE
C
350   JJ=J2
```

```
      KEY=0
      DO 360 N=1,4
      IF (R(J2).LT.RI(N)) GO TO 360
      IF (RI(N).LT.RX) GO TO 360
      IF (KEY.EQ.1) GO TO 355
      KEY=1
      KEEP=N
      GO TO 360
355   DIF1=RI(KEEP)-RX
      DIF2=RI(N)-RX
      IF (DIF1.LE.DIF2) GO TO 360
      KEEP=N
360   CONTINUE
375   IF (KEY.EQ.1) GO TO 400
C
C         NO POINTS BETWEEN RX AND GRID POINTS
C
      ANS2(J,1)=Z(II)
      ANS2(J,2)=R(JJ)
      ANS2(J,3)=XMESH(II,JJ,1)
      ANS2(J,4)=XMESH(II,JJ,2)
      ANS2(J,5)=XMESH(II,JJ,3)
      ANS2(J,6)=XMESH(II,JJ,4)
      ANS2(J,7)=XMESH(II,JJ,5)
      ANS2(J,8)=XMESH(II,JJ,6)
      GO TO 700
C
C         POINT FOUND BETWEEN RX AND GRID POINTS
C
400   GO TO (405,410,470,481),KEEP
C
C         INTERSECTION ON PROJECTILE SHOCK
C
405   N1=MPS
      RY=RI(KEEP)
      ZY=Z(II)
```

```
      GO TO 520
C
C           INTERSECTION ON TARGET SHOCK
C
410   N1=MTS
      RY=RI(KEEP)
      ZY=Z(II)
      GO TO 520
C
C          INTERSECTION ON RAREFACTION
C
470   N1=MR
      RY=RI(KEEP)
      ZY=Z(II)
      GO TO 520
C
C     INTERSECTION ON FREE SURFACE
C
481   N1=MS
      RY=RI(KEEP)
      ZY=Z(II)
      GO TO 520
C
C
485   WRITE (3,488) KEEP,II,JJ,ZX,RX
488   FORMAT (25H0ERROR NEAR STATEMENT 485/1X5HKEEP=,I4,4X3HII=,I4,4X3HJ
     1J=,I4/1X3HZX=,E15.8,4X3HRX=,E15.8/1H1)
      CALL EXIT
C
C           FIND TABLE VALUES
C
520   IF (KEEP.EQ.3) GO TO 580
      IF (KEEP.EQ.4) GO TO 591
      DO 550 N=3,8
      ANS2(J,N)=TAB(N1,N,KEEP)+(TAB(N1+1,N,KEEP)-TAB(N1,N,KEEP))*SQRT(((
     1RY-TAB(N1,2,KEEP))**2+(ZY-TAB(N1,1,KEEP))**2)/((TAB(N1+1,2,KEEP)-T
```

```
     1AB(N1,2,KEEP))**2+(TAB(N1+1,1,KEEP)-TAB(N1,1,KEEP))**2))
550   CONTINUE
      IF (ZX.LT.0..AND.ABS(RX-RADIUS).LT.1.E-6) GO TO 552
      IF (RX.LT.RADIUS.OR.ABS(Z(II)).GT.1.E-6) GO TO 551
552   CONTINUE
      ANS2(J,3)=0.
      ANS2(J,6)=RHOSTR
      ANS2(J,7)=0.
      ANS2(J,8)=SQRT(BIGAPR/RHOSTR)
551   CONTINUE
      GO TO 600
580   DO 590 N=3,8
      ANS2(J,N)=RARF(N1,N)+(RARF(N1+1,N)-RARF(N1,N))*SQRT(((RY-RARF(N1,2
     1))**2+(ZY-RARF(N1,1))**2)/((RARF(N1+1,2)-RARF(N1,2))**2+(RARF(N1+1
     1,1)-RARF(N1,1))**2))
590   CONTINUE
      GO TO 600
591   DO 592 N=3,8
      ANS2(J,N)=SURF(N1,N)+(SURF(N1+1,N)-SURF(N1,N))*SQRT(((RY-SURF(N1,2
     1))**2+(ZY-SURF(N1,1))**2)/((SURF(N1+1,2)-SURF(N1,2))**2+(SURF(N1+1
     1,1)-SURF(N1,1))**2))
592   CONTINUE
600   CALL DVCHK(NO)
      IF (NO.EQ.2) GO TO 605
      NO=600
      GO TO 940
605   ANS2(J,1)=ZY
      ANS2(J,2)=RY
C
C          END OF LOOP FOR BOTH R GRID LINES
C
700   CONTINUE
C
C          INTERPOLATE FOR UPPER AND LOWER VALUES
C
      DO 720 J=3,8
```

```
      ANS1(I,J)=ANS2(1,J)+(ANS2(2,J)-ANS2(1,J))*(RX-ANS2(1,2))/(ANS2(2,2
     1)-ANS2(1,2))
  720 CONTINUE
      CALL DVCHK(NO)
      IF (NO.EQ.2) GO TO 730
      NO=720
      GO TO 940
  730 ANS1(I,1)=Z(II)
      ANS1(I,2)=RX
C
C             END OF LOOP FOR BOTH Z GRID LINES
C
  800 CONTINUE
C
C             FIND FINAL VALUES
C
      DO 810 J=1,6
      ANS(J)=ANS1(1,J+2)+(ANS1(2,J+2)-ANS1(1,J+2))*(ZX-ANS1(1,1))/(ANS1(
     12,1)-ANS1(1,1))
  810 CONTINUE
      CALL DVCHK(NO)
      IF (NO.EQ.2) GO TO 820
      NO=810
      GO TO 940
  820 RETURN
C
  940 WRITE (3,942)
  942 FORMAT (35HODIVIDE CHECK ERROR IN SUBR. DBLTRP)
  950 WRITE (3,952) NO,ZX,RX,I1,J1,KEEP,ZI,RI
  952 FORMAT (19H NEAR STATEMENT NO.,I4/1X3HZX=,E15.8,4X3HRX=,E15.8/1X3H
     1I1=,I4,4X3HJ1=,I4,4X5HKEEP=,I4/1X3HZI=,4E18.8/1X3HRI=,4E18.8)
      WRITE (3,955) ((ANS1(I,J),J=1,8),I=1,2),((ANS2(I,J),J=1,8),I=1,2)
  955 FORMAT (1X5HANS1=/8E16.8/8E16.8/1X5HANS2=/8E16.8/8E16.8/1H1)
      XYZ=-2.
      ZYX=SQRT(XYZ)
      CALL EXIT
```

```
      RETURN
      DEBUG SUBCHK
      END
      SUBROUTINE SHOCK
C         COMPUTES SHOCK VALUES
      COMMON CASEID(14),ITS1,ITS2,ITS3,ITS4,ITI1,ITI2,ITI3,ITI4,EPS1,EPS
     12,EPS3,EPS4,EPS5,EPS6,EPI1,EPI2,EPI3,EPI4,EPI5,EPI6,EPI7,VP,AR,LEN
     1GTH,APR,BPR,BIGAPR,BIGBPR,ESTAR,ALPHA,BETA,RHOSTR,EPRS,RHOS
      COMMON XMESH(20,20,6),XMESH2(20,20,6),Z(20),R(20),SURF(15,8),SURF2
     1(15,8),TAB(15,14,2),TAB2(15,14,2),SPART(15,2,2),RARF(15,11),RARF2(
     115,4),RPART(15,2)
C
      COMMON ZO,RO,PO,UO,VO,LO,MO,RHOO,EO,AO,UBARO,VBARO
C
      COMMON NP,NT,NR,NI,NDEL,ISUB
C
      COMMON ZMIN,ZMAX,RMIN,RMAX,RADIUS,GZ,GR,DELTA,H
      COMMON DIRCOS
      COMMON TIME
      COMMON IRARF
      COMMON KSTOP
      COMMON TPSI
      COMMON KKK
C
      REAL LO,MO,LENGTH,MU,KO
C
      DIMENSION ANS(6)
      EXTERNAL FGOF1
      EPS=.0000001
C
C         BEGIN SHOCK POINT COMPUTATIONS
      DO 505 K=1,2
      GO TO (158,160),K
158   NN=NP
      GO TO 162
160   NN=NT
```

```
      VBARS=0.
  162 DO 500 I=1,NN
      MPROJ=0
      IF (TAB(I,14,K).LT.0.) GO TO 500
  164 CONTINUE
C
C         INITIALIZE TO ITERATE ON 1 SHOCK POINT
C
      NBIC=0
      ZO=TAB2(I,1,K)
      RO=TAB2(I,2,K)
      PO=TAB(I,3,K)
      UO=TAB(I,4,K)
      VO=TAB(I,5,K)
      RHOO=TAB(I,6,K)
      EO=TAB(I,7,K)
      AO=TAB(I,8,K)
      LO=TAB(I,9,K)
      MO=TAB(I,10,K)
      UBARO=TAB(I,11,K)
      VBARO=TAB(I,12,K)
      UTOH=TAB(I,13,K)
      UTO=UTOH
      ITS44=ITS4
      IF (IRARF.EQ.1) GO TO 170
      M=1-(NR-2)*(K-2)
      FF=RO-RARF2(M+1,2)-(RARF2(M,2)-RARF2(M+1,2))*(ZO-RARF2(M+1,1))/(RA
     1RF2(M,1)-RARF2(M+1,1))
  169 CONTINUE
      IF (FF.LT..001) GO TO 350
  170 IF (I.NE.1) GO TO 180
      MO=TAB(I,10,K)
      LO=0.
      GO TO 190
  180 IF (I.LT.NN) GO TO 184
      UP=H*(TAB(I-1,13,K)-TAB(I,13,K))
```

```
      TMP=SQRT((TAB2(I-1,2,K)-RO)**2+(TAB2(I-1,1,K)-ZO)**2)
      DOMEG=UP/TMP
      GO TO 186
184   DR1=TAB2(I+1,2,K)-RO
      DR2=RO-TAB2(I-1,2,K)
      DZ1=TAB2(I+1,1,K)-ZO
      DZ2=ZO-TAB2(I-1,1,K)
      UP=H*(TAB(I-1,13,K)-TAB(I+1,13,K))
      TMP=SQRT(DR1**2+DZ1**2)+SQRT(DR2**2+DZ2**2)
      DOMEG=UP/TMP
      KICK=184
      CALL DVCHK(KQ)
      IF (KQ.EQ.1) GO TO 9980
C
C         COMPUTE NEW LO,MO
C
186   COMEG=COS(DOMEG)
      SOMEG=SIN(DOMEG)
      XLO=LO*COMEG+MO*SOMEG
      XMO=MO*COMEG-LO*SOMEG
      LO=XLO
      MO=XMO
      IF (PO.GT..0025) GO TO 190
      PO=0.
      UO=0.
      VO=VP*(1.-(-1.)**K)/2.
      RHOO=RHOSTR
      EO=0.
      AO=SQRT(BIGAPR/RHOSTR)
      UBARO=MO*VO
      VBARO=VBARS
      UTO=UBARO+AO*(-1.)**K
      GO TO 350
190   ITS33=ITS3
C
C         FIND GUESS TO START ITERATION
```

```
C
195   CALL GUESS(1,KOD2,Z0,R0,I,K,ZZ,RR,DZ,DR)
      IF (KOD2.EQ.1) GO TO 200
      WRITE (3,198) I,K,Z0,R0
      WRITE (3,7002) ZZ,RR,DZ,DR
198   FORMAT (31HONO GUESS FOUND FOR SHOCK POINT/3H0I=,I4,6X2HK=,I4,10X3
     1HZ0=,E15.8,10X3HR0=,E15.8/1H1)
      CALL EXIT
200   CONTINUE
      KY=K
      NTW=0
      IF (K.EQ.2) GO TO 201
      VBARS=VP*L0
      DIRCOS=-M0
      GO TO 203
201   DIRCOS=M0
203   CONTINUE
      CALL NRIT2(Z1,R1,ZZ,DZ,RR,DR,EPS1,EPS2,FGOF1,ITS1,KODE)
      IF (KODE.EQ.0) GO TO 205
C
C     BICHARACTERISTIC SELECTION SCHEME
C
      IF (NBIC.EQ.0) GO TO 204
      IF (NTW.EQ.8)KY=KY+1
      IF (NTW.GT.21) GO TO 7000
      ANG1=ANG1+DTPSI*(-1.)**KY
      DIRCOS=SIN(ANG1)
      L0=COS(ANG1)
      NTW=NTW+1
      GO TO 203
204   CONTINUE
      NBIC=1
      CALL DBLTRP(ZZ,RR,ANS)
      UA=ANS(2)
      VA=ANS(3)
      AA=ANS(6)
```

```
      ZZZ=ZZ+DZ
      CALL DBLTRP(ZZZ,RR,ANS)
      UB=ANS(2)
      VB=ANS(3)
      AB=ANS(6)
      RRR=RR+DR
      CALL DBLTRP(ZZ,RRR,ANS)
      UC=ANS(2)
      VC=ANS(3)
      AC=ANS(6)
      MM=0
      TPSI=1.5708*(-1.)**K
      XB=ZZ
      YB=RR
      NOM=5
      CA=NOM
 6201 DTPSI=.01745
      DTPSI=CA*DTPSI
      TPSI=TPSI+DTPSI*(-1.)**K
      A1=1.+H*(VB-VA+(AB-AA)*SIN(TPSI))/DZ
      B1=H*(VC-VA+(AC-AA)*SIN(TPSI))/DR
      C1=-(ZZ-Z0+H*(VA+AA*SIN(TPSI)))
      A2=H*(UB-UA+(AB-AA)*COS(TPSI))/DZ
      B2=1.+H*(UC-UA+(AC-AA)*COS(TPSI))/DR
      C2=-(RR-R0+H*(UA+AA*COS(TPSI)))
      DET=A1*B2-A2*B1
      DELX=(B2*C1-B1*C2)/DET
      DELY=(A1*C2-A2*C1)/DET
C
C         TEST FOR SAME REGION
C
      XB1=XB+DELX
      YB1=YB+DELY
      M=COMP(XB,YB,XB1,YB1)
      IF (M.EQ.1) GO TO 6203
      MM=MM+1
```

```
      IF (MM.LT.360/NOM) GO TO 6201
7000  WRITE (3,7001)
7001  FORMAT (41HOBICHARACTERISTIC SELECTION SCHEME FAILED)
      WRITE (3,614) ZO,RO
614   FORMAT (1X5HZO  =,E15.8,4X5HRO  =,E15.8)
      WRITE (3,7002) UA,VA,AA,UB,VB,AB,UC,VC,AC,ZZ,DZ,RR,DR,ANG1
7002  FORMAT (4E16.8)
      CALL EXIT
6203  CONTINUE
      WRITE (3,6210)
6210  FORMAT (53HOBICHARACTERISTIC SELECTION SCHEME EMPLOYED BY SHOCKX)
6204  ANG1=TPSI
      T1=DIRCOS
      T2=LO
      DIRCOS=SIN(ANG1)
      LO=COS(ANG1)
      GO TO 203
205   CONTINUE
      UBARS1=0.
      IF (K.EQ.1)UBARS1=MO*VP
      CALL DBLTRP(Z1,R1,ANS)
      P1=ANS(1)
      U1=ANS(2)
      V1=ANS(3)
      RHO1=ANS(4)
      E1=ANS(5)
      A1=ANS(6)
206   CONTINUE
      KICK=205
      CALL DVCHK(KQ)
      IF (KQ.EQ.1) GO TO 9980
      IF (NBIC.EQ.0) GO TO 207
7003  SINTH=ABS(DIRCOS)
      COSTH=ABS(LO)
      DIRCOS=T1
      LO=T2
```

```
207   CONTINUE
      UBAR1=LO*U1+MO*V1
      IF (K.EQ.2) GO TO 208
      IF (UBAR1.LT.VP/2.) GO TO 208
      UBAR1=UBARS1-UBAR1
208   CONTINUE
218   CONTINUE
      M1=PART(1,Z1,R1,ZZ,RR,DELTA,NDEL)
      IF (M1.EQ.1) GO TO 210
      PUR=0.
      PVR=0.
      GO TO 215
210   CALL DBLTRP(ZZ,RR,ANS)
      DP=RR-R1
      PUR=(ANS(2)-U1)/DP
219   CONTINUE
      PVR=(ANS(3)-V1)/DP
215   M1=PART(2,Z1,R1,ZZ,RR,DELTA,NDEL)
      IF (M1.EQ.1) GO TO 220
      PUZ=0.
      PVZ=0.
      PAZ=0.
      GO TO 225
220   CALL DBLTRP(ZZ,RR,ANS)
      DP=ZZ-Z1
      PUZ=(ANS(2)-U1)/DP
      PVZ=(ANS(3)-V1)/DP
225   CONTINUE
      IF (NBIC.EQ.1) GO TO 7004
      PURB1=LO*PUR+MO*PVR
      PVRB1=LO*PVR-MO*PUR
      PVZB1=LO*PVZ-MO*PUZ
      PVEB1=-MO*PVRB1+LO*PVZB1
      SBAR1=PVEB1
226   CONTINUE
      IF (ABS(R1).LE.EPS) GO TO 235
```

```
      SBAR1=SBAR1+U1/R1
      GO TO 240
 7004 CONTINUE
      IF (V1.GT.VP/2..AND.K.EQ.1)V1=VP-V1
      SBAR1=SINTH**2*PUR-SINTH*COSTH*(PUZ+PVR)+COSTH**2*PVZ
      GO TO 226
  235 SBAR1=SBAR1+PUR
C
C
  240 ITS22=ITS2
      MMM=0
  250 CONTINUE
      CALL EQOSS(PFR,PFE)
      BIGA1=RHO1*A1
      KICK=250
      CALL DVCHK(KQ)
      IF (KQ.EQ.1) GO TO 9980
      TEMP=1.-RHOSTR/RHOO
      TMP=SQRT(PO*TEMP/RHOSTR)
      IF (K.EQ.2) GO TO 251
      IF (TMP.LT.VP/2.) GO TO 251
      MPROJ=1
      TMP=UBARS1-TMP
  251 CONTINUE
      TMP6=TMP
  256 CONTINUE
      FNBIC=NBIC
      TMP1=P1+BIGA1*UBAR1-RHO1*H*SBAR1*A1**2+BIGA1*(-UBAR1+COSTH*U1+SINT
     1H*V1-SINTH*LO*VBARS+COSTH*MO*VBARS)*(FNBIC)
      TMP2=PFR*TEMP+PO*RHOSTR/RHOO**2
      TMP5=PFE*TEMP
      GTMP=-RHO1*A1
      IF (NBIC.EQ.0) GO TO 259
      GTMP=GTMP*(COSTH*LO+SINTH*MO)
  259 CONTINUE
      BIGG=PO-(GTMP*TMP+TMP1)
```

```
      PGR=PFR-((GTMP*TMP2)/(2.*RHOSTR*TMP6))
      PGE=PFE-((GTMP*TMP5)/(2.*RHOSTR*TMP6))
  265 TMP=.5*(1./RHOSTR-1./RHO0)
      BIGH=E0-TMP*P0
      PHR=-TMP*PFR-.5*P0/RHO0**2
      PHE=1.-TMP*PFE
      IF (ABS(BIGH).GT..0001) GO TO 267
      BIGH=0.
  267 IF (ABS(BIGG).GT..0001) GO TO 269
      BIGG=0.
  269 CONTINUE
C
C         COMPUTE DELTA E0,DELTA RHO0
C
      DOWN=PGE*PHR-PGR*PHE
      DE0=(-BIGG*PHR+BIGH*PGR)/DOWN
      DRHO0=(-BIGH*PGE+BIGG*PHE)/DOWN
C
      E02=E0+DE0
      IF (E02.LT.0.)E02=0.
      RHO02=RHO0+DRHO0
      IF (RHO02.LT.RHOSTR)RHO02=RHO0
      KICK=265
      CALL DVCHK(KQ)
      IF (KQ.EQ.1) GO TO 9980
      CALL EQOSP(RHO02,E02,P02)
      UBAR02=(1.-RHOSTR/RHO02)*(P02/RHOSTR)
      IF (UBAR02.GT.0.) GO TO 2669
      WRITE (3,2700) P02,RHO02,E02,R0,Z0
      WRITE (3,7002) P1,U1,V1,RHO1,E1,Z1TR1,SBAR1
 2700 FORMAT (4E16.8)
 2669 CONTINUE
      UBAR02=SQRT(UBAR02)
      IF (E02.LT.1.E-5) GO TO 273
      IF (ABS((E02-E0)/E02).LT.EPS4) GO TO 273
      IF (ABS(DE0).GT..01*EPS4) GO TO 275
```

```
273   IF (ABS((RHOO2-RHOO)/RHOO2).LE.EPS3) GO TO 285
      IF (ABS(DRHOO).LT.EPS3) GO TO 285
275   ITS22=ITS22-1
      IF (ITS22.GT.0) GO TO 280
      WRITE (3,278) ITS2
278   FORMAT (35HOE AND RHO FAILED TO CONVERGE AFTER,I4,6H TRIES)
      WRITE (3,279) I,K,ZO,RO,EO,RHOO,PO,EO2,RHOO2,PO2
279   FORMAT (1X2HI=,I4,4X2HK=,I4/1X4HZO =,E15.8,4X4HRO =,E15.8,4X4HEO =
     1,E15.8,4X6HRHOO =,E15.8,4X4HPO =,E15.8/1X4HEO2=,E15.8,4X6HRHOO2=,E
     115.8,4X4HPO2=,E15.8/1H1)
      STOP
280   EO=EO2
      RHOO=RHOO2
      PO=PO2
      UBARO=UBARO2
      GO TO 250
285   EO=EO2
      RHOO=RHOO2
      UBARO=UBARO2
      AO=SQRT(PFR+PO2*PFE/RHOO**2)
C
C
      CALL DVCHK(KQ)
      KICK=285
      IF (KQ.EQ.1) GO TO 9980
      IF (K.EQ.2) GO TO 286
      VBARO=VP*LO
      GO TO 287
286   VBARO=0.
287   CONTINUE
295   PO=PO2
      IF (K.EQ.2) GO TO 296
      UBARO=UBARS1-UBARO
296   CONTINUE
      UTO=(RHOO*UBARO-RHOSTR*UBARS1)/(RHOO-RHOSTR)
      VO=MO*UBARO+LO*VBARO
```

```
      UO=LO*UBARO-MO*VBARO
      UBAR=.5*(UTOH+UTO)
      IF (ABS((UBAR-UTOH)/UBAR).LE.EPS6) GO TO 350
      IF (ABS(UBAR-UTOH).LT.EPS6) GO TO 350
      ITS44=ITS44-1
      IF (ITS44.GT.0) GO TO 325
      WRITE (3,297) ITS4,UTOH,UTO
297   FORMAT (30HOUBAR FAILED TO CONVERGE AFTER,I4,6H TRIES/1X5HUTOH=,E1
     15.8,4X4HUTO=,E15.8)
      CALL EXIT
      WRITE (3,279) I,K,ZO,RO,EO,RHOO,PO,EO2,RHOO2,PO2
C
C         INIT. FOR MORE U BAR ITERATIONS
C
325   UTOH=UBAR
      AVMO=(TAB(I,10,K)+MO)*.5
      AVLO=(TAB(I,9,K)+LO)*.5
      ZO=TAB(I,1,K)+UBAR*H*AVMO-VBARS*AVLO*H
      RO=TAB(I,2,K)+UBAR*H*AVLO-VBARS*AVMO*H
      LO=AVLO
      MO=AVMO
      GO TO 195
C
C         ONE SHOCK POINT HAS CONVERGED
C
350   TAB2(I,1,K)=ZO
      TAB2(I,2,K)=RO
      TAB2(I,3,K)=PO
      TAB2(I,4,K)=UO
      TAB2(I,5,K)=VO
      TAB2(I,6,K)=RHOO
      TAB2(I,7,K)=EO
      TAB2(I,8,K)=AO
      TAB2(I,9,K)=LO
      TAB2(I,10,K)=MO
      TAB2(I,11,K)=UBARO
```

```
      TAB2(I,12,K)=VBARO
      TAB2(I,13,K)=UTO
      KICK=500
      CALL DVCHK(KQ)
      IF (KQ.EQ.1) GO TO 9980
C
C
500   CONTINUE
505   CONTINUE
      RETURN
9980  WRITE (3,9985) KICK
9985  FORMAT (32H0DIVIDE CHECK NEAR STATEMENT NO.,I5,15H IN SUBR. SHOCK/
     11H1)
      CALL EXIT
      RETURN
      END
      SUBROUTINE FGOF1(ZX,RX,SS,QQ)
C
C          COMPUTES S1,Q1 FOR SHOCK LINE
C          ITERATION FOR Z1,R1
C
      COMMON CASEID(14),ITS1,ITS2,ITS3,ITS4,ITI1,ITI2,ITI3,ITI4,EPS1,EPS
     12,EPS3,EPS4,EPS5,EPS6,EPI1,EPI2,EPI3,EPI4,EPI5,EPI6,EPI7,VP,AR,LEN
     1GTH,APR,BPR,BIGAPR,BIGBPR,ESTAR,ALPHA,BETA,RHOSTR,EPRS,RHOS
      COMMON XMESH(20,20,6),XMESH2(20,20,6),Z(20),R(20),SURF(15,8),SURF2
     1(15,8),TAB(15,14,2),TAB2(15,14,2),SPART(15,2,2),RARF(15,11),RARF2(
     115,4),RPART(15,2)
C
C
      COMMON ZO,RO,PO,UO,VO,LO,MO,RHOO,EO,AO,UBARO,VBARO
C
      COMMON NP,NT,NR,NI,NDEL,ISUB
C
      COMMON ZMIN,ZMAX,RMIN,RMAX,RADIUS,GZ,GR,DELTA,H
      COMMON DIRCOS
      COMMON TIME
```

```
      COMMON IRARF
      COMMON KSTOP
      COMMON TPSI
      COMMON KKK
      REAL LO,MO,LENGTH,MU,KO
C
      DIMENSION ANS(6)
C
      REAL LO,MO
      CALL DBLTRP(ZX,RX,ANS)
      U1=ANS(2)
      V1=ANS(3)
      A1=ANS(6)
      SS=ZX-ZO+H*(V1+A1*DIRCOS)
      QQ=RX-RO+H*(U1+A1*LO)
      RETURN
      END
      SUBROUTINE INTER(PHI,NMAX,MMAX)
C     SUBROUTINE INTER
C         COMPUTES INTERIOR REGION POINTS
      COMMON CASEID(14),ITS1,ITS2,ITS3,ITS4,ITI1,ITI2,ITI3,ITI4,EPS1,EPS
     12,EPS3,EPS4,EPS5,EPS6,EPI1,EPI2,EPI3,EPI4,EPI5,EPI6,EPI7,VP,AR,LEN
     1GTH,APR,BPR,BIGAPR,BIGBPR,ESTAR,ALPHA,BETA,RHOSTR,EPRS,RHOS
      COMMON XMESH(20,20,6),XMESH2(20,20,6),Z(20),R(20),SURF(15,8),SURF2
     1(15,8),TAB(15,14,2),TAB2(15,14,2),SPART(15,2,2),RARF(15,11),RARF2(
     115,4),RPART(15,2)
C
C
      COMMON ZO,RO,PO,UO,VO,LO,MO,RHOO,EO,AO,UBARO,VBARO
C
      COMMON NP,NT,NR,NI,NDEL,ISUB
C
      COMMON ZMIN,ZMAX,RMIN,RMAX,RADIUS,GZ,GR,DELTA,H
      COMMON DIRCOS
      COMMON TIME
      COMMON IRARF
```

```
      COMMON KSTOP
      COMMON TPSI
      COMMON KKK
C
C
      REAL LO,MO,LENGTH,MU,KO
      DOUBLE PRECISION PHI(20,20,6)
      DIMENSION ANS(6),LL(3),ZI(11),RI(11),PI(11),UI(11),VI(11),RHOI(11)
     1,EI(11),AI(11),PUR(11),PVR(11),PAR(11),PUZ(11),PVZ(11),PAZ(11),PSI
     1(7),SPSI(11),CPSI(11),S(11)
C
      EXTERNAL FGOFI,FGOF5
      INTEGER CHECK,CHECK2
C
1     FORMAT (1H1)
      TSSS=1.1
      EPS=.0000001
      DO 905 J=1,20
      DO 900 I=1,20
      M=TEST(Z(I),R(J))
      ZO=Z(I)
      RO=R(J)
      KICK=1
      CALL DVCHK(KQ)
      IF (KQ.EQ.1) GO TO 9980
      IF (M.EQ.3.AND.ZO.LT.EPS.AND.ABS(RO-RADIUS).LT.EPS)M=1
      IF (M.NE.1) GO TO 900
      DO 2 L=1,NP
      IF (TAB(L,14,1).LT.0.) GO TO 20
2     CONTINUE
      IF (IRARF.EQ.1) GO TO 20
      DO 3 N=1,NR
      IF (R(J).GT.RARF(N,2)) GO TO 5
3     CONTINUE
      GO TO 6
5     CONTINUE
```

```
      M=PICK(Z(I),R(J),3)
      FF=R(J)-RARF(M+1,2)-(RARF(M,2)-RARF(M+1,2))*(Z(I)-RARF(M+1,1))/(RA
     1RF(M,1)-RARF(M+1,1))
      IF (FF.GT.0.) GO TO 20
6     CONTINUE
      PO2=RARF(1,3)
      UO2=RARF(1,4)
      VO2=RARF(1,5)
      RHOO2=RARF(1,6)
      EO2=RARF(1,7)
      AO2=RARF(1,8)
      GO TO 870
20    CONTINUE
      CALL GUESS(2,KOD,ZO,RO,I,J,ZZ,RR,DZ,DR)
      IF (KOD.EQ.1) GO TO 580
      WRITE (3,575) I,J,ZO,RO
575   FORMAT (41HONO GUESS FOUND FOR INTERIOR REGION POINT/3HOI=I4,6X2HK
     1=,I4,10X3HZO=,E15.8,10X3HRO=,E15.8/1H1)
      CALL EXIT
  580 IF(TIME.GT.TSSS) GO TO 150
      CALL DBLTRP(ZZ,RR,ANS)
      GO TO 151
  150 CALL  DSURFT(ZZ,RR,ANS,PHI,NMAX,MMAX)
C
C          INITIALIZE FOR 1 POINT
C
C     PSI(1)=0.
  151 PSI(1)=0.
      PSI(3)=1.0472
      PSI(4)=2.0944
      PSI(6)=4.18879
      PSI(7)=5.23599
      NBIC=0
      ITI22=ITI2
      PO=ANS(1)
      UO=ANS(2)
```

```
      V0=ANS(3)
      RHO0=ANS(4)
      E0=ANS(5)
      A0=ANS(6)
      KICK=580
      CALL DVCHK(KQ)
      IF (KQ.EQ.1) GO TO 9980
590   IF (ABS(R0).GT.EPS) GO TO 594
      L1=1
      LL(1)=4
      LL(2)=6
      LLL=2
      GO TO 620
C
C
594   IF (ABS(R0-RADIUS).GT.EPS) GO TO 600
      IF (Z0.GT.EPS) GO TO 610
      L1=2
      LL(1)=3
      LL(2)=7
      LLL=2
      GO TO 620
600   IF (R0.LE.RADIUS.OR.ABS(Z0).GT.EPS) GO TO 610
      L1=3
      LL(1)=6
      LL(2)=7
      LLL=2
      GO TO 620
C
C
610   L1=4
      LL(1)=1
      LL(2)=4
      LL(3)=6
      LLL=3
C
```

```
C          ITERATE FOR I VALUES
C
619    CONTINUE
620    DO 630 KK=1,LLL
       LUMP=L1
       ISUB=LL(KK)
621    CONTINUE
       TPSI=PSI(ISUB)
       SPSI(ISUB)=SIN(TPSI)
       CPSI(ISUB)=COS(TPSI)
C      CALL NRIT2(ZI(ISUB),RI(ISUB),ZZ,DZ,RR,DR,EPI1,EPI2,FGOFI,ITI1,KODE
C     1)
       CALL NRIT2(ZI(ISUB),RI(ISUB),ZZ,DZ,RR,DR,EPI1,EPI2,FGOFI,ITI1,KODE
      1,PHI,NMAX,MMAX)
       IF (KODE.NE.0) GO TO 6200
  625 IF(TIME.GT.TSSS) GO TO 125
       CALL DBLTRP(ZI(ISUB),RI(ISUB),ANS)
       GO TO 122
  125 CALL DSURFT(ZI(ISUB),RI(ISUB),ANS,PHI,NMAX,MMAX)
  122 PI(ISUB)=ANS(1)
C      PI(ISUB)=ANS(1)
       UI(ISUB)=ANS(2)
       VI(ISUB)=ANS(3)
       RHOI(ISUB)=ANS(4)
       EI(ISUB)=ANS(5)
       AI(ISUB)=ANS(6)
630    CONTINUE
C
C
       KICK=630
       CALL DVCHK(KQ)
       IF (KQ.EQ.1) GO TO 9980
       GO TO 6400
C
C     BICHARACTERISTIC SELECTION SCHEME
C
```

```
7000  WRITE (3,7001)
7001  FORMAT (41HOBICHARACTERISTIC SELECTION SCHEME FAILED)
      WRITE (3,614) ZO,RO
      WRITE (3,7002) (PSI(MNMN),MNMN=1,7),UA,VA,AA,UB,VB,AB,UC,VC,AC,ZZ,
     1DZ,RR,DR,ANG1,ANG2
      SUB=ISUB
      WRITE (3,7002) SUB,ZI(ISUB),RI(ISUB)
7002  FORMAT (4E16.8)
      CALL EXIT
6200  CONTINUE
      IF (NBIC.NE.0) GO TO 7000
      IF (L1.NE.2.OR.LL(1).EQ.1) GO TO 7300
      LL(1)=1
      GO TO 619
7300  CONTINUE
      IF (L1.NE.3) GO TO 7310
      IF (PSI(6).GT.4.2) GO TO 7310
      PSI(6)=5.75959
      GO TO 619
7310  CONTINUE
      IF(TIME.GT.TSSS) GO TO 222
      CALL DBLTRP(ZZ,RR,ANS)
      GO TO 223
  222 CALL DSURFT(ZZ,RR,ANS,PHI,NMAX,MMAX)
  223 UA=ANS(2)
C     UA=ANS(2)
      VA=ANS(3)
      AA=ANS(6)
      ZZZ=ZZ+DZ
      IF(TIME.GT.TSSS) GO TO 128
      CALL DBLTRP(ZZZ,RR,ANS)
      GO TO 129
  128 CALL DSURFT(ZZZ,RR, ANS,PHI,NMAX,MMAX)
  129 UB=ANS(2)
C     UB=ANS(2)
      VB=ANS(3)
```

```
      AB=ANS(6)
      RRR=RR+DR
      IF(TIME.GT.TSSS) GO TO 130
      CALL DBLTRP(ZZ,RRR,ANS)
      GO TO 131
  130 CALL DSURFT(ZZ,RRR,ANS,PHI,NMAX,MMAX)
  131 UC=ANS(2)
C     UC=ANS(2)
      VC=ANS(3)
      AC=ANS(6)
      MM=0
      TPSI=PSI(ISUB)
      XB=ZZ
      YB=RR
      NOM=5
      CA=NOM
      DO 6210 LM=1,2
 6201 DTPSI=.01745
      DTPSI=CA*DTPSI
      TPSI=TPSI+DTPSI
      A1=1.+H*(VB-VA+(AB-AA)*SIN(TPSI))/DZ
      B1=H*(VC-VA+(AC-AA)*SIN(TPSI))/DR
      C1=-(ZZ-Z0+H*(VA+AA*SIN(TPSI)))
      A2=H*(UB-UA+(AB-AA)*COS(TPSI))/DZ
      B2=1.+H*(UC-UA+(AC-AA)*COS(TPSI))/DR
      C2=-(RR-R0+H*(UA+AA*COS(TPSI)))
      DET=A1*B2-A2*B1
      DELX=(B2*C1-B1*C2)/DET
      DELY=(A1*C2-A2*C1)/DET
C
C         TEST FOR SAME REGION
C
      XB1=XB+DELX
      YB1=YB+DELY
      M=COMP(XB,YB,XB1,YB1)
      IF (LM.EQ.2) GO TO 6700
```

```
      IF (M.EQ.1) GO TO 6203
      GO TO 6800
6700  CONTINUE
      IF (M.NE.1) GO TO 6203
6800  CONTINUE
      MM=MM+1
      IF (MM.LE.360/NOM) GO TO 6201
612   WRITE (3,613) ITI1
613   FORMAT (44H0FAILED TO FIND 2 POINTS IN THE SAME REGION 21H IN SUBR
     1. NRIT2 AFTER,I4,6H TRIES)
      WRITE (3,614) ZO,RO
614   FORMAT (1X5HZO  =,E15.8,4X5HRO  =,E15.8)
      WRITE (3,6144) LM
      WRITE (3,6145) M
      WRITE (3,6146) KODE
      WRITE (3,7002) XB,YB,XB1,YB1
6144  FORMAT (4H LM=,I4)
6145  FORMAT (3H M=,I4)
6146  FORMAT (6H KODE=,I4)
      CALL EXIT
6203  GO TO (6204,6205),LM
6204  ANG1=TPSI
      MM=0
      GO TO 6210
6205  ANG2=TPSI-DTPSI
6210  CONTINUE
      AL=LLL+1
      DO 6300 KK=1,LLL
      ISUB=LL(KK)
      AK=KK
      PSI(ISUB)=ANG1+(ANG2-ANG1)*AK/AL
6300  CONTINUE
      NBIC=1
      GO TO 619
C
C
```

```
6400  CONTINUE
      IF (L1.EQ.2.OR.L1.EQ.3) GO TO 642
C     CALL NRIT2(ZI(8),RI(8),ZZ,DZ,RR,DR,EPI1,EPI2,FGOF5,ITI1,KODE)
      CALL NRIT2(ZI(8),RI(8),ZZ,DZ,RR,DR,EPI1,EPI2,FGOF5,ITI1,KODE,
     1 PHI,NMAX,MMAX)
      IF (KODE.EQ.0) GO TO 635
      ISUB=8
      WRITE (3,622) ITI1,I,J,ISUB,ZO,RO,ZZ,RR,ZI(8),RI(8)
622   FORMAT (27HOFAILED TO FIND ZI,RI AFTER,I4,6H TRIES,3X2HI=,I4,3X2HJ
     1=,I4,3X5HISUB=,I4/1X3HZO=,E15.8,6X3HRO=,E15.8/1X3HZZ=,E15.8,6X3HRR
     1=,E15.8/1X3HZI=,E15.8,6X3HRI=,E15.8/1H1)
      CALL EXIT
C
C
  635 IF(TIME.GT.TSSS) GO TO 132
      CALL DBLTRP(ZI(8),RI(8),ANS)
       GO TO 133
  132 CALL DSURFT(ZI(8),RI(8),ANS,PHI,NMAX,MMAX)
  133 PI(8)=ANS(1)
C     PI(8)=ANS(1)
      UI(8)=ANS(2)
      VI(8)=ANS(3)
      RHOI(8)=ANS(4)
      EI(8)=ANS(5)
      AI(8)=ANS(6)
C
642   DO 670 IL=1,LLL
      NN=LL(IL)
      M=PART(1,ZI(NN),RI(NN),ZX,RX,DELTA,NDEL)
      IF (M.EQ.1) GO TO 645
      PUR(NN)=0.
      PVR(NN)=0.
      GO TO 648
  645 IF(TIME.GT.TSSS) GO TO 134
      CALL DBLTRP(ZX,RX,ANS)
      GO TO 135
```

```
  134 CALL DSURFT(ZX,RX,ANS,PHI,NMAX,MMAX)
  135 DEN=RX-RI(NN)
C     DEN=RX-RI(NN)
      PUR(NN)=(ANS(2)-UI(NN))/DEN
      PVR(NN)=(ANS(3)-VI(NN))/DEN
648   M=PART(2,ZI(NN),RI(NN),ZX,RX,DELTA,NDEL)
      IF (M.EQ.1) GO TO 650
      PUZ(NN)=0.
      PVZ(NN)=0.
      GO TO 655
  650 IF(TIME.GT.TSSS) GO TO 136
      CALL DBLTRP(ZX,RX,ANS)
      GO TO 137
  136 CALL DSURFT(ZX,RX,ANS,PHI,NMAX,MMAX)
  137 DEN=ZX-ZI(NN)
      PUZ(NN)=(ANS(2)-UI(NN))/DEN
      PVZ(NN)=(ANS(3)-VI(NN))/DEN
655   S(NN)=SPSI(NN)**2*PUR(NN)-CPSI(NN)*SPSI(NN)*(PVR(NN)+PUZ(NN))+CPSI
     1(NN)**2*PVZ(NN)
C
      IF (ABS(RI(NN)).GT.EPS) GO TO 660
      CON=PUR(NN)
      GO TO 662
660   CON=UI(NN)/RI(NN)
662   S(NN)=-RHOI(NN)*H*AI(NN)**2*(S(NN)+CON)+PI(NN)+RHOI(NN)*AI(NN)*CPS
     1I(NN)*UI(NN)+RHOI(NN)*AI(NN)*SPSI(NN)*VI(NN)
670   CONTINUE
1005  CONTINUE
1002  FORMAT (4E16.8)
      KICK=670
      CALL DVCHK(KQ)
      IF (KQ.EQ.1) GO TO 9980
C
C         COMPUTE NEW P,U,V
C
      GO TO (690,692,695,698),L1
```

```
690   DUO=0.
      U02=0.
      V02=(S(4)-S(6))/(RHOI(4)*AI(4)*SPSI(4)-RHOI(6)*AI(6)*SPSI(6))
      P02=S(4)-RHOI(4)*AI(4)*SPSI(4)*V02
      GO TO 700
C
C
692   DPO=0.
      P02=0.
      L=LL(1)
      TMP1=RHOI(7)*RHOI(L)*AI(7)*AI(L)*(CPSI(7)*SPSI(L)-CPSI(L)*SPSI(7))
      V02=(S(L)*RHOI(7)*AI(7)*CPSI(7)-S(7)*RHOI(L)*AI(L)*CPSI(L))/TMP1
      U02=(S(L)-RHOI(L)*AI(L)*SPSI(L)*V02)/(RHOI(L)*AI(L)*CPSI(L))
      GO TO 700
C
C
695   DPO=0.
      P02=0.
      TMP1=RHOI(7)*RHOI(6)*AI(7)*AI(6)*(CPSI(7)*SPSI(6)-SPSI(7)*CPSI(6))
      V02=(S(6)*RHOI(7)*AI(7)*CPSI(7)-S(7)*RHOI(6)*AI(6)*CPSI(6))/TMP1
      U02=(S(6)-RHOI(6)*AI(6)*SPSI(6)*V02)/(RHOI(6)*AI(6)*CPSI(6))
      GO TO 700
698   CONTINUE
      L=LL(1)
      TMP1=RHOI(4)*AI(4)*CPSI(4)-RHOI(L)*AI(L)*CPSI(L)
      TMP2=RHOI(4)*AI(4)*SPSI(4)-RHOI(L)*AI(L)*SPSI(L)
      TMP3=RHOI(6)*AI(6)*CPSI(6)-RHOI(L)*AI(L)*CPSI(L)
      TMP4=RHOI(6)*AI(6)*SPSI(6)-RHOI(L)*AI(L)*SPSI(L)
      V02=((S(4)-S(L))*TMP3-(S(6)-S(L))*TMP1)/(TMP3*TMP2-TMP1*TMP4)
      U02=(S(4)-S(L)-TMP2*V02)/TMP1
      P02=S(6)-RHOI(6)*AI(6)*CPSI(6)*U02-RHOI(6)*AI(6)*SPSI(6)*V02
700   KICK=700
      CALL DVCHK(KQ)
      IF (KQ.EQ.1) GO TO 9980
C
C
```

```
C           ITERATE FOR RHOO,EO
C
705    ITI33=ITI3
       ITI44=ITI4
       KM=1
708    CONTINUE
       CALL EQOSI(PO2,PGRHO,PGE,BIGG,CHECK,KRTT,AO2,EO2,RHOO2,KM,EPS)
       IF (KRTT.EQ.1) GO TO 871
725    T1=RHOO-RHOI(8)
       T2=PI(8)/RHOI(8)**2
       BIGH=EI(8)+T2*T1-EO
       PHE=-1.
       PHRHO=T2
       KICK=725
       CALL DVCHK(KQ)
       IF (KQ.EQ.1) GO TO 9980
C
C           COMPUTE NEW EO,RHOO
C
       DOWN=PGE*PHRHO-PGRHO*PHE
       DEO=(-BIGG*PHRHO+BIGH*PGRHO)/DOWN
       DRHOO=(-BIGH*PGE+BIGG*PHE)/DOWN
       EO2=EO+DEO
       RHOO2=RHOO+DRHOO
C
C           CHECK EO2,RHOO2 FOR CONVERGENCE
       KICK=726
       CALL DVCHK(KQ)
       IF (KQ.EQ.1) GO TO 9980
C
       IF (ABS(DEO/EO).LT.EPI7) GO TO 726
       IF (ABS(DEO).GT..01*EPI7) GO TO 730
726    IF (ABS(DRHOO/RHOO).LE.EPI6) GO TO 740
       IF (ABS(DRHOO).LT.EPI6) GO TO 740
730    ITI33=ITI33-1
       IF (ITI33.NE.0) GO TO 735
```

```
      WRITE (6,732) ITI3,I,J,Z0,R0,P0,U0,V0,RHO0,E0,P02,U02,V02,RHO02,E0
     12
  732 FORMAT (33H0E0,RHO0 FAILED TO CONVERGE AFTER,I4,6H TRIES/1X2HI=,I4
     1,4X2HJ=,I4,4X2HZ=,E15.8,4X2HR=,E15.8/5X2HP018X2HU018X2HV018X4HRHO0
     116X2HE0/5X3HP0217X3HU0217X3HV0217X5HRHO0215X3HE02//(5E20.8))
      WRITE (3,1)
      CALL EXIT
  735 E0=E02
      RHO0=RHO02
      KM=0
      GO TO 708
C
C         CHECK FOR PROPER EQUATIONS
C
  740 CONTINUE
      PGE=-PGE
      PGRHO=-PGRHO
      IF (RHO02.GE.RHOSTR) GO TO 750
      IF (E02.LT.EPRS) GO TO 750
  742 CHECK2=0
      GO TO 752
  750 CHECK2=1
  752 A02=SQRT(+PGRHO+P02*PGE/RHO02**2)
      IF (CHECK.EQ.CHECK2) GO TO 870
      ITI44=ITI44-1
      IF (ITI44.NE.0) GO TO 770
      WRITE (3,755) ITI4,I,J,Z0,R0,P0,U0,V0,RHO0,E0,A0,P02,U02,V02,RHO02
     1,E02,A02
  755 FORMAT (38H0FAILED TO USE CORRECT EQUATIONS AFTER,I4,6H TRIES/1X2H
     1I=,I4,4X2HJ=,I4,4X2HZ=,E15.8,4X2HR=,E15.8/5X2HP018X2HU018X2HV018X4
     1HRHO016X2HE018X2HA0/5X3HP0217X3HU0217X3HV0217X5HRHO0215X3HE0217X3H
     1A02//(6E20.8))
      WRITE (3,1)
      CALL EXIT
  770 KICK=770
      CALL DVCHK(KQ)
```

```
      IF (KQ.EQ.1) GO TO 9980
      ITI33=ITI3
      GO TO 735
C
C         ALL VALUES HAVE CONVERGED FOR 1 INTERIOR POINT
C
871   KRTT=0
870   XMESH2(I,J,1)=P02
      XMESH2(I,J,2)=U02
      XMESH2(I,J,3)=V02
      XMESH2(I,J,4)=RHO02
      XMESH2(I,J,5)=E02
      XMESH2(I,J,6)=A02
      KICK=900
      CALL DVCHK(KQ)
      IF (KQ.EQ.1) GO TO 9980
900   CONTINUE
905   CONTINUE
      IF (ITS3.EQ.1) GO TO 950
      CALL ITRP
      RETURN
950   CONTINUE
9980  WRITE (3,9985) KICK
      WRITE (3,614) ZO,RO
9985  FORMAT (32HODIVIDE CHECK NEAR STATEMENT NO.,I5,15H IN SUBR. INTER/
     11H1)
      CALL EXIT
      RETURN
      DEBUG SUBCHK
      END
      SUBROUTINE EQOS1(PRHO,PPP,PVV,PEE,TEE,TRHO,KICK)
      COMMON CASEID(14),ITS1,ITS2,ITS3,ITS4,ITI1,ITI2,ITI3,ITI4,EPS1,EPS
     12,EPS3,EPS4,EPS5,EPS6,EPI1,EPI2,EPI3,EPI4,EPI5,EPI6,EPI7,VP,AR,LEN
     1GTH,APR,BPR,BIGAPR,BIGBPR,ESTAR,ALPHA,BETA,RHOSTR,EPRS,RHOS
      COMMON XMESH(20,20,6),XMESH2(20,20,6),Z(20),R(20),SURF(15,8),SURF2
     1(15,8),TAB(15,14,2),TAB2(15,14,2),SPART(15,2,2),RARF(15,11),RARF2(
```

```
     115,4),RPART(15,2)
C
C
      COMMON ZO,RO,PO,UO,VO,LO,MO,RHOO,EO,AO,UBARO,VBARO
C
      COMMON NP,NT,NR,NI,NDEL,ISUB
C
      COMMON ZMIN,ZMAX,RMIN,RMAX,RADIUS,GZ,GR,DELTA,H
      COMMON DIRCOS
      COMMON TIME
      COMMON IRARF
      COMMON KSTOP
      COMMON TPSI
      COMMON KKK
C
C
      REAL LO,MO,LENGTH,MU,KO
      RHO=RHOSTR
      E=VP**2/8.
      DO 100 M=1,100
      ETA=RHO/RHOSTR
      MU=ETA-1.
      G=-RHOSTR*(VP/2.)**2+((APR+BPR/(E/(ESTAR*ETA**2)+1.))*E*RHO+BIGAPR
     1*MU+BIGBPR*MU**2)*(1.-RHOSTR/RHO)
      DERIVG=((APR+BPR/(E/(ESTAR*ETA**2)+1.))*E+BIGAPR/RHOSTR+2.*BIGBPR*
     1MU/RHOSTR+2.*E**2*BPR/(ESTAR*ETA**2*(E/(ESTAR*ETA**2)+1.)**2))*(1.
     1-RHOSTR/RHO)+((APR+BPR/(E/(ESTAR*ETA**2)+1.))*E*RHO+BIGAPR*MU+BIGB
     1PR*MU**2)*RHOSTR/RHO**2
      DLTRHO=-G/DERIVG
      RHO=RHO+DLTRHO
C     IF(ABS(DLTRHO).LT.1.E-07) GO TO 101
      IF (ABS(DLTRHO).LT.1.E-06) GO TO 101
100   CONTINUE
      KICK=2200
      GO TO 9980
101   CONTINUE
```

```
      PRHO=RHO
      TRHO=RHO
      PEE=E
      TEE=E
      PVV=VP/2.
      PPP=(APR+BPR/(E/(ESTAR*ETA**2)+1.))*E*RHO+BIGAPR*MU+BIGBPR*MU**2
 9980 RETURN
      DEBUG SUBCHK
      END
      SUBROUTINE EQOS2(PPP,PRHO,PEE)
      COMMON CASEID(14),ITS1,ITS2,ITS3,ITS4,ITI1,ITI2,ITI3,ITI4,EPS1,EPS
     12,EPS3,EPS4,EPS5,EPS6,EPI1,EPI2,EPI3,EPI4,EPI5,EPI6,EPI7,VP,AR,LEN
     1GTH,APR,BPR,BIGAPR,BIGBPR,ESTAR,ALPHA,BETA,RHOSTR,EPRS,RHOS
      COMMON XMESH(20,20,6),XMESH2(20,20,6),Z(20),R(20),SURF(15,8),SURF2
     1(15,8),TAB(15,14,2),TAB2(15,14,2),SPART(15,2,2),RARF(15,11),RARF2(
     115,4),RPART(15,2)
C
C
      COMMON Z0,R0,P0,U0,V0,L0,M0,RHO0,E0,A0,UBAR0,VBAR0
C
      COMMON NP,NT,NR,NI,NDEL,ISUB
C
      COMMON ZMIN,ZMAX,RMIN,RMAX,RADIUS,GZ,GR,DELTA,H
      COMMON DIRCOS
      COMMON TIME
      COMMON IRARF
      COMMON KSTOP
C
      COMMON TPSI
      COMMON KKK
C
      REAL L0,M0,LENGTH,MU,K0
      P=PPP
      RHO=PRHO
      E=PEE
      ETA=RHO/RHOSTR
```

```
      MU=ETA-1.
      EE=E/(ESTAR*ETA**2)+1.
      PGRHO=E*(APR+BPR/EE)+BIGAPR/RHOSTR+(2.*BIGBPR*MU)/RHOSTR+(2.*E**2*
     1BPR)/(ESTAR*ETA**2*EE**2)
      PGE=(APR+BPR/EE)*RHO-(E*BPR*RHO)/(ESTAR*ETA**2*EE**2)
      AR=SQRT(PGRHO+PGE*P/RHO**2)
      RETURN
      DEBUG SUBCHK
      END
      SUBROUTINE EQOS3(RHO,AA,E,P)
      COMMON CASEID(14),ITS1,ITS2,ITS3,ITS4,ITI1,ITI2,ITI3,ITI4,EPS1,EPS
     12,EPS3,EPS4,EPS5,EPS6,EPI1,EPI2,EPI3,EPI4,EPI5,EPI6,EPI7,VP,AR,LEN
     1GTH,APR,BPR,BIGAPR,BIGBPR,ESTAR,ALPHA,BETA,RHOSTR,EPRS,RHOS
      COMMON XMESH(20,20,6),XMESH2(20,20,6),Z(20),R(20),SURF(15,8),SURF2
     1(15,8),TAB(15,14,2),TAB2(15,14,2),SPART(15,2,2),RARF(15,11),RARF2(
     115,4),RPART(15,2)
C
C
      COMMON ZO,RO,PO,UO,VO,LO,MO,RHOO,EO,AO,UBARO,VBARO
C
      COMMON NP,NT,NR,NI,NDEL,ISUB
C
      COMMON ZMIN,ZMAX,RMIN,RMAX,RADIUS,GZ,GR,DELTA,H
      COMMON DIRCOS
      COMMON TIME
      COMMON IRARF
      COMMON KSTOP
      COMMON TPSI
      COMMON KKK
C
C
      REAL LO,MO,LENGTH,MU,KO
70    ETA=RHO/RHOSTR
      MU=ETA-1.
      EE=E/(ESTAR*ETA**2)+1.
      IF (RHO.GT.RHOSTR) GO TO 72
```

```
      IF (E.GE.EPRS) GO TO 74
72    PGRHO=E*(APR+BPR/EE)+BIGAPR/RHOSTR+(2.*BIGBPR*MU)/RHOSTR+(2.*E**2*
     1BPR)/(ESTAR*ETA**2*EE**2)
      PGE=(APR+BPR/EE)*RHO-(E*BPR*RHO)/(ESTAR*ETA**2*EE**2)
      GO TO 75
74    C1=RHOSTR/RHO-1.
      C2=EXP(-BETA*C1)
      C3=EXP(-ALPHA*C1**2)
      T1=(BPR*E*RHO)/EE+BIGAPR*MU*C2
      T2=2.*ALPHA*C1*(RHOSTR/(RHO**2))
      T3=BPR*E/EE
      T4=(2.*E)/(ESTAR*ETA**2*EE)
      T4=T3*T4
      T5=(BIGAPR*C2)/RHOSTR
      T6=(BIGAPR*MU*BETA*RHOSTR*C2)/(RHO**2)
      PGRHO=APR*E+C3*(T1*T2+T3+T4+T5+T6)
      T7=(BPR*RHO)/EE
      PGE=APR*RHO+C3*(T7-T7*(E/(ESTAR*ETA**2*EE)))
75    AA=SQRT(PGRHO+PGE*P/RHO**2)
      RETURN
      DEBUG SUBCHK
      END
      SUBROUTINE EQOSS(PFR,PFE)
      COMMON CASEID(14),ITS1,ITS2,ITS3,ITS4,ITI1,ITI2,ITI3,ITI4,EPS1,EPS
     12,EPS3,EPS4,EPS5,EPS6,EPI1,EPI2,EPI3,EPI4,EPI5,EPI6,EPI7,VP,AR,LEN
     1GTH,APR,BPR,BIGAPR,BIGBPR,ESTAR,ALPHA,BETA,RHOSTR,EPRS,RHOS
      COMMON XMESH(20,20,6),XMESH2(20,20,6),Z(20),R(20),SURF(15,8),SURF2
     1(15,8),TAB(15,14,2),TAB2(15,14,2),SPART(15,2,2),RARF(15,11),RARF2(
     115,4),RPART(15,2)
C
C
      COMMON Z0,R0,P0,U0,V0,L0,M0,RHO0,E0,A0,UBAR0,VBAR0
C
      COMMON NP,NT,NR,NI,NDEL,ISUB
C
      COMMON ZMIN,ZMAX,RMIN,RMAX,RADIUS,GZ,GR,DELTA,H
```

```
      COMMON DIRCOS
      COMMON TIME
      COMMON IRARF
      COMMON KSTOP
      COMMON TPSI
      COMMON KKK
C
C
      REAL LO,MO,LENGTH,MU,KO
250   ETA=RHOO/RHOSTR
      MU=ETA-1.
C
C
      EPP=EO/(ESTAR*ETA**2)+1.
      TMP=APR+BPR/EPP
      TMP1=BPR/(ESTAR*ETA**2*EPP**2)
      PFR=TMP*EO+(BIGAPR+2.*BIGBPR*MU)/RHOSTR+2.*EO**2*TMP1
      PFE=TMP*RHOO-EO*RHOO*TMP1
      RETURN
      DEBUG SUBCHK
      END
      SUBROUTINE EQOSP(RHOO2,EO2,PO2)
      COMMON CASEID(14),ITS1,ITS2,ITS3,ITS4,ITI1,ITI2,ITI3,ITI4,EPS1,EPS
     12,EPS3,EPS4,EPS5,EPS6,EPI1,EPI2,EPI3,EPI4,EPI5,EPI6,EPI7,VP,AR,LEN
     1GTH,APR,BPR,BIGAPR,BIGBPR,ESTAR,ALPHA,BETA,RHOSTR,EPRS,RHOS
      COMMON XMESH(20,20,6),XMESH2(20,20,6),Z(20),R(20),SURF(15,8),SURF2
     1(15,8),TAB(15,14,2),TAB2(15,14,2),SPART(15,2,2),RARF(15,11),RARF2(
     115,4),RPART(15,2)
C
C
      COMMON ZO,RO,PO,UO,VO,LO,MO,RHOO,EO,AO,UBARO,VBARO
C
      COMMON NP,NT,NR,NI,NDEL,ISUB
C
      COMMON ZMIN,ZMAX,RMIN,RMAX,RADIUS,GZ,GR,DELTA,H
      COMMON DIRCOS
```

```
      COMMON TIME
      COMMON IRARF
      COMMON KSTOP
      COMMON TPSI
      COMMON KKK
C
C
      REAL LO,MO,LENGTH,MU,KO
      ETA=RHOO2/RHOSTR
      MU=ETA-1.
      PO2=EO2*RHOO2*(APR+(BPR*ESTAR*ETA**2)/(EO2+ESTAR*ETA**2))+BIGAPR*M
     1U+BIGBPR*MU**2
      RETURN
      DEBUG SUBCHK
      END
      SUBROUTINE EQOSI(PO2,PGRHO,PGE,BIGG,CHECK,KRTT,AO2,EO2,RHOO2,KM,EP
     1S)
      COMMON CASEID(14),ITS1,ITS2,ITS3,ITS4,ITI1,ITI2,ITI3,ITI4,EPS1,EPS
     12,EPS3,EPS4,EPS5,EPS6,EPI1,EPI2,EPI3,EPI4,EPI5,EPI6,EPI7,VP,AR,LEN
     1GTH,APR,BPR,BIGAPR,BIGBPR,ESTAR,ALPHA,BETA,RHOSTR,EPRS,RHOS
      COMMON XMESH(20,20,6),XMESH2(20,20,6),Z(20),R(20),SURF(15,8),SURF2
     1(15,8),TAB(15,14,2),TAB2(15,14,2),SPART(15,2,2),RARF(15,11),RARF2(
     115,4),RPART(15,2)
C
C
      COMMON ZO,RO,PO,UO,VO,LO,MO,RHOO,EO,AO,UBARO,VBARO
C
      COMMON NP,NT,NR,NI,NDEL,ISUB
C
      COMMON ZMIN,ZMAX,RMIN,RMAX,RADIUS,GZ,GR,DELTA,H
      COMMON DIRCOS
      COMMON TIME
      COMMON IRARF
      COMMON KSTOP
      COMMON TPSI
      COMMON KKK
```

```
C
C
      REAL LO,MO,LENGTH,MU,KO
      INTEGER CHECK,CHECK2
      IF (KM.EQ.0) GO TO 708
      RHOO=RHOSTR
      TMP1=(APR+BPR)*RHOSTR-PO2/ESTAR
      TMP2=SQRT(TMP1**2+4.*PO2*APR*RHOSTR/ESTAR)
      EO=(-TMP1+TMP2)/(2.*APR*RHOSTR/ESTAR)
      IF (PO2.GT.EPS) GO TO 708
      PO2=0.
      EO2=0.
      RHOO2=RHOSTR
      AO2=SQRT(BIGAPR/RHOSTR)
      KRTT=1
      GO TO 870
708   KRTT=0
      ETA=RHOO/RHOSTR
      MU=ETA-1.
      EE=EO/(ESTAR*ETA**2)+1.
      IF (RHOO.GT.RHOSTR) GO TO 720
      IF (EO.LT.EPRS) GO TO 720
715   C1=RHOSTR/RHOO-1.
      BEC1=BETA*C1
      IF (BEC1.LT.10.E10) GO TO 716
      C2=0.0
      GO TO 717
716   C2=EXP(-BEC1)
717   C3AL=ALPHA*C1**2
      IF (C3AL.LT.10.E12) GO TO 718
      C3=0.0
      GO TO 719
718   C3=EXP(-C3AL)
719   CONTINUE
      T1=(BPR*EO*RHOO)/EE+BIGAPR*MU*C2
      T2=2.*ALPHA*C1*(RHOSTR/(RHOO**2))
```

```
      T3=BPR*EO/EE
      T4=(2.*EO)/(ESTAR*ETA**2*EE)
      T4=T3*T4
      T5=(BIGAPR*C2)/RHOSTR
      T6=(BIGAPR*MU*BETA*RHOSTR*C2)/(RHOO**2)
      T7=(BPR*RHOO)/EE
      PGRHO=APR*EO+C3*(T1*T2+T3+T4+T5+T6)
      PGE=APR*RHOO+C3*(T7-T7*(EO/(ESTAR*ETA**2*EE)))
      BIGG=PO2-APR*EO*RHOO-T1*C3
      CHECK=0
      GO TO 725
720   T1=APR+BPR/EE
      T2=(BPR*EO)/(ESTAR*ETA**2*EE**2)
      BIGG=PO2-T1*EO*RHOO-BIGAPR*MU-BIGBPR*MU**2
      PGRHO=T1*EO+BIGAPR/RHOSTR+2.*BIGBPR*MU/RHOSTR+T2*2.*EO
      PGRHO=-PGRHO
      PGE=T1*RHOO-RHOO*T2
      PGE=-PGE
      CHECK=1
725   CONTINUE
870   CONTINUE
      RETURN
      DEBUG SUBCHK
      END
      SUBROUTINE SOUT2
C
C         PRINTS 6 LINES OF DISCONTINUITY AT TO
C
       COMMON CASEID(14),ITS1,ITS2,ITS3,ITS4,ITI1,ITI2,ITI3,ITI4,EPS1,EPS
     12,EPS3,EPS4,EPS5,EPS6,EPI1,EPI2,EPI3,EPI4,EPI5,EPI6,EPI7,VP,AR,LEN
     1GTH,APR,BPR,BIGAPR,BIGBPR,ESTAR,ALPHA,BETA,RHOSTR,EPRS,RHOS
       COMMON XMESH(20,20,6),XMESH2(20,20,6),Z(20),R(20),SURF(15,8),SURF2
     1(15,8),TAB(15,14,2),TAB2(15,14,2),SPART(15,2,2),RARF(15,11),RARF2(
     115,4),RPART(15,2)
C
C
```

```
      COMMON ZO,RO,PO,UO,VO,LO,MO,RHOO,EO,AO,UBARO,VBARO
C
      COMMON NP,NT,NR,NI,NDEL,ISUB
C
      COMMON ZMIN,ZMAX,RMIN,RMAX,RADIUS,GZ,GR,DELTA,H
      COMMON DIRCOS
      COMMON TIME
      COMMON IRARF
      COMMON KSTOP
      COMMON TPSI
      COMMON KKK
      REAL LO,MO,LENGTH,MU,KO
C
4     FORMAT (///30H CURVES OF DISCONTINUITY AT TO//40X20H--PROJECTILE S
     1HOCK--//)
6     FORMAT (//35X29H--PROJECTILE PARTICLE CURVE--//)
8     FORMAT (//42X16H--TARGET SHOCK--//)
10    FORMAT (//38X25H--TARGET PARTICLE CURVE--//)
12    FORMAT (//42X15H--RAREFACTION--//)
14    FORMAT (//35X30H--RAREFACTION PARTICLE CURVE--//)
16    FORMAT (7X1HZ19X1HR19X1HP19X1HU19X1HV/7X3HRHO17X1HE19X1HA19X1HL19X
     11HM//)
18    FORMAT (7X1HZ19X1HR//)
20    FORMAT (7X1HZ19X1HR19X1HL19X1HM//)
30    FORMAT (5E20.8/5E20.8//)
35    FORMAT (2E20.8)
38    FORMAT (4E20.8)
39    FORMAT (//35X16H--FREE SURFACE--//)
40    FORMAT (1H1)
      WRITE (3,4)
      WRITE (3,16)
      WRITE (3,30) ((TAB2(I,J,1),J=1,10),I=1,NP)
      WRITE (3,6)
      WRITE (3,18)
      WRITE (3,35) ((SPART(I,J,1),J=1,2),I=1,NP)
      WRITE (3,8)
```

```
      WRITE (3,16)
      WRITE (3,30) ((TAB2(I,J,2),J=1,10),I=1,NT)
      WRITE (3,10)
      WRITE (3,18)
      WRITE (3,35) ((SPART(I,J,2),J=1,2),I=1,NT)
      WRITE (3,12)
      WRITE (3,20)
      WRITE (3,38) ((RARF2(I,J),J=1,4),I=1,NR)
      WRITE (3,14)
      WRITE (3,39)
      WRITE (3,35) ((SURF2(I,J),J=1,2),I=1,NP)
      WRITE (3,40)
      RETURN
      DEBUG SUBCHK
      END
      SUBROUTINE SOUT
C
C       PRINTS 4 LINES OF DISCONTINUITY AT TO-H
C
      COMMON CASEID(14),ITS1,ITS2,ITS3,ITS4,ITI1,ITI2,ITI3,ITI4,EPS1,EPS
     12,EPS3,EPS4,EPS5,EPS6,EPI1,EPI2,EPI3,EPI4,EPI5,EPI6,EPI7,VP,AR,LEN
     1GTH,APR,BPR,BIGAPR,BIGBPR,ESTAR,ALPHA,BETA,RHOSTR,EPRS,RHOS
      COMMON XMESH(20,20,6),XMESH2(20,20,6),Z(20),R(20),SURF(15,8),SURF2
     1(15,8),TAB(15,14,2),TAB2(15,14,2),SPART(15,2,2),RARF(15,11),RARF2(
     115,4),RPART(15,2)
C
C
      COMMON ZO,RO,PO,UO,VO,LO,MO,RHOO,EO,AO,UBARO,VBARO
C
      COMMON NP,NT,NR,NI,NDEL,ISUB
C
      COMMON ZMIN,ZMAX,RMIN,RMAX,RADIUS,GZ,GR,DELTA,H
      COMMON DIRCOS
      COMMON TIME
      COMMON IRARF
      COMMON KSTOP
```

```
      COMMON TPSI
      COMMON KKK
      REAL LO,MO,LENGTH,MU,KO
C
4     FORMAT (///32H CURVES OF DISCONTINUITY AT TO-H//40X20H--PROJECTILE
     1 SHOCK--//)
6     FORMAT (//42X16H--TARGET SHOCK--//)
8     FORMAT (//42X15H--RAREFACTION--//)
10    FORMAT (7X1HZ19X1HR19X1HP19X1HU19X1HV/7X3HRHO17X1HE19X1HA19X1HL19X
     11HM//)
15    FORMAT (5E20.8/5E20.8//)
18    FORMAT (1H1)
21    FORMAT (//35X16H--FREE SURFACE--//)
25    FORMAT (2E20.8)
      WRITE (3,4)
      WRITE (3,10)
      WRITE (3,15) ((TAB(I,J,1),J=1,10),I=1,NP)
      WRITE (3,6)
      WRITE (3,10)
      WRITE (3,15) ((TAB(I,J,2),J=1,10),I=1,NT)
      WRITE (3,8)
      WRITE (3,10)
      WRITE (3,15) ((RARF(I,J),J=1,10),I=1,NR)
      WRITE (3,21)
      WRITE (3,25) ((SURF(I,J),J=1,2),I=1,NP)
      WRITE (3,18)
      RETURN
      DEBUG SUBCHK
      END
      SUBROUTINE PRINT(BL,ZTAB,RTAB,KK,PHI,NMAX,MMAX)
C     SUBROUTINE PRINT(BL,ZTAB,RTAB,KK)
      DOUBLE PRECISION XS(20),RU(20),ZU(20,20,6),UU(20),WW(20),
     1ZCOMP(20,20,6),PHI(20,20,6),CETA(20,20),DENC,POLY
C         PRINTS INTERIOR REGION
C
      COMMON CASEID(14),ITS1,ITS2,ITS3,ITS4,ITI1,ITI2,ITI3,ITI4,EPS1,EPS
```

```
     12,EPS3,EPS4,EPS5,EPS6,EPI1,EPI2,EPI3,EPI4,EPI5,EPI6,EPI7,VP,AR,LEN
     1GTH,APR,BPR,BIGAPR,BIGBPR,ESTAR,ALPHA,BETA,RHOSTR,EPRS,RHOS
      COMMON XMESH(20,20,6),XMESH2(20,20,6),Z(20),R(20),SURF(15,8),SURF2
     1(15,8),TAB(15,14,2),TAB2(15,14,2),SPART(15,2,2),RARF(15,11),RARF2(
     115,4),RPART(15,2)
C
C
      COMMON ZO,RO,PO,UO,VO,LO,MO,RHOO,EO,AO,UBARO,VBARO
C
      COMMON NP,NT,NR,NI,NDEL,ISUB
C
      COMMON ZMIN,ZMAX,RMIN,RMAX,RADIUS,GZ,GR,DELTA,H
      COMMON DIRCOS
      COMMON TIME
      COMMON IRARF
      COMMON KSTOP
      COMMON TPSI
      COMMON KKK
      REAL LO,MO,LENGTH,MU,KO
C
      DIMENSION BL(20,20,6),ZTAB(20),RTAB(20)
C
      TSSS=1.1
      M=0
      N=0
      DO 15 I=1,20
      DO 15 J=1,20
      IF (ABS(BL(I,J,1))+ABS(BL(I,J,2))+ABS(BL(I,J,3)))  20,15,20
15    CONTINUE
      WRITE (3,18)
18    FORMAT (15H1TABLES ALL = 0/1H1)
      CALL EXIT
20    I1=I
      DO 30 I=I1,20
      IF (ABS(BL(I,1,1))+ABS(BL(I,1,2))+ABS(BL(I,1,3)))  30,22,30
22    DO 25 J=1,20
```

```
      IF (ABS(BL(I,J,1))+ABS(BL(I,J,2))+ABS(BL(I,J,3)))  30,25,30
25    CONTINUE
      I2=I-1
      GO TO 35
30    CONTINUE
      I2=20
35    DO 45 J=1,20
      IF (ABS(BL(I1,J,1))+ABS(BL(I1,J,2))+ABS(BL(I1,J,3)))  45,37,45
37    DO 40 I=I1,I2
      IF (ABS(BL(I,J,1))+ABS(BL(I,J,2))+ABS(BL(I,J,3)))  45,40,45
40    CONTINUE
      J2=J-1
      GO TO 50
45    CONTINUE
      J2=20
50    J1=1
C
C         PRINT TABLE
C
      GO TO (52,56),KK
52    WRITE (3,53)
53    FORMAT (//24HOINTERIOR REGION AT TO-H///)
      GO TO 62
56    WRITE (3,57)
57    FORMAT (//22HOINTERIOR REGION AT TO///)
62    DO 70 I=I1,I2
      WRITE (3,64) ZTAB(I)
64    FORMAT (///7HOZTAB =,F10.4//7X1HR9X1HP17X1HU17X1HV17X3HRHO15X1HE17
     1X1HA//)
      M=M+1
      XS(M)=ZTAB(I)
      UU(M)=1.0
      DO 69 J=J1,J2
      WRITE (3,68) RTAB(J),(BL(I,J,K),K=1,6)
      N=N+1
      RU(N)=RTAB(J)
```

```
      WW(N)=1.0
      DO 156 IK=1,6
C     ZU(M,N)=BL(I,J,4)
C     ZZ(M,N)=BL(I,J,1)
  156 ZU(M,N,IK)=BL(I,J,IK)
68    FORMAT (F12.4,6E18.8)
69    CONTINUE
      MMAX=N
      N=0
70    CONTINUE
      NMAX=M
C     IF(TIME.LT.TSSS) GO TO 80
  333 IMAX=I2+1-I1
      JMAX=J2+1-J1
      CALL SURFIT(XS,UU,RU,WW,ZU,NMAX,MMAX,IMAX,JMAX,CETA,PHI,ZCOMP,
     1SQD,SQDC,SDC,DFC)
      WRITE(3,100)
  100 FORMAT('  *** ')
      DO 88 IK=1,6
      DO 48 I=1,IMAX
      DO 48 J=1,JMAX
      DENC=0.D0
      DO 43 IS=1,NMAX
      K=NMAX-IS+1
      POLY=PHI(K,MMAX,IK)
      IF(MMAX-1)43,43,46
   46 DO 42 IT=2,MMAX
      L=MMAX-IT+1
   42 POLY=POLY*RU(J)+PHI(K,L,IK)
   43 DENC=DENC*XS(I)+POLY
      ZCOMP(I,J,IK)=DENC
   48 CONTINUE
   88 CONTINUE
80    WRITE (3,82)
82    FORMAT (1H1)
      RETURN
```

```
      DEBUG SUBCHK
      END
      SUBROUTINE NRIT2(X,Y,XO,DX,YO,DY,EX,EY,FGOF,IT,KODE,
     1PHI,NMAX,MMAX)
C     SUBROUTINE NRIT2(X,Y,XO,DX,YO,DY,EX,EY,FGOF,IT,KODE)
C
C         NEWTON-RAPHSON METHOD FOR SOLUTION OF
C         TWO NON LINEAR EQUATIONS IN TWO UNKNOWNS
C
      COMMON CASEID(14),ITS1,ITS2,ITS3,ITS4,ITI1,ITI2,ITI3,ITI4,EPS1,EPS
     12,EPS3,EPS4,EPS5,EPS6,EPI1,EPI2,EPI3,EPI4,EPI5,EPI6,EPI7,VP,AR,LEN
     1GTH,APR,BPR,BIGAPR,BIGBPR,ESTAR,ALPHA,BETA,RHOSTR,EPRS,RHOS
      COMMON XMESH(20,20,6),XMESH2(20,20,6),Z(20),R(20),SURF(15,8),SURF2
     1(15,8),TAB(15,14,2),TAB2(15,14,2),SPART(15,2,2),RARF(15,11),RARF2(
     115,4),RPART(15,2)
C
C
      COMMON ZO,RO,PO,UO,VO,LO,MO,RHOO,EO,AO,UBARO,VBARO
C
      COMMON NP,NT,NR,NI,NDEL,ISUB
C
      COMMON ZMIN,ZMAX,RMIN,RMAX,RADIUS,GZ,GR,DELTA,H
      COMMON DIRCOS
      COMMON TIME
      COMMON IRARF
      COMMON KSTOP
      COMMON TPSI
      COMMON KKK
      REAL LO,MO,LENGTH,MU,KO
      DOUBLE PRECISION PHI(20,20,6)
C
      TSSS=1.1
      XB=XO
      YB=YO
      DXX=DX
      DYY=DY
```

```
      DELX1=0
      DELY1=0
      KODE=0
 1    CONTINUE
      DO 50 I=1,IT
      KK=0
      XX=XB+DXX
      YY=YB+DYY
C
C
      IF(TIME.LT.TSSS) GO TO 266
      CALL FGOF(XB,YY,F2,G2,PHI,NMAX,MMAX)
      CALL FGOF(XX,YB,F1,G1,PHI,NMAX,MMAX)
      CALL FGOF(XB,YB,F0,G0,PHI,NMAX,MMAX)
      GO TO 267
  266 CALL FGOF(XB,YY,F2,G2)
      CALL FGOF(XX,YB,F1,G1)
      CALL FGOF(XB,YB,F0,G0)
  267 A1=(F1-F0)/DXX
      B1=(F2-F0)/DYY
      C1=-F0
      A2=(G1-G0)/DXX
      B2=(G2-G0)/DYY
      C2=-G0
      DET=A1*B2-A2*B1
      IF (DET.EQ.0.) GO TO 920
      DELX=(B2*C1-B1*C2)/DET
      DELY=(A1*C2-A2*C1)/DET
      IF (ABS(DELX).GT..001) GO TO 8
      DELX=0.
 8    IF (ABS(DELY).GT..001) GO TO 9
      DELY=0.
 9    CONTINUE
      SDEL=ABS(DELX+DELX1)+ABS(DELY+DELY1)
      DELX1=DELX
      DELY1=DELY
```

```
C
C        TEST FOR SAME REGION
C
      DO 10 J=1,IT
      XB1=XB+DELX
      YB1=YB+DELY
      IF (YB1.LE.0.)YB1=0.
      M=COMP(XB,YB,XB1,YB1)
      IF (M.EQ.1) GO TO 15
11    CONTINUE
      KK=1
      DELX=.5*DELX
      DELY=.5*DELY
10    CONTINUE
      GO TO 930
15    IF (ABS(XB-XB1).GT.EX) GO TO 45
      IF (ABS(YB-YB1).GT.EY) GO TO 45
      IF (KK.NE.0) GO TO 45
      X=XB1
      Y=YB1
      KODE=0
      RETURN
45    CONTINUE
      IF (KODE.NE.1) GO TO 46
      IF (SDEL.GT.EPI1) GO TO 46
      DELX=.5*DELX
      DELY=.5*DELY
      GO TO 9
46    XB=XB1
      YB=YB1
      DEL=DELTA
      DO 70 N=1,NDEL
      XB2=XB+DEL
      M=COMP(XB,YB,XB2,YB)
      IF (M.NE.1) GO TO 55
      DXX=DEL
```

```
      GO TO 80
55    XB2=XB-DEL
      M=COMP(XB,YB,XB2,YB)
      IF (M.NE.1) GO TO 60
      DXX=-DEL
      GO TO 80
60    DEL=.5*DEL
70    CONTINUE
      GO TO 980
80    DEL=DELTA
      DO 100 N=1,NDEL
      YB2=YB+DEL
      M=COMP(XB,YB,XB,YB2)
      IF (M.NE.1) GO TO 85
      DYY=DEL
      GO TO 50
85    YB2=YB-DEL
      M=COMP(XB,YB,XB,YB2)
      IF (M.NE.1) GO TO 90
      DYY=-DEL
      GO TO 50
90    DEL=.5*DEL
100   CONTINUE
      GO TO 990
50    CONTINUE
      X=XB1
      Y=YB1
      IF (KODE.EQ.1) RETURN
      KODE=1
      GO TO 1
920   WRITE (3,922) I
922   FORMAT (46HODETERMINANT IS 0 IN SUBR. NRIT2 FOR ITERATION,I4)
      GO TO 950
930   KODE=2
      RETURN
950   WRITE (3,952) XO,YO,XB,YB,XB1,YB1,DELX,DELY
```

```
952   FORMAT (1X5HZO  =,E15.8,4X5HRO  =,E15.8/1X5HZB  =,E15.8,4X5HRB  =,
     1E15.8/1X5HZB1 =,E15.8,4X5HRB1 =,E15.8/1X5HDELZ=,E15.8,4X5HDELR=,E1
     15.8/1H1)
      CALL EXIT
      RETURN
980   KODE=3
      RETURN
990   KODE=4
      RETURN
      DEBUG SUBCHK
      END
      FUNCTION COMP(ZP,RP,ZP1,RP1)
C
C         DETERMINES IF 2 POINTS ARE IN THE SAME REGION
      COMMON CASEID(14),ITS1,ITS2,ITS3,ITS4,ITI1,ITI2,ITI3,ITI4,EPS1,EPS
     12,EPS3,EPS4,EPS5,EPS6,EPI1,EPI2,EPI3,EPI4,EPI5,EPI6,EPI7,VP,AR,LEN
     1GTH,APR,BPR,BIGAPR,BIGBPR,ESTAR,ALPHA,BETA,RHOSTR,EPRS,RHOS
      COMMON XMESH(20,20,6),XMESH2(20,20,6),Z(20),R(20),SURF(15,8),SURF2
     1(15,8),TAB(15,14,2),TAB2(15,14,2),SPART(15,2,2),RARF(15,11),RARF2(
     115,4),RPART(15,2)
C
      COMMON ZO,RO,PO,UO,VO,LO,MO,RHOO,EO,AO,UBARO,VBARO
C
      COMMON NP,NT,NR,NI,NDEL,ISUB
C
      COMMON ZMIN,ZMAX,RMIN,RMAX,RADIUS,GZ,GR,DELTA,H
      COMMON DIRCOS
      COMMON TIME
      COMMON IRARF
      COMMON KSTOP
      COMMON TPSI
      COMMON KKK
      REAL LO,MO,LENGTH,MU,KO
      EPS=.0000001
      IF (RP1.LT.0.) GO TO 80
      IF (ZP1.GE.0.) GO TO 4
```

```
      IF (RP1.GT.RADIUS) GO TO 80
C
C         FIND CONTROL CONSTANTS FOR ZP,RP
C
4     CONTINUE
      IF (ITS3.EQ.1) GO TO 33
      IF (IRARF.EQ.1) GO TO 13
      M=PICK(ZP,RP,3)
      IF (ZP.GT.RARF(M,1).AND.M.NE.1)M=M-1
      FF=RP-RARF(M+1,2)-(RARF(M,2)-RARF(M+1,2))*(ZP-RARF(M+1,1))/(RARF(M
     1,1)-RARF(M+1,1))
      IF (FF.LT.0.) GO TO 11
10    NN=1
      GO TO 13
11    NN=0
13    CONTINUE
      DO 22 K=1,2
      M=PICK(ZP1,RP1,K)
      IF (RP1.LT.TAB(M,2,K).AND.M.NE.1)M=M-1
5     CONTINUE
      FF=ZP1-TAB(M+1,1,K)-(TAB(M,1,K)-TAB(M+1,1,K))*(RP1-TAB(M+1,2,K))/(
     1TAB(M,2,K)-TAB(M+1,2,K))
      IF (K.EQ.2) GO TO 17
      IF (RP1.GT.RADIUS) GO TO 21
      IF (FF.LT.-EPS) GO TO 90
      GO TO 21
17    IF (FF.GT.EPS) GO TO 100
21    IF (RP.GT.RADIUS) GO TO 22
      M=PICK(ZP1,RP1,4)
      FF=ZP1-SURF(M+1,1)-(SURF(M,1)-SURF(M+1,1))*(RP1-SURF(M+1,2))/(SURF
     1(M,2)-SURF(M+1,2))
      IF (FF)  80,22,22
22    CONTINUE
      IF (IRARF.EQ.1) GO TO 33
      M=PICK(ZP1,RP1,3)
      IF (ZP1.GT.RARF(M,1).AND.M.NE.1)M=M-1
```

```
      FF=RP1-RARF(M+1,2)-(RARF(M,2)-RARF(M+1,2))*(ZP1-RARF(M+1,1))/(RARF
     1(M,1)-RARF(M+1,1))
      IF (FF.LT.O.) GO TO 31
30    NN1=1
      GO TO 32
31    NN1=0
32    IF (NN1.NE.NN) GO TO 110
33    CONTINUE
      COMP=1
      COMP=COMP+.2
      RETURN
80    COMP=2
      COMP=COMP+.2
      RETURN
90    COMP=3.
      COMP=COMP+.2
      RETURN
100   COMP=4.
      COMP=COMP+.2
      RETURN
110   COMP=5.
      COMP=COMP+.2
      RETURN
      DEBUG SUBCHK
      END
      FUNCTION PICK(ZP,RP,KODE)
C
C         DETERMINES 2 CLOSEST CONSECUTIVE POINTS ON SPECIFIED
C         LINE OF DISCONTINUITY TO A GIVEN POINT
C
      COMMON CASEID(14),ITS1,ITS2,ITS3,ITS4,ITI1,ITI2,ITI3,ITI4,EPS1,EPS
     12,EPS3,EPS4,EPS5,EPS6,EPI1,EPI2,EPI3,EPI4,EPI5,EPI6,EPI7,VP,AR,LEN
     1GTH,APR,BPR,BIGAPR,BIGBPR,ESTAR,ALPHA,BETA,RHOSTR,EPRS,RHOS
      COMMON XMESH(20,20,6),XMESH2(20,20,6),Z(20),R(20),SURF(15,8),SURF2
     1(15,8),TAB(15,14,2),TAB2(15,14,2),SPART(15,2,2),RARF(15,11),RARF2(
     115,4),RPART(15,2)
```

```
C
C
      COMMON ZO,RO,PO,UO,VO,LO,MO,RHOO,EO,AO,UBARO,VBARO
C
      COMMON NP,NT,NR,NI,NDEL,ISUB
C
      COMMON ZMIN,ZMAX,RMIN,RMAX,RADIUS,GZ,GR,DELTA,H
      COMMON DIRCOS
      COMMON TIME
      COMMON IRARF
      COMMON KSTOP
      COMMON TPSI
      COMMON KKK
      REAL LO,MO,LENGTH,MU,KO
C
      GO TO (5,10,100,300),KODE
5     NN=NP
      K=1
      GO TO 15
10    NN=NT
      K=2
15    AA=(TAB(1,1,K)-ZP)**2+(TAB(1,2,K)-RP)**2
C
C         SEARCH SHOCK TABLES
C
      DO 60 N=2,NN
      A=(TAB(N,1,K)-ZP)**2+(TAB(N,2,K)-RP)**2
      IF (A.GE.AA) GO TO 23
      AA=A
60    CONTINUE
      PICK=NN-1
      PICK=PICK+.2
      RETURN
23    PICK=N-1
      PICK=PICK+.2
      RETURN
```

```
100   AA=(RARF(1,1)-ZP)**2+(RARF(1,2)-RP)**2
C
C         SEARCH RAREFACTION TABLE
C
      DO 200 N=2,NR
      A=(RARF(N,1)-ZP)**2+(RARF(N,2)-RP)**2
      IF (A.GE.AA) GO TO 203
      AA=A
200   CONTINUE
      PICK=NR-1
      PICK=PICK+.2
      RETURN
203   PICK=N-1
      PICK=PICK+.2
      RETURN
300   AA=(SURF(1,1)-ZP)**2+(SURF(1,2)-RP)**2
C
C     SEARCH FREE SURFACE TABLE
C
      DO 400 N=2,NP
      A=(SURF(N,1)-ZP)**2+(SURF(N,2)-RP)**2
      IF (A.GE.AA) GO TO 303
      AA=A
400   CONTINUE
      PICK=NP-1
      PICK=PICK+.2
      RETURN
303   PICK=N-1
      PICK=PICK+.2
304   CONTINUE
      RETURN
      DEBUG SUBCHK
      END
      SUBROUTINE GUESS(KOD1,KOD2,ZP,RP,I2,K2,ZG,RG,DZ,DR)
C
C         DETERMINES STARTING POINT AND DELTAS
```

```
C          FOR NEWTON-RAPHSON ITERATION
C
      COMMON CASEID(14),ITS1,ITS2,ITS3,ITS4,ITI1,ITI2,ITI3,ITI4,EPS1,EPS
     12,EPS3,EPS4,EPS5,EPS6,EPI1,EPI2,EPI3,EPI4,EPI5,EPI6,EPI7,VP,AR,LEN
     1GTH,APR,BPR,BIGAPR,BIGBPR,ESTAR,ALPHA,BETA,RHOSTR,EPRS,RHOS
      COMMON XMESH(20,20,6),XMESH2(20,20,6),Z(20),R(20),SURF(15,8),SURF2
     1(15,8),TAB(15,14,2),TAB2(15,14,2),SPART(15,2,2),RARF(15,11),RARF2(
     115,4),RPART(15,2)
C
C
      COMMON ZO,RO,PO,UO,VO,LO,MO,RHOO,EO,AO,UBARO,VBARO
C
      COMMON NP,NT,NR,NI,NDEL,ISUB
C
      COMMON ZMIN,ZMAX,RMIN,RMAX,RADIUS,GZ,GR,DELTA,H
      COMMON DIRCOS
      COMMON TIME
      COMMON IRARF
      COMMON KSTOP
      COMMON TPSI
      COMMON KKK
      REAL LO,MO,LENGTH,MU,KO
C
      KS=0
      IF (KOD1.EQ.2) GO TO 10
      ZG=TAB(I2,1,K2)
      RG=TAB(I2,2,K2)
      IF (IRARF.EQ.1) GO TO 9
 2    M=1-(NR-2)*(K2-2)
      FF=RG-RARF(M+1,2)-(RARF(M,2)-RARF(M+1,2))*(ZG-RARF(M+1,1))/(RARF(M
     1,1)-RARF(M+1,1))
      IF (FF.GT.0.) GO TO 9
      ZG=(1.-.02/(RADIUS-RG))*ZG
      RG=RG+.02
      IF (RG.GT.(RADIUS-.01)) GO TO 110
      GO TO 2
```

```
9     CONTINUE
      GO TO 50
10    JJJ=NT-1
      IF (ITS3.EQ.1) GO TO 26
      DO 24 M=1,JJJ
      IF (RP.GT.TAB(M+1,2,2).OR.RP.LT.TAB(M,2,2)) GO TO 24
      GO TO 25
24    CONTINUE
25    CONTINUE
      FF=ZP-TAB(M+1,1,2)-(TAB(M,1,2)-TAB(M+1,1,2))*(RP-TAB(M+1,2,2))/(TA
     1B(M,2,2)-TAB(M+1,2,2))
      IF (FF.GT.0.) GO TO 20
26    CONTINUE
      ZG=ZP
      RG=RP
      GO TO 50
20    IK=M
      M=CROSS(TAB(IK,1,2),TAB(IK,2,2),TAB(IK+1,1,2),TAB(IK+1,2,2),0.,0.,
     1ZP,RP,ZG,RG)
      GO TO (50,920,930),M
C
C         COMPUTE DELTAS
C
50    DEL=DELTA
C
C         Z DELTA
C
      LL=0
52    DO 70 N=1,NDEL
      ZZ=ZG+DEL
      M=COMP(ZG,RG,ZZ,RG)
      IF (M.NE.1) GO TO 55
      DZ=DEL
      GO TO 80
55    ZZ=ZG-DEL
      M=COMP(ZG,RG,ZZ,RG)
```

```
      IF (M.NE.1) GO TO 60
      DZ=-DEL
      GO TO 80
60    DEL=.5*DEL
70    CONTINUE
      LL=LL+1
      IF (LL.EQ.3) GO TO 75
      RG=RG-DELTA/5.
      DEL=DELTA
      GO TO 52
75    KOD2=2
      RETURN
80    DEL=DELTA
      IF (KS.EQ.1) GO TO 120
C
C         R DELTA
C
      LL=0
82    DO 100 N=1,NDEL
      RR=RG+DEL
      M=COMP(ZG,RG,ZG,RR)
      IF (M.NE.1) GO TO 85
      DR=DEL
      IF (KS.EQ.1) GO TO 50
      GO TO 120
85    RR=RG-DEL
      M=COMP(ZG,RG,ZG,RR)
      IF (M.NE.1) GO TO 90
      DR=-DEL
      IF (KS.EQ.1) GO TO 50
      GO TO 120
90    DEL=.5*DEL
100   CONTINUE
108   CONTINUE
      LL=LL+1
      FLL=LL
```

```
      IF (LL.EQ.5) GO TO 110
C
104   ZG1=ZG+DELTA/5.*FLL*(-1.)**LL
      M=COMP(ZG,RG,ZG1,RG)
      ZG=ZG1
      IF (M.NE.1) GO TO 108
      KS=1
      GO TO 82
110   KOD2=2
      RETURN
120   KOD2=1
      RETURN
920   WRITE (3,922)
922   FORMAT (42H0ERROR FOR COINCIDENT LINES IN SUBR. GUESS)
      GO TO 950
C
930   WRITE (3,932)
932   FORMAT (40H0ERROR FOR PARALLEL LINES IN SUBR. GUESS)
C
950   WRITE (3,952) KOD1,I2,K2,ZP,RP
952   FORMAT (1X5HKOD1=,I4,4X3HI2=,I4,4X3HK2=,I4/1X3HZP=,E15.8,4X3HRP=,E
     115.8/1H1)
      XYZ=-2.
      ZYX=SQRT(XYZ)
      CALL EXIT
      RETURN
      END
      FUNCTION CROSS(X1,Y1,X2,Y2,X3,Y3,X4,Y4,X,Y)
C
C         FINDS INTERSECTION OF TWO STRAIGHT LINES
C
      EPS=.0000001
      A1=Y2-Y1
      B1=X1-X2
      C1=X1*A1+Y1*B1
      A2=Y4-Y3
```

```
      B2=X3-X4
      C2=X3*A2+Y3*B2
      DET=A1*B2-A2*B1
      D1=C1*B2-C2*B1
      D2=A1*C2-A2*C1
      IF (ABS(DET).LE.EPS) GO TO 10
      X=D1/DET
      Y=D2/DET
      CROSS=1
      CROSS=CROSS+.2
      RETURN
10    IF (ABS(D1).GT.EPS) GO TO 20
      IF (ABS(D2).LE.EPS) GO TO 30
20    CROSS=3
      CROSS=CROSS+.2
      RETURN
30    X=X1
      Y=Y1
      CROSS=2
      CROSS=CROSS+.2
316   CONTINUE
      RETURN
      DEBUG SUBCHK
      END
      FUNCTION PART(MODE,ZP,RP,ZX,RX,DELTA,NDEL)
C
C         LOCATES A POINT IN THE SAME REGION AS A GIVEN POINT
C         TO BE USED IN COMPUTING A PARTIAL
C     MODE=1,WITH RESPECT TO R
C     MODE=2,WITH RESPECT TO Z
C
      GO TO (2,4),MODE
2     DR=DELTA
      DZ=0.
      GO TO 8
4     DR=0.
```

```
      DZ=DELTA
8     DO 50 NN=1,NDEL
      RR=RP+DR
      ZZ=ZP+DZ
      M=COMP(ZP,RP,ZZ,RR)
      IF (M.EQ.1) GO TO 60
      RR=RP-DR
      ZZ=ZP-DZ
      M=COMP(ZP,RP,ZZ,RR)
      IF (M.EQ.1) GO TO 60
      DZ=DZ*.5
      DR=DR*.5
50    CONTINUE
      PART=2
      PART=PART+.2
      RETURN
60    ZX=ZZ
      RX=RR
      PART=1
      PART=PART+.2
      RETURN
      DEBUG SUBCHK
      END
      FUNCTION PICK2(ZP,RP,KODE)
C
C         DETERMINES 2 CLOSEST CONSECUTIVE POINTS ON SPECIFIED
C         LINE OF DISCONTINUITY TO A GIVEN POINT
      COMMON CASEID(14),ITS1,ITS2,ITS3,ITS4,ITI1,ITI2,ITI3,ITI4,EPS1,EPS
     12,EPS3,EPS4,EPS5,EPS6,EPI1,EPI2,EPI3,EPI4,EPI5,EPI6,EPI7,VP,AR,LEN
     1GTH,APR,BPR,BIGAPR,BIGBPR,ESTAR,ALPHA,BETA,RHOSTR,EPRS,RHOS
      COMMON XMESH(20,20,6),XMESH2(20,20,6),Z(20),R(20),SURF(15,8),SURF2
     1(15,8),TAB(15,14,2),TAB2(15,14,2),SPART(15,2,2),RARF(15,11),RARF2(
     115,4),RPART(15,2)
C
      COMMON Z0,R0,P0,U0,V0,L0,M0,RHO0,E0,A0,UBAR0,VBAR0
      COMMON NP,NT,NR,NI,NDEL,ISUB
```

```
C
      COMMON ZMIN,ZMAX,RMIN,RMAX,RADIUS,GZ,GR,DELTA,H
      COMMON DIRCOS
      COMMON TIME
      COMMON IRARF
      COMMON KSTOP
      COMMON TPSI
      COMMON KKK
      REAL LO,MO,LENGTH,MU,KO
C
      GO TO (5,10,100,205,210,300,500),KODE
5     NN=NP
      K=1
      GO TO 15
10    NN=NT
      K=2
15    AA=(TAB2(1,1,K)-ZP)**2+(TAB2(1,2,K)-RP)**2
C
C              SEARCH SHOCK TABLES
C
      DO 60 N=2,NN
      A=(TAB2(N,1,K)-ZP)**2+(TAB2(N,2,K)-RP)**2
      IF (A.GE.AA) GO TO 23
      AA=A
60    CONTINUE
      PICK2=NN-1
      PICK2=PICK2+.2
      RETURN
23    PICK2=N-1
      PICK2=PICK2+.2
      RETURN
100   AA=(RARF2(1,1)-ZP)**2+(RARF2(1,2)-RP)**2
C
C              SEARCH RAREFACTION TABLE
C
      DO 200 N=2,NR
```

```
      A=(RARF2(N,1)-ZP)**2+(RARF2(N,2)-RP)**2
      IF (A.GE.AA) GO TO 203
      AA=A
200   CONTINUE
      PICK2=NR-1
      PICK2=PICK2+.2
      RETURN
203   PICK2=N-1
      PICK2=PICK2+.2
      RETURN
205   NN=NP
      K=1
      GO TO 215
210   NN=NT
      K=2
215   AA=(SPART(1,1,K)-ZP)**2+(SPART(1,2,K)-RP)**2
C
C              SEARCH SHOCK PARTICLE TABLES
C
      DO 260 N=2,NN
      A=(SPART(N,1,K)-ZP)**2+(SPART(N,2,K)-RP)**2
      IF (A.GE.AA) GO TO 223
      AA=A
260   CONTINUE
      PICK2=NN-1
      PICK2=PICK2+.2
      RETURN
223   PICK2=N-1
      PICK2=PICK2+.2
      RETURN
300   AA=(RPART(1,1)-ZP)**2+(RPART(1,2)-RP)**2
C
C              SEARCH RAREFACTION PARTICLE TABLE
C
      DO 400 N=2,NR
      A=(RPART(N,1)-ZP)**2+(RPART(N,2)-RP)**2
```

```
      IF (A.GE.AA) GO TO 403
      AA=A
  400 CONTINUE
      PICK2=NR-1
      PICK2=PICK2+.2
      RETURN
  403 PICK2=N-1
      PICK2=PICK2+.2
      RETURN
  500 AA=(SURF2(1,1)-ZP)**2+(SURF2(1,2)-RP)**2
C
C     SEARCH FREE SURFACE TABLE
C
      DO 520 N=2,NP
      A=(SURF2(N,1)-ZP)**2+(SURF2(N,2)-RP)**2
      IF (A.GE.AA) GO TO 523
      AA=A
  520 CONTINUE
      PICK2=NP-1
      PICK2=PICK2+.2
      RETURN
  523 PICK2=N-1
      PICK2=PICK2+.2
      RETURN
      DEBUG SUBCHK
      END
      FUNCTION TEST(ZP,RP)
C
C
C         DETERMINES IF A GIVEN INTERIOR POINT IS IN
C         THE REGION TO BE CONSIDERED
C
      COMMON CASEID(14),ITS1,ITS2,ITS3,ITS4,ITI1,ITI2,ITI3,ITI4,EPS1,EPS
     12,EPS3,EPS4,EPS5,EPS6,EPI1,EPI2,EPI3,EPI4,EPI5,EPI6,EPI7,VP,AR,LEN
     1GTH,APR,BPR,BIGAPR,BIGBPR,ESTAR,ALPHA,BETA,RHOSTR,EPRS,RHOS
      COMMON XMESH(20,20,6),XMESH2(20,20,6),Z(20),R(20),SURF(15,8),SURF2
```

```
     1(15,8),TAB(15,14,2),TAB2(15,14,2),SPART(15,2,2),RARF(15,11),RARF2(
     115,4),RPART(15,2)
C
C
      COMMON ZO,RO,PO,UO,VO,LO,MO,RHOO,EO,AO,UBARO,VBARO
C
      COMMON NP,NT,NR,NI,NDEL,ISUB
C
      COMMON ZMIN,ZMAX,RMIN,RMAX,RADIUS,GZ,GR,DELTA,H
      COMMON DIRCOS
      COMMON TIME
      COMMON IRARF
      COMMON KSTOP
      COMMON TPSI
      COMMON KKK
      REAL LO,MO,LENGTH,MU,KO
C
      EPS=.0001
      IF (ITS3.EQ.1) GO TO 5
      IF (RP.GT.(RADIUS+EPS)) GO TO 5
      M=PICK2(ZP,RP,7)
      FF=ZP-SURF2(M+1,1)-(SURF2(M,1)-SURF2(M+1,1))*(RP-SURF2(M,2))/(SURF
     12(M,2)-SURF2(M+1,2))
      KICK=5
      CALL DVCHK(KQ)
      IF (KQ.EQ.1) GO TO 9980
      IF (FF)  200,5,5
5     CONTINUE
      IF (ZP.GT.-EPS) GO TO 1
      IF (RP.GT.(RADIUS+EPS)) GO TO 200
1     DO 10 K=1,2
      IF (ITS3.EQ.1) GO TO 100
      M=PICK2(ZP,RP,K)
      IF (TAB2(M,2,K).GT.RP.AND.M.NE.1)M=M-1
      FF=ZP-TAB2(M+1,1,K)-(TAB2(M,1,K)-TAB2(M+1,1,K))*(RP-TAB2(M+1,2,K))
     1/(TAB2(M,2,K)-TAB2(M+1,2,K))
```

```
      KICK=50
      CALL DVCHK(KQ)
      IF (KQ.EQ.1) GO TO 9980
      IF (K.EQ.2) GO TO 50
      IF (RP.GT.RADIUS) GO TO 10
      IF (FF)  200,10,10
50    IF (FF)  10,10,200
10    CONTINUE
      DO 20 K=1,2
      J=K+3
      M=PICK2(ZP,RP,J)
      IF (SPART(M,2,K).GT.RP.AND.M.NE.1)M=M-1
      FF=ZP-SPART(M+1,1,K)-(SPART(M,1,K)-SPART(M+1,1,K))*(RP-SPART(M+1,2
     1,K))/(SPART(M,2,K)-SPART(M+1,2,K))
      KICK=15
      CALL DVCHK(KQ)
      IF (KQ.EQ.1) GO TO 9980
      IF (K.EQ.2) GO TO 15
      IF (RP.GT.RADIUS) GO TO 20
      IF (FF.LT..001) GO TO 300
      GO TO 20
15    IF (FF.GT.-.001) GO TO 400
20    CONTINUE
      IF (IRARF.EQ.1) GO TO 100
      M=PICK2(ZP,RP,3)
      FF=RP-RARF2(M+1,2)-(RARF2(M,2)-RARF2(M+1,2))*(ZP-RARF2(M+1,1))/(RA
     1RF2(M,1)-RARF2(M+1,1))
      KICK=20
      CALL DVCHK(KQ)
      IF (KQ.EQ.1) GO TO 9980
      IF (FF.LT.0.) GO TO 100
      M=PICK2(ZP,RP,6)
      FF=RP-RPART(M+1,2)-(RPART(M,2)-RPART(M+1,2))*(ZP-RPART(M+1,1))/(RP
     1ART(M,1)-RPART(M+1,1))
      KICK=100
      CALL DVCHK(KQ)
```

```
      IF (KQ.EQ.1) GO TO 9980
      IF (FF.LT.0.) GO TO 500
100   TEST=1
      TEST=TEST+.2
      RETURN
200   TEST=2
      TEST=TEST+.2
      RETURN
300   TEST=3
      TEST=TEST+.2
      RETURN
400   TEST=4
      TEST=TEST+.2
      RETURN
500   TEST=5
      TEST=TEST+.2
      RETURN
9980  WRITE (3,9985) KICK
9985  FORMAT (32HODIVIDE CHECK NEAR STATEMENT NO.,I5,14H IN SUBR. TEST/1
     1H1)
      RETURN
      DEBUG SUBCHK
      END
      SUBROUTINE FGOF5(Z5,R5,SS,QQ,PHI,NMAX,MMAX)
C     SUBROUTINE FGOF5(Z5,R5,SS,QQ)
C
C         COMPUTES S5,Q5 FOR INTERIOR REGION
C         ITERATION FOR Z5,R5
C
      COMMON CASEID(14),ITS1,ITS2,ITS3,ITS4,ITI1,ITI2,ITI3,ITI4,EPS1,EPS
     12,EPS3,EPS4,EPS5,EPS6,EPI1,EPI2,EPI3,EPI4,EPI5,EPI6,EPI7,VP,AR,LEN
     1GTH,APR,BPR,BIGAPR,BIGBPR,ESTAR,ALPHA,BETA,RHOSTR,EPRS,RHOS
      COMMON XMESH(20,20,6),XMESH2(20,20,6),Z(20),R(20),SURF(15,8),SURF2
     1(15,8),TAB(15,14,2),TAB2(15,14,2),SPART(15,2,2),RARF(15,11),RARF2(
     115,4),RPART(15,2)
C
```

```
C
      COMMON ZO,RO,PO,UO,VO,LO,MO,RHOO,EO,AO,UBARO,VBARO
C
      COMMON NP,NT,NR,NI,NDEL,ISUB
C
      COMMON ZMIN,ZMAX,RMIN,RMAX,RADIUS,GZ,GR,DELTA,H
      COMMON DIRCOS
      COMMON TIME
      COMMON IRARF
      COMMON KSTOP
      COMMON TPSI
      COMMON KKK
      REAL LO,MO,LENGTH,MU,KO
      DOUBLE PRECISION PHI(20,20,6)
C
      DIMENSION ANS(6)
C
      TSSS=1.1
      IF(TIME.GT.TSSS) GO TO 100
      CALL DBLTRP(Z5,R5,ANS)
      GO TO 101
  100 CALL DSURFT(Z5,R5,ANS,PHI,NMAX,MMAX)
  101 U5=ANS(2)
C     U5=ANS(2)
      V5=ANS(3)
      SS=Z5-ZO+H*V5
      QQ=R5-RO+H*U5
      RETURN
      DEBUG SUBCHK
      END
      SUBROUTINE ITRP
      COMMON CASEID(14),ITS1,ITS2,ITS3,ITS4,ITI1,ITI2,ITI3,ITI4,EPS1,EPS
     12,EPS3,EPS4,EPS5,EPS6,EPI1,EPI2,EPI3,EPI4,EPI5,EPI6,EPI7,VP,AR,LEN
     1GTH,APR,BPR,BIGAPR,BIGBPR,ESTAR,ALPHA,BETA,RHOSTR,EPRS,RHOS
      COMMON XMESH(20,20,6),XMESH2(20,20,6),Z(20),R(20),SURF(15,8),SURF2
     1(15,8),TAB(15,14,2),TAB2(15,14,2),SPART(15,2,2),RARF(15,11),RARF2(
```

```
     115,4),RPART(15,2)
C
C
      COMMON ZO,RO,PO,UO,VO,LO,MO,RHOO,EO,AO,UBARO,VBARO
C
      COMMON NP,NT,NR,NI,NDEL,ISUB
C
      COMMON ZMIN,ZMAX,RMIN,RMAX,RADIUS,GZ,GR,DELTA,H
      COMMON DIRCOS
      COMMON TIME
      COMMON IRARF
      COMMON KSTOP
      COMMON TPSI
      COMMON KKK
C
C
      REAL LO,MO,LENGTH,MU,KO
C
C INTERPOLATION SCHEME FOR POINTS BETWEEN PARTICLE CURVES
C AND DISCONTINUITIES
C
      EPS=.0000001
      KOD1=0
      KOD2=0
      DO 1000 J=1,20
      DO 1000 I=1,20
      M=TEST(Z(I),R(J))
      IF (M.NE.5) GO TO 906
      IF (IRARF.EQ.1) GO TO 906
      NR1=NR-1
      DO 907 JJ=1,NR1
      IF (RARF2(JJ,1).LT.Z(I).AND.RARF2(JJ+1,1).GT.Z(I)) GO TO 908
907   CONTINUE
908   CONTINUE
      FF=R(J)-RARF2(JJ+1,2)+(RARF2(JJ,2)-RARF2(JJ+1,2))*(Z(I)-RARF2(JJ+1
     1,1))/(RARF2(JJ,1)-RARF2(JJ+1,1))
```

```
      IF (FF.LT.0.) GO TO 1000
906   CONTINUE
      IF (M.EQ.3.AND.Z(I).LT.EPS.AND.ABS(R(J)-RADIUS).LT.EPS) GO TO 1000
      IF (M.LT.3) GO TO 8051
      WRITE (3,8050)
8050  FORMAT (30H0INTERPOLATION SCHEME EMPLOYED)
614   FORMAT (1X5HZO  =,E15.8,4X5HRO  =,E15.8)
      ZO=Z(I)
      RO=R(J)
      WRITE (3,614) ZO,RO
      WRITE (3,8888) M
8888  FORMAT (1X4HM  =,I4)
8051  CONTINUE
      GO TO (1000,1000,1001,1010,1100),M
1001  IF (IRARF.EQ.1) GO TO 1003
      M=PICK2(Z(I),R(J),3)
      FF=R(J)-RARF2(M+1,2)+(RARF2(M,2)-RARF2(M+1,2))*(Z(I)-RARF2(M+1,1))
     1/(RARF2(M,1)-RARF2(M+1,1))
      IF (FF.GT.0.) GO TO 1003
      DO 8002 K=1,6
      L=K+2
8002  XMESH2(I,J,K)=RARF(1,L)
      GO TO 1000
1003  L=I+1
      N=TEST(Z(L),R(J))
      GO TO (1004,1007,1030,1030,1050),N
1004  M=PICK2(Z(I),R(J),1)
      DO 1006 K=1,8
      ANS=TAB2(M,K,1)+(TAB2(M+1,K,1)-TAB2(M,K,1))*(R(J)-TAB2(M,2,1))/(TA
     1B2(M+1,2,1)-TAB2(M,2,1))
      IF (K.NE.1) GO TO 8005
      ANS1=ANS
      GO TO 1006
8005  CONTINUE
      IF (K.EQ.2) GO TO 1006
      KX=K-2
```

```
      IF (ABS(R(J)-RADIUS).GT.EPS) GO TO 9024
      IF (K.GT.5.OR.K.LT.4) GO TO 9024
      ANS=TAB2(M+1,K,1)
 9024 CONTINUE
      XMESH2(I,J,KX)=ANS+(XMESH2(L,J,KX)-ANS)*(Z(I)-ANS1)/(Z(L)-ANS1)
      IF (ABS(R(J)-RADIUS).GT.EPS) GO TO 1006
      XMESH2(I,J,1)=0.
      XMESH2(I,J,4)=RHOSTR
      XMESH2(I,J,5)=0.
      XMESH2(I,J,6)=SQRT(BIGAPR/RHOSTR)
 1006 CONTINUE
      GO TO 1000
 1007 MM=PICK2(Z(I),R(J),2)
      M=PICK2(Z(I),R(J),1)
      DO 1009 K=1,8
      ANS=TAB2(M,K,1)+(TAB2(M+1,K,1)-TAB2(M,K,1))*(R(J)-TAB2(M,2,1))/(TA
     1B2(M+1,2,1)-TAB2(M,2,1))
      ANSW=TAB2(MM,K,2)+(TAB2(MM+1,K,2)-TAB2(MM,K,2))*(R(J)-TAB2(MM,2,2)
     1)/(TAB2(MM+1,2,2)-TAB2(MM,2,1))
      IF (K.NE.1) GO TO 1008
      ANS1=ANS
      ANS2=ANSW
      GO TO 1009
 1008 CONTINUE
      IF (K.EQ.2) GO TO 1009
      KX=K-2
      XMESH2(I,J,KX)=ANS+(ANSW-ANS)*(Z(I)-ANS1)/(ANS2-ANS1)
 1009 CONTINUE
      GO TO 1000
 1010 IF (IRARF.EQ.1) GO TO 1013
      M=PICK2(Z(I),R(J),3)
      FF=R(J)-RARF2(M+1,2)+(RARF2(M,2)-RARF2(M+1,2))*(Z(I)-RARF2(M+1,1))
     1/(RARF2(M,1)-RARF2(M+1,1))
      IF (FF.GT.0.) GO TO 1013
      DO 1012 K=1,6
      L=K+2
```

```
1012  XMESH2(I,J,K)=RARF(1,L)
      GO TO 1000
1013  L=I-1
      IF (ABS(Z(I)).LT.EPS) GO TO 1017
      N=TEST(Z(L),R(J))
      GO TO (1014,1017,1030,1017,1051),N
1014  M=PICK2(Z(I),R(J),2)
      DO 1016 K=1,8
      ANS=TAB2(M,K,2)+(TAB2(M+1,K,2)-TAB2(M,K,2))*(R(J)-TAB2(M,2,2))/(TA
     1B2(M+1,2,2)-TAB2(M,2,2))
      IF (K.NE.1) GO TO 1015
      ANS1=ANS
      GO TO 1016
1015  CONTINUE
      IF (K.EQ.2) GO TO 1016
      KX=K-2
      XMESH2(I,J,KX)=ANS+(XMESH2(L,J,KX)-ANS)*(Z(I)-ANS1)/(Z(L)-ANS1)
1016  CONTINUE
      GO TO 1000
1017  L=J-1
      N=TEST(Z(I),R(L))
      GO TO (1024,1030,1030,1030,1051),N
1024  M=PICK2(Z(I),R(J),2)
      DO 1026 K=2,8
      ANS=TAB2(M,K,2)+(TAB2(M+1,K,2)-TAB2(M,K,2))*(Z(I)-TAB2(M,1,2))/(TA
     1B2(M+1,1,2)-TAB2(M,1,2))
      IF (K.NE.2) GO TO 1025
      ANS1=ANS
      GO TO 1026
1025  CONTINUE
      KX=K-2
      IF (ABS(Z(I)).GT.EPS) GO TO 9125
      IF (K.GT.5.OR.K.LT.4) GO TO 9125
      ANS=TAB2(M+1,K,2)
9125  CONTINUE
      XMESH2(I,J,KX)=ANS+(XMESH2(I,L,KX)-ANS)*(R(J)-ANS1)/(R(L)-ANS1)
```

```
      IF (ABS(Z(I)).GT.EPS) GO TO 1026
      XMESH2(I,J,1)=0.
      XMESH2(I,J,4)=RHOSTR
      XMESH2(I,J,5)=0.
      XMESH2(I,J,6)=SQRT(BIGAPR/RHOSTR)
 1026 CONTINUE
      GO TO 1000
 1100 M=PICK2(Z(I),R(J),3)
      ANS1=RARF2(M+1,2)+(RARF2(M,2)-RARF2(M+1,2))*(Z(I)-RARF2(M+1,1))/(R
     1ARF2(M,1)-RARF2(M+1,1))
      L=J+1
      M=TEST(Z(I),R(L))
      GO TO (1101,1030,1051,1030),M
 1101 CONTINUE
      DO 1106 K=1,6
      LL=K+2
      XMESH2(I,J,K)=RARF(1,LL)+(XMESH2(I,L,K)-RARF(1,LL))*(R(J)-ANS1)/(R
     1(L)-ANS1)
 1106 CONTINUE
      GO TO 1000
 1050 JJ1=J
      II1=I
      KOD1=1
      GO TO 1000
 1051 JJ2=J
      II2=I
      KOD2=1
 1000 CONTINUE
      IF (KOD1.EQ.0) GO TO 2000
      M=PICK2(Z(II1),R(JJ1),1)
      DO 2016 K=1,8
      ANS=TAB2(M,K,1)+(TAB2(M+1,K,1)-TAB2(M,K,1))*(R(JJ1)-TAB2(M,2,1))/(
     1TAB2(M+1,2,1)-TAB2(M,2,1))
      IF (K.NE.1) GO TO 2005
      ANS1=ANS
      GO TO 2016
```

```
 2005 CONTINUE
      I=II1
      J=JJ1
      L=II1+1
      IF (K.EQ.2) GO TO 2016
      KX=K-2
      XMESH2(I,J,KX)=ANS+(XMESH2(L,J,KX)-ANS)*(Z(I)-ANS1)/(Z(L)-ANS1)
 2016 CONTINUE
 2000 IF (KOD2.EQ.0) GO TO 3000
      M=PICK2(Z(II2),R(JJ2),2)
      DO 3016 K=1,8
      ANS=TAB2(M,K,2)+(TAB2(M+1,K,2)-TAB2(M,K,2))*(R(JJ2)-TAB2(M,2,2))/(
     1TAB2(M+1,2,2)-TAB2(M,2,2))
      IF (K.NE.1) GO TO 3015
      ANS1=ANS
      GO TO 3016
 3015 CONTINUE
      I=II2
      J=JJ2
      L=II2-1
      IF (K.EQ.2) GO TO 3016
      KX=K-2
      XMESH2(I,J,KX)=ANS+(XMESH2(L,J,KX)-ANS)*(Z(I)-ANS1)/(Z(L)-ANS1)
 3016 CONTINUE
 3000 CONTINUE
      GO TO 3017
 1030 WRITE (3,1040) I,J
 1040 FORMAT (27H0 TIME STEP TOO LARGE AT I=,I4,2HJ=,I4,///)
      CALL EXIT
 3017 CONTINUE
C
C
      RETURN
      DEBUG SUBCHK
      END
      SUBROUTINE EXIT
```

```
C
      COMMON CASEID(14),ITS1,ITS2,ITS3,ITS4,ITI1,ITI2,ITI3,ITI4,EPS1,EPS
     12,EPS3,EPS4,EPS5,EPS6,EPI1,EPI2,EPI3,EPI4,EPI5,EPI6,EPI7,VP,AR,LEN
     1GTH,APR,BPR,BIGAPR,BIGBPR,ESTAR,ALPHA,BETA,RHOSTR,EPRS,RHOS
      COMMON XMESH(20,20,6),XMESH2(20,20,6),Z(20),R(20),SURF(15,8),SURF2
     1(15,8),TAB(15,14,2),TAB2(15,14,2),SPART(15,2,2),RARF(15,11),RARF2(
     115,4),RPART(15,2)
C
C
      COMMON ZO,RO,PO,UO,VO,LO,MO,RHOO,EO,AO,UBARO,VBARO
C
      COMMON NP,NT,NR,NI,NDEL,ISUB
C
      COMMON ZMIN,ZMAX,RMIN,RMAX,RADIUS,GZ,GR,DELTA,H
      COMMON DIRCOS
      COMMON TIME
      COMMON IRARF
      COMMON KSTOP
      COMMON TPSI
      COMMON KKK
      REAL LO,MO,LENGTH,MU,KO
      KSTOP=1
      STOP
      END
      SUBROUTINE FGOFI(ZX,RX,SS,QQ,PHI,NMAX,MMAX)
C     SUBROUTINE FGOFI(ZX,RX,SS,QQ)
C
C         COMPUTES SI,QI FOR INTERIOR REGION
C         ITERATION FOR ZI,RI
C
      COMMON CASEID(14),ITS1,ITS2,ITS3,ITS4,ITI1,ITI2,ITI3,ITI4,EPS1,EPS
     12,EPS3,EPS4,EPS5,EPS6,EPI1,EPI2,EPI3,EPI4,EPI5,EPI6,EPI7,VP,AR,LEN
     1GTH,APR,BPR,BIGAPR,BIGBPR,ESTAR,ALPHA,BETA,RHOSTR,EPRS,RHOS
      COMMON XMESH(20,20,6),XMESH2(20,20,6),Z(20),R(20),SURF(15,8),SURF2
     1(15,8),TAB(15,14,2),TAB2(15,14,2),SPART(15,2,2),RARF(15,11),RARF2(
     115,4),RPART(15,2)
```

```
C
C
      COMMON ZO,RO,PO,UO,VO,LO,MO,RHOO,EO,AO,UBARO,VBARO
C
      COMMON NP,NT,NR,NI,NDEL,ISUB
C
      COMMON ZMIN,ZMAX,RMIN,RMAX,RADIUS,GZ,GR,DELTA,H
      COMMON DIRCOS
      COMMON TIME
      COMMON IRARF
      COMMON KSTOP
      COMMON TPSI
      COMMON KKK
      REAL LO,MO,LENGTH,MU,KO
C
      DIMENSION ANS(6),PSI(4),SPSI(11),CPSI(11)
      DOUBLE PRECISION PHI(20,20,6)
C
C
C
C
C
      TSSS=1.1
      IF(TIME.GT.TSSS) GO TO 100
      CALL DBLTRP(ZX,RX,ANS)
      GO TO 101
  100 CALL DSURFT(ZX,RX,ANS,PHI,NMAX,MMAX)
  101 UI=ANS(2)
C     UI=ANS(2)
      VI=ANS(3)
      AI=ANS(6)
      SS=ZX-ZO+H*(VI+AI*SIN(TPSI))
      QQ=RX-RO+H*(UI+AI*COS(TPSI))
      RETURN
```

II.2. Method of Characteristics Calculations and the Computer Code for Materials with Arbitrary Equations of State.

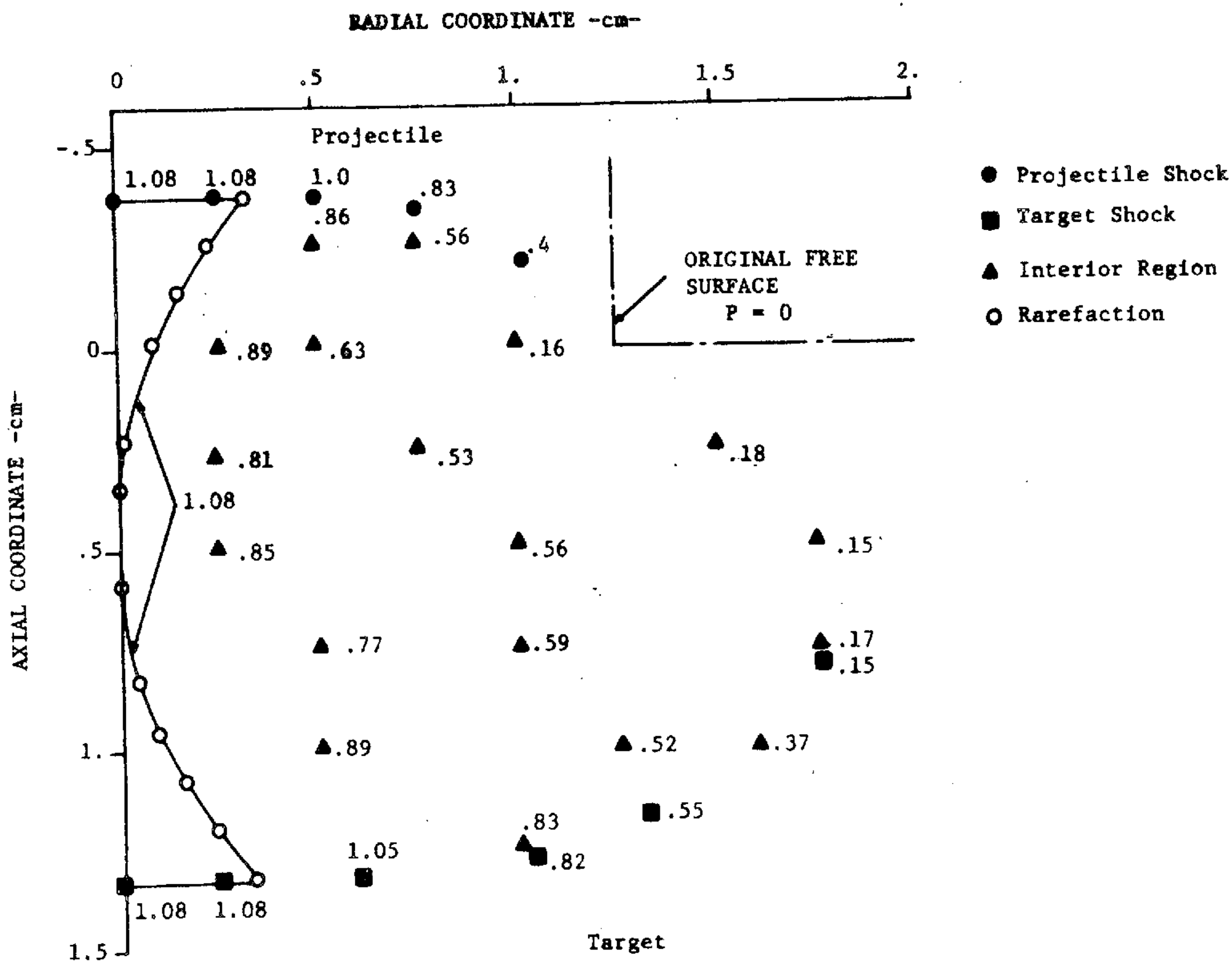

Fig. 1. Pressure distribution from the characteristic solution at t = 1.25 μsec after impact of a 2.5 -cm- diameter projectile at 0.76 cm/μsec on an aluminum half-space.

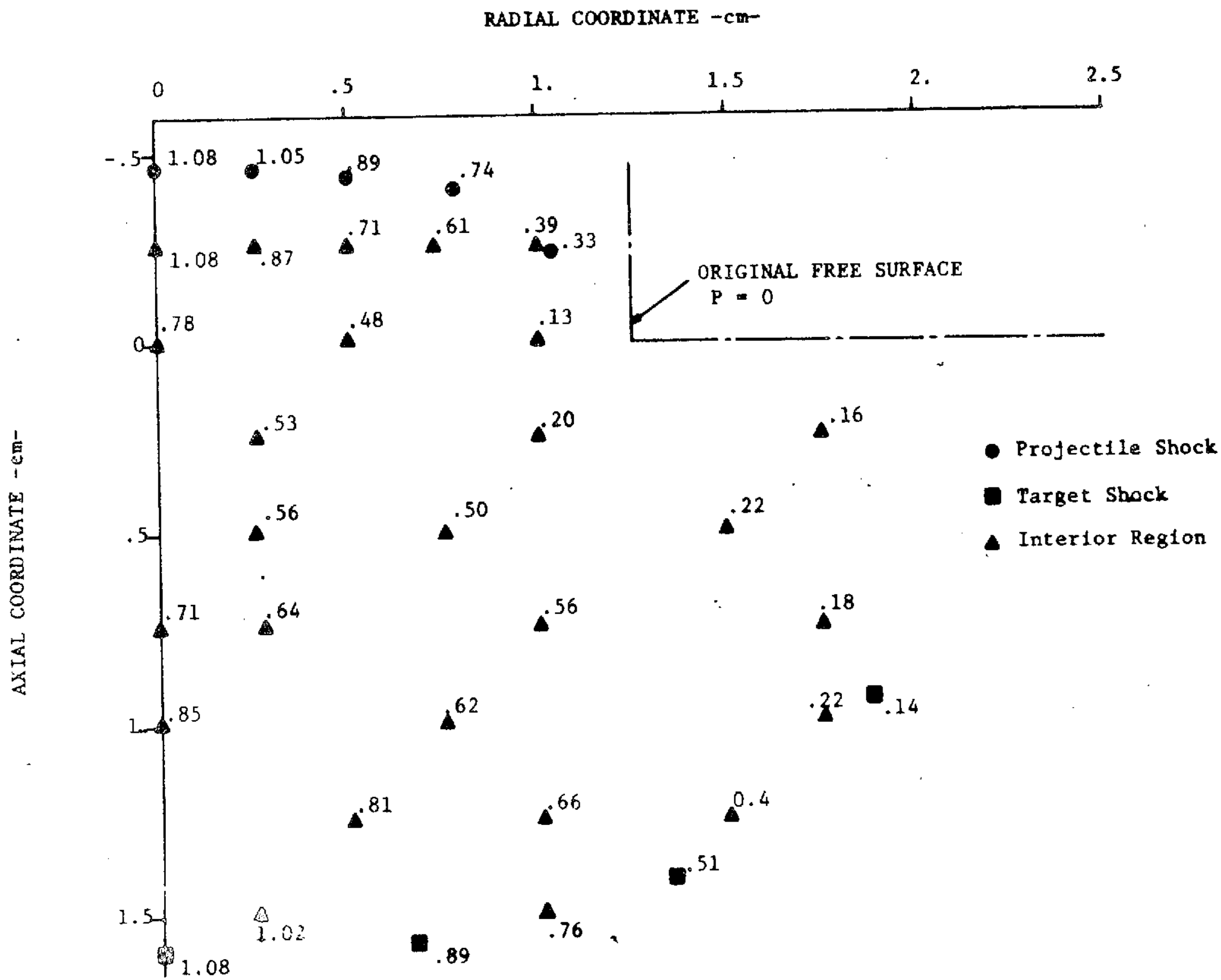

Fig. 2. Pressure distribtuion from the characteristic solution at t = 1.52 μsec after impact of a 2.5 -cm- diameter projectile at 0.76 cm/μsec on an aluminum half-space.

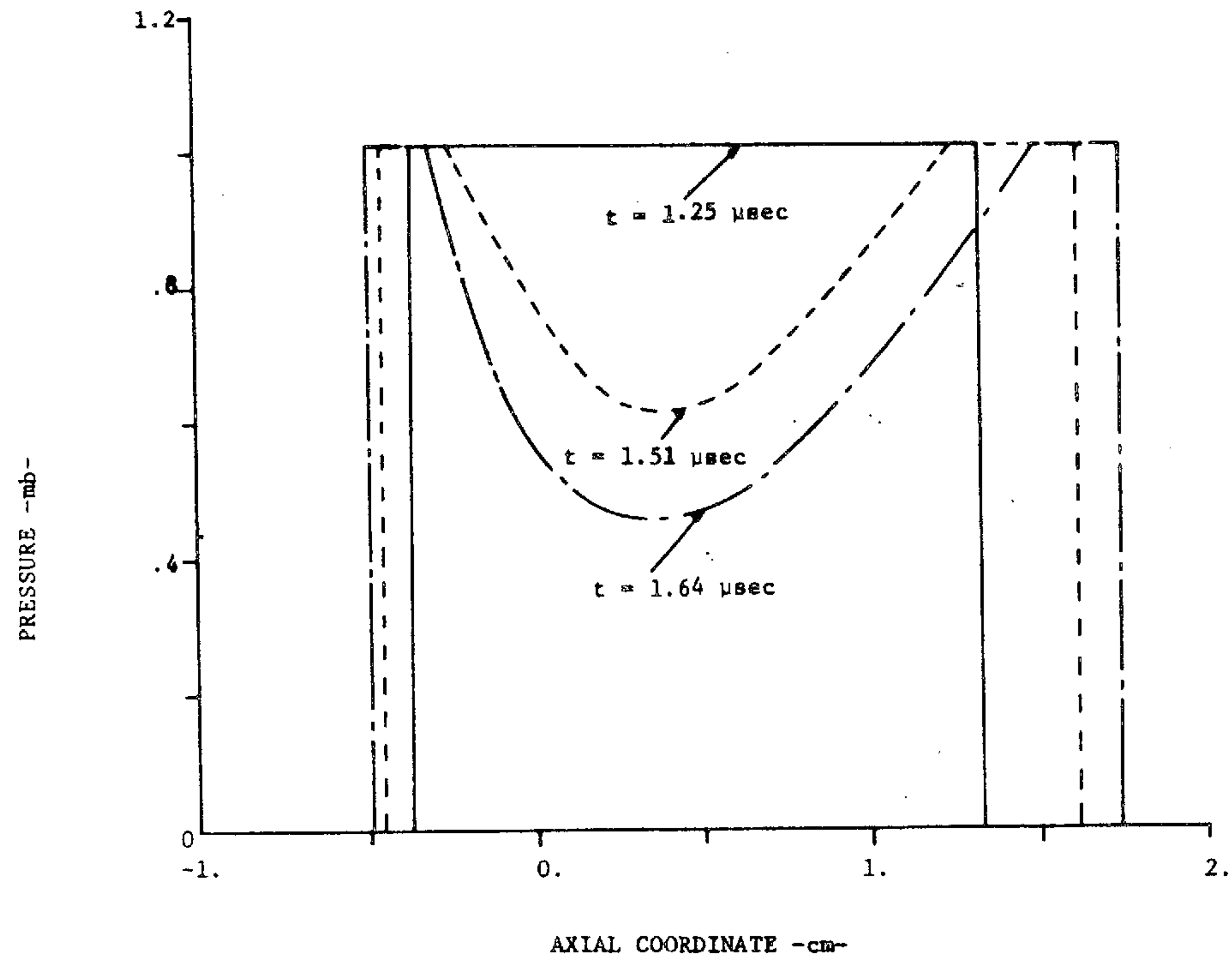

Fig 3. Axial pressure profiles at various times as predicted by the charactersitc method for a 2.5 -cm- diameter aluminum projectile impacting on aluminum half-space at 0.76 cm/μsec.

```
      COMMON CASEID(14),ITS1,ITS2,ITS3,ITS4,ITI1,ITI2,ITI3,ITI4,EPS1,EPS
     12,EPS3,EPS4,EPS5,EPS6,EPI1,EPI2,EPI3,EPI4,EPI5,EPI6,EPI7,VP,AR,LEN
     1GTH,APR,BPR,BIGAPR,BIGBPR,ESTAR,ALPHA,BETA,RHOSTR,EPRS,RHOS
      COMMON XMESH(20,20,6),XMESH2(20,20,6),Z(20),R(20),SURF(15,8),SURF2
     1(15,8),TAB(15,14,2),TAB2(15,14,2),SPART(15,2,2),RARF(15,11),RARF2(
     115,4),RPART(15,2)
C
C
      COMMON ZO,RO,PO,UO,VO,LO,MO,RHOO,EO,AO,UBARO,VBARO
C
      COMMON NP,NT,NR,NI,NDEL,ISUB
C
      COMMON ZMIN,ZMAX,RMIN,RMAX,RADIUS,GZ,GR,DELTA,H
      COMMON DIRCOS
      COMMON TIME
      COMMON IRARF
      COMMON KSTOP
      COMMON TPSI
      COMMON KKK
C
C
      REAL LO,MO,LENGTH,MU,KO
      KR=10
      EPS=.0000001
      KSTOP=0
1     FORMAT (1H1)
      CALL DVCHK(KEY)
      KICK=0
      IF (KEY.EQ.1) GO TO 9980
C
      DO 2 K=1,6
      DO 2 J=1,20
      DO 2 I=1,20
      XMESH(I,J,K)=0.
      XMESH2(I,J,K)=0.
2     CONTINUE
```

```
C     KRW=0
      NUZON=0
C
C
      WRITE (3,4)
C
C          DATA INPUT SECTION
C
4     FORMAT (52H1HYPERVELOCITY IMPACT METHOD OF CHARACTERISTICS CODE///
     1)
C       IO AND FX. PT. CONSTANTS
C
      READ (1,8) CASEID,ITS1,ITS2,ITS3,ITS4,ITI1,ITI2,ITI3,ITI4,NDEL
8     FORMAT (13A6,A2/9I3)
      IRARF=ITI2
C
C       FL. PT. CONSTANTS
C
      READ (1,15) EPS1,EPS2,EPS3,EPS4,EPS5,EPS6,EPI1,EPI2,EPI3,EPI4,EPI5
     1,EPI6,EPI7
      READ (1,14) NP,NT,NR
14    FORMAT (3I3)
      READ (1,15) APR,BPR,BIGAPR,BIGBPR,ESTAR,ALPHA,BETA,RHOSTR,EPRS,REF
     1L
      READ (1,15) ZMIN,ZMAX,RMIN,RMAX,GR,GZ,DELTA,VP,LENGTH,RADIUS,HSTAR
15    FORMAT (6E12.8)
      READ (1,15) RST
      IF (RST.GT.0.) GO TO 16
      REWIND 9
C     DO 1529 JTP=1,200
      READ (9)TIME
C     IF(ABS(RST+TIME).LT..001) GO TO 1530
C     READ(9)BLOB
C1529 CONTINUE
1530  CONTINUE
C     KRW=1
```

```
      READ (9)(((XMESH(I,J,K),I=1,20),J=1,20),K=1,6),(Z(I),I=1,20),(R(I)
     1,I=1,20),((SURF(I,J),I=1,15),J=1,8),(((TAB(I,J,K),I=1,15),J=1,14),
     1K=1,2),((RARF(I,J),I=1,15),J=1,11),TIME,ZMIN,ZMAX,RMIN,RMAX,GR,GZ,
     1AR
      DO 1500 J=1,20
      DO 1500 I=1,20
      DO 1500 K=1,6
1500  XMESH2(I,J,K)=XMESH(I,J,K)
      DO 1501 I=1,15
      DO 1501 J=1,8
1501  SURF2(I,J)=SURF(I,J)
      WRITE (3,145) TIME
      CALL SOUT
      CALL PRINT(XMESH2,Z,R,1)
      KREFL=0
16    CONTINUE
      WRITE (3,10) CASEID,ITS1,ITS2,ITS3,ITS4,ITI1,ITI2,ITI3,ITI4,NDEL
10    FORMAT (1X13A6,A2//17H SHOCK ITERATIONS6X,4I4//20H INTERIOR ITERAT
     1IONS3X,4I4//7H NDEL =,I4///)
      WRITE (3,18) EPS1,EPS2,EPS3,EPS4,EPS5,EPS6,EPI1,EPI2,EPI3,EPI4,EPI
     15,EPI6,EPI7,ZMIN,ZMAX,RMIN,RMAX,DELTA,VP,LENGTH,RADIUS,APR,BPR,BIG
     1APR,BIGBPR,ESTAR,ALPHA,BETA,RHOSTR,EPRS,REFL
18    FORMAT (///38H ERROR CRITERIA FOR SHOCK COMPUTATIONS//5X8HDELTA Z1
     18X8HDELTA R18X9HDELTA RHO7X7HDELTA E9X7HDELTA P9X7HDELTA U/6E16.6/
     1//41H ERROR CRITERIA FOR INTERIOR COMPUTATIONS//5X8HDELTA Z18X8HDE
     1LTA R18X7HDELTA P9X7HDELTA U9X7HDELTA V9X9HDELTA RHO7X7HDELTA E/7E
     116.6///5X4HZMIN12X4HZMAX12X4HRMIN12X4HRMAX12X5HDELTA11X2HVP14X6HLE
     1NGTH10X6HRADIUS/8E16.6///5X2HA'14X2HB'14X6HBIG A'10X6HBIG B'10X2HE
     1*14X5HALPHA11X4HBETA12X4HRHO*/8E16.6//5X3HE'S13X4HREFL/2E16.6///)
      IF (RST.LT.0.) GO TO 140
C
C           STORE RHO* IN ALL XMESH
C
      DO 22 J=1,20
      DO 22 I=1,20
22    XMESH(I,J,4)=RHOSTR
```

```
40    FORMAT (5E12.8)                                                  MAIN 109
C                                                                      MAIN 110
C       PROJECTILE SHOCK                                               MAIN 111
C                                                                      MAIN 112
      CALL EQOS1(PRHO,PPP,PVV,PEE,TEE,TRHO,KICK)                       MAIN 113
      IF (KICK.EQ.2200) GO TO 9980                                     MAIN 114
      DO 230 N=1,NP                                                    MAIN 115
      TAB(N,1,1)=(PRHO*PVV-RHOSTR*VP)*HSTAR/(PRHO-RHOSTR)              MAIN 116
      EE=N-1                                                           MAIN 117
      FNP=NP                                                           MAIN 118
      TAB(N,2,1)=RMIN+EE*(RADIUS-RMIN)/FNP                             MAIN 119
      TAB(N,3,1)=PPP                                                   MAIN 120
      TAB(N,4,1)=0.0                                                   MAIN 121
      TAB(N,5,1)=PVV                                                   MAIN 122
      TAB(N,6,1)=PRHO                                                  MAIN 123
      TAB(N,7,1)=PEE                                                   MAIN 124
      TAB(N,9,1)=0.0                                                   MAIN 125
      TAB(N,10,1)=1.0                                                  MAIN 126
230   CONTINUE                                                         MAIN 127
C                                                                      MAIN 128
C       TARGET SHOCK                                                   MAIN 129
C                                                                      MAIN 130
      M=0                                                              MAIN 131
      DO 240 N=1,NT                                                    MAIN 132
      EE=N-1                                                           MAIN 133
      FNT=NT-4                                                         MAIN 134
      TAB(N,2,2)=RMIN+EE*(RADIUS-RMIN)/FNT                             MAIN 135
      TAB(N,7,2)=TEE                                                   MAIN 136
      TAB(N,6,2)=TRHO                                                  MAIN 137
      TAB(N,3,2)=PPP                                                   MAIN 138
      IF (TAB(N,2,2).GT.RADIUS) GO TO 250                              MAIN 139
      TAB(N,1,2)=TRHO*PVV*HSTAR/(TRHO-RHOSTR)                          MAIN 140
      TAB(N,4,2)=0.0                                                   MAIN 141
      TAB(N,5,2)=PVV                                                   MAIN 142
      TAB(N,9,2)=0.0                                                   MAIN 143
      TAB(N,10,2)=1.0                                                  MAIN 144
```

```
      GO TO 240
250   EF=M
      TAB(N,9,2)=SIN(.5236+EF*.2618)
      TAB(N,10,2)=COS(.5236+EF*.2618)
      TAB(N,4,2)=PVV*TAB(N,9,2)
      TAB(N,5,2)=PVV*TAB(N,10,2)
      TAB(N,1,2)=TAB(1,1,2)*TAB(N,10,2)
      TAB(N,2,2)=RADIUS+TAB(1,1,2)*TAB(N,9,2)
      M=M+1
240   CONTINUE
C
C       RAREFACTION
C
      CALL EQOS2(PPP,PRHO,PEE)
      EE=NR-1
      ADEL=(TAB(1,1,2)-TAB(1,1,1))/EE
      RARF(1,1)=TAB(1,1,2)
      DO 205 N=2,NR
      RARF(N,1)=RARF(N-1,1)-ADEL
205   CONTINUE
      DO 210 N=1,NR
      RARF(N,10)=(RARF(N,1)/HSTAR-.5*VP)/AR
      RARF(N,9)=-SQRT(1.-RARF(N,10)**2)
      RARF(N,2)=RADIUS+HSTAR*AR*RARF(N,9)
210   CONTINUE
      DO 220 N=1,NR
      RARF(N,3)=TAB(1,3,1)
      RARF(N,4)=0.
      RARF(N,5)=TAB(1,5,1)
      RARF(N,6)=TAB(1,6,1)
      RARF(N,7)=TAB(1,7,1)
220   CONTINUE
C       REGION INTERIOR TO SHOCKS
      I=-ZMIN/GZ+1.2
      J=0
260   J=J+1
```

```
      XMESH(I,J,1)=PPP
      XMESH(I,J,3)=PVV
      XMESH(I,J,4)=PRHO
      XMESH(I,J,5)=PEE
      EE=(J-1)
      IF ((EE*GR-RADIUS).LT.-EPS) GO TO 260
      XMESH(I,J,1)=0.
      XMESH(I,J,4)=RHOSTR
      XMESH(I,J,5)=0.
C
C       FREE SURFACE
C
      DO 50 I=1,NP
      SURF(I,1)=-LENGTH+VP*HSTAR
      SURF(I,2)=TAB(I,2,1)
      SURF(I,3)=0.
      SURF(I,4)=0.
      SURF(I,5)=VP
      SURF(I,6)=RHOSTR
      SURF(I,7)=0.
      SURF(I,8)=SQRT(BIGAPR/RHOSTR)
50    CONTINUE
      DO 51 I=1,NP
      DO 51 J=1,8
51    SURF2(I,J)=SURF(I,J)
      IF (NUZON.EQ.0) GO TO 5001
5000  GR=GR*2.
      GZ=GZ*2.
      ZMAX=ZMAX*2.-ZMIN
      RMAX=RMAX*2.
      NUZON=1
      WRITE (3,5003)
5003  FORMAT (7H REZONE///)
5001  CONTINUF
C
C
```

```
      DO 55 I=1,20
      EE=I-1
      Z(I)=ZMIN+EE*GZ
      R(I)=RMIN+EE*GR
55    CONTINUE
      IF (NUZON.EQ.0) GO TO 5101
      DO 5100 I=1,10
      DO 5100 J=1,10
      DO 5100 K=1,6
      L=2*I-1
      M=2*J-1
      XMESH(I,J,K)=XMESH(L,M,K)
5100  CONTINUE
      GO TO 157
5101  CONTINUE
C
C          COMPUTE A FOR 2 SHOCKS AND MESH
C
      DO 86 K=1,3
      GO TO (57,59,61),K
57    NN=NP
      JJ=1
      GO TO 63
59    NN=NT
      JJ=1
      GO TO 63
61    NN=20
      JJ=20
63    DO 84 N=1,NN
      DO 82 J=1,JJ
      GO TO (65,65,68),K
65    P=TAB(N,3,K)
      RHO=TAB(N,6,K)
      E=TAB(N,7,K)
      GO TO 70
68    P=XMESH(J,N,1)
```

```
      RHO=XMESH(J,N,4)
      E=XMESH(J,N,5)
70    CONTINUE
      CALL EQOS3(RHO,AA,E,P)
      GO TO (76,76,78),K
76    TAB(N,8,K)=AA
      GO TO 82
78    XMESH(J,N,6)=AA
82    CONTINUE
84    CONTINUE
86    CONTINUE
      KICK=86
      CALL DVCHK(KQ)
      IF (KQ.EQ.1) GO TO 9980
C
C          STORE A FOR RAREFACTION
C
      DO 90 I=1,NR
90    RARF(I,8)=AR
C
C          COMPLETE SHOCK TABLES
C
      DO 99 K=1,2
      GO TO (92,94),K
92    NN=NP
      GO TO 95
94    NN=NT
      US=0.
95    DO 97 N=1,NN
      GO TO (93,96),K
93    CONTINUE
      US=VP*TAB(N,10,1)
96    CONTINUE
      TAB(N,11,K)=TAB(N,9,K)*TAB(N,4,K)+TAB(N,10,K)*TAB(N,5,K)
      TAB(N,12,K)=TAB(N,9,K)*TAB(N,5,K)-TAB(N,10,K)*TAB(N,4,K)
      TAB(N,13,K)=((TAB(N,6,K)*ABS(TAB(N,11,K)))/(TAB(N,6,K)-RHOSTR)-US)
```

```
     1*(-1.)**K
      TAB(N,14,K)=1.
97    CONTINUE
99    CONTINUE
C
C
C         STORE ALL XMESH IN XMESH2
C
130   DO 135 K=1,6
      DO 135 J=1,20
      DO 135 I=1,20
      XMESH2(I,J,K)=XMESH(I,J,K)
135   CONTINUE
      TIME=HSTAR
      WRITE (3,145) TIME
      CALL SOUT
      CALL PRINT(XMESH2,Z,R,1)
C
      KREFL=0
139   IF (KREFL.NE.0) GO TO 143
C         ENTRY FOR TIME STEP
C
140   READ (1,142) H
142   FORMAT (E12.8)
143   CONTINUE
      TIME=TIME+H
      WRITE (3,145) TIME
145   FORMAT (1H1///6H TIME=,E15.8///)
      WRITE (3,999) KR
999   FORMAT (5X,4H KR=,I5)
C
C
C         ADVANCE SHOCK POINTS
C
      DO 159 N=1,NP
      IF (TAB(N,14,1).LT.0.) GO TO 156
```

```
      IF ((TAB(N,1,1)-SURF(N,1)).GT.EPS) GO TO 154
156   TAB2(N,1,1)=TAB(N,1,1)
      TAB2(N,2,1)=TAB(N,2,1)
      TAB(N,14,1)=-1.
      GO TO 159
154   TAB2(N,1,1)=TAB(N,1,1)+TAB(N,13,1)*H*TAB(N,10,1)-VP*TAB(N,9,1)*TAB
     1(N,10,1)*H
150   TAB2(N,2,1)=TAB(N,2,1)+TAB(N,13,1)*H*TAB(N,9,1)-VP*TAB(N,9,1)**2*H
159   CONTINUE
      DO 155 N=1,NT
      TAB2(N,1,2)=TAB(N,1,2)+TAB(N,13,2)*H*TAB(N,10,2)
155   TAB2(N,2,2)=TAB(N,2,2)+TAB(N,13,2)*H*TAB(N,9,2)
      DO 158 M=1,NT
      IF (TAB2(M,1,2).GT.ZMAX) GO TO 5000
      IF (TAB2(M,2,2).GT.RMAX) GO TO 5000
158   CONTINUE
157   NUZON=0
C          ADVANCE RAREFACTION
C
      IF (RARF(1,2).LT.0.)IRARF=1
      IF (IRARF.EQ.1) GO TO 516
      ENR=NR-1
      ADEL=(TAB2(1,1,2)-TAB2(1,1,1))/ENR
      RARF2(1,1)=TAB2(1,1,2)
      DO 510 N=2,NR
      RARF2(N,1)=RARF2(N-1,1)-ADEL
510   CONTINUE
      DO 515 N=1,NR
      RARF2(N,3)=(RARF2(N,1)/TIME-.5*VP)/AR
      RARF2(N,4)=-SQRT(1.-RARF2(N,3)**2)
      RARF2(N,2)=RADIUS+TIME*AR*RARF2(N,4)
515   CONTINUE
516   CONTINUE
      CALL SHOCK
C
C
```

```
      IF (ITS3.EQ.1) GO TO 569
C         SHOCK COMPUTATIONS COMPLETED
C         COMPUTE PARTICLE CURVES
C
      TMP=.5*VP*H
      DO 520 N=1,NP
      SPART(N,1,1)=TAB(N,1,1)+TAB(N,5,1)*H
520   SPART(N,2,1)=TAB(N,2,1)+TAB(N,4,1)*H
      DO 525 N=1,NT
      SPART(N,1,2)=TAB(N,1,2)+TAB(N,5,2)*H
525   SPART(N,2,2)=TAB(N,2,2)+TAB(N,4,2)*H
      IF (IRARF.EQ.1) GO TO 531
      DO 530 N=1,NR
      RPART(N,1)=RARF(N,1)+TMP
530   RPART(N,2)=RARF(N,2)
531   CONTINUE
C
C
568   CALL SOUT2
569   CONTINUE
C       ADVANCE PROJECTILE REAR SURFACE
      DO 5300 I=1,NP
      DO 5300 J=1,8
5300  SURF2(I,J)=SURF(I,J)
      KICK=568
      CALL DVCHK(KQ)
      IF (KQ.EQ.1) GO TO 9980
C
C         START INTERIOR REGION COMPUTATIONS
C
      CALL INTER
C
C         INTERIOR REGION COMPUTATIONS COMPLETED
C
      CALL PRINT(XMESH2,Z,R,2)
570   CONTINUE
```

```
C
C          INITIALIZE FOR NEXT TIME STEP
C
      DO 920 K=1,6
      DO 920 J=1,20
      DO 920 I=1,20
      XMESH(I,J,K)=XMESH2(I,J,K)
  920 CONTINUE
      DO 930 J=1,13
      DO 930 I=1,NP
      TAB(I,J,1)=TAB2(I,J,1)
  930 CONTINUE
      DO 940 J=1,13
      DO 940 I=1,NT
      TAB(I,J,2)=TAB2(I,J,2)
  940 CONTINUE
      IF (IRARF.EQ.1) GO TO 951
      DO 950 I=1,NR
      RARF(I,1)=RARF2(I,1)
      RARF(I,2)=RARF2(I,2)
  950 CONTINUE
  951 CONTINUE
      DO 960 I=1,NP
      DO 959 J=1,5
      SURF(I,J)=SURF2(I,J)
  959 CONTINUE
  960 CONTINUE
      IF (KR.EQ.10) GO TO 888
      REWIND 4
      WRITE (4)TIME
      WRITE (4)(((XMESH(I,J,K),I=1,20),J=1,20),K=1,6),(Z(I),I=1,20),(R(I
     1),I=1,20),((SURF(I,J),I=1,15),J=1,8),(((TAB(I,J,K),I=1,15),J=1,14)
     1,K=1,2),((RARF(I,J),I=1,15),J=1,11),TIME,ZMIN,ZMAX,RMIN,RMAX,GR,GZ
     1,AR
      KR=10
      GO TO 777
```

```
888   REWIND 10
C     IF(KRW.EQ.1)REWIND10
C     KRW=0
      WRITE (10)TIME
      WRITE (10)(((XMESH(I,J,K),I=1,20),J=1,20),K=1,6),(Z(I),I=1,20),(R(
     1I),I=1,20),((SURF(I,J),I=1,15),J=1,8),(((TAB(I,J,K),I=1,15),J=1,14
     1),K=1,2),((RARF(I,J),I=1,15),J=1,11),TIME,ZMIN,ZMAX,RMIN,RMAX,GR,G
     1Z,AR
      KR=4
777   IF (KREFL.EQ.0) GO TO 980
      KREFL=0
      H=H1
      GO TO 143
980   CONTINUE
      CALL DVCHK(KICK)
      IF (KICK.EQ.2) GO TO 140
      WRITE (3,970)
970   FORMAT (28H0DIVIDE CHECK AT END OF CASE/1H1)
      CALL EXIT
C
C         DIVIDE CHECK
C
9980  WRITE (3,9985) KICK
9985  FORMAT (32H0DIVIDE CHECK NEAR STATEMENT NO.,I5/1H1)
      RETURN
      END
      SUBROUTINE DBLTRP(ZX,RX,ANS)
C
C         1ST ORDER DOUBLE INTERPOLATION THAT CONSIDERS
C         LINES OF DISCONTINUITY IF IN CONSIDERED REGION
C
      COMMON CASEID(14),ITS1,ITS2,ITS3,ITS4,ITI1,ITI2,ITI3,ITI4,EPS1,EPS
     12,EPS3,EPS4,EPS5,EPS6,EPI1,EPI2,EPI3,EPI4,EPI5,EPI6,EPI7,VP,AR,LEN
     1GTH,APR,BPR,BIGAPR,BIGBPR,ESTAR,ALPHA,BETA,RHOSTR,EPRS,RHOS
      COMMON XMESH(20,20,6),XMESH2(20,20,6),Z(20),R(20),SURF(15,8),SURF2
     1(15,8),TAB(15,14,2),TAB2(15,14,2),SPART(15,2,2),RARF(15,11),RARF2(
```

```
     115,4),RPART(15,2)
C
C
      COMMON Z0,R0,P0,U0,V0,L0,M0,RHO0,E0,A0,UBAR0,VBAR0
C
      COMMON NP,NT,NR,NI,NDEL,ISUB
C
      COMMON ZMIN,ZMAX,RMIN,RMAX,RADIUS,GZ,GR,DELTA,H
      COMMON DIRCOS
      COMMON TIME
      COMMON IRARF
      COMMON KSTOP
      COMMON TPSI
      COMMON KKK
      REAL L0,M0,LENGTH,MU,K0
C
      DIMENSION ANS(6),ANS1(2,8),ANS2(2,8),ZI(4),RI(4),IK(4)
      CALL OVCHK(KEY)
      IF (KEY.EQ.2) GO TO 4
      NO=0
      GO TO 940
C
C         FIND SUBSCRIPTS FOR GRID
C
4     I1=(ZX-ZMIN)/GZ+1.000001
      I2=I1+1
      J1=(RX-RMIN)/GR+1.000001
      J2=J1+1
      NN=NP
      IF (ITS3.EQ.1) GO TO 3
      DO 1 K=1,2
      IF (K.EQ.2)NN=NT
      DO 1 I=1,NN
      ALF=SQRT((TAB(I,1,K)-ZX)**2+(TAB(I,2,K)-RX)**2)
      IF (ALF.GT.EPS1) GO TO 1
      ANS(1)=TAB(I,3,K)
```

```
      ANS(2)=TAB(I,4,K)
      ANS(3)=TAB(I,5,K)
      ANS(4)=TAB(I,6,K)
      ANS(5)=TAB(I,7,K)
      ANS(6)=TAB(I,8,K)
      RETURN
1     CONTINUE
      IF (IRARF.EQ.1) GO TO 3
      DO 2 I=1,NR
      ALF=SQRT((RARF(I,1)-ZX)**2+(RARF(I,2)-RX)**2)
      IF (ALF.GT.EPI1) GO TO 2
      ANS(1)=RARF(I,3)
      ANS(2)=RARF(I,4)
      ANS(3)=RARF(I,5)
      ANS(4)=RARF(I,6)
      ANS(5)=RARF(I,7)
      ANS(6)=RARF(I,8)
      RETURN
2     CONTINUE
3     CONTINUE
C
C
      ZXX=ZX+.01
      RXX=RX+.01
C
C          I LOOP FOR UPPER AND LOWER Z GRID LINES
C
      DO 800 I=1,2
      IF (ITS3.EQ.1) GO TO 14
      IF (I.EQ.2) GO TO 8
      II=I1
      GO TO 12
8     II=I2
12    M=COMP(ZX,RX,Z(II),R(J1))
      IF (M.EQ.1) GO TO 13
      MCOM=1
```

```
      GO TO 20
13    M=COMP(ZX,RX,Z(II),R(J2))
      IF (M.EQ.1) GO TO 14
      MCOM=2
      GO TO 20
C
C          GET 6 VALUES ON GRID LINES
C
14    DO 15 K=1,6
      ANS1(I,K+2)=XMESH(II,J1,K)+(XMESH(II,J2,K)-XMESH(II,J1,K))*(RX-R(J
     11))/(R(J2)-R(J1))
15    CONTINUE
      CALL OVCHK(NO)
      IF (NO.EQ.2) GO TO 17
      NO=15
      GO TO 940
17    ANS1(I,1)=Z(II)
      ANS1(I,2)=RX
      GO TO 800
C
C
20    ZZ=Z(II)
      RR=RX
      M=COMP(ZX,RX,ZZ,RR)
      IF (M.EQ.1) GO TO 300
C
C
      DO 25 K=1,2
      KATCH=0
      GO TO (21,22),K
21    NN=NP
      GO TO 23
22    NN=NT
23    JJJ=NN-1
      DO 24 M=1,JJJ
      IF (M.EQ.JJJ) GO TO 210
```

```
      IF (RX.GT.TAB(M+1,2,K).OR.RX.LT.TAB(M,2,K)) GO TO 24
210   ZI(K)=TAB(M+1,1,K)+(TAB(M,1,K)-TAB(M+1,1,K))*(RX-TAB(M+1,2,K))/(TA
     1B(M,2,K)-TAB(M+1,2,K))
      NO=210
      CALL DVCHK(KQ)
      IF (KQ.EQ.1) GO TO 940
      IF (I.EQ.2) GO TO 211
      IF (KATCH.EQ.1) GO TO 212
      KATCH=1
      GO TO 213
212   IF ((ZX-ZI(K)).GT.(ZX-ZM)) GO TO 24
      IF (ZI(K).GT.ZX) GO TO 24
213   ZM=ZI(K)
      IF (K.EQ.2) GO TO 215
      NPS=M
      GO TO 24
215   NTS=M
      GO TO 24
211   CONTINUE
      IF (KATCH.EQ.1) GO TO 26
      KATCH=1
      GO TO 213
26    IF ((ZI(K)-ZX).GT.(ZM-ZX)) GO TO 24
      IF (ZI(K).LT.ZX) GO TO 24
      GO TO 213
24    CONTINUE
      ZI(K)=ZM
      IF (KATCH.NE.0) GO TO 25
      ZI(K)=ZMAX+1.
25    CONTINUE
      IF (IRARF.EQ.1)ZI(3)=ZMAX+1.
      IF (IRARF.EQ.1) GO TO 2504
      KATCH=0
      JJJ=NR-1
      DO 27 M=1,JJJ
      ZI(3)=RARF(M+1,1)+(RARF(M,1)-RARF(M+1,1))*(RX-RARF(M+1,2))/(RARF(M
```

```
     1,2)-RARF(M+1,2))
      NO=25
      CALL DVCHK(KQ)
      IF (KQ.EQ.1) GO TO 940
      IF (ABS(ZI(3)-ZX).GT.1.E-5) GO TO 279
      DO 2799 LN=1,6
      LNN=LN+2
      ANS(LN)=RARF(1,LNN)
 2799 CONTINUE
      GO TO 820
  279 CONTINUE
      IF (I.EQ.2) GO TO 28
      IF (ZI(3).GT.ZX) GO TO 27
      IF (KATCH.EQ.1) GO TO 280
      KATCH=1
      GO TO 281
  280 IF ((ZX-ZI(3)).GT.(ZX-ZM)) GO TO 27
  281 ZM=ZI(3)
      MR=M
      GO TO 27
   28 IF (ZI(3).LT.ZX) GO TO 27
      IF (KATCH.EQ.1) GO TO 282
      KATCH=1
      GO TO 281
  282 IF ((ZI(3)-ZX).GT.(ZM-ZX)) GO TO 27
      GO TO 281
   27 CONTINUE
      ZI(3)=ZM
 2504 CONTINUE
      KATCH=0
      K=4
      JJJ=NP-1
      DO 2700 M=1,JJJ
      IF (M.EQ.JJJ) GO TO 2710
      IF (RX.GT.SURF(M+1,2).OR.RX.LT.SURF(M,2)) GO TO 2700
 2710 ZI(4)=SURF(M+1,1)+(SURF(M,1)-SURF(M+1,1))*(RX-SURF(M+1,2))/(SURF(M
```

```
     1,2)-SURF(M+1,2))
      IF (KQ.EQ.1) GO TO 940
      CALL DVCHK(KQ)
      NO=2710
      IF (I.EQ.2) GO TO 2711
      IF (KATCH.EQ.1) GO TO 2712
      KATCH=1
      GO TO 2713
2712  IF ((ZX-ZI(K)).GT.(ZX-ZM)) GO TO 2700
2713  ZM=ZI(4)
      MS=M
      GO TO 2700
2711  CONTINUE
      IF (KATCH.EQ.1) GO TO 2726
      KATCH=1
      GO TO 2713
2726  IF ((ZI(K)-ZX).GT.(ZM-ZX)) GO TO 2700
      GO TO 2713
2700  CONTINUE
      ZI(4)=ZM
      IF (KATCH.NE.0) GO TO 2701
      ZI(4)=ZMAX+1.
2701  CONTINUE
      RI(1)=RX
      RI(2)=RX
      RI(3)=RX
      RI(4)=RX
C           FIND INTERSECTION TO USE
C
30    KEY=0
      IF (I.EQ.2) GO TO 50
C
C           UPPER GRID LINE
C
      DO 40 KK=1,4
      IF (Z(II).GT.ZI(KK)) GO TO 40
```

```
      IF (ABS(ZI(KK)-ZX).LT.1.E-5) GO TO 35
      IF (ZI(KK).GT.ZX) GO TO 40
      IF (KEY.EQ.0) GO TO 35
      IF (ZI(KK).LE.ZI(KEEP)) GO TO 40
      KEEP=KK
      GO TO 40
35    KEEP=KK
      KEY=1
40    CONTINUE
      GO TO 65
C
C         LOWER GRID LINE
C
50    DO 60 KK=1,4
      IF (Z(II).LT.ZI(KK)) GO TO 60
      IF (ABS(ZI(KK)-ZX).LT.1.E-5) GO TO 55
      IF (ZI(KK).LT.ZX) GO TO 60
      IF (KEY.EQ.0) GO TO 55
      IF (ZI(KK).GE.ZI(KEEP)) GO TO 60
      KEEP=KK
      GO TO 60
55    KEEP=KK
      KEY=1
60    CONTINUE
C
65    IF (KEY.NE.0) GO TO 70
      WRITE (6,67) ZX,RX,I,(ZI(KEY),KEY=1,4),(RI(KEY),KEY=1,4)
67    FORMAT (34HOERROR NEAR STATEMENT 65 IN DBLTRP/1X3HZX=,E15.8,4X3HRX
     1=,F15.8,4X2HI=,I3/1X3HZI=,4E20.8/1X3HRI=,4E20.8/1H1)
      XYZ=-2.
      ZYX=SQRT(XYZ)
      CALL EXIT
C
C         FIND 6 VALUES ON SELECTED DISCONTINUITY
C
70    IF (KEEP.EQ.3) GO TO 80
```

```
      IF (KEEP.EQ.4) GO TO 81
      IF (KEEP.EQ.2) GO TO 71
      N=NPS
      GO TO 72
71    N=NTS
72    CONTINUE
      ZY=ZI(KEEP)
      RY=RX
      DO 75 K=3,8
      ANS1(I,K)=TAB(N,K,KEEP)+(TAB(N+1,K,KEEP)-TAB(N,K,KEEP))*SQRT(((RY-
     1TAB(N,2,KEEP))**2+(ZY-TAB(N,1,KEEP))**2)/((TAB(N+1,2,KEEP)-TAB(N,2
     1,KEEP))**2+(TAB(N+1,1,KEEP)-TAB(N,1,KEEP))**2))
      NO=75
      CALL DVCHK(KQ)
      IF (KQ.EQ.1) GO TO 940
75    CONTINUE
      GO TO 90
80    N=MR
      ZY=ZI(3)
      RY=RX
      DO 85 K=3,8
      ANS1(I,K)=RARF(N,K)+(RARF(N+1,K)-RARF(N,K))*SQRT(((RY-RARF(N,2))**
     12+(ZY-RARF(N,1))**2)/((RARF(N+1,2)-RARF(N,2))**2+(RARF(N+1,1)-RARF
     1(N,1))**2))
      NO=85
      CALL DVCHK(KQ)
      IF (KQ.EQ.1) GO TO 940
85    CONTINUE
      GO TO 90
81    N=MS
      ZY=ZI(4)
      RY=RX
      DO 86 K=3,8
      ANS1(I,K)=SURF(N,K)+(SURF(N+1,K)-SURF(N,K))*SQRT(((RY-SURF(N,2))**
     12+(ZY-SURF(N,1))**2)/((SURF(N+1,2)-SURF(N,2))**2+(SURF(N+1,1)-SURF
     1(N,1))**2))
```

```
86    CONTINUE
90    CALL DVCHK(NO)
      IF (NO.EQ.2) GO TO 92
      NO=90
      GO TO 940
92    ANS1(I,1)=ZY
      ANS1(I,2)=RY
      GO TO 800
C
C         FIND INTERSECTIONS OF 3 DISCONTINUITIES AND Z GRID LINE
C
300   CONTINUE
      KATCHP=0
      KATCHR=0
      KATCHT=0
      KATCHS=0
      DO 310 K=1,2
      KATCH=0
      GO TO (303,301),K
303   NN=NP
      GO TO 302
301   NN=NT
302   JJJ=NN-1
      DO 309 M=1,JJJ
      IF ((TAB(M,1,K)-TAB(M+1,1,K)).GT.1.E-6) GO TO 3030
      GO TO 309
3030  RI(K)=TAB(M+1,2,K)+(TAB(M,2,K)-TAB(M+1,2,K))*(Z(II)-TAB(M+1,1,K))/
     1(TAB(M,1,K)-TAB(M+1,1,K))
      CALL DVCHK(NO)
      IF (NO.EQ.2) GO TO 3031
      NO=3030
      GO TO 940
3031  CONTINUE
      IF (M.EQ.JJJ) GO TO 3022
      IF (RI(K).GT.TAB(M+1,2,K).OR.RI(K).LT.TAB(M,2,K)) GO TO 309
3022  IF (MCOM.EQ.2) GO TO 305
```

```
      IF (KATCH.EQ.1) GO TO 304
      KATCH=1
      GO TO 3050
304   IF ((RX-RI(K)).GT.(RX-RM)) GO TO 309
3050  RM=RI(K)
      IF (K.EQ.2) GO TO 3040
      MPS=M
      KATCHP=1
      GO TO 309
3040  MTS=M
      KATCHT=1
      GO TO 309
305   CONTINUE
      IF (KATCH.EQ.1) GO TO 306
      KATCH=1
      GO TO 3050
306   IF ((RI(K)-RX).GT.(RM-RX)) GO TO 309
      GO TO 3050
309   CONTINUE
      RI(K)=RM
      IF (KATCH.NE.0) GO TO 310
      RI(K)=RMAX+1.
310   CONTINUE
      K=3
      IF (IRARF.EQ.1)RI(3)=RMAX+1.
      IF (IRARF.EQ.1) GO TO 315
      JJJ=NR-1
      KATCH=0
      DO 312 M=1,JJJ
      RI(3)=RARF(M+1,2)+(RARF(M,2)-RARF(M+1,2))*(Z(II)-RARF(M+1,2))/(RAR
     1F(M,1)-RARF(M+1,1))
      NO=3122
      CALL DVCHK(KQ)
      IF (KQ.EQ.1) GO TO 940
      IF (M.EQ.JJJ.OR.M.EQ.1) GO TO 3122
      IF (RI(K).GT.RARF(M+1,2).OR.RI(K).LT.RARF(M,2)) GO TO 312
```

```
 3122 IF (MCOM.EQ.2) GO TO 316
      IF (KATCH.EQ.1) GO TO 317
      KATCH=1
      GO TO 3051
 317  IF ((RX-RI(K)).GT.(RX-RM)) GO TO 312
 3051 RM=RI(K)
      MR=M
      KATCHR=1
      GO TO 312
 316  CONTINUE
      IF (KATCH.EQ.1) GO TO 318
      KATCH=1
      GO TO 3051
 318  IF ((RI(K)-RX).GT.(RM-RX)) GO TO 312
      GO TO 3051
 312  CONTINUE
      RI(K)=RM
      IF (KATCH.NE.0) GO TO 315
      RI(K)=RMAX+1.
 315  CONTINUE
      KATCH=0
      JJJ=NP-1
      DO 3150 M=1,JJJ
      IF ((SURF(M,1)-SURF(M+1,1)).GT.1.E-6) GO TO 3130
      GO TO 3150
 3130 RI(4)=SURF(M+1,2)+(SURF(M,2)-SURF(M+1,2))*(Z(II)-SURF(M+1,1))/(SUR
     1F(M,1)-SURF(M+1,1))
      NO=3130
      CALL DVCHK(KQ)
      IF (KQ.EQ.1) GO TO 940
      IF (M.EQ.JJJ) GO TO 3123
      IF (RI(4).GT.SURF(M+1,2).OR.RI(4).LT.SURF(M,2)) GO TO 3150
 3123 IF (MCOM.EQ.2) GO TO 3105
      IF (KATCH.EQ.1) GO TO 3104
      KATCH=1
      GO TO 3109
```

```
3104  IF ((RX-RI(4)).GT.(RX-RM)) GO TO 3150                              SUB1 407
3109  RM=RI(4)                                                           SUB1 408
      MS=M                                                               SUB1 409
      KATCHS=1                                                           SUB1 410
      GO TO 3150                                                         SUB1 411
3105  IF (KATCH.EQ.1) GO TO 3106                                         SUB1 412
      KATCH=1                                                            SUB1 413
      GO TO 3109                                                         SUB1 414
3106  IF ((RI(4)-RX).GT.(RM-RX)) GO TO 3150                              SUB1 415
      GO TO 3109                                                         SUB1 416
3150  CONTINUE                                                           SUB1 417
      RI(4)=RM                                                           SUB1 418
      IF (KATCH.NE.0) GO TO 3107                                         SUB1 419
      RI(4)=RMAX+1.                                                      SUB1 420
3107  CONTINUE                                                           SUB1 421
      IF (KATCHP+KATCHT+KATCHR+KATCHS.EQ.0) GO TO 485                    SUB1 422
      ZI(1)=Z(II)                                                        SUB1 423
      ZI(2)=Z(II)                                                        SUB1 424
      ZI(3)=Z(II)                                                        SUB1 425
      ZI(4)=Z(II)                                                        SUB1 426
C          J LOOP FOR LEFT AND RIGHT R GRID LINES                        SUB1 427
C                                                                        SUB1 428
      DO 700 J=1,2                                                       SUB1 429
      IF (J.EQ.2) GO TO 350                                              SUB1 430
C                                                                        SUB1 431
C          LEFT R GRID LINE                                              SUB1 432
C                                                                        SUB1 433
      JJ=J1                                                              SUB1 434
      KEY=0                                                              SUB1 435
      DO 340 N=1,4                                                       SUB1 436
      IF (R(J1).GT.RI(N)) GO TO 340                                      SUB1 437
      IF (RI(N).GT.RX) GO TO 340                                         SUB1 438
      IF (KEY.EQ.1) GO TO 330                                            SUB1 439
      KEY=1                                                              SUB1 440
      KEEP=N                                                             SUB1 441
      GO TO 340                                                          SUB1 442
```

```
C
C          FIND CLOSEST
C
330   DIF1=RX-RI(KEEP)
      DIF2=RX-RI(N)
      IF (DIF1.LE.DIF2) GO TO 340
      KEEP=N
340   CONTINUE
      GO TO 375
C
C          RIGHT R GRID LINE
C
350   JJ=J2
      KEY=0
      DO 360 N=1,4
      IF (R(J2).LT.RI(N)) GO TO 360
      IF (RI(N).LT.RX) GO TO 360
      IF (KEY.EQ.1) GO TO 355
      KEY=1
      KEEP=N
      GO TO 360
355   DIF1=RI(KEEP)-RX
      DIF2=RI(N)-RX
      IF (DIF1.LE.DIF2) GO TO 360
      KEEP=N
360   CONTINUE
375   IF (KEY.EQ.1) GO TO 400
C
C          NO POINTS BETWEEN RX AND GRID POINTS
C
      ANS2(J,1)=Z(II)
      ANS2(J,2)=R(JJ)
      ANS2(J,3)=XMESH(II,JJ,1)
      ANS2(J,4)=XMESH(II,JJ,2)
      ANS2(J,5)=XMESH(II,JJ,3)
      ANS2(J,6)=XMESH(II,JJ,4)
```

```
      ANS2(J,7)=XMESH(II,JJ,5)
      ANS2(J,8)=XMESH(II,JJ,6)
      GO TO 700
C
C         POINT FOUND BETWEEN RX AND GRID POINTS
C
400   GO TO (405,410,470,481),KEEP
C
C         INTERSECTION ON PROJECTILE SHOCK
C
405   N1=MPS
      RY=RI(KEEP)
      ZY=Z(II)
      GO TO 520
C
C         INTERSECTION ON TARGET SHOCK
C
410   N1=MTS
      RY=RI(KEEP)
      ZY=Z(II)
      GO TO 520
C
C        INTERSECTION ON RAREFACTION
C
470   N1=MR
      RY=RI(KEEP)
      ZY=Z(II)
      GO TO 520
C
C     INTERSECTION ON FREE SURFACE
C
481   N1=MS
      RY=RI(KEEP)
      ZY=Z(II)
      GO TO 520
C
```

```
C                                                                       SUB1 515
485   WRITE (3,488) KEEP,II,JJ,ZX,RX                                    SUB1 516
488   FORMAT (25HOERROR NEAR STATEMENT 485/1X5HKEEP=,I4,4X3HII=,I4,4X3HJSUB1 517
     1J=,I4/1X3HZX=,E15.8,4X3HRX=,E15.8/1H1)                            SUB1 518
      CALL EXIT                                                         SUB1 519
C                                                                       SUB1 520
C         FIND TABLE VALUES                                             SUB1 521
C                                                                       SUB1 522
520   IF (KEEP.EQ.3) GO TO 580                                          SUB1 523
      IF (KEEP.EQ.4) GO TO 591                                          SUB1 524
      DO 550 N=3,8                                                      SUB1 525
      ANS2(J,N)=TAB(N1,N,KEEP)+(TAB(N1+1,N,KEEP)-TAB(N1,N,KEEP))*SQRT(((SUB1 526
     1RY-TAB(N1,2,KEEP))**2+(ZY-TAB(N1,1,KEEP))**2)/((TAB(N1+1,2,KEEP)-TSUB1 527
     1AB(N1,2,KEEP))**2+(TAB(N1+1,1,KEEP)-TAB(N1,1,KEEP))**2))          SUB1 528
550   CONTINUE                                                          SUB1 529
      IF (ZX.LT.0..AND.ABS(RX-RADIUS).LT.1.E-6) GO TO 552               SUB1 530
      IF (RX.LT.RADIUS.OR.ABS(Z(II)).GT.1.E-6) GO TO 551                SUB1 531
552   CONTINUE                                                          SUB1 532
      ANS2(J,3)=0.                                                      SUB1 533
      ANS2(J,6)=RHOSTR                                                  SUB1 534
      ANS2(J,7)=0.                                                      SUB1 535
      ANS2(J,8)=SQRT(BIGAPR/RHOSTR)                                     SUB1 536
551   CONTINUE                                                          SUB1 537
      GO TO 600                                                         SUB1 538
580   DO 590 N=3,8                                                      SUB1 539
      ANS2(J,N)=RARF(N1,N)+(RARF(N1+1,N)-RARF(N1,N))*SQRT(((RY-RARF(N1,2SUB1 540
     1))**2+(ZY-RARF(N1,1))**2)/((RARF(N1+1,2)-RARF(N1,2))**2+(RARF(N1+1SUB1 541
     1,1)-RARF(N1,1))**2))                                              SUB1 542
590   CONTINUE                                                          SUB1 543
      GO TO 600                                                         SUB1 544
591   DO 592 N=3,8                                                      SUB1 545
      ANS2(J,N)=SURF(N1,N)+(SURF(N1+1,N)-SURF(N1,N))*SQRT(((RY-SURF(N1,2SUB1 546
     1))**2+(ZY-SURF(N1,1))**2)/((SURF(N1+1,2)-SURF(N1,2))**2+(SURF(N1+1SUB1 547
     1,1)-SURF(N1,1))**2))                                              SUB1 548
592   CONTINUE                                                          SUB1 549
600   CALL DVCHK(NO)                                                    SUB1 550
```

```
      IF (NO.EQ.2) GO TO 605
      NO=600
      GO TO 940
605   ANS2(J,1)=ZY
      ANS2(J,2)=RY
C
C          END OF LOOP FOR BOTH R GRID LINES
C
700   CONTINUE
C
C          INTERPOLATE FOR UPPER AND LOWER VALUES
C
      DO 720 J=3,8
      ANS1(I,J)=ANS2(1,J)+(ANS2(2,J)-ANS2(1,J))*(RX-ANS2(1,2))/(ANS2(2,2
     1)-ANS2(1,2))
720   CONTINUE
      CALL DVCHK(NO)
      IF (NO.EQ.2) GO TO 730
      NO=720
      GO TO 940
730   ANS1(I,1)=Z(II)
      ANS1(I,2)=RX
C
C          END OF LOOP FOR BOTH Z GRID LINES
C
800   CONTINUE
C
C          FIND FINAL VALUES
C
      DO 810 J=1,6
      ANS(J)=ANS1(1,J+2)+(ANS1(2,J+2)-ANS1(1,J+2))*(ZX-ANS1(1,1))/(ANS1(
     12,1)-ANS1(1,1))
810   CONTINUE
      CALL DVCHK(NO)
      IF (NO.EQ.2) GO TO 820
      NO=810
```

```
      GO TO 940
  820 RETURN
C
  940 WRITE (3,942)
  942 FORMAT (35HODIVIDE CHECK ERROR IN SUBR. DBLTRP)
  950 WRITE (3,952) NO,ZX,RX,I1,J1,KEEP,ZI,RI
  952 FORMAT (19H NEAR STATEMENT NO.,I4/1X3HZX=,E15.8,4X3HRX=,E15.8/1X3H
     1I1=,I4,4X3HJ1=,I4,4X5HKEEP=,I4/1X3HZI=,4E18.8/1X3HRI=,4E18.8)
      WRITE (3,955) ((ANS1(I,J),J=1,8),I=1,2),((ANS2(I,J),J=1,8),I=1,2)
  955 FORMAT (1X5HANS1=/8E16.8/8E16.8/1X5HANS2=/8E16.8/8E16.8/1H1)
      XYZ=-2.
      ZYX=SQRT(XYZ)
      CALL EXIT
      RETURN
      END
      SUBROUTINE SHOCK
C         COMPUTES SHOCK VALUES
      COMMON CASEID(14),ITS1,ITS2,ITS3,ITS4,ITI1,ITI2,ITI3,ITI4,EPS1,EPS
     12,EPS3,EPS4,EPS5,EPS6,EPI1,EPI2,EPI3,EPI4,EPI5,EPI6,EPI7,VP,AR,LEN
     1GTH,APR,BPR,BIGAPR,BIGBPR,ESTAR,ALPHA,BETA,RHOSTR,EPRS,RHOS
      COMMON XMESH(20,20,6),XMESH2(20,20,6),Z(20),R(20),SURF(15,8),SURF2
     1(15,8),TAB(15,14,2),TAB2(15,14,2),SPART(15,2,2),RARF(15,11),RARF2(
     115,4),RPART(15,2)
C
      COMMON Z0,R0,P0,U0,V0,L0,M0,RHO0,E0,A0,UBAR0,VBAR0
C
      COMMON NP,NT,NR,NI,NDEL,ISUB
C
      COMMON ZMIN,ZMAX,RMIN,RMAX,RADIUS,GZ,GR,DELTA,H
      COMMON DIRCOS
      COMMON TIME
      COMMON IRARF
      COMMON KSTOP
      COMMON TPSI
      COMMON KKK
C
```

```
      REAL LO,MO,LENGTH,MU,KO
C
      DIMENSION ANS(6)
      EXTERNAL FGOF1
      EPS=.0000001
C
C           BEGIN SHOCK POINT COMPUTATIONS
      DO 505 K=1,2
      GO TO (158,160),K
158   NN=NP
      GO TO 162
160   NN=NT
      VBARS=0.
162   DO 500 I=1,NN
      MPROJ=0
      IF (TAB(I,14,K).LT.0.) GO TO 500
164   CONTINUE
C
C           INITIALIZE TO ITERATE ON 1 SHOCK POINT
C
      NBIC=0
      ZO=TAB2(I,1,K)
      RO=TAB2(I,2,K)
      PO=TAB(I,3,K)
      UO=TAB(I,4,K)
      VO=TAB(I,5,K)
      RHOO=TAB(I,6,K)
      EO=TAB(I,7,K)
      AO=TAB(I,8,K)
      LO=TAB(I,9,K)
      MO=TAB(I,10,K)
      UBARO=TAB(I,11,K)
      VBARO=TAB(I,12,K)
      UTOH=TAB(I,13,K)
      UTO=UTOH
      ITS44=ITS4
```

```
      IF (IRARF.EQ.1) GO TO 170
      M=1-(NR-2)*(K-2)
      FF=RO-RARF2(M+1,2)-(RARF2(M,2)-RARF2(M+1,2))*(ZO-RARF2(M+1,1))/(RA
     1RF2(M,1)-RARF2(M+1,1))
  169 CONTINUE
      IF (FF.LT..001) GO TO 350
  170 IF (I.NE.1) GO TO 180
      MO=TAB(I,10,K)
      LO=0.
      GO TO 190
  180 IF (I.LT.NN) GO TO 184
      UP=H*(TAB(I-1,13,K)-TAB(I,13,K))
      TMP=SQRT((TAB2(I-1,2,K)-RO)**2+(TAB2(I-1,1,K)-ZO)**2)
      DOMEG=UP/TMP
      GO TO 186
  184 DR1=TAB2(I+1,2,K)-RO
      DR2=RO-TAB2(I-1,2,K)
      DZ1=TAB2(I+1,1,K)-ZO
      DZ2=ZO-TAB2(I-1,1,K)
      UP=H*(TAB(I-1,13,K)-TAB(I+1,13,K))
      TMP=SQRT(DR1**2+DZ1**2)+SQRT(DR2**2+DZ2**2)
      DOMEG=UP/TMP
      KICK=184
      CALL DVCHK(KQ)
      IF (KQ.EQ.1) GO TO 9980
C
C         COMPUTE NEW LO,MO
C
  186 COMEG=COS(DOMEG)
      SOMEG=SIN(DOMEG)
      XLO=LO*COMEG+MO*SOMEG
      XMO=MO*COMEG-LO*SOMEG
      LO=XLO
      MO=XMO
      IF (PO.GT..0025) GO TO 190
      PO=0.
```

```
      U0=0.
      V0=VP*(1.-(-1.)**K)/2.
      RHO0=RHOSTR
      E0=0.
      A0=SQRT(BIGAPR/RHOSTR)
      UBAR0=M0*V0
      VBAR0=VBARS
      UT0=UBAR0+A0*(-1.)**K
      GO TO 350
  190 ITS33=ITS3
C
C          FIND GUESS TO START ITERATION
C
  195 CALL GUESS(1,KOD2,Z0,R0,I,K,ZZ,RR,DZ,DR)
      IF (KOD2.EQ.1) GO TO 200
      WRITE (3,198) I,K,Z0,R0
      WRITE (3,7002) ZZ,RR,DZ,DR
  198 FORMAT (31HONO GUESS FOUND FOR SHOCK POINT/3H0I=,I4,6X2HK=,I4,10X3
     1HZ0=,E15.8,10X3HR0=,E15.8/1H1)
      CALL EXIT
  200 CONTINUE
      KY=K
      NTW=0
      IF (K.EQ.2) GO TO 201
      VBARS=VP*L0
      DIRCOS=-M0
      GO TO 203
  201 DIRCOS=M0
  203 CONTINUE
      CALL NRIT2(Z1,R1,ZZ,DZ,RR,DR,EPS1,EPS2,FGOF1,ITS1,KODE)
      IF (KODE.EQ.0) GO TO 205
C
C     BICHARACTERISTIC SELECTION SCHEME
C
      IF (NBIC.EQ.0) GO TO 204
      IF (NTW.EQ.8)KY=KY+1
```

```
      IF (NTW.GT.21) GO TO 7000
      ANG1=ANG1+DTPSI*(-1.)**KY
      DIRCOS=SIN(ANG1)
      LO=COS(ANG1)
      NTW=NTW+1
      GO TO 203
204   CONTINUE
      NBIC=1
      CALL DBLTRP(ZZ,RR,ANS)
      UA=ANS(2)
      VA=ANS(3)
      AA=ANS(6)
      ZZZ=ZZ+DZ
      CALL DBLTRP(ZZZ,RR,ANS)
      UB=ANS(2)
      VB=ANS(3)
      AB=ANS(6)
      RRR=RR+DR
      CALL DBLTRP(ZZ,RRR,ANS)
      UC=ANS(2)
      VC=ANS(3)
      AC=ANS(6)
      MM=0
      TPSI=1.5708*(-1.)**K
      XB=ZZ
      YB=RR
      NOM=5
      CA=NOM
6201  DTPSI=.01745
      DTPSI=CA*DTPSI
      TPSI=TPSI+DTPSI*(-1.)**K
      A1=1.+H*(VB-VA+(AB-AA)*SIN(TPSI))/DZ
      B1=H*(VC-VA+(AC-AA)*SIN(TPSI))/DR
      C1=-(ZZ-Z0+H*(VA+AA*SIN(TPSI)))
      A2=H*(UB-UA+(AB-AA)*COS(TPSI))/DZ
      B2=1.+H*(UC-UA+(AC-AA)*COS(TPSI))/DR
```

```
      C2=-(RR-RO+H*(UA+AA*COS(TPSI)))
      DET=A1*B2-A2*B1
      DELX=(B2*C1-B1*C2)/DET
      DELY=(A1*C2-A2*C1)/DET
C
C         TEST FOR SAME REGION
C
      XB1=XB+DELX
      YB1=YB+DELY
      M=COMP(XB,YB,XB1,YB1)
      IF (M.EQ.1) GO TO 6203
      MM=MM+1
      IF (MM.LT.360/NOM) GO TO 6201
7000  WRITE (3,7001)
7001  FORMAT (41H0BICHARACTERISTIC SELECTION SCHEME FAILED)
      WRITE (3,614) ZO,RO
614   FORMAT (1X5HZO   =,E15.8,4X5HRO   =,E15.8)
      WRITE (3,7002) UA,VA,AA,UB,VB,AB,UC,VC,AC,ZZ,DZ,RR,DR,ANG1
7002  FORMAT (4E16.8)
      CALL EXIT
6203  CONTINUE
      WRITE (3,6210)
6210  FORMAT (53H0BICHARACTERISTIC SELECTION SCHEME EMPLOYED BY SHOCKX)
6204  ANG1=TPSI
      T1=DIRCOS
      T2=LO
      DIRCOS=SIN(ANG1)
      LO=COS(ANG1)
      GO TO 203
205   CONTINUE
      UBARS1=0.
      IF (K.EQ.1)UBARS1=MO*VP
      CALL DBLTRP(Z1,R1,ANS)
      P1=ANS(1)
      U1=ANS(2)
      V1=ANS(3)
```

```
      RHO1=ANS(4)
      E1=ANS(5)
      A1=ANS(6)
  206 CONTINUE
      KICK=205
      CALL DVCHK(KQ)
      IF (KQ.EQ.1) GO TO 9980
      IF (NBIC.EQ.0) GO TO 207
 7003 SINTH=ABS(DIRCOS)
      COSTH=ABS(LO)
      DIRCOS=T1
      LO=T2
  207 CONTINUE
      UBAR1=LO*U1+MO*V1
      IF (K.EQ.2) GO TO 208
      IF (UBAR1.LT.VP/2.) GO TO 208
      UBAR1=UBARS1-UBAR1
  208 CONTINUE
  218 CONTINUE
      M1=PART(1,Z1,R1,ZZ,RR,DELTA,NDEL)
      IF (M1.EQ.1) GO TO 210
      PUR=0.
      PVR=0.
      GO TO 215
  210 CALL DBLTRP(ZZ,RR,ANS)
      DP=RR-R1
      PUR=(ANS(2)-U1)/DP
  219 CONTINUE
      PVR=(ANS(3)-V1)/DP
  215 M1=PART(2,Z1,R1,ZZ,RR,DELTA,NDEL)
      IF (M1.EQ.1) GO TO 220
      PUZ=0.
      PVZ=0.
      PAZ=0.
      GO TO 225
  220 CALL DBLTRP(ZZ,RR,ANS)
```

```
      DP=ZZ-Z1
      PUZ=(ANS(2)-U1)/DP
      PVZ=(ANS(3)-V1)/DP
225   CONTINUE
      IF (NBIC.EQ.1) GO TO 7004
      PURB1=LO*PUR+MO*PVR
      PVRB1=LO*PVR-MO*PUR
      PVZB1=LO*PVZ-MO*PUZ
      PVEB1=-MO*PVRB1+LO*PVZB1
      SBAR1=PVEB1
226   CONTINUE
      IF (ABS(R1).LE.EPS) GO TO 235
      SBAR1=SBAR1+U1/R1
      GO TO 240
7004  CONTINUE
      IF (V1.GT.VP/2..AND.K.EQ.1)V1=VP-V1
      SBAR1=SINTH**2*PUR-SINTH*COSTH*(PUZ+PVR)+COSTH**2*PVZ
      GO TO 226
235   SBAR1=SBAR1+PUR
C
C
240   ITS22=ITS2
      MMM=0
250   CONTINUE
      CALL EQOSS(PFR,PFE)
      BIGA1=RHO1*A1
      KICK=250
      CALL DVCHK(KQ)
      IF (KQ.EQ.1) GO TO 9980
      TEMP=1.-RHOSTR/RHOO
      TMP=SQRT(PO*TEMP/RHOSTR)
      IF (K.EQ.2) GO TO 251
      IF (TMP.LT.VP/2.) GO TO 251
      MPROJ=1
      TMP=UBARS1-TMP
251   CONTINUE
```

```
      TMP6=TMP
  256 CONTINUE
      FNBIC=NBIC
      TMP1=P1+BIGA1*UBAR1-RHO1*H*SBAR1*A1**2+BIGA1*(-UBAR1+COSTH*U1+SINT
     1H*V1-SINTH*LO*VBARS+COSTH*MO*VBARS)*(FNBIC)
      TMP2=PFR*TEMP+PO*RHOSTR/RHOO**2
      TMP5=PFE*TEMP
      GTMP=-RHO1*A1
      IF (NBIC.EQ.0) GO TO 259
      GTMP=GTMP*(COSTH*LO+SINTH*MO)
  259 CONTINUE
      BIGG=PO-(GTMP*TMP+TMP1)
      PGR=PFR-((GTMP*TMP2)/(2.*RHOSTR*TMP6))
      PGE=PFE-((GTMP*TMP5)/(2.*RHOSTR*TMP6))
  265 TMP=.5*(1./RHOSTR-1./RHOO)
      BIGH=EO-TMP*PO
      PHR=-TMP*PFR-.5*PO/RHOO**2
      PHE=1.-TMP*PFE
      IF (ABS(BIGH).GT..0001) GO TO 267
      BIGH=0.
  267 IF (ABS(BIGG).GT..0001) GO TO 269
      BIGG=0.
  269 CONTINUE
C
C          COMPUTE DELTA EO,DELTA RHOO
C
      DOWN=PGE*PHR-PGR*PHE
      DEO=(-BIGG*PHR+BIGH*PGR)/DOWN
      DRHOO=(-BIGH*PGE+BIGG*PHE)/DOWN
C
      EO2=EO+DEO
      IF (EO2.LT.0.)EO2=0.
      RHOO2=RHOO+DRHOO
      IF (RHOO2.LT.RHOSTR)RHOO2=RHOO
      KICK=265
      CALL DVCHK(KQ)
```

```
      IF (KQ.EQ.1) GO TO 9980                                           SUB2 310
      CALL EQOSP(RHOO2,EO2,PO2)                                         SUB2 311
      UBARO2=(1.-RHOSTR/RHOO2)*(PO2/RHOSTR)                             SUB2 312
      IF (UBARO2.GT.0.) GO TO 2669                                      SUB2 313
      WRITE (3,2700) PO2,RHOO2,EO2,RO,ZO                                SUB2 314
      WRITE (3,7002) P1,U1,V1,RHO1,E1,Z1TR1,SBAR1                       SUB2 315
 2700 FORMAT (4E16.8)                                                   SUB2 316
 2669 CONTINUE                                                          SUB2 317
      UBARO2=SQRT(UBARO2)                                               SUB2 318
      IF (EO2.LT.1.E-5) GO TO 273                                       SUB2 319
      IF (ABS((EO2-EO)/EO2).LT.EPS4) GO TO 273                          SUB2 320
      IF (ABS(DEO).GT..01*EPS4) GO TO 275                               SUB2 321
  273 IF (ABS((RHOO2-RHOO)/RHOO2).LE.EPS3) GO TO 285                    SUB2 322
      IF (ABS(DRHOO).LT.EPS3) GO TO 285                                 SUB2 323
  275 ITS22=ITS22-1                                                     SUB2 324
      IF (ITS22.GT.0) GO TO 280                                         SUB2 325
      WRITE (3,278) ITS2                                                SUB2 326
  278 FORMAT (35HOE AND RHO FAILED TO CONVERGE AFTER,I4,6H TRIES)       SUB2 327
      WRITE (3,279) I,K,ZO,RO,EO,RHOO,PO,EO2,RHOO2,PO2                  SUB2 328
  279 FORMAT (1X2HI=,I4,4X2HK=,I4/1X4HZO =,E15.8,4X4HRO =,E15.8,4X4HEO =SUB2 329
     1,E15.8,4X6HRHOO =,E15.8,4X4HPO =,E15.8/1X4HEO2=,E15.8,4X6HRHOO2=,ESUB2 330
     115.8,4X4HPO2=,E15.8/1H1)                                          SUB2 331
      STOP                                                              SUB2 332
  280 EO=EO2                                                            SUB2 333
      RHOO=RHOO2                                                        SUB2 334
      PO=PO2                                                            SUB2 335
      UBARO=UBARO2                                                      SUB2 336
      GO TO 250                                                         SUB2 337
  285 EO=EO2                                                            SUB2 338
      RHOO=RHOO2                                                        SUB2 339
      UBARO=UBARO2                                                      SUB2 340
      AO=SQRT(PFR+PO2*PFE/RHOO**2)                                      SUB2 341
C                                                                       SUB2 342
C                                                                       SUB2 343
      CALL DVCHK(KQ)                                                    SUB2 344
      KICK=285                                                          SUB2 345
```

```
      IF (KQ.EQ.1) GO TO 9980
      IF (K.EQ.2) GO TO 286
      VBARO=VP*LO
      GO TO 287
  286 VBARO=0.
  287 CONTINUE
  295 PO=PO2
      IF (K.EQ.2) GO TO 296
      UBARO=UBARS1-UBARO
  296 CONTINUE
      UTO=(RHOO*UBARO-RHOSTR*UBARS1)/(RHOO-RHOSTR)
      VO=MO*UBARO+LO*VBARO
      UO=LO*UBARO-MO*VBARO
      UBAR=.5*(UTOH+UTO)
      IF (ABS((UBAR-UTOH)/UBAR).LE.EPS6) GO TO 350
      IF (ABS(UBAR-UTOH).LT.EPS6) GO TO 350
      ITS44=ITS44-1
      IF (ITS44.GT.0) GO TO 325
      WRITE (3,297) ITS4,UTOH,UTO
  297 FORMAT (30HOUBAR FAILED TO CONVERGE AFTER,I4,6H TRIES/1X5HUTOH=,E1
     15.8,4X4HUTO=,E15.8)
      CALL EXIT
      WRITE (3,279) I,K,ZO,RO,EO,RHOO,PO,EO2,RHOO2,PO2
C
C         INIT. FOR MORE U BAR ITERATIONS
C
  325 UTOH=UBAR
      AVMO=(TAB(I,10,K)+MO)*.5
      AVLO=(TAB(I,9,K)+LO)*.5
      ZO=TAB(I,1,K)+UBAR*H*AVMO-VBARS*AVLO*H
      RO=TAB(I,2,K)+UBAR*H*AVLO-VBARS*AVMO*H
      LO=AVLO
      MO=AVMO
      GO TO 195
C
C         ONE SHOCK POINT HAS CONVERGED
```

```
C
350   TAB2(I,1,K)=Z0
      TAB2(I,2,K)=R0
      TAB2(I,3,K)=P0
      TAB2(I,4,K)=U0
      TAB2(I,5,K)=V0
      TAB2(I,6,K)=RHO0
      TAB2(I,7,K)=E0
      TAB2(I,8,K)=A0
      TAB2(I,9,K)=L0
      TAB2(I,10,K)=M0
      TAB2(I,11,K)=UBAR0
      TAB2(I,12,K)=VBAR0
      TAB2(I,13,K)=UT0
      KICK=500
      CALL DVCHK(KQ)
      IF (KQ.EQ.1) GO TO 9980
C
C
500   CONTINUE
505   CONTINUE
      RETURN
9980  WRITE (3,9985) KICK
9985  FORMAT (32H0DIVIDE CHECK NEAR STATEMENT NO.,I5,15H IN SUBR. SHOCK/
     11H1)
      CALL EXIT
      RETURN
      END
      SUBROUTINE FGOF1(ZX,RX,SS,QQ)
C
C         COMPUTES S1,Q1 FOR SHOCK LINE
C         ITERATION FOR Z1,R1
C
      COMMON CASEID(14),ITS1,ITS2,ITS3,ITS4,ITI1,ITI2,ITI3,ITI4,EPS1,EPS
     12,EPS3,EPS4,EPS5,EPS6,EPI1,EPI2,EPI3,EPI4,EPI5,EPI6,EPI7,VP,AR,LEN
     1GTH,APR,BPR,BIGAPR,BIGBPR,ESTAR,ALPHA,BETA,RHOSTR,EPRS,RHOS
```

```
      COMMON XMESH(20,20,6),XMESH2(20,20,6),Z(20),R(20),SURF(15,8),SURF2SUB3    9
     1(15,8),TAB(15,14,2),TAB2(15,14,2),SPART(15,2,2),RARF(15,11),RARF2(SUB3   10
     115,4),RPART(15,2)                                                 SUB3   11
C                                                                       SUB3   12
C                                                                       SUB3   13
      COMMON Z0,R0,P0,U0,V0,L0,M0,RHO0,E0,A0,UBAR0,VBAR0                SUB3   14
C                                                                       SUB3   15
      COMMON NP,NT,NR,NI,NDEL,ISUB                                      SUB3   16
C                                                                       SUB3   17
      COMMON ZMIN,ZMAX,RMIN,RMAX,RADIUS,GZ,GR,DELTA,H                   SUB3   18
      COMMON DIRCOS                                                     SUB3   19
      COMMON TIME                                                       SUB3   20
      COMMON IRARF                                                      SUB3   21
      COMMON KSTOP                                                      SUB3   22
      COMMON TPSI                                                       SUB3   23
      COMMON KKK                                                        SUB3   24
      REAL L0,M0,LENGTH,MU,K0                                           SUB3   25
C                                                                       SUB3   26
      DIMENSION ANS(6)                                                  SUB3   27
C                                                                       SUB3   28
      REAL L0,M0                                                        SUB3   29
      CALL DBLTRP(ZX,RX,ANS)                                            SUB3   30
      U1=ANS(2)                                                         SUB3   31
      V1=ANS(3)                                                         SUB3   32
      A1=ANS(6)                                                         SUB3   33
      SS=ZX-Z0+H*(V1+A1*DIRCOS)                                         SUB3   34
      QQ=RX-R0+H*(U1+A1*L0)                                             SUB3   35
      RETURN                                                            SUB3   36
      END                                                               SUB3   37
      SUBROUTINE INTER                                                  SUB4    1
C         COMPUTES INTERIOR REGION POINTS                               SUB4    2
      COMMON CASEID(14),ITS1,ITS2,ITS3,ITS4,ITI1,ITI2,ITI3,ITI4,EPS1,EPSSUB4    3
     12,EPS3,EPS4,EPS5,EPS6,EPI1,EPI2,EPI3,EPI4,EPI5,EPI6,EPI7,VP,AR,LENSUB4    4
     1GTH,APR,BPR,BIGAPR,BIGBPR,ESTAR,ALPHA,BETA,RHOSTR,EPRS,RHOS       SUB4    5
      COMMON XMESH(20,20,6),XMESH2(20,20,6),Z(20),R(20),SURF(15,8),SURF2SUB4    6
     1(15,8),TAB(15,14,2),TAB2(15,14,2),SPART(15,2,2),RARF(15,11),RARF2(SUB4    7
```

```
     115,4),RPART(15,2)
C
C
      COMMON Z0,R0,P0,U0,V0,L0,M0,RHO0,E0,A0,UBAR0,VBAR0
C
      COMMON NP,NT,NR,NI,NDEL,ISUB
C
      COMMON ZMIN,ZMAX,RMIN,RMAX,RADIUS,GZ,GR,DELTA,H
      COMMON DIRCOS
      COMMON TIME
      COMMON IRARF
      COMMON KSTOP
      COMMON TPSI
      COMMON KKK
C
C
      REAL L0,M0,LENGTH,MU,K0
      DIMENSION ANS(6),LL(3),ZI(11),RI(11),PI(11),UI(11),VI(11),RHOI(11)
     1,EI(11),AI(11),PUR(11),PVR(11),PAR(11),PUZ(11),PVZ(11),PAZ(11),PSI
     1(7),SPSI(11),CPSI(11),S(11)
C
      EXTERNAL FGOF1,FGOF5
      INTEGER CHECK,CHECK2
C
1     FORMAT (1H1)
      EPS=.0000001
      DO 905 J=1,20
      DO 900 I=1,20
      M=TEST(Z(I),R(J))
      Z0=Z(I)
      R0=R(J)
      KICK=1
      CALL DVCHK(KQ)
      IF (KQ.EQ.1) GO TO 9980
      IF (M.EQ.3.AND.Z0.LT.EPS.AND.ABS(R0-RADIUS).LT.EPS)M=1
      IF (M.NE.1) GO TO 900
```

```
      DO 2 L=1,NP
      IF (TAB(L,14,1).LT.0.) GO TO 20
2     CONTINUE
      IF (IRARF.EQ.1) GO TO 20
      DO 3 N=1,NR
      IF (R(J).GT.RARF(N,2)) GO TO 5
3     CONTINUE
      GO TO 6
5     CONTINUE
      M=PICK(Z(I),R(J),3)
      FF=R(J)-RARF(M+1,2)-(RARF(M,2)-RARF(M+1,2))*(Z(I)-RARF(M+1,1))/(RA
     1RF(M,1)-RARF(M+1,1))
      IF (FF.GT.0.) GO TO 20
6     CONTINUE
      PO2=RARF(1,3)
      UO2=RARF(1,4)
      VO2=RARF(1,5)
      RHOO2=RARF(1,6)
      EO2=RARF(1,7)
      AO2=RARF(1,8)
      GO TO 870
20    CONTINUE
      CALL GUESS(2,KOD,ZO,RO,I,J,ZZ,RR,DZ,DR)
      IF (KOD.EQ.1) GO TO 580
      WRITE (3,575) I,J,ZO,RO
575   FORMAT (41HONO GUESS FOUND FOR INTERIOR REGION POINT/3HOI=I4,6X2HK
     1=,I4,10X3HZO=,E15.8,10X3HRO=,E15.8/1H1)
      CALL EXIT
580   CALL DBLTRP(ZZ,RR,ANS)
C
C          INITIALIZE FOR 1 POINT
C
      PSI(1)=0.
      PSI(3)=1.0472
      PSI(4)=2.0944
      PSI(6)=4.18879
```

```
      PSI(7)=5.23599
      NBIC=0
      ITI22=ITI2
      PO=ANS(1)
      UO=ANS(2)
      VO=ANS(3)
      RHOO=ANS(4)
      EO=ANS(5)
      AO=ANS(6)
      KICK=580
      CALL DVCHK(KQ)
      IF (KQ.EQ.1) GO TO 9980
590   IF (ABS(RO).GT.EPS) GO TO 594
      L1=1
      LL(1)=4
      LL(2)=6
      LLL=2
      GO TO 620
C
C
594   IF (ABS(RO-RADIUS).GT.EPS) GO TO 600
      IF (ZO.GT.EPS) GO TO 610
      L1=2
      LL(1)=3
      LL(2)=7
      LLL=2
      GO TO 620
600   IF (RO.LE.RADIUS.OR.ABS(ZO).GT.EPS) GO TO 610
      L1=3
      LL(1)=6
      LL(2)=7
      LLL=2
      GO TO 620
C
C
610   L1=4
```

```
      LL(1)=1
      LL(2)=4
      LL(3)=6
      LLL=3
C
C          ITERATE FOR I VALUES
C
619   CONTINUE
620   DO 630 KK=1,LLL
      LUMP=L1
      ISUB=LL(KK)
621   CONTINUE
      TPSI=PSI(ISUB)
      SPSI(ISUB)=SIN(TPSI)
      CPSI(ISUB)=COS(TPSI)
      CALL NRIT2(ZI(ISUB),RI(ISUB),ZZ,DZ,RR,DR,EPI1,EPI2,FGOFI,ITI1,KODE
     1)
      IF (KODE.NE.0) GO TO 6200
625   CALL DBLTRP(ZI(ISUB),RI(ISUB),ANS)
      PI(ISUB)=ANS(1)
      UI(ISUB)=ANS(2)
      VI(ISUB)=ANS(3)
      RHOI(ISUB)=ANS(4)
      EI(ISUB)=ANS(5)
      AI(ISUB)=ANS(6)
630   CONTINUE
C
C
      KICK=630
      CALL DVCHK(KQ)
      IF (KQ.EQ.1) GO TO 9980
      GO TO 6400
C
C     BICHARACTERISTIC SELECTION SCHEME
C
7000  WRITE (3,7001)
```

```
7001  FORMAT (41HOBICHARACTERISTIC SELECTION SCHEME FAILED)
      WRITE (3,614) ZO,RO
      WRITE (3,7002) (PSI(MNMN),MNMN=1,7),UA,VA,AA,UB,VB,AB,UC,VC,AC,ZZ,
     1DZ,RR,DR,ANG1,ANG2
      SUB=ISUB
      WRITE (3,7002) SUB,ZI(ISUB),RI(ISUB)
7002  FORMAT (4E16.8)
      CALL EXIT
6200  CONTINUE
      IF (NBIC.NE.0) GO TO 7000
      IF (L1.NE.2.OR.LL(1).EQ.1) GO TO 7300
      LL(1)=1
      GO TO 619
7300  CONTINUE
      IF (L1.NE.3) GO TO 7310
      IF (PSI(6).GT.4.2) GO TO 7310
      PSI(6)=5.75959
      GO TO 619
7310  CONTINUE
      CALL DBLTRP(ZZ,RR,ANS)
      UA=ANS(2)
      VA=ANS(3)
      AA=ANS(6)
      ZZZ=ZZ+DZ
      CALL DBLTRP(ZZZ,RR,ANS)
      UB=ANS(2)
      VB=ANS(3)
      AB=ANS(6)
      RRR=RR+DR
      CALL DBLTRP(ZZ,RRR,ANS)
      UC=ANS(2)
      VC=ANS(3)
      AC=ANS(6)
      MM=0
      TPSI=PSI(ISUB)
      XB=ZZ
```

```
      YB=RR
      NOM=5
      CA=NOM
      DO 6210 LM=1,2
6201  DTPSI=.01745
      DTPSI=CA*DTPSI
      TPSI=TPSI+DTPSI
      A1=1.+H*(VB-VA+(AB-AA)*SIN(TPSI))/DZ
      B1=H*(VC-VA+(AC-AA)*SIN(TPSI))/DR
      C1=-(ZZ-ZO+H*(VA+AA*SIN(TPSI)))
      A2=H*(UB-UA+(AB-AA)*COS(TPSI))/DZ
      B2=1.+H*(UC-UA+(AC-AA)*COS(TPSI))/DR
      C2=-(RR-RO+H*(UA+AA*COS(TPSI)))
      DET=A1*B2-A2*B1
      DELX=(B2*C1-B1*C2)/DET
      DELY=(A1*C2-A2*C1)/DET
C
C         TEST FOR SAME REGION
C
      XB1=XB+DELX
      YB1=YB+DELY
      M=COMP(XB,YB,XB1,YB1)
      IF (LM.EQ.2) GO TO 6700
      IF (M.EQ.1) GO TO 6203
      GO TO 6800
6700  CONTINUE
      IF (M.NE.1) GO TO 6203
6800  CONTINUE
      MM=MM+1
      IF (MM.LE.360/NOM) GO TO 6201
612   WRITE (3,613) ITI1
613   FORMAT (44HOFAILED TO FIND 2 POINTS IN THE SAME REGION 21H IN SUBR
     1. NRIT2 AFTER,I4,6H TRIES)
      WRITE (3,614) ZO,RO
614   FORMAT (1X5HZO  =,E15.8,4X5HRO  =,E15.8)
      WRITE (3,6144) LM
```

```
      WRITE (3,6145) M
      WRITE (3,6146) KODE
      WRITE (3,7002) XB,YB,XB1,YB1
 6144 FORMAT (4H LM=,I4)
 6145 FORMAT (3H M=,I4)
 6146 FORMAT (6H KODE=,I4)
      CALL EXIT
 6203 GO TO (6204,6205),LM
 6204 ANG1=TPSI
      MM=0
      GO TO 6210
 6205 ANG2=TPSI-DTPSI
 6210 CONTINUE
      AL=LLL+1
      DO 6300 KK=1,LLL
      ISUB=LL(KK)
      AK=KK
      PSI(ISUB)=ANG1+(ANG2-ANG1)*AK/AL
 6300 CONTINUE
      NBIC=1
      GO TO 619
C
C
 6400 CONTINUE
      IF (L1.EQ.2.OR.L1.EQ.3) GO TO 642
      CALL NRIT2(ZI(8),RI(8),ZZ,DZ,RR,DR,EPI1,EPI2,FGOF5,ITI1,KODE)
      IF (KODE.EQ.0) GO TO 635
      ISUB=8
      WRITE (3,622) ITI1,I,J,ISUB,ZO,RO,ZZ,RR,ZI(8),RI(8)
 622  FORMAT (27HOFAILED TO FIND ZI,RI AFTER,I4,6H TRIES,3X2HI=,I4,3X2HJ
     1=,I4,3X5HISUB=,I4/1X3HZO=,E15.8,6X3HRO=,E15.8/1X3HZZ=,E15.8,6X3HRR
     1=,E15.8/1X3HZI=,E15.8,6X3HRI=,E15.8/1H1)
      CALL EXIT
C
C
 635  CALL DBLTRP(ZI(8),RI(8),ANS)
```

```
      PI(8)=ANS(1)
      UI(8)=ANS(2)
      VI(8)=ANS(3)
      RHOI(8)=ANS(4)
      EI(8)=ANS(5)
      AI(8)=ANS(6)
C
642   DO 670 IL=1,LLL
      NN=LL(IL)
      M=PART(1,ZI(NN),RI(NN),ZX,RX,DELTA,NDEL)
      IF (M.EQ.1) GO TO 645
      PUR(NN)=0.
      PVR(NN)=0.
      GO TO 648
645   CALL DBLTRP(ZX,RX,ANS)
      DEN=RX-RI(NN)
      PUR(NN)=(ANS(2)-UI(NN))/DEN
      PVR(NN)=(ANS(3)-VI(NN))/DEN
648   M=PART(2,ZI(NN),RI(NN),ZX,RX,DELTA,NDEL)
      IF (M.EQ.1) GO TO 650
      PUZ(NN)=0.
      PVZ(NN)=0.
      GO TO 655
650   CALL DBLTRP(ZX,RX,ANS)
      DEN=ZX-ZI(NN)
      PUZ(NN)=(ANS(2)-UI(NN))/DEN
      PVZ(NN)=(ANS(3)-VI(NN))/DEN
655   S(NN)=SPSI(NN)**2*PUR(NN)-CPSI(NN)*SPSI(NN)*(PVR(NN)+PUZ(NN))+CPSI
     1(NN)**2*PVZ(NN)
C
      IF (ABS(RI(NN)).GT.EPS) GO TO 660
      CON=PUR(NN)
      GO TO 662
660   CON=UI(NN)/RI(NN)
662   S(NN)=-RHOI(NN)*H*AI(NN)**2*(S(NN)+CON)+PI(NN)+RHOI(NN)*AI(NN)*CPS
     1I(NN)*UI(NN)+RHOI(NN)*AI(NN)*SPSI(NN)*VI(NN)
```

```
670   CONTINUE
1005  CONTINUE
1002  FORMAT (4E16.8)
      KICK=670
      CALL DVCHK(KQ)
      IF (KQ.EQ.1) GO TO 9980
C
C         COMPUTE NEW P,U,V
C
      GO TO (690,692,695,698),L1
690   DUO=0.
      U02=0.
      V02=(S(4)-S(6))/(RHOI(4)*AI(4)*SPSI(4)-RHOI(6)*AI(6)*SPSI(6))
      P02=S(4)-RHOI(4)*AI(4)*SPSI(4)*V02
      GO TO 700
C
C
692   DPO=0.
      P02=0.
      L=LL(1)
      TMP1=RHOI(7)*RHOI(L)*AI(7)*AI(L)*(CPSI(7)*SPSI(L)-CPSI(L)*SPSI(7))
      V02=(S(L)*RHOI(7)*AI(7)*CPSI(7)-S(7)*RHOI(L)*AI(L)*CPSI(L))/TMP1
      U02=(S(L)-RHOI(L)*AI(L)*SPSI(L)*V02)/(RHOI(L)*AI(L)*CPSI(L))
      GO TO 700
C
C
695   DPO=0.
      P02=0.
      TMP1=RHOI(7)*RHOI(6)*AI(7)*AI(6)*(CPSI(7)*SPSI(6)-SPSI(7)*CPSI(6))
      V02=(S(6)*RHOI(7)*AI(7)*CPSI(7)-S(7)*RHOI(6)*AI(6)*CPSI(6))/TMP1
      U02=(S(6)-RHOI(6)*AI(6)*SPSI(6)*V02)/(RHOI(6)*AI(6)*CPSI(6))
      GO TO 700
698   CONTINUE
      L=LL(1)
      TMP1=RHOI(4)*AI(4)*CPSI(4)-RHOI(L)*AI(L)*CPSI(L)
      TMP2=RHOI(4)*AI(4)*SPSI(4)-RHOI(L)*AI(L)*SPSI(L)
```

```
      TMP3=RHOI(6)*AI(6)*CPSI(6)-RHOI(L)*AI(L)*CPSI(L)
      TMP4=RHOI(6)*AI(6)*SPSI(6)-RHOI(L)*AI(L)*SPSI(L)
      V02=((S(4)-S(L))*TMP3-(S(6)-S(L))*TMP1)/(TMP3*TMP2-TMP1*TMP4)
      U02=(S(4)-S(L)-TMP2*V02)/TMP1
      P02=S(6)-RHOI(6)*AI(6)*CPSI(6)*U02-RHOI(6)*AI(6)*SPSI(6)*V02
 700  KICK=700
      CALL DVCHK(KQ)
      IF (KQ.EQ.1) GO TO 9980
C
C
C         ITERATE FOR RHOO,EO
C
 705  ITI33=ITI3
      ITI44=ITI4
      KM=1
 708  CONTINUE
      CALL EQOSI(P02,PGRHO,PGE,BIGG,CHECK,KRTT,A02,E02,RHOO2,KM,EPS)
      IF (KRTT.EQ.1) GO TO 871
 725  T1=RHOO-RHOI(8)
      T2=PI(8)/RHOI(8)**2
      BIGH=EI(8)+T2*T1-EO
      PHE=-1.
      PHRHO=T2
      KICK=725
      CALL DVCHK(KQ)
      IF (KQ.EQ.1) GO TO 9980
C
C         COMPUTE NEW EO,RHOO
C
      DOWN=PGE*PHRHO-PGRHO*PHE
      DEO=(-BIGG*PHRHO+BIGH*PGRHO)/DOWN
      DRHOO=(-BIGH*PGE+BIGG*PHE)/DOWN
      E02=EO+DEO
      RHOO2=RHOO+DRHOO
C
C         CHECK E02,RHOO2 FOR CONVERGENCE
```

```
      KICK=726
      CALL DVCHK(KQ)
      IF (KQ.EQ.1) GO TO 9980
C
      IF (ABS(DEO/EO).LT.EPI7) GO TO 726
      IF (ABS(DEO).GT..01*EPI7) GO TO 730
  726 IF (ABS(DRHOO/RHOO).LE.EPI6) GO TO 740
      IF (ABS(DRHOO).LT.EPI6) GO TO 740
  730 ITI33=ITI33-1
      IF (ITI33.NE.0) GO TO 735
      WRITE (6,732) ITI3,I,J,ZO,RO,PO,UO,VO,RHOO,EO,PO2,UO2,VO2,RHOO2,EO
     12
  732 FORMAT (33HOEO,RHOO FAILED TO CONVERGE AFTER,I4,6H TRIES/1X2HI=,I4
     1,4X2HJ=,I4,4X2HZ=,E15.8,4X2HR=,E15.8/5X2HPO18X2HUO18X2HVO18X4HRHOO
     116X2HEO/5X3HPO217X3HUO217X3HVO217X5HRHOO215X3HEO2//(5E20.8))
      WRITE (3,1)
      CALL EXIT
  735 EO=EO2
      RHOO=RHOO2
      KM=0
      GO TO 708
C
C         CHECK FOR PROPER EQUATIONS
C
  740 CONTINUE
      PGE=-PGE
      PGRHO=-PGRHO
      IF (RHOO2.GE.RHOSTR) GO TO 750
      IF (EO2.LT.EPRS) GO TO 750
  742 CHECK2=0
      GO TO 752
  750 CHECK2=1
  752 AO2=SQRT(+PGRHO+PO2*PGE/RHOO2**2)
      IF (CHECK.EQ.CHECK2) GO TO 870
      ITI44=ITI44-1
      IF (ITI44.NE.0) GO TO 770
```

```
      WRITE (3,755) ITI4,I,J,Z0,R0,P0,U0,V0,RHO0,E0,A0,P02,U02,V02,RHO02
     1,E02,A02
755   FORMAT (38H0FAILED TO USE CORRECT EQUATIONS AFTER,I4,6H TRIES/1X2H
     1I=,I4,4X2HJ=,I4,4X2HZ=,E15.8,4X2HR=,E15.8/5X2HP018X2HU018X2HV018X4
     1HRHO016X2HE018X2HA0/5X3HP0217X3HU0217X3HV0217X5HRHO0215X3HE0217X3H
     1A02//(6E20.8))
      WRITE (3,1)
      CALL EXIT
770   KICK=770
      CALL DVCHK(KQ)
      IF (KQ.EQ.1) GO TO 9980
      ITI33=ITI3
      GO TO 735
C
C          ALL VALUES HAVE CONVERGED FOR 1 INTERIOR POINT
C
871   KRTT=0
870   XMESH2(I,J,1)=P02
      XMESH2(I,J,2)=U02
      XMESH2(I,J,3)=V02
      XMESH2(I,J,4)=RHO02
      XMESH2(I,J,5)=E02
      XMESH2(I,J,6)=A02
      KICK=900
      CALL DVCHK(KQ)
      IF (KQ.EQ.1) GO TO 9980
900   CONTINUE
905   CONTINUE
      IF (ITS3.EQ.1) GO TO 950
      CALL ITRP
      RETURN
950   CONTINUE
9980  WRITE (3,9985) KICK
      WRITE (3,614) Z0,R0
9985  FORMAT (32H0DIVIDE CHECK NEAR STATEMENT NO.,I5,15H IN SUBR. INTER/
     11H1)
```

```
      CALL EXIT
      RETURN
      END
      SUBROUTINE EQOS1(PRHO,PPP,PVV,PEE,TEE,TRHO,KICK)
      COMMON CASEID(14),ITS1,ITS2,ITS3,ITS4,ITI1,ITI2,ITI3,ITI4,EPS1,EPS
     12,EPS3,EPS4,EPS5,EPS6,EPI1,EPI2,EPI3,EPI4,EPI5,EPI6,EPI7,VP,AR,LEN
     1GTH,APR,BPR,BIGAPR,BIGBPR,ESTAR,ALPHA,BETA,RHOSTR,EPRS,RHOS
      COMMON XMESH(20,20,6),XMESH2(20,20,6),Z(20),R(20),SURF(15,8),SURF2
     1(15,8),TAB(15,14,2),TAB2(15,14,2),SPART(15,2,2),RARF(15,11),RARF2(
     115,4),RPART(15,2)
C
C
      COMMON Z0,R0,P0,U0,V0,L0,M0,RHO0,E0,A0,UBAR0,VBAR0
C
      COMMON NP,NT,NR,NI,NDEL,ISUB
C
      COMMON ZMIN,ZMAX,RMIN,RMAX,RADIUS,GZ,GR,DELTA,H
      COMMON DIRCOS
      COMMON TIME
      COMMON IRARF
      COMMON KSTOP
      COMMON TPSI
      COMMON KKK
C
C
      REAL L0,M0,LENGTH,MU,K0
      RHO=RHOSTR
      E=VP**2/8.
      DO 100 M=1,100
      ETA=RHO/RHOSTR
      MU=ETA-1.
      G=-RHOSTR*(VP/2.)**2+((APR+BPR/(E/(ESTAR*ETA**2)+1.))*E*RHO+BIGAPR
     1*MU+BIGBPR*MU**2)*(1.-RHOSTR/RHO)
      DERIVG=((APR+BPR/(E/(ESTAR*ETA**2)+1.))*E+BIGAPR/RHOSTR+2.*BIGBPR*
     1MU/RHOSTR+2.*E**2*BPR/(ESTAR*ETA**2*(E/(ESTAR*ETA**2)+1.)**2))*(1.
     1-RHOSTR/RHO)+((APR+BPR/(E/(ESTAR*ETA**2)+1.))*E*RHO+BIGAPR*MU+BIGB
```

```
     1PR*MU**2)*RHOSTR/RHO**2
      DLTRHO=-G/DERIVG
      RHO=RHO+DLTRHO
      IF(ABS(DLTRHO).LT.1.E-07) GO TO 101
C     IF (ABS(DLTRHO).LT.1.E-06) GO TO 101
100   CONTINUE
      KICK=2200
      GO TO 9980
101   CONTINUE
      PRHO=RHO
      TRHO=RHO
      PEE=E
      TEE=E
      PVV=VP/2.
      PPP=(APR+BPR/(E/(ESTAR*ETA**2)+1.))*E*RHO+BIGAPR*MU+BIGBPR*MU**2
9980  RETURN
      END
      SUBROUTINE EQOS2(PPP,PRHO,PEE)
      COMMON CASEID(14),ITS1,ITS2,ITS3,ITS4,ITI1,ITI2,ITI3,ITI4,EPS1,EPS
     12,EPS3,EPS4,EPS5,EPS6,EPI1,EPI2,EPI3,EPI4,EPI5,EPI6,EPI7,VP,AR,LEN
     1GTH,APR,BPR,BIGAPR,BIGBPR,ESTAR,ALPHA,BETA,RHOSTR,EPRS,RHOS
      COMMON XMESH(20,20,6),XMESH2(20,20,6),Z(20),R(20),SURF(15,8),SURF2
     1(15,8),TAB(15,14,2),TAB2(15,14,2),SPART(15,2,2),RARF(15,11),RARF2(
     115,4),RPART(15,2)
C
C
      COMMON Z0,R0,P0,U0,V0,L0,M0,RHO0,E0,A0,UBAR0,VBAR0
C
      COMMON NP,NT,NR,NI,NDEL,ISUB
C
      COMMON ZMIN,ZMAX,RMIN,RMAX,RADIUS,GZ,GR,DELTA,H
      COMMON DIRCOS
      COMMON TIME
      COMMON IRARF
      COMMON KSTOP
C
```

```
      COMMON TPSI
      COMMON KKK
C
      REAL LO,MO,LENGTH,MU,KO
      P=PPP
      RHO=PRHO
      E=PEE
      ETA=RHO/RHOSTR
      MU=ETA-1.
      EE=E/(ESTAR*ETA**2)+1.
      PGRHO=E*(APR+BPR/EE)+BIGAPR/RHOSTR+(2.*BIGBPR*MU)/RHOSTR+(2.*E**2*
     1BPR)/(ESTAR*ETA**2*EE**2)
      PGE=(APR+BPR/EE)*RHO-(E*BPR*RHO)/(ESTAR*ETA**2*EE**2)
      AR=SQRT(PGRHO+PGE*P/RHO**2)
      RETURN
      END
      SUBROUTINE EQOS3(RHO,AA,E,P)
      COMMON CASEID(14),ITS1,ITS2,ITS3,ITS4,ITI1,ITI2,ITI3,ITI4,EPS1,EPS
     12,EPS3,EPS4,EPS5,EPS6,EPI1,EPI2,EPI3,EPI4,EPI5,EPI6,EPI7,VP,AR,LEN
     1GTH,APR,BPR,BIGAPR,BIGBPR,ESTAR,ALPHA,BETA,RHOSTR,EPRS,RHOS
      COMMON XMESH(20,20,6),XMESH2(20,20,6),Z(20),R(20),SURF(15,8),SURF2
     1(15,8),TAB(15,14,2),TAB2(15,14,2),SPART(15,2,2),RARF(15,11),RARF2(
     115,4),RPART(15,2)
C
C
      COMMON ZO,RO,PO,UO,VO,LO,MO,RHOO,EO,AO,UBARO,VBARO
C
      COMMON NP,NT,NR,NI,NOEL,ISUB
C
      COMMON ZMIN,ZMAX,RMIN,RMAX,RADIUS,GZ,GR,DELTA,H
      COMMON DIRCOS
      COMMON TIME
      COMMON IRARF
      COMMON KSTOP
      COMMON TPSI
      COMMON KKK
```

```
C
C
      REAL LO,MO,LENGTH,MU,KO
70    ETA=RHO/RHOSTR
      MU=ETA-1.
      EE=E/(ESTAR*ETA**2)+1.
      IF (RHO.GT.RHOSTR) GO TO 72
      IF (E.GE.EPRS) GO TO 74
72    PGRHO=E*(APR+BPR/EE)+BIGAPR/RHOSTR+(2.*BIGBPR*MU)/RHOSTR+(2.*E**2*
     1BPR)/(ESTAR*ETA**2*EE**2)
      PGE=(APR+BPR/EE)*RHO-(E*BPR*RHO)/(ESTAR*ETA**2*EE**2)
      GO TO 75
74    C1=RHOSTR/RHO-1.
      C2=EXP(-BETA*C1)
      C3=EXP(-ALPHA*C1**2)
      T1=(BPR*E*RHO)/EE+BIGAPR*MU*C2
      T2=2.*ALPHA*C1*(RHOSTR/(RHO**2))
      T3=BPR*E/EE
      T4=(2.*E)/(ESTAR*ETA**2*EE)
      T4=T3*T4
      T5=(BIGAPR*C2)/RHOSTR
      T6=(BIGAPR*MU*BETA*RHOSTR*C2)/(RHO**2)
      PGRHO=APR*E+C3*(T1*T2+T3+T4+T5+T6)
      T7=(BPR*RHO)/EE
      PGE=APR*RHO+C3*(T7-T7*(E/(ESTAR*ETA**2*EE)))
75    AA=SQRT(PGRHO+PGE*P/RHO**2)
      RETURN
      END
      SUBROUTINE EQOSS(PFR,PFE)
      COMMON CASEID(14),ITS1,ITS2,ITS3,ITS4,ITI1,ITI2,ITI3,ITI4,EPS1,EPS
     12,EPS3,EPS4,EPS5,EPS6,EPI1,EPI2,EPI3,EPI4,EPI5,EPI6,EPI7,VP,AR,LEN
     1GTH,APR,BPR,BIGAPR,BIGBPR,ESTAR,ALPHA,BETA,RHOSTR,EPRS,RHOS
      COMMON XMESH(20,20,6),XMESH2(20,20,6),Z(20),R(20),SURF(15,8),SURF2
     1(15,8),TAB(15,14,2),TAB2(15,14,2),SPART(15,2,2),RARF(15,11),RARF2(
     115,4),RPART(15,2)
C
```

```
C                                                                       SUB8   9
      COMMON Z0,R0,P0,U0,V0,L0,M0,RHO0,E0,A0,UBAR0,VBAR0                SUB8  10
C                                                                       SUB8  11
      COMMON NP,NT,NR,NI,NDEL,ISUB                                      SUB8  12
C                                                                       SUB8  13
      COMMON ZMIN,ZMAX,RMIN,RMAX,RADIUS,GZ,GR,DELTA,H                   SUB8  14
      COMMON DIRCOS                                                     SUB8  15
      COMMON TIME                                                       SUB8  16
      COMMON IRARF                                                      SUB8  17
      COMMON KSTOP                                                      SUB8  18
      COMMON TPSI                                                       SUB8  19
      COMMON KKK                                                        SUB8  20
C                                                                       SUB8  21
C                                                                       SUB8  22
      REAL L0,M0,LENGTH,MU,K0                                           SUB8  23
250   ETA=RHO0/RHOSTR                                                   SUB8  24
      MU=ETA-1.                                                         SUB8  25
C                                                                       SUB8  26
C                                                                       SUB8  27
      EPP=E0/(ESTAR*ETA**2)+1.                                          SUB8  28
      TMP=APR+BPR/EPP                                                   SUB8  29
      TMP1=BPR/(ESTAR*ETA**2*EPP**2)                                    SUB8  30
      PFR=TMP*E0+(BIGAPR+2.*BIGBPR*MU)/RHOSTR+2.*E0**2*TMP1             SUB8  31
      PFE=TMP*RHO0-E0*RHO0*TMP1                                         SUB8  32
      RETURN                                                            SUB8  33
      END                                                               SUB8  34
      SUBROUTINE EQOSP(RHO02,E02,P02)                                   SUB9   1
      COMMON CASEID(14),ITS1,ITS2,ITS3,ITS4,ITI1,ITI2,ITI3,ITI4,EPS1,EPSSUB9   2
     12,EPS3,EPS4,EPS5,EPS6,EPI1,EPI2,EPI3,EPI4,EPI5,EPI6,EPI7,VP,AR,LENSUB9   3
     1GTH,APR,BPR,BIGAPR,BIGBPR,ESTAR,ALPHA,BETA,RHOSTR,EPRS,RHOS       SUB9   4
      COMMON XMESH(20,20,6),XMESH2(20,20,6),Z(20),R(20),SURF(15,8),SURF2SUB9   5
     1(15,8),TAB(15,14,2),TAB2(15,14,2),SPART(15,2,2),RARF(15,11),RARF2(SUB9   6
     115,4),RPART(15,2)                                                 SUB9   7
C                                                                       SUB9   8
C                                                                       SUB9   9
      COMMON Z0,R0,P0,U0,V0,L0,M0,RHO0,E0,A0,UBAR0,VBAR0                SUB9  10
```

```
C
      COMMON NP,NT,NR,NI,NDEL,ISUB
C
      COMMON ZMIN,ZMAX,RMIN,RMAX,RADIUS,GZ,GR,DELTA,H
      COMMON DIRCOS
      COMMON TIME
      COMMON IRARF
      COMMON KSTOP
      COMMON TPSI
      COMMON KKK
C
C
      REAL LO,MO,LENGTH,MU,KO
      ETA=RHO02/RHOSTR
      MU=ETA-1.
      P02=E02*RHO02*(APR+(BPR*ESTAR*ETA**2)/(E02+ESTAR*ETA**2))+BIGAPR*M
     1U+BIGBPR*MU**2
      RETURN
      END
      SUBROUTINE EQOSI(P02,PGRHO,PGE,BIGG,CHECK,KRTT,A02,E02,RHO02,KM,EP
     1S)
      COMMON CASEID(14),ITS1,ITS2,ITS3,ITS4,ITI1,ITI2,ITI3,ITI4,EPS1,EPS
     12,EPS3,EPS4,EPS5,EPS6,EPI1,EPI2,EPI3,EPI4,EPI5,EPI6,EPI7,VP,AR,LEN
     1GTH,APR,BPR,BIGAPR,BIGBPR,ESTAR,ALPHA,BETA,RHOSTR,EPRS,RHOS
      COMMON XMESH(20,20,6),XMESH2(20,20,6),Z(20),R(20),SURF(15,8),SURF2
     1(15,8),TAB(15,14,2),TAB2(15,14,2),SPART(15,2,2),RARF(15,11),RARF2(
     115,4),RPART(15,2)
C
C
      COMMON ZO,RO,PO,UO,VO,LO,MO,RHOO,EO,AO,UBARO,VBARO
C
      COMMON NP,NT,NR,NI,NDEL,ISUB
C
      COMMON ZMIN,ZMAX,RMIN,RMAX,RADIUS,GZ,GR,DELTA,H
      COMMON DIRCOS
      COMMON TIME
```

```
      COMMON IRARF
      COMMON KSTOP
      COMMON TPSI
      COMMON KKK
C
C
      REAL LO,MO,LENGTH,MU,KO
      INTEGER CHECK,CHECK2
      IF (KM.EQ.0) GO TO 708
      RHOO=RHOSTR
      TMP1=(APR+BPR)*RHOSTR-PO2/ESTAR
      TMP2=SQRT(TMP1**2+4.*PO2*APR*RHOSTR/ESTAR)
      EO=(-TMP1+TMP2)/(2.*APR*RHOSTR/ESTAR)
      IF (PO2.GT.EPS) GO TO 708
      PO2=0.
      EO2=0.
      RHOO2=RHOSTR
      AO2=SQRT(BIGAPR/RHOSTR)
      KRTT=1
      GO TO 870
  708 KRTT=0
      ETA=RHOO/RHOSTR
      MU=ETA-1.
      EE=EO/(ESTAR*ETA**2)+1.
      IF (RHOO.GT.RHOSTR) GO TO 720
      IF (EO.LT.EPRS) GO TO 720
  715 C1=RHOSTR/RHOO-1.
      BEC1=BETA*C1
      IF (BEC1.LT.10.E10) GO TO 716
      C2=0.0
      GO TO 717
  716 C2=EXP(-BEC1)
  717 C3AL=ALPHA*C1**2
      IF (C3AL.LT.10.E12) GO TO 718
      C3=0.0
      GO TO 719
```

```
718   C3=EXP(-C3AL)                                                     SU10  54
719   CONTINUE                                                          SU10  55
      T1=(BPR*EO*RHOO)/EE+BIGAPR*MU*C2                                  SU10  56
      T2=2.*ALPHA*C1*(RHOSTR/(RHOO**2))                                 SU10  57
      T3=BPR*EO/EE                                                      SU10  58
      T4=(2.*EO)/(ESTAR*ETA**2*EE)                                      SU10  59
      T4=T3*T4                                                          SU10  60
      T5=(BIGAPR*C2)/RHOSTR                                             SU10  61
      T6=(BIGAPR*MU*BETA*RHOSTR*C2)/(RHOO**2)                           SU10  62
      T7=(BPR*RHOO)/EE                                                  SU10  63
      PGRHO=APR*EO+C3*(T1*T2+T3+T4+T5+T6)                               SU10  64
      PGE=APR*RHOO+C3*(T7-T7*(EO/(ESTAR*ETA**2*EE)))                    SU10  65
      BIGG=PO2-APR*EO*RHOO-T1*C3                                        SU10  66
      CHECK=0                                                           SU10  67
      GO TO 725                                                         SU10  68
720   T1=APR+BPR/EE                                                     SU10  69
      T2=(BPR*EO)/(ESTAR*ETA**2*EE**2)                                  SU10  70
      BIGG=PO2-T1*EO*RHOO-BIGAPR*MU-BIGBPR*MU**2                        SU10  71
      PGRHO=T1*EO+BIGAPR/RHOSTR+2.*BIGBPR*MU/RHOSTR+T2*2.*EO            SU10  72
      PGRHO=-PGRHO                                                      SU10  73
      PGE=T1*RHOO-RHOO*T2                                               SU10  74
      PGE=-PGE                                                          SU10  75
      CHECK=1                                                           SU10  76
725   CONTINUE                                                          SU10  77
870   CONTINUE                                                          SU10  78
      RETURN                                                            SU10  79
      END                                                               SU10  80
      SUBROUTINE SOUT2                                                  SU11   1
C                                                                       SU11   2
C            PRINTS 6 LINES OF DISCONTINUITY AT TO                      SU11   3
C                                                                       SU11   4
      COMMON CASEID(14),ITS1,ITS2,ITS3,ITS4,ITI1,ITI2,ITI3,ITI4,EPS1,EPSSU11   5
     12,EPS3,EPS4,EPS5,EPS6,EPI1,EPI2,EPI3,EPI4,EPI5,EPI6,EPI7,VP,AR,LENSU11   6
     1GTH,APR,BPR,BIGAPR,BIGBPR,ESTAR,ALPHA,BETA,RHOSTR,EPRS,RHOS       SU11   7
      COMMON XMESH(20,20,6),XMESH2(20,20,6),Z(20),R(20),SURF(15,8),SURF2SU11   8
     1(15,8),TAB(15,14,2),TAB2(15,14,2),SPART(15,2,2),RARF(15,11),RARF2(SU11   9
```

```
     115,4),RPART(15,2)
C
C
      COMMON Z0,R0,P0,U0,V0,L0,M0,RHO0,E0,A0,UBAR0,VBAR0
C
      COMMON NP,NT,NR,NI,NDEL,ISUB
C
      COMMON ZMIN,ZMAX,RMIN,RMAX,RADIUS,GZ,GR,DELTA,H
      COMMON DIRCOS
      COMMON TIME
      COMMON IRARF
      COMMON KSTOP
      COMMON TPSI
      COMMON KKK
      REAL L0,M0,LENGTH,MU,K0
C
4     FORMAT (///30H CURVES OF DISCONTINUITY AT T0//40X20H--PROJECTILE S
     1HOCK--//)
6     FORMAT (//35X29H--PROJECTILE PARTICLE CURVE--//)
8     FORMAT (//42X16H--TARGET SHOCK--//)
10    FORMAT (//38X25H--TARGET PARTICLE CURVE--//)
12    FORMAT (//42X15H--RAREFACTION--//)
14    FORMAT (//35X30H--RAREFACTION PARTICLE CURVE--//)
16    FORMAT (7X1HZ19X1HR19X1HP19X1HU19X1HV/7X3HRHO17X1HE19X1HA19X1HL19X
     11HM//)
18    FORMAT (7X1HZ19X1HR//)
20    FORMAT (7X1HZ19X1HR19X1HL19X1HM//)
30    FORMAT (5E20.8/5E20.8//)
35    FORMAT (2E20.8)
38    FORMAT (4E20.8)
39    FORMAT (//35X16H--FREE SURFACE--//)
40    FORMAT (1H1)
      WRITE (3,4)
      WRITE (3,16)
      WRITE (3,30) ((TAB2(I,J,1),J=1,10),I=1,NP)
      WRITE (3,6)
```

```
      WRITE (3,18)
      WRITE (3,35) ((SPART(I,J,1),J=1,2),I=1,NP)
      WRITE (3,8)
      WRITE (3,16)
      WRITE (3,30) ((TAB2(I,J,2),J=1,10),I=1,NT)
      WRITE (3,10)
      WRITE (3,18)
      WRITE (3,35) ((SPART(I,J,2),J=1,2),I=1,NT)
      WRITE (3,12)
      WRITE (3,20)
      WRITE (3,38) ((RARF2(I,J),J=1,4),I=1,NR)
      WRITE (3,14)
      WRITE (3,39)
      WRITE (3,35) ((SURF2(I,J),J=1,2),I=1,NP)
      WRITE (3,40)
      RETURN
      END
      SUBROUTINE SOUT
C
C       PRINTS 4 LINES OF DISCONTINUITY AT TO-H
C
      COMMON CASEID(14),ITS1,ITS2,ITS3,ITS4,ITI1,ITI2,ITI3,ITI4,EPS1,EPS
     12,EPS3,EPS4,EPS5,EPS6,EPI1,EPI2,EPI3,EPI4,EPI5,EPI6,EPI7,VP,AR,LEN
     1GTH,APR,BPR,BIGAPR,BIGBPR,ESTAR,ALPHA,BETA,RHOSTR,EPRS,RHOS
      COMMON XMESH(20,20,6),XMESH2(20,20,6),Z(20),R(20),SURF(15,8),SURF2
     1(15,8),TAB(15,14,2),TAB2(15,14,2),SPART(15,2,2),RARF(15,11),RARF2(
     115,4),RPART(15,2)
C
C
      COMMON ZO,RO,PO,UO,VO,LO,MO,RHOO,EO,AO,UBARO,VBARO
C
      COMMON NP,NT,NR,NI,NDEL,ISUB
C
      COMMON ZMIN,ZMAX,RMIN,RMAX,RADIUS,GZ,GR,DELTA,H
      COMMON DIRCOS
      COMMON TIME
```

```
      COMMON IRARF                                                      SU12  20
      COMMON KSTOP                                                      SU12  21
      COMMON TPSI                                                       SU12  22
      COMMON KKK                                                        SU12  23
      REAL LO,MO,LENGTH,MU,KO                                           SU12  24
C                                                                       SU12  25
4     FORMAT (///32H CURVES OF DISCONTINUITY AT TO-H//40X20H--PROJECTILESU12  26
     1 SHOCK--//)                                                       SU12  27
6     FORMAT (//42X16H--TARGET SHOCK--//)                               SU12  28
8     FORMAT (//42X15H--RAREFACTION--//)                                SU12  29
10    FORMAT (7X1HZ19X1HR19X1HP19X1HU19X1HV/7X3HRHO17X1HE19X1HA19X1HL19XSU12  30
     11HM//)                                                            SU12  31
15    FORMAT (5E20.8/5E20.8//)                                          SU12  32
18    FORMAT (1H1)                                                      SU12  33
21    FORMAT (//35X16H--FREE SURFACE--//)                               SU12  34
25    FORMAT (2E20.8)                                                   SU12  35
      WRITE (3,4)                                                       SU12  36
      WRITE (3,10)                                                      SU12  37
      WRITE (3,15) ((TAB(I,J,1),J=1,10),I=1,NP)                         SU12  38
      WRITE (3,6)                                                       SU12  39
      WRITE (3,10)                                                      SU12  40
      WRITE (3,15) ((TAB(I,J,2),J=1,10),I=1,NT)                         SU12  41
      WRITE (3,8)                                                       SU12  42
      WRITE (3,10)                                                      SU12  43
      WRITE (3,15) ((RARF(I,J),J=1,10),I=1,NR)                          SU12  44
      WRITE (3,21)                                                      SU12  45
      WRITE (3,25) ((SURF(I,J),J=1,2),I=1,NP)                           SU12  46
      WRITE (3,18)                                                      SU12  47
      RETURN                                                            SU12  48
      END                                                               SU12  49
      SUBROUTINE PRINT(BL,ZTAB,RTAB,KK)                                 SU13   1
C         PRINTS INTERIOR REGION                                        SU13   2
C                                                                       SU13   3
      COMMON CASEID(14),ITS1,ITS2,ITS3,ITS4,ITI1,ITI2,ITI3,ITI4,EPS1,EPSSU13   4
     12,EPS3,EPS4,EPS5,EPS6,EPI1,EPI2,EPI3,EPI4,EPI5,EPI6,EPI7,VP,AR,LENSU13   5
     1GTH,APR,BPR,BIGAPR,BIGBPR,ESTAR,ALPHA,BETA,RHOSTR,EPRS,RHOS       SU13   6
```

```
      COMMON XMESH(20,20,6),XMESH2(20,20,6),Z(20),R(20),SURF(15,8),SURF2
     1(15,8),TAB(15,14,2),TAB2(15,14,2),SPART(15,2,2),RARF(15,11),RARF2(
     115,4),RPART(15,2)
C
C
      COMMON Z0,R0,P0,U0,V0,L0,M0,RHO0,E0,A0,UBAR0,VBAR0
C
      COMMON NP,NT,NR,NI,NDEL,ISUB
C
      COMMON ZMIN,ZMAX,RMIN,RMAX,RADIUS,GZ,GR,DELTA,H
      COMMON DIRCOS
      COMMON TIME
      COMMON IRARF
      COMMON KSTOP
      COMMON TPSI
      COMMON KKK
      REAL L0,M0,LENGTH,MU,K0
C
      DIMENSION BL(20,20,6),ZTAB(20),RTAB(20)
C
      DO 15 I=1,20
      DO 15 J=1,20
      IF (ABS(BL(I,J,1))+ABS(BL(I,J,2))+ABS(BL(I,J,3)))  20,15,20
15    CONTINUE
      WRITE (3,18)
18    FORMAT (15H1TABLES ALL = 0/1H1)
      CALL EXIT
20    I1=I
      DO 30 I=I1,20
      IF (ABS(BL(I,1,1))+ABS(BL(I,1,2))+ABS(BL(I,1,3)))  30,22,30
22    DO 25 J=1,20
      IF (ABS(BL(I,J,1))+ABS(BL(I,J,2))+ABS(BL(I,J,3)))  30,25,30
25    CONTINUE
      I2=I-1
      GO TO 35
30    CONTINUE
```

```
      I2=20                                                             SU13  43
35    DO 45 J=1,20                                                      SU13  44
      IF (ABS(BL(I1,J,1))+ABS(BL(I1,J,2))+ABS(BL(I1,J,3)))  45,37,45    SU13  45
37    DO 40 I=I1,I2                                                     SU13  46
      IF (ABS(BL(I,J,1))+ABS(BL(I,J,2))+ABS(BL(I,J,3)))  45,40,45       SU13  47
40    CONTINUE                                                          SU13  48
      J2=J-1                                                            SU13  49
      GO TO 50                                                          SU13  50
45    CONTINUE                                                          SU13  51
      J2=20                                                             SU13  52
50    J1=1                                                              SU13  53
C                                                                       SU13  54
C         PRINT TABLE                                                   SU13  55
C                                                                       SU13  56
      GO TO (52,56),KK                                                  SU13  57
52    WRITE (3,53)                                                      SU13  58
53    FORMAT (//24H0INTERIOR REGION AT TO-H///)                         SU13  59
      GO TO 62                                                          SU13  60
56    WRITE (3,57)                                                      SU13  61
57    FORMAT (//22H0INTERIOR REGION AT TO///)                           SU13  62
62    DO 70 I=I1,I2                                                     SU13  63
      WRITE (3,64) ZTAB(I)                                              SU13  64
64    FORMAT (///7H0ZTAB =,F10.4//7X1HR9X1HP17X1HU17X1HV17X3HRHO15X1HE17SU13  65
     1X1HA//)                                                           SU13  66
      DO 69 J=J1,J2                                                     SU13  67
      WRITE (3,68) RTAB(J),(BL(I,J,K),K=1,6)                            SU13  68
68    FORMAT (F12.4,6E18.8)                                             SU13  69
69    CONTINUE                                                          SU13  70
70    CONTINUE                                                          SU13  71
80    WRITE (3,82)                                                      SU13  72
82    FORMAT (1H1)                                                      SU13  73
      RETURN                                                            SU13  74
      END                                                               SU13  75
      SUBROUTINE NRIT2(X,Y,X0,DX,Y0,DY,EX,EY,FGOF,IT,KODE)              SU14   1
C                                                                       SU14   2
C         NEWTON-RAPHSON METHOD FOR SOLUTION OF                         SU14   3
```

```
C          TWO NON LINEAR EQUATIONS IN TWO UNKNOWNS
C
      COMMON CASEID(14),ITS1,ITS2,ITS3,ITS4,ITI1,ITI2,ITI3,ITI4,EPS1,EPS
     12,EPS3,EPS4,EPS5,EPS6,EPI1,EPI2,EPI3,EPI4,EPI5,EPI6,EPI7,VP,AR,LEN
     1GTH,APR,BPR,BIGAPR,BIGBPR,ESTAR,ALPHA,BETA,RHOSTR,EPRS,RHOS
      COMMON XMESH(20,20,6),XMESH2(20,20,6),Z(20),R(20),SURF(15,8),SURF2
     1(15,8),TAB(15,14,2),TAB2(15,14,2),SPART(15,2,2),RARF(15,11),RARF2(
     115,4),RPART(15,2)
C
C
      COMMON ZO,RO,PO,UO,VO,LO,MO,RHOO,EO,AO,UBARO,VBARO
C
      COMMON NP,NT,NR,NI,NDEL,ISUB
C
      COMMON ZMIN,ZMAX,RMIN,RMAX,RADIUS,GZ,GR,DELTA,H
      COMMON DIRCOS
      COMMON TIME
      COMMON IRARF
      COMMON KSTOP
      COMMON TPSI
      COMMON KKK
      REAL LO,MO,LENGTH,MU,KO
C
      XB=XO
      YB=YO
      DXX=DX
      DYY=DY
      DELX1=0
      DELY1=0
      KODE=0
1     CONTINUE
      DO 50 I=1,IT
      KK=0
      XX=XB+DXX
      YY=YB+DYY
C
```

```
C
      CALL FGOF(XB,YY,F2,G2)
      CALL FGOF(XX,YB,F1,G1)
      CALL FGOF(XB,YB,F0,G0)
      A1=(F1-F0)/DXX
      B1=(F2-F0)/DYY
      C1=-F0
      A2=(G1-G0)/DXX
      B2=(G2-G0)/DYY
      C2=-G0
      DET=A1*B2-A2*B1
      IF (DET.EQ.0.) GO TO 920
      DELX=(B2*C1-B1*C2)/DET
      DELY=(A1*C2-A2*C1)/DET
      IF (ABS(DELX).GT..001) GO TO 8
      DELX=0.
8     IF (ABS(DELY).GT..001) GO TO 9
      DELY=0.
9     CONTINUE
      SDEL=ABS(DELX+DELX1)+ABS(DELY+DELY1)
      DELX1=DELX
      DELY1=DELY
C
C         TEST FOR SAME REGION
C
      DO 10 J=1,IT
      XB1=XB+DELX
      YB1=YB+DELY
      IF (YB1.LE.0.)YB1=0.
      M=COMP(XB,YB,XB1,YB1)
      IF (M.EQ.1) GO TO 15
11    CONTINUE
      KK=1
      DELX=.5*DELX
      DELY=.5*DELY
10    CONTINUE
```

```
      GO TO 930
15    IF (ABS(XB-XB1).GT.EX) GO TO 45
      IF (ABS(YB-YB1).GT.EY) GO TO 45
      IF (KK.NE.0) GO TO 45
      X=XB1
      Y=YB1
      KODE=0
      RETURN
45    CONTINUE
      IF (KODE.NE.1) GO TO 46
      IF (SDEL.GT.EPI1) GO TO 46
      DELX=.5*DELX
      DELY=.5*DELY
      GO TO 9
46    XB=XB1
      YB=YB1
      DEL=DELTA
      DO 70 N=1,NDEL
      XB2=XB+DEL
      M=COMP(XB,YB,XB2,YB)
      IF (M.NE.1) GO TO 55
      DXX=DEL
      GO TO 80
55    XB2=XB-DEL
      M=COMP(XB,YB,XB2,YB)
      IF (M.NE.1) GO TO 60
      DXX=-DEL
      GO TO 80
60    DEL=.5*DEL
70    CONTINUE
      GO TO 980
80    DEL=DELTA
      DO 100 N=1,NDEL
      YB2=YB+DEL
      M=COMP(XB,YB,XB,YB2)
      IF (M.NE.1) GO TO 85
```

```
      DYY=DEL                                                           SU14 112
      GO TO 50                                                          SU14 113
85    YB2=YB-DEL                                                        SU14 114
      M=COMP(XB,YB,XB,YB2)                                              SU14 115
      IF (M.NE.1) GO TO 90                                              SU14 116
      DYY=-DEL                                                          SU14 117
      GO TO 50                                                          SU14 118
90    DEL=.5*DEL                                                        SU14 119
100   CONTINUE                                                          SU14 120
      GO TO 990                                                         SU14 121
50    CONTINUE                                                          SU14 122
      X=XB1                                                             SU14 123
      Y=YB1                                                             SU14 124
      IF (KODE.EQ.1) RETURN                                             SU14 125
      KODE=1                                                            SU14 126
      GO TO 1                                                           SU14 127
920   WRITE (3,922) I                                                   SU14 128
922   FORMAT (46HODETERMINANT IS 0 IN SUBR. NRIT2 FOR ITERATION,I4)     SU14 129
      GO TO 950                                                         SU14 130
930   KODE=2                                                            SU14 131
      RETURN                                                            SU14 132
950   WRITE (3,952) XO,YO,XB,YB,XB1,YB1,DELX,DELY                       SU14 133
952   FORMAT (1X5HZO  =,E15.8,4X5HRO  =,E15.8/1X5HZB  =,E15.8,4X5HRB  =,SU14 134
     1E15.8/1X5HZB1 =,E15.8,4X5HRB1 =,E15.8/1X5HDELZ=,E15.8,4X5HDELR=,E1SU14 135
     15.8/1H1)                                                          SU14 136
      CALL EXIT                                                         SU14 137
      RETURN                                                            SU14 138
980   KODE=3                                                            SU14 139
      RETURN                                                            SU14 140
990   KODE=4                                                            SU14 141
      RETURN                                                            SU14 142
      END                                                               SU14 143
      FUNCTION COMP(ZP,RP,ZP1,RP1)                                      SU15   1
C                                                                       SU15   2
C         DETERMINES IF 2 POINTS ARE IN THE SAME REGION                 SU15   3
      COMMON CASEID(14),ITS1,ITS2,ITS3,ITS4,ITI1,ITI2,ITI3,ITI4,EPS1,EPSSU15   4
```

```
     12,EPS3,EPS4,EPS5,EPS6,EPI1,EPI2,EPI3,EPI4,EPI5,EPI6,EPI7,VP,AR,LEN
     1GTH,APR,BPR,BIGAPR,BIGBPR,ESTAR,ALPHA,BETA,RHOSTR,EPRS,RHOS
      COMMON XMESH(20,20,6),XMESH2(20,20,6),Z(20),R(20),SURF(15,8),SURF2
     1(15,8),TAB(15,14,2),TAB2(15,14,2),SPART(15,2,2),RARF(15,11),RARF2(
     115,4),RPART(15,2)
C
      COMMON Z0,R0,P0,U0,V0,L0,M0,RHO0,E0,A0,UBAR0,VBAR0
C
      COMMON NP,NT,NR,NI,NDEL,ISUB
C
      COMMON ZMIN,ZMAX,RMIN,RMAX,RADIUS,GZ,GR,DELTA,H
      COMMON DIRCOS
      COMMON TIME
      COMMON IRARF
      COMMON KSTOP
      COMMON TPSI
      COMMON KKK
      REAL L0,M0,LENGTH,MU,K0
      EPS=.0000001
      IF (RP1.LT.0.) GO TO 80
      IF (ZP1.GE.0.) GO TO 4
      IF (RP1.GT.RADIUS) GO TO 80
C
C         FIND CONTROL CONSTANTS FOR ZP,RP
C
4     CONTINUE
      IF (ITS3.EQ.1) GO TO 33
      IF (IRARF.EQ.1) GO TO 13
      M=PICK(ZP,RP,3)
      IF (ZP.GT.RARF(M,1).AND.M.NE.1)M=M-1
      FF=RP-RARF(M+1,2)-(RARF(M,2)-RARF(M+1,2))*(ZP-RARF(M+1,1))/(RARF(M
     1,1)-RARF(M+1,1))
      IF (FF.LT.0.) GO TO 11
10    NN=1
      GO TO 13
11    NN=0
```

```
 13      CONTINUE
         DO 22 K=1,2
         M=PICK(ZP1,RP1,K)
         IF (RP1.LT.TAB(M,2,K).AND.M.NE.1)M=M-1
 5       CONTINUE
         FF=ZP1-TAB(M+1,1,K)-(TAB(M,1,K)-TAB(M+1,1,K))*(RP1-TAB(M+1,2,K))/(
        1TAB(M,2,K)-TAB(M+1,2,K))
         IF (K.EQ.2) GO TO 17
         IF (RP1.GT.RADIUS) GO TO 21
         IF (FF.LT.-EPS) GO TO 90
         GO TO 21
 17      IF (FF.GT.EPS) GO TO 100
 21      IF (RP.GT.RADIUS) GO TO 22
         M=PICK(ZP1,RP1,4)
         FF=ZP1-SURF(M+1,1)-(SURF(M,1)-SURF(M+1,1))*(RP1-SURF(M+1,2))/(SURF
        1(M,2)-SURF(M+1,2))
         IF (FF)  80,22,22
 22      CONTINUE
         IF (IRARF.EQ.1) GO TO 33
         M=PICK(ZP1,RP1,3)
         IF (ZP1.GT.RARF(M,1).AND.M.NE.1)M=M-1
         FF=RP1-RARF(M+1,2)-(RARF(M,2)-RARF(M+1,2))*(ZP1-RARF(M+1,1))/(RARF
        1(M,1)-RARF(M+1,1))
         IF (FF.LT.0.) GO TO 31
 30      NN1=1
         GO TO 32
 31      NN1=0
 32      IF (NN1.NE.NN) GO TO 110
 33      CONTINUE
         COMP=1
         COMP=COMP+.2
         RETURN
 80      COMP=2
         COMP=COMP+.2
         RETURN
 90      COMP=3.
```

```
      COMP=COMP+.2
      RETURN
  100 COMP=4.
      COMP=COMP+.2
      RETURN
  110 COMP=5.
      COMP=COMP+.2
      RETURN
      END
      FUNCTION PICK(ZP,RP,KODE)
C
C         DETERMINES 2 CLOSEST CONSECUTIVE POINTS ON SPECIFIED
C         LINE OF DISCONTINUITY TO A GIVEN POINT
C
      COMMON CASEID(14),ITS1,ITS2,ITS3,ITS4,ITI1,ITI2,ITI3,ITI4,EPS1,EPS
     12,EPS3,EPS4,EPS5,EPS6,EPI1,EPI2,EPI3,EPI4,EPI5,EPI6,EPI7,VP,AR,LEN
     1GTH,APR,BPR,BIGAPR,BIGBPR,ESTAR,ALPHA,BETA,RHOSTR,EPRS,RHOS
      COMMON XMESH(20,20,6),XMESH2(20,20,6),Z(20),R(20),SURF(15,8),SURF2
     1(15,8),TAB(15,14,2),TAB2(15,14,2),SPART(15,2,2),RARF(15,11),RARF2(
     115,4),RPART(15,2)
C
C
      COMMON Z0,R0,P0,U0,V0,L0,M0,RHO0,E0,A0,UBAR0,VBAR0
C
      COMMON NP,NT,NR,NI,NDEL,ISUB
C
      COMMON ZMIN,ZMAX,RMIN,RMAX,RADIUS,GZ,GR,DELTA,H
      COMMON DIRCOS
      COMMON TIME
      COMMON IRARF
      COMMON KSTOP
      COMMON TPSI
      COMMON KKK
      REAL L0,M0,LENGTH,MU,K0
C
      GO TO (5,10,100,300),KODE
```

```
5     NN=NP
      K=1
      GO TO 15
10    NN=NT
      K=2
15    AA=(TAB(1,1,K)-ZP)**2+(TAB(1,2,K)-RP)**2
C
C          SEARCH SHOCK TABLES
C
      DO 60 N=2,NN
      A=(TAB(N,1,K)-ZP)**2+(TAB(N,2,K)-RP)**2
      IF (A.GE.AA) GO TO 23
      AA=A
60    CONTINUE
      PICK=NN-1
      PICK=PICK+.2
      RETURN
23    PICK=N-1
      PICK=PICK+.2
      RETURN
100   AA=(RARF(1,1)-ZP)**2+(RARF(1,2)-RP)**2
C
C          SEARCH RAREFACTION TABLE
C
      DO 200 N=2,NR
      A=(RARF(N,1)-ZP)**2+(RARF(N,2)-RP)**2
      IF (A.GE.AA) GO TO 203
      AA=A
200   CONTINUE
      PICK=NR-1
      PICK=PICK+.2
      RETURN
203   PICK=N-1
      PICK=PICK+.2
      RETURN
300   AA=(SURF(1,1)-ZP)**2+(SURF(1,2)-RP)**2
```

```
C
C     SEARCH FREE SURFACE TABLE
C
      DO 400 N=2,NP
      A=(SURF(N,1)-ZP)**2+(SURF(N,2)-RP)**2
      IF (A.GE.AA) GO TO 303
      AA=A
400   CONTINUE
      PICK=NP-1
      PICK=PICK+.2
      RETURN
303   PICK=N-1
      PICK=PICK+.2
304   CONTINUE
      RETURN
      END
      SUBROUTINE GUESS(KOD1,KOD2,ZP,RP,I2,K2,ZG,RG,DZ,DR)
C
C         DETERMINES STARTING POINT AND DELTAS
C         FOR NEWTON-RAPHSON ITERATION
C
      COMMON CASEID(14),ITS1,ITS2,ITS3,ITS4,ITI1,ITI2,ITI3,ITI4,EPS1,EPS
     12,EPS3,EPS4,EPS5,EPS6,EPI1,EPI2,EPI3,EPI4,EPI5,EPI6,EPI7,VP,AR,LEN
     1GTH,APR,BPR,BIGAPR,BIGBPR,ESTAR,ALPHA,BETA,RHOSTR,EPRS,RHOS
      COMMON XMESH(20,20,6),XMESH2(20,20,6),Z(20),R(20),SURF(15,8),SURF2
     1(15,8),TAB(15,14,2),TAB2(15,14,2),SPART(15,2,2),RARF(15,11),RARF2(
     115,4),RPART(15,2)
C
C
      COMMON Z0,R0,P0,U0,V0,L0,M0,RHO0,E0,A0,UBAR0,VBAR0
C
      COMMON NP,NT,NR,NI,NDEL,ISUB
C
      COMMON ZMIN,ZMAX,RMIN,RMAX,RADIUS,GZ,GR,DELTA,H
      COMMON DIRCOS
      COMMON TIME
```

```
      COMMON IRARF
      COMMON KSTOP
      COMMON TPSI
      COMMON KKK
      REAL LO,MO,LENGTH,MU,KO
C
      KS=0
      IF (KOD1.EQ.2) GO TO 10
      ZG=TAB(I2,1,K2)
      RG=TAB(I2,2,K2)
      IF (IRARF.EQ.1) GO TO 9
2     M=1-(NR-2)*(K2-2)
      FF=RG-RARF(M+1,2)-(RARF(M,2)-RARF(M+1,2))*(ZG-RARF(M+1,1))/(RARF(M
     1,1)-RARF(M+1,1))
      IF (FF.GT.0.) GO TO 9
      ZG=(1.-.02/(RADIUS-RG))*ZG
      RG=RG+.02
      IF (RG.GT.(RADIUS-.01)) GO TO 110
      GO TO 2
9     CONTINUE
      GO TO 50
10    JJJ=NT-1
      IF (ITS3.EQ.1) GO TO 26
      DO 24 M=1,JJJ
      IF (RP.GT.TAB(M+1,2,2).OR.RP.LT.TAB(M,2,2)) GO TO 24
      GO TO 25
24    CONTINUE
25    CONTINUE
      FF=ZP-TAB(M+1,1,2)-(TAB(M,1,2)-TAB(M+1,1,2))*(RP-TAB(M+1,2,2))/(TA
     1B(M,2,2)-TAB(M+1,2,2))
      IF (FF.GT.0.) GO TO 20
26    CONTINUE
      ZG=ZP
      RG=RP
      GO TO 50
20    IK=M
```

```
      M=CROSS(TAB(IK,1,2),TAB(IK,2,2),TAB(IK+1,1,2),TAB(IK+1,2,2),0.,0.,
     1ZP,RP,ZG,RG)
      GO TO (50,920,930),M
C
C           COMPUTE DELTAS
C
50    DEL=DELTA
C
C           Z DELTA
C
      LL=0
52    DO 70 N=1,NDEL
      ZZ=ZG+DEL
      M=COMP(ZG,RG,ZZ,RG)
      IF (M.NE.1) GO TO 55
      DZ=DEL
      GO TO 80
55    ZZ=ZG-DEL
      M=COMP(ZG,RG,ZZ,RG)
      IF (M.NE.1) GO TO 60
      DZ=-DEL
      GO TO 80
60    DEL=.5*DEL
70    CONTINUE
      LL=LL+1
      IF (LL.EQ.3) GO TO 75
      RG=RG-DELTA/5.
      DEL=DELTA
      GO TO 52
75    KOD2=2
      RETURN
80    DEL=DELTA
      IF (KS.EQ.1) GO TO 120
C
C           R DELTA
C
```

```
      LL=0
82    DO 100 N=1,NDEL
      RR=RG+DEL
      M=COMP(ZG,RG,ZG,RR)
      IF (M.NE.1) GO TO 85
      DR=DEL
      IF (KS.EQ.1) GO TO 50
      GO TO 120
85    RR=RG-DEL
      M=COMP(ZG,RG,ZG,RR)
      IF (M.NE.1) GO TO 90
      DR=-DEL
      IF (KS.EQ.1) GO TO 50
      GO TO 120
90    DEL=.5*DEL
100   CONTINUE
108   CONTINUE
      LL=LL+1
      FLL=LL
      IF (LL.EQ.5) GO TO 110
C
104   ZG1=ZG+DELTA/5.*FLL*(-1.)**LL
      M=COMP(ZG,RG,ZG1,RG)
      ZG=ZG1
      IF (M.NE.1) GO TO 108
      KS=1
      GO TO 82
110   KOD2=2
      RETURN
120   KOD2=1
      RETURN
920   WRITE (3,922)
922   FORMAT (42H0ERROR FOR COINCIDENT LINES IN SUBR. GUESS)
      GO TO 950
C
930   WRITE (3,932)
```

```
932   FORMAT (40HOERROR FOR PARALLEL LINES IN SUBR. GUESS)
C
950   WRITE (3,952) KOD1,I2,K2,ZP,RP
952   FORMAT (1X5HKOD1=,I4,4X3HI2=,I4,4X3HK2=,I4/1X3HZP=,E15.8,4X3HRP=,E
     115.8/1H1)
      XYZ=-2.
      ZYX=SQRT(XYZ)
      CALL EXIT
      RETURN
      END
      FUNCTION CROSS(X1,Y1,X2,Y2,X3,Y3,X4,Y4,X,Y)
C
C         FINDS INTERSECTION OF TWO STRAIGHT LINES
C
      EPS=.0000001
      A1=Y2-Y1
      B1=X1-X2
      C1=X1*A1+Y1*B1
      A2=Y4-Y3
      B2=X3-X4
      C2=X3*A2+Y3*B2
      DET=A1*B2-A2*B1
      D1=C1*B2-C2*B1
      D2=A1*C2-A2*C1
      IF (ABS(DET).LE.EPS) GO TO 10
      X=D1/DET
      Y=D2/DET
      CROSS=1
      CROSS=CROSS+.2
      RETURN
10    IF (ABS(D1).GT.EPS) GO TO 20
      IF (ABS(D2).LE.EPS) GO TO 30
20    CROSS=3
      CROSS=CROSS+.2
      RETURN
30    X=X1
```

```
      Y=Y1
      CROSS=2
      CROSS=CROSS+.2
316   CONTINUE
      RETURN
      END
      FUNCTION PART(MODE,ZP,RP,ZX,RX,DELTA,NDEL)
C
C         LOCATES A POINT IN THE SAME REGION AS A GIVEN POINT
C         TO BE USED IN COMPUTING A PARTIAL
C     MODE=1,WITH RESPECT TO R
C     MODE=2,WITH RESPECT TO Z
C
      GO TO (2,4),MODE
2     DR=DELTA
      DZ=0.
      GO TO 8
4     DR=0.
      DZ=DELTA
8     DO 50 NN=1,NDEL
      RR=RP+DR
      ZZ=ZP+DZ
      M=COMP(ZP,RP,ZZ,RR)
      IF (M.EQ.1) GO TO 60
      RR=RP-DR
      ZZ=ZP-DZ
      M=COMP(ZP,RP,ZZ,RR)
      IF (M.EQ.1) GO TO 60
      DZ=DZ*.5
      DR=DR*.5
50    CONTINUE
      PART=2
      PART=PART+.2
      RETURN
60    ZX=ZZ
      RX=RR
```

```
      PART=1
      PART=PART+.2
      RETURN
      END
      FUNCTION PICK2(ZP,RP,KODE)
C
C          DETERMINES 2 CLOSEST CONSECUTIVE POINTS ON SPECIFIED
C          LINE OF DISCONTINUITY TO A GIVEN POINT
      COMMON CASEID(14),ITS1,ITS2,ITS3,ITS4,ITI1,ITI2,ITI3,ITI4,EPS1,EPS
     12,EPS3,EPS4,EPS5,EPS6,EPI1,EPI2,EPI3,EPI4,EPI5,EPI6,EPI7,VP,AR,LEN
     1GTH,APR,BPR,BIGAPR,BIGBPR,ESTAR,ALPHA,BETA,RHOSTR,EPRS,RHOS
      COMMON XMESH(20,20,6),XMESH2(20,20,6),Z(20),R(20),SURF(15,8),SURF2
     1(15,8),TAB(15,14,2),TAB2(15,14,2),SPART(15,2,2),RARF(15,11),RARF2(
     115,4),RPART(15,2)
C
      COMMON ZO,RO,PO,UO,VO,LO,MO,RHOO,EO,AO,UBARO,VBARO
      COMMON NP,NT,NR,NI,NDEL,ISUB
C
      COMMON ZMIN,ZMAX,RMIN,RMAX,RADIUS,GZ,GR,DELTA,H
      COMMON DIRCOS
      COMMON TIME
      COMMON IRARF
      COMMON KSTOP
      COMMON TPSI
      COMMON KKK
      REAL LO,MO,LENGTH,MU,KO
C
      GO TO (5,10,100,205,210,300,500),KODE
5     NN=NP
      K=1
      GO TO 15
10    NN=NT
      K=2
15    AA=(TAB2(1,1,K)-ZP)**2+(TAB2(1,2,K)-RP)**2
C
C                SEARCH SHOCK TABLES
```

```
C
      DO 60 N=2,NN
      A=(TAB2(N,1,K)-ZP)**2+(TAB2(N,2,K)-RP)**2
      IF (A.GE.AA) GO TO 23
      AA=A
60    CONTINUE
      PICK2=NN-1
      PICK2=PICK2+.2
      RETURN
23    PICK2=N-1
      PICK2=PICK2+.2
      RETURN
100   AA=(RARF2(1,1)-ZP)**2+(RARF2(1,2)-RP)**2
C
C              SEARCH RAREFACTION TABLE
C
      DO 200 N=2,NR
      A=(RARF2(N,1)-ZP)**2+(RARF2(N,2)-RP)**2
      IF (A.GE.AA) GO TO 203
      AA=A
200   CONTINUE
      PICK2=NR-1
      PICK2=PICK2+.2
      RETURN
203   PICK2=N-1
      PICK2=PICK2+.2
      RETURN
205   NN=NP
      K=1
      GO TO 215
210   NN=NT
      K=2
215   AA=(SPART(1,1,K)-ZP)**2+(SPART(1,2,K)-RP)**2
C
C              SEARCH SHOCK PARTICLE TABLES
C
```

```
      DO 260 N=2,NN
      A=(SPART(N,1,K)-ZP)**2+(SPART(N,2,K)-RP)**2
      IF (A.GE.AA) GO TO 223
      AA=A
260   CONTINUE
      PICK2=NN-1
      PICK2=PICK2+.2
      RETURN
223   PICK2=N-1
      PICK2=PICK2+.2
      RETURN
300   AA=(RPART(1,1)-ZP)**2+(RPART(1,2)-RP)**2
C
C               SEARCH RAREFACTION PARTICLE TABLE
C
      DO 400 N=2,NR
      A=(RPART(N,1)-ZP)**2+(RPART(N,2)-RP)**2
      IF (A.GE.AA) GO TO 403
      AA=A
400   CONTINUE
      PICK2=NR-1
      PICK2=PICK2+.2
      RETURN
403   PICK2=N-1
      PICK2=PICK2+.2
      RETURN
500   AA=(SURF2(1,1)-ZP)**2+(SURF2(1,2)-RP)**2
C
C     SEARCH FREE SURFACE TABLE
C
      DO 520 N=2,NP
      A=(SURF2(N,1)-ZP)**2+(SURF2(N,2)-RP)**2
      IF (A.GE.AA) GO TO 523
      AA=A
520   CONTINUE
      PICK2=NP-1
```

```
      PICK2=PICK2+.2
      RETURN
  523 PICK2=N-1
      PICK2=PICK2+.2
      RETURN
      END
      FUNCTION TEST(ZP,RP)
C
C
C           DETERMINES IF A GIVEN INTERIOR POINT IS IN
C           THE REGION TO BE CONSIDERED
C
      COMMON CASEID(14),ITS1,ITS2,ITS3,ITS4,ITI1,ITI2,ITI3,ITI4,EPS1,EPS
     12,EPS3,EPS4,EPS5,EPS6,EPI1,EPI2,EPI3,EPI4,EPI5,EPI6,EPI7,VP,AR,LEN
     1GTH,APR,BPR,BIGAPR,BIGBPR,ESTAR,ALPHA,BETA,RHOSTR,EPRS,RHOS
      COMMON XMESH(20,20,6),XMESH2(20,20,6),Z(20),R(20),SURF(15,8),SURF2
     1(15,8),TAB(15,14,2),TAB2(15,14,2),SPART(15,2,2),RARF(15,11),RARF2(
     115,4),RPART(15,2)
C
C
      COMMON Z0,R0,P0,U0,V0,L0,M0,RHO0,E0,A0,UBAR0,VBAR0
C
      COMMON NP,NT,NR,NI,NDEL,ISUB
C
      COMMON ZMIN,ZMAX,RMIN,RMAX,RADIUS,GZ,GR,DELTA,H
      COMMON DIRCOS
      COMMON TIME
      COMMON IRARF
      COMMON KSTOP
      COMMON TPSI
      COMMON KKK
      REAL L0,M0,LENGTH,MU,K0
C
      EPS=.0001
      IF (ITS3.EQ.1) GO TO 5
      IF (RP.GT.(RADIUS+EPS)) GO TO 5
```

```
      M=PICK2(ZP,RP,7)
      FF=ZP-SURF2(M+1,1)-(SURF2(M,1)-SURF2(M+1,1))*(RP-SURF2(M,2))/(SURF
     12(M,2)-SURF2(M+1,2))
      KICK=5
      CALL DVCHK(KQ)
      IF (KQ.EQ.1) GO TO 9980
      IF (FF)  200,5,5
5     CONTINUE
      IF (ZP.GT.-EPS) GO TO 1
      IF (RP.GT.(RADIUS+EPS)) GO TO 200
1     DO 10 K=1,2
      IF (ITS3.EQ.1) GO TO 100
      M=PICK2(ZP,RP,K)
      IF (TAB2(M,2,K).GT.RP.AND.M.NE.1)M=M-1
      FF=ZP-TAB2(M+1,1,K)-(TAB2(M,1,K)-TAB2(M+1,1,K))*(RP-TAB2(M+1,2,K))
     1/(TAB2(M,2,K)-TAB2(M+1,2,K))
      KICK=50
      CALL DVCHK(KQ)
      IF (KQ.EQ.1) GO TO 9980
      IF (K.EQ.2) GO TO 50
      IF (RP.GT.RADIUS) GO TO 10
      IF (FF)  200,10,10
50    IF (FF)  10,10,200
10    CONTINUE
      DO 20 K=1,2
      J=K+3
      M=PICK2(ZP,RP,J)
      IF (SPART(M,2,K).GT.RP.AND.M.NE.1)M=M-1
      FF=ZP-SPART(M+1,1,K)-(SPART(M,1,K)-SPART(M+1,1,K))*(RP-SPART(M+1,2
     1,K))/(SPART(M,2,K)-SPART(M+1,2,K))
      KICK=15
      CALL DVCHK(KQ)
      IF (KQ.EQ.1) GO TO 9980
      IF (K.EQ.2) GO TO 15
      IF (RP.GT.RADIUS) GO TO 20
      IF (FF.LT..001) GO TO 300
```

```
      GO TO 20                                                          SU21
15    IF (FF.GT.-.001) GO TO 400                                        SU21
20    CONTINUE                                                          SU21
      IF (IRARF.EQ.1) GO TO 100                                         SU21
      M=PICK2(ZP,RP,3)                                                  SU21
      FF=RP-RARF2(M+1,2)-(RARF2(M,2)-RARF2(M+1,2))*(ZP-RARF2(M+1,1))/(RASU21
     1RF2(M,1)-RARF2(M+1,1))                                            SU21
      KICK=20                                                           SU21
      CALL DVCHK(KQ)                                                    SU21
      IF (KQ.EQ.1) GO TO 9980                                           SU21
      IF (FF.LT.0.) GO TO 100                                           SU21
      M=PICK2(ZP,RP,6)                                                  SU21
      FF=RP-RPART(M+1,2)-(RPART(M,2)-RPART(M+1,2))*(ZP-RPART(M+1,1))/(RPSU21
     1ART(M,1)-RPART(M+1,1))                                            SU21
      KICK=100                                                          SU21
      CALL DVCHK(KQ)                                                    SU21
      IF (KQ.EQ.1) GO TO 9980                                           SU21
      IF (FF.LT.0.) GO TO 500                                           SU21
100   TEST=1                                                            SU21
      TEST=TEST+.2                                                      SU21
      RETURN                                                            SU21
200   TEST=2                                                            SU21
      TEST=TEST+.2                                                      SU21
      RETURN                                                            SU21
300   TEST=3                                                            SU21
      TEST=TEST+.2                                                      SU21
      RETURN                                                            SU21
400   TEST=4                                                            SU21
      TEST=TEST+.2                                                      SU21
      RETURN                                                            SU21
500   TEST=5                                                            SU21
      TEST=TEST+.2                                                      SU21
      RETURN                                                            SU21
9980  WRITE (3,9985) KICK                                               SU21
9985  FORMAT (32H0DIVIDE CHECK NEAR STATEMENT NO.,I5,14H IN SUBR. TEST/1SU21
     1H1)                                                               SU21
```

```
      RETURN
      END
      SUBROUTINE FGOF5(Z5,R5,SS,QQ)
C
C          COMPUTES S5,Q5 FOR INTERIOR REGION
C          ITERATION FOR Z5,R5
C
      COMMON CASEID(14),ITS1,ITS2,ITS3,ITS4,ITI1,ITI2,ITI3,ITI4,EPS1,EPS
     12,EPS3,EPS4,EPS5,EPS6,EPI1,EPI2,EPI3,EPI4,EPI5,EPI6,EPI7,VP,AR,LEN
     1GTH,APR,BPR,BIGAPR,BIGBPR,ESTAR,ALPHA,BETA,RHOSTR,EPRS,RHOS
      COMMON XMESH(20,20,6),XMESH2(20,20,6),Z(20),R(20),SURF(15,8),SURF2
     1(15,8),TAB(15,14,2),TAB2(15,14,2),SPART(15,2,2),RARF(15,11),RARF2(
     115,4),RPART(15,2)
C
C
      COMMON Z0,R0,P0,U0,V0,L0,M0,RHO0,E0,A0,UBAR0,VBAR0
C
      COMMON NP,NT,NR,NI,NDEL,ISUB
C
      COMMON ZMIN,ZMAX,RMIN,RMAX,RADIUS,GZ,GR,DELTA,H
      COMMON DIRCOS
      COMMON TIME
      COMMON IRARF
      COMMON KSTOP
      COMMON TPSI
      COMMON KKK
      REAL L0,M0,LENGTH,MU,K0
C
      DIMENSION ANS(6)
C
      CALL DBLTRP(Z5,R5,ANS)
      U5=ANS(2)
      V5=ANS(3)
      SS=Z5-Z0+H*V5
      QQ=R5-R0+H*U5
      RETURN
```

```
      END
      SUBROUTINE ITRP
      COMMON CASEID(14),ITS1,ITS2,ITS3,ITS4,ITI1,ITI2,ITI3,ITI4,EPS1,EPS
     12,EPS3,EPS4,EPS5,EPS6,EPI1,EPI2,EPI3,EPI4,EPI5,EPI6,EPI7,VP,AR,LEN
     1GTH,APR,BPR,BIGAPR,BIGBPR,ESTAR,ALPHA,BETA,RHOSTR,EPRS,RHOS
      COMMON XMESH(20,20,6),XMESH2(20,20,6),Z(20),R(20),SURF(15,8),SURF2
     1(15,8),TAB(15,14,2),TAB2(15,14,2),SPART(15,2,2),RARF(15,11),RARF2(
     115,4),RPART(15,2)
C
C
      COMMON ZO,RO,PO,UO,VO,LO,MO,RHOO,EO,AO,UBARO,VBARO
C
      COMMON NP,NT,NR,NI,NDEL,ISUB
C
      COMMON ZMIN,ZMAX,RMIN,RMAX,RADIUS,GZ,GR,DELTA,H
      COMMON DIRCOS
      COMMON TIME
      COMMON IRARF
      COMMON KSTOP
      COMMON TPSI
      COMMON KKK
C
C
      REAL LO,MO,LENGTH,MU,KO
C
C INTERPOLATION SCHEME FOR POINTS BETWEEN PARTICLE CURVES
C AND DISCONTINUITIES
C
      EPS=.0000001
      KOD1=0
      KOD2=0
      DO 1000 J=1,20
      DO 1000 I=1,20
      M=TEST(Z(I),R(J))
      IF (M.NE.5) GO TO 906
      IF (IRARF.EQ.1) GO TO 906
```

```
      NR1=NR-1
      DO 907 JJ=1,NR1
      IF (RARF2(JJ,1).LT.Z(I).AND.RARF2(JJ+1,1).GT.Z(I)) GO TO 908
  907 CONTINUE
  908 CONTINUE
      FF=R(J)-RARF2(JJ+1,2)+(RARF2(JJ,2)-RARF2(JJ+1,2))*(Z(I)-RARF2(JJ+1
     1,1))/(RARF2(JJ,1)-RARF2(JJ+1,1))
      IF (FF.LT.0.) GO TO 1000
  906 CONTINUE
      IF (M.EQ.3.AND.Z(I).LT.EPS.AND.ABS(R(J)-RADIUS).LT.EPS) GO TO 1000
      IF (M.LT.3) GO TO 8051
      WRITE (3,8050)
 8050 FORMAT (30HOINTERPOLATION SCHEME EMPLOYED)
  614 FORMAT (1X5HZO  =,E15.8,4X5HRO  =,E15.8)
      ZO=Z(I)
      RO=R(J)
      WRITE (3,614) ZO,RO
      WRITE (3,8888) M
 8888 FORMAT (1X4HM  =,I4)
 8051 CONTINUE
      GO TO (1000,1000,1001,1010,1100),M
 1001 IF (IRARF.EQ.1) GO TO 1003
      M=PICK2(Z(I),R(J),3)
      FF=R(J)-RARF2(M+1,2)+(RARF2(M,2)-RARF2(M+1,2))*(Z(I)-RARF2(M+1,1))
     1/(RARF2(M,1)-RARF2(M+1,1))
      IF (FF.GT.0.) GO TO 1003
      DO 8002 K=1,6
      L=K+2
 8002 XMESH2(I,J,K)=RARF(1,L)
      GO TO 1000
 1003 L=I+1
      N=TEST(Z(L),R(J))
      GO TO (1004,1007,1030,1030,1050),N
 1004 M=PICK2(Z(I),R(J),1)
      DO 1006 K=1,8
      ANS=TAB2(M,K,1)+(TAB2(M+1,K,1)-TAB2(M,K,1))*(R(J)-TAB2(M,2,1))/(TA
```

```
     1B2(M+1,2,1)-TAB2(M,2,1))
      IF (K.NE.1) GO TO 8005
      ANS1=ANS
      GO TO 1006
 8005 CONTINUE
      IF (K.EQ.2) GO TO 1006
      KX=K-2
      IF (ABS(R(J)-RADIUS).GT.EPS) GO TO 9024
      IF (K.GT.5.OR.K.LT.4) GO TO 9024
      ANS=TAB2(M+1,K,1)
 9024 CONTINUE
      XMESH2(I,J,KX)=ANS+(XMESH2(L,J,KX)-ANS)*(Z(I)-ANS1)/(Z(L)-ANS1)
      IF (ABS(R(J)-RADIUS).GT.EPS) GO TO 1006
      XMESH2(I,J,1)=0.
      XMESH2(I,J,4)=RHOSTR
      XMESH2(I,J,5)=0.
      XMESH2(I,J,6)=SQRT(BIGAPR/RHOSTR)
 1006 CONTINUE
      GO TO 1000
 1007 MM=PICK2(Z(I),R(J),2)
      M=PICK2(Z(I),R(J),1)
      DO 1009 K=1,8
      ANS=TAB2(M,K,1)+(TAB2(M+1,K,1)-TAB2(M,K,1))*(R(J)-TAB2(M,2,1))/(TA
     1B2(M+1,2,1)-TAB2(M,2,1))
      ANSW=TAB2(MM,K,2)+(TAB2(MM+1,K,2)-TAB2(MM,K,2))*(R(J)-TAB2(MM,2,2
     1)/(TAB2(MM+1,2,2)-TAB2(MM,2,1))
      IF (K.NE.1) GO TO 1008
      ANS1=ANS
      ANS2=ANSW
      GO TO 1009
 1008 CONTINUE
      IF (K.EQ.2) GO TO 1009
      KX=K-2
      XMESH2(I,J,KX)=ANS+(ANSW-ANS)*(Z(I)-ANS1)/(ANS2-ANS1)
 1009 CONTINUE
      GO TO 1000
```

```
1010  IF (IRARF.EQ.1) GO TO 1013                                           SU23 108
      M=PICK2(Z(I),R(J),3)                                                 SU23 109
      FF=R(J)-RARF2(M+1,2)+(RARF2(M,2)-RARF2(M+1,2))*(Z(I)-RARF2(M+1,1))SU23 110
     1/(RARF2(M,1)-RARF2(M+1,1))                                           SU23 111
      IF (FF.GT.0.) GO TO 1013                                             SU23 112
      DO 1012 K=1,6                                                        SU23 113
      L=K+2                                                                SU23 114
1012  XMESH2(I,J,K)=RARF(1,L)                                              SU23 115
      GO TO 1000                                                           SU23 116
1013  L=I-1                                                                SU23 117
      IF (ABS(Z(I)).LT.EPS) GO TO 1017                                     SU23 118
      N=TEST(Z(L),R(J))                                                    SU23 119
      GO TO (1014,1017,1030,1017,1051),N                                   SU23 120
1014  M=PICK2(Z(I),R(J),2)                                                 SU23 121
      DO 1016 K=1,8                                                        SU23 122
      ANS=TAB2(M,K,2)+(TAB2(M+1,K,2)-TAB2(M,K,2))*(R(J)-TAB2(M,2,2))/(TASU23 123
     1B2(M+1,2,2)-TAB2(M,2,2))                                             SU23 124
      IF (K.NE.1) GO TO 1015                                               SU23 125
      ANS1=ANS                                                             SU23 126
      GO TO 1016                                                           SU23 127
1015  CONTINUE                                                             SU23 128
      IF (K.EQ.2) GO TO 1016                                               SU23 129
      KX=K-2                                                               SU23 130
      XMESH2(I,J,KX)=ANS+(XMESH2(L,J,KX)-ANS)*(Z(I)-ANS1)/(Z(L)-ANS1)      SU23 131
1016  CONTINUE                                                             SU23 132
      GO TO 1000                                                           SU23 133
1017  L=J-1                                                                SU23 134
      N=TEST(Z(I),R(L))                                                    SU23 135
      GO TO (1024,1030,1030,1030,1051),N                                   SU23 136
1024  M=PICK2(Z(I),R(J),2)                                                 SU23 137
      DO 1026 K=2,8                                                        SU23 138
      ANS=TAB2(M,K,2)+(TAB2(M+1,K,2)-TAB2(M,K,2))*(Z(I)-TAB2(M,1,2))/(TASU23 139
     1B2(M+1,1,2)-TAB2(M,1,2))                                             SU23 140
      IF (K.NE.2) GO TO 1025                                               SU23 141
      ANS1=ANS                                                             SU23 142
      GO TO 1026                                                           SU23 143
```

```
1025  CONTINUE
      KX=K-2
      IF (ABS(Z(I)).GT.EPS) GO TO 9125
      IF (K.GT.5.OR.K.LT.4) GO TO 9125
      ANS=TAB2(M+1,K,2)
9125  CONTINUE
      XMESH2(I,J,KX)=ANS+(XMESH2(I,L,KX)-ANS)*(R(J)-ANS1)/(R(L)-ANS1)
      IF (ABS(Z(I)).GT.EPS) GO TO 1026
      XMESH2(I,J,1)=0.
      XMESH2(I,J,4)=RHOSTR
      XMESH2(I,J,5)=0.
      XMESH2(I,J,6)=SQRT(BIGAPR/RHOSTR)
1026  CONTINUE
      GO TO 1000
1100  M=PICK2(Z(I),R(J),3)
      ANS1=RARF2(M+1,2)+(RARF2(M,2)-RARF2(M+1,2))*(Z(I)-RARF2(M+1,1))/(R
     1ARF2(M,1)-RARF2(M+1,1))
      L=J+1
      M=TEST(Z(I),R(L))
      GO TO (1101,1030,1051,1030),M
1101  CONTINUE
      DO 1106 K=1,6
      LL=K+2
      XMESH2(I,J,K)=RARF(1,LL)+(XMESH2(I,L,K)-RARF(1,LL))*(R(J)-ANS1)/(R
     1(L)-ANS1)
1106  CONTINUE
      GO TO 1000
1050  JJ1=J
      II1=I
      KOD1=1
      GO TO 1000
1051  JJ2=J
      II2=I
      KOD2=1
1000  CONTINUE
      IF (KOD1.EQ.0) GO TO 2000
```

```
      M=PICK2(Z(II1),R(JJ1),1)
      DO 2016 K=1,8
      ANS=TAB2(M,K,1)+(TAB2(M+1,K,1)-TAB2(M,K,1))*(R(JJ1)-TAB2(M,2,1))/(
     1TAB2(M+1,2,1)-TAB2(M,2,1))
      IF (K.NE.1) GO TO 2005
      ANS1=ANS
      GO TO 2016
 2005 CONTINUE
      I=II1
      J=JJ1
      L=II1+1
      IF (K.EQ.2) GO TO 2016
      KX=K-2
      XMESH2(I,J,KX)=ANS+(XMESH2(L,J,KX)-ANS)*(Z(I)-ANS1)/(Z(L)-ANS1)
 2016 CONTINUE
 2000 IF (KOD2.EQ.0) GO TO 3000
      M=PICK2(Z(II2),R(JJ2),2)
      DO 3016 K=1,8
      ANS=TAB2(M,K,2)+(TAB2(M+1,K,2)-TAB2(M,K,2))*(R(JJ2)-TAB2(M,2,2))/(
     1TAB2(M+1,2,2)-TAB2(M,2,2))
      IF (K.NE.1) GO TO 3015
      ANS1=ANS
      GO TO 3016
 3015 CONTINUE
      I=II2
      J=JJ2
      L=II2-1
      IF (K.EQ.2) GO TO 3016
      KX=K-2
      XMESH2(I,J,KX)=ANS+(XMESH2(L,J,KX)-ANS)*(Z(I)-ANS1)/(Z(L)-ANS1)
 3016 CONTINUE
 3000 CONTINUE
      GO TO 3017
 1030 WRITE (3,1040) I,J
 1040 FORMAT (27H0 TIME STEP TOO LARGE AT I=,I4,2HJ=,I4,///)
      CALL EXIT
```

```
3017  CONTINUE
C
C
      RETURN
      END
      SUBROUTINE EXIT
C
      COMMON CASEID(14),ITS1,ITS2,ITS3,ITS4,ITI1,ITI2,ITI3,ITI4,EPS1,EPS
     12,EPS3,EPS4,EPS5,EPS6,EPI1,EPI2,EPI3,EPI4,EPI5,EPI6,EPI7,VP,AR,LEN
     1GTH,APR,BPR,BIGAPR,BIGBPR,ESTAR,ALPHA,BETA,RHOSTR,EPRS,RHOS
      COMMON XMESH(20,20,6),XMESH2(20,20,6),Z(20),R(20),SURF(15,8),SURF2
     1(15,8),TAB(15,14,2),TAB2(15,14,2),SPART(15,2,2),RARF(15,11),RARF2(
     115,4),RPART(15,2)
C
C
      COMMON Z0,R0,P0,U0,V0,L0,M0,RHO0,E0,A0,UBAR0,VBAR0
C
      COMMON NP,NT,NR,NI,NOEL,ISUB
C
      COMMON ZMIN,ZMAX,RMIN,RMAX,RADIUS,GZ,GR,DELTA,H
      COMMON DIRCOS
      COMMON TIME
      COMMON IRARF
      COMMON KSTOP
      COMMON TPSI
      COMMON KKK
      REAL L0,M0,LENGTH,MU,K0
      KSTOP=1
      STOP
      END
      SUBROUTINE FGOFI(ZX,RX,SS,QQ)
C
C         COMPUTES SI,QI FOR INTERIOR REGION
C         ITERATION FOR ZI,RI
C
      COMMON CASEID(14),ITS1,ITS2,ITS3,ITS4,ITI1,ITI2,ITI3,ITI4,EPS1,EPS
```

```
     12,EPS3,EPS4,EPS5,EPS6,EPI1,EPI2,EPI3,EPI4,EPI5,EPI6,EPI7,VP,AR,LEN
     1GTH,APR,BPR,BIGAPR,BIGBPR,ESTAR,ALPHA,BETA,RHOSTR,EPRS,RHOS
      COMMON XMESH(20,20,6),XMESH2(20,20,6),Z(20),R(20),SURF(15,8),SURF2
     1(15,8),TAB(15,14,2),TAB2(15,14,2),SPART(15,2,2),RARF(15,11),RARF2(
     115,4),RPART(15,2)
C
C
      COMMON Z0,R0,P0,U0,V0,L0,M0,RHO0,E0,A0,UBAR0,VBAR0
C
      COMMON NP,NT,NR,NI,NDEL,ISUB
C
      COMMON ZMIN,ZMAX,RMIN,RMAX,RADIUS,GZ,GR,DELTA,H
      COMMON DIRCOS
      COMMON TIME
      COMMON IRARF
      COMMON KSTOP
      COMMON TPSI
      COMMON KKK
      REAL L0,M0,LENGTH,MU,K0
C
      DIMENSION ANS(6),PSI(4),SPSI(11),CPSI(11)
C
C
C
C
C
      CALL DBLTRP(ZX,RX,ANS)
      UI=ANS(2)
      VI=ANS(3)
      AI=ANS(6)
      SS=ZX-Z0+H*(VI+AI*SIN(TPSI))
      QQ=RX-R0+H*(UI+AI*COS(TPSI))
      RETURN
      END
```

III.1. "Elementary Solutions of Coupled Model Equations in the Kinetic Tehory of Gases"

III.2. "Tricritical Points in Multicomponent Fluid Mixtures"

III.3. "Generalized Scaling Hypothesis in Multicomponent Systems. I. Classification of Critical Points by Order and Scaling at Tricritical Points"

III.4. "Double-Power Scaling Functions Near Tricritical Points"

PAPERS INTENTIONALLY OMITTED

75-04939
N75- 15329

AIAA Paper No. 69-355

STRESS WAVES RESULTING FROM HYPERVELOCITY IMPACT

by

R. MADDEN
Northeastern University
Boston, Massachusetts
and
T. S. CHANG
North Carolina State University
Raleigh, North Carolina

AIAA Hypervelocity Impact Conference

CINCINNATI, OHIO/APRIL 30 – MAY 2, 1969

STRESS WAVES RESULTING FROM HYPERVELOCITY IMPACT†

R. Madden
Assistant Professor of Mechanical Engineering
Northeastern University
Boston, Massachusetts

and

T. S. Chang
NSF Professor and Chairman of Mechanics Program
North Carolina State University
Raleigh, North Carolina

Abstract

Results from a numerical scheme based on the method of characteristics are presented for the axially symmetric, hypervelocity impact of similar materials. The analysis is restricted to the early stages of the impact of a right circular cylinder on a halfspace. The resulting rarefaction and shock waves produced by the impact are considered as discrete wavefronts which divide the impacted zone into regions. Numerical diffusion is then controlled by requiring that the values of the dependent variables at a given point in the impacted zone to depend on only the calculated values at earlier times at points in the same region as the point in question. The numerical results give accurate representations of the stress wave profiles (i.e., rarefaction and shock waves) which should be useful as inputs for a later stage elastoplastic analysis and/or spallation analysis. The effects of "numerical diffusion" on the calculated pressure and flow fields when the rarefaction wave is not considered as discrete is investigated and the "diffused" results are compared with the more exact analysis.

Nomenclature

a = isentropic speed of sound
e = specific internal energy
e_s = sublimation energy
h = time step
P = pressure
r = radial coordinate
t = time
U = radial velocity
V = axial velocity
z = axial coordinate
η = ρ/ρ^*
θ = parameter defining a bicharacteristic, $(0 \leq \theta \leq 2\pi)$
μ = $\eta - 1$
ρ = mass density
ρ^* = ambient density
ϕ = function of r, z, and t

Introduction

Most of the existing numerical codes[1-3] for hypervelocity impact calculations are based on procedures which allow some smearing of the resulting rarefaction and shock waves. The present analysis of the initial hydrodynamic phase of an axially symmetric, hypervelocity impact is based on the method of characteristics while treating the rarefaction and shock waves as discrete discontinuities. The definitiveness of the resulting flow field obtained from such an analysis should be useful as inputs to a subsequent elastoplastic analysis for studying later stage cratering effects and/or spallation calculations which require rather accurate representations of both the peak pressure and the incident shock wave profile at reflection. The results based on a numerical code using the method of characteristics for the impact of a right circular aluminum cylinder on an aluminum halfspace are presented. The impact configuration is depicted schematically in Fig. 1.

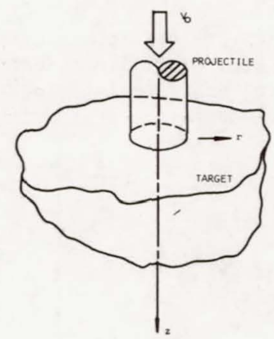

Figure 1 Impact configuration

In order to give some insight into the mechanism of "numerical diffusion", an analysis using the method of characteristics by not considering the rarefaction as discrete is also considered. In

†The authors are grateful to Mr. P. Townsend of Northeastern University for his assistance in adapting the computer program to the Northeastern University Computer, the running of the programs, and the preparation of the figures. The research of one of us (T.S.C.) was partially supported by the National Aeronautics and Space Administration under Contract No. NGR 34-002-084, and the Advanced Research Projects of the Department of Defense while monitored by the Office of Naval Research under Contract No. N00014-68-A-0187.

69-355

doing so, the speed of the release wave from the free surface of the projectile and the free surface of the target is not controlled. Results from such an approximate analysis are compared with the discrete rarefaction case and the limitations of the "diffused" solution are delineated.

Characteristic Surfaces

As described in references 4 and 5, during the initial stages of a hypervelocity impact, the material in the impacted zone may be assumed to obey the inviscid fluid dynamic equations. For axially symmetric impact, these equations may be expressed as follows:

Conservation of Mass

$$\frac{D\rho}{Dt} + \rho\left(\frac{\partial U}{\partial r} + \frac{\partial V}{\partial z} + \frac{U}{r}\right) = 0 , \tag{1}$$

Conservation of Momentum

$$\rho\frac{DU}{Dt} + \frac{\partial P}{\partial r} = 0 , \tag{2}$$

$$\rho\frac{DV}{Dt} + \frac{\partial P}{\partial z} = 0 , \tag{3}$$

Conservation of Entropy along a Particle Path

$$\frac{DP}{Dt} - a^2\frac{D\rho}{Dt} = 0 , \tag{4}$$

where,

$$\frac{D}{Dt} = \frac{\partial}{\partial t} + U\frac{\partial}{\partial r} + V\frac{\partial}{\partial z} , \tag{5}$$

and P is the pressure, ρ is the density, a is the isentropic speed of sound, t is the time, and (r,z) and (U,V) are the radial and axial coordinates and velocities, respectively.

Equations (1) to (4) form a system of nonlinear, hyperbolic, partial differential equations. The corresponding characteristic equation for this system of equations is:

$$\begin{vmatrix} 0 & \frac{D\phi}{Dt} & \rho\frac{\partial\phi}{\partial r} & \rho\frac{\partial\phi}{\partial z} \\ \frac{\partial\phi}{\partial r} & 0 & \rho\frac{D\phi}{Dt} & 0 \\ \frac{\partial\phi}{\partial z} & 0 & 0 & \rho\frac{D\phi}{Dt} \\ \frac{D\phi}{Dt} & -a^2\frac{D\phi}{Dt} & 0 & 0 \end{vmatrix} = 0 \tag{6}$$

where $\phi = \phi(r,z,t)$, and surfaces of ϕ = constants are the characteristic surfaces.

The solutions of Eq. (6) are given by

$$\left(\frac{D\phi}{Dt}\right)^2 - a^2\left[\left(\frac{\partial\phi}{\partial r}\right)^2 + \left(\frac{\partial\phi}{\partial z}\right)^2\right] = 0 , \tag{7}$$

and

$$\frac{D\phi}{Dt} = 0 . \tag{8}$$

The characteristic surfaces described by Eqs. (7) and (8) correspond to two distinct types of characteristic propagations. Corresponding to Eq. (7), the characteristic propagation is described by the differential equations of the bicharacteristics

$$\frac{dr}{dt} = U + a\cos\theta , \tag{9}$$

$$\frac{dz}{dt} = V + a\sin\theta , \tag{10}$$

where, $0 \le \theta \le 2\pi$. These bicharacteristics describe the propagation of pressure, density, or velocity disturbances. Corresponding to Eq. (8), the characteristic propagation is described by

$$\frac{dr}{dt} = U , \tag{11}$$

$$\frac{dz}{dt} = V , \tag{12}$$

which are the particle path equations and describe the propagation of entropy disturbances.

The set of bicharacteristics from a point, with $0 \le \theta \le 2\pi$, forms the conoid of dependence for the point which is at its vertex. The interior of the conoid contains all the points whose values of U,V,P,ρ, etc. may influence the corresponding values at the point at the vertex. The intersection of this conoid and a particular time plane forms the domain of dependence of the point at the vertex of the conoid and contains all the points whose values of U,V,P,ρ, etc. influence the corresponding values at the point at the vertex. A schematic representation of these ideas are given in Fig. 2.

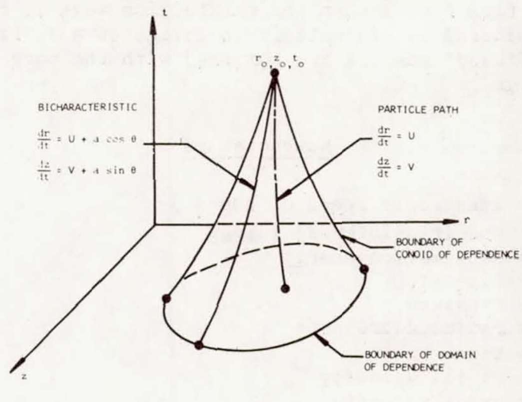

Figure 2 Conoid and domain of dependence

Compatibility Conditions

It will not be difficult to demonstrate that along a bicharacteristic, U,V, and P must satisfy the following differential relation in a time interval dt:

$$dP + \rho a\cos\theta dU + \rho a\sin\theta dV$$

$$= -\rho a^2 dt\left[\left(\frac{\partial U}{\partial r}\right)\sin^2\theta - \left(\frac{\partial U}{\partial z} + \frac{\partial V}{\partial r}\right)\sin\theta\cos\theta + \left(\frac{\partial V}{\partial z}\right)\cos^2\theta + \frac{U}{r}\right] . \tag{13}$$

Similarly, along the particle path, the following differential expression must be satisfied:

$$\rho^2 de = p d\rho \ , \tag{14}$$

where e is the specific internal energy. Equations (13) and (14) are called the bicharacteristic and particle path compatibility conditions, respectively.

Equation (14) is essentially the first law of thermodynamics expressed along the particle path for an isentropic process. This choice of a particle path compatibility equation was made in order to introduce the internal energy variable. The P,ρ,e variables are related by an equation of state of the form,

$$P = P(\rho, e) \ . \tag{15}$$

The particular form of the equation of state used in this analysis is that of Tillotson.[6] For aluminum, it can be expressed as follows:

For $\rho > \rho_*$, with $e > 0$ or $e \leq e_s$,

$$P = [0.5 + \frac{1.63}{1+e/(e_s \eta^2)}]e\rho + 0.752\mu + 0.65\mu^2 \ , \tag{16}$$

and for $\rho < \rho_*$, with $e > e_s$,

$$P = 0.5e\rho + [\frac{1.63e\rho}{1+e/(e_s \eta^2)} + 0.752\mu e^{+5(1-1/\eta)}]e^{-5(1-1/\eta)^2} \ , \tag{17}$$

where,

$$\eta = \rho/\rho_* \ , \quad \mu = \eta - 1 \ , \tag{18}$$

$\rho_* = 2.70$ gm/cm^3 is the ambient density for aluminum, and $e_s = 0.03$ megabar cm^3/gm is the sublimation energy for aluminum. In Eqs. (16) and (17), P is expressed in megabars, ρ in gm/cm^3, and e in megabars cm^3/gm.

Numerical Procedure

The differential expressions, Eqs. (9)-(14), are cast in finite difference forms accurate to the order of h^2, where h is the time step. For example, the bicharacteristic compatibility equation for a particular value of θ is

$$P_o - P_i + \rho_i a_i [\cos\theta_i (U_o - U_i) + \sin\theta_i (V_o - V_i)]$$
$$= -\rho_i a_i^2 h [(\frac{\partial U}{\partial r})_i \sin^2\theta_i - (\frac{\partial U}{\partial z} + \frac{\partial V}{\partial r})_i \sin\theta_i \cos\theta_i + (\frac{\partial V}{\partial z})_i \sin^2\theta_i + \frac{U_i}{r_i}] + O(h^2) \ , \tag{19}$$

where the subscript "o" refers to $t = t_o$ and the point where the values of U,V,P,ρ, etc. are being calculated and the subscript "i" refers to the corresponding values at the intersection of the bicharacteristic θ_i with an (t_o-h) - time plane at which all data has been previously calculated. In spite of the fact that the error over each time step is of order h^2, the accumulated errors reduce the aggregate solution to the order of h.

The unknowns in Eq. (19) are P_o, U_o, V_o and therefore unless one (or more) of these values is specified, three bicharacteristics are required for each calculation. After P_o, U_o, V_o are determined, the values ρ_o and e_o are obtained with the aid of the particle path compatibility condition and the equation of state. This procedure is applicable at points not on the boundary of the impacted zone, (i.e., on the shocks, rarefaction, free surfaces, or axis of symmetry). At points on the boundary, auxiliary relations are available and consequently, fewer independent bicharacteristic conditions are required for each calculation. A scheme is also used to insure that finite difference relations are not written across discontinuities and "numerical diffusion" across these discontinuities is minimized. The details of the various calculational procedures are given in references 4 and 5.

Numerical Stability

The problem of constructing a stable numerical procedure for the present analysis is resolved by following certain qualitative guidelines. The basic idea is suggested by the stability criterion of Courant, Friedrichs, and Lewy, (or the C.F.L. Condition). According to this condition, the domain of dependence of the difference equations must *encompass the domain of dependence of the original* hyperbolic differential equations for numerical stability. The following is a brief account of the approach used in this analysis to ascertain numerical stability.

Consider the domain of dependenee of the partial differential equations in the (t_o-h) - time plane as illustrated in Fig. 3(a). If the conoid of dependence is approximated by the three bicharacteristics passing through the triangular points (1,2,3), the domain of dependence is described by the triangle of dashed lines connecting the three points. Since, for the purpose of attaining numerical convergence, the points (1,2,3) must be relatively close to the circular region which is the domain of dependence of the differential equations, instabilities cannot be avoided. To insure numerical stability, the values at points (1,2,3) are obtained by interpolation using the values at the twelve grid points (circular dots) which surround the three original points as shown in Fig. 3(b). In doing so, the domain of depend-

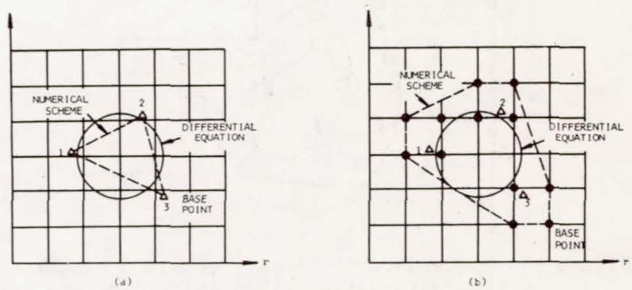

Figure 3 Domains of dependence: (a) without interpolation, (b) with interpolation

ence of the difference equations is increased to the convex hull of dashed lines indicated in Fig. 3(b). This convex hull should encompass the circular domain of the differential equations. Such an interpolation scheme seems to be sufficient to insure the required numerical stability for the present analysis.

Results and Discussion

The example chosen in this paper to illustrate the results of the characteristic method is the axially symmetric impact of an infinitely long cylindrical aluminum projectile with a diameter d_o equal to 2.5 cm on an aluminum halfspace. The initial velocity V_o of the projectile is taken to be 7.6 km/sec and the halfspace is assumed to be at rest. The results of the characteristic method are compared with the results obtained from the well-known "OIL Code" of reference 1. Results from the discrete rarefaction case is then compared with those for a case where the "numerical diffusion" of the rarefaction wave is allowed.

Figure 4 shows the pressure distributions for both the "OIL" solution of reference 1 and the method of characteristics with discrete rarefaction at a time of t = 0.74 μsec after impact when the rarefaction has not yet propagated near the axis of symmetry. The pressure distributions are compared by mapping the isobars for P = 1.08, 0.8, 0.5, and 0.2 megabars (MB). The results of the method of characteristics are shown as solid lines and the "OIL" distributions as dashed lines. The locations of the two shocks and the rarefaction (P = 1.08 MB) are quite clearly defined for the characteristic method. One difference immediately apparent between the two sets of results is that the isobars for the "OIL" approach begin and end on the axis of symmetry, whereas the isobars for the characteristic method begin and end on the projectile and target shocks. The difference, of course, comes from the smearing of the shock fronts in the "OIL" solution. The "OIL" approach predicts additionally two regions of pressure higher than the one-dimensional region which is bounded by the two shocks and the rarefaction. The reduction in pressure in the rarefied region compares quite favorably for both methods. Major differences among the isobars of P = 0.5 and 0.2 MB obtained from the two methods are noted in the region near the original free surface where the pressure has been controlled by the characteristic method.

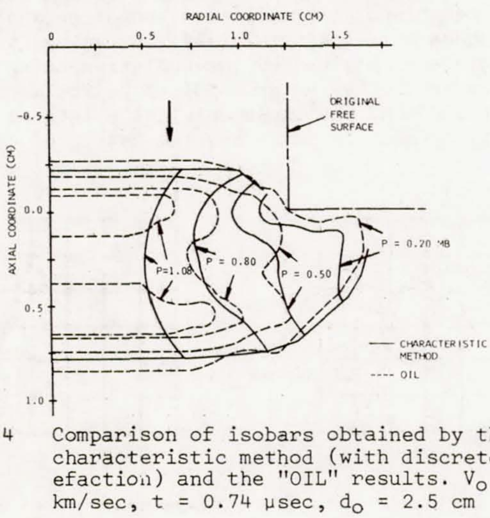

Figure 4 Comparison of isobars obtained by the characteristic method (with discrete rarefaction) and the "OIL" results. V_o = 7.6 km/sec, t = 0.74 μsec, d_o = 2.5 cm

Figure 5 shows the pressure distribution along the axis of symmetry at a time of t = 1.28 μsec after impact just prior to the actual reflection of the rarefaction wave from the axis of symmetry. The dashed curve shows the correct uniform pressure distribution based on the discrete rarefaction solution. The solid line shows the pressure distribution predicted by the numerical method which allows "diffusion" across the rarefaction wave. In the latter case, the pressure along the axis is underestimated. The lowest value is approximately 60% of the actual value. This drop in pressure is due to the fact that the effective speed of the rarefaction for the "diffused" case is equal to the actual rarefaction speed plus the mesh speed (i.e., the rarefaction front travels one additional grid spacing in each time cycle). The fact that the pressures are in error by 40% could be serious if the target shock wave were to be reflected from a free surface at the back of a target with a finite thickness or if these results were to be used as inputs for an elastoplastic analysis for later stage cratering and subsequent spallation calculations.

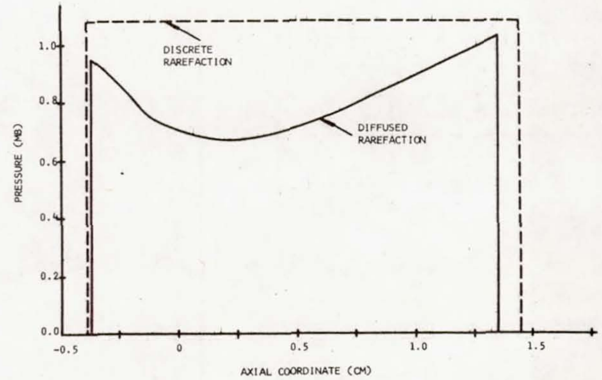

Figure 5 Pressure distribution along the axis of symmetry. V_o = 7.6 km/sec, t = 1.28 μsec, d_o = 2.5 cm

Figure 6 shows the pressure distribution along the axis of symmetry at a later time (t = 1.55 μsec) after the rarefaction has been re-

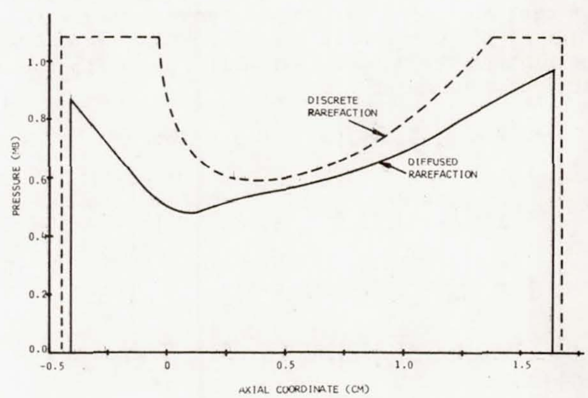

Figure 6 Pressure distribution along the axis of symmetry. V_o = 7.6 km/sec, t = 1.28 μsec, d_o = 2.5 cm

flected. Again the dashed curve is that of the discrete rarefaction solution and the solid curve is the "diffused" solution. At or near this time and for subsequent times, the results of the two solutions are very close to each other and the discrepancies among the results diminish with the increase of time.

Figure 7 maps the isobars for the entire flow field for both the discrete rarefaction solution (dashed curves) and the "diffused" solution (solid curves) at t = 1.28 μsec after impact. It is noted that in regions close to the axis of symmetry and the rarefaction, there are large discrepancies among the numerically calculated pressures using the two different methods. In addition, due to the premature decay of the projectile shock near the projectile free surface, the calculated pressures near the target shock close to the free surface using the "diffused" scheme are much higher than those for the discrete rarefaction solution. This effect also causes a slightly higher target shock velocity near the free surface. In other regions far away from the free surface and the rarefaction front, the calculated pressures from the two methods are in good agreement.

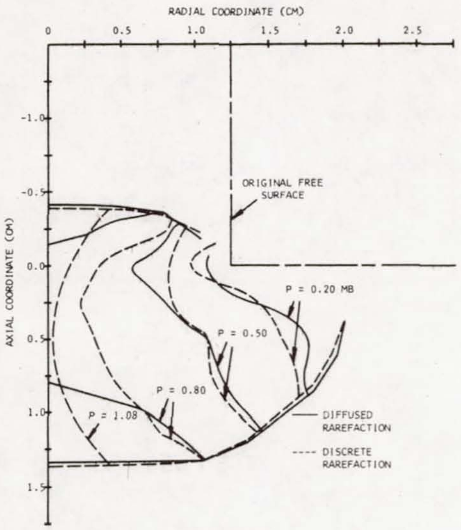

Figure 7 Pressure field. V_o = 7.6 km/sec t = 1.28 μsec, d_o = 2.5 cm

Figure 8 shows a comparison of the isobars in the impacted zone at t = 1.55 μsec after impact. At this time, the isobars are in close agreement throughout the flow field. Nevertheless, some of the effects of the "diffused" rarefaction can still be observed. For instance, there is a slightly higher pressure region predicted by the "diffused" results near the target shock close to the axis of symmetry.

Figure 9 compares the velocity vectors for the two methods of calculations at t = 1.50 μsec after impact. For all practical purposes, the results are nearly identical. It is apparent that the effect of "numerical diffusion" is more important in the pressure calculations.

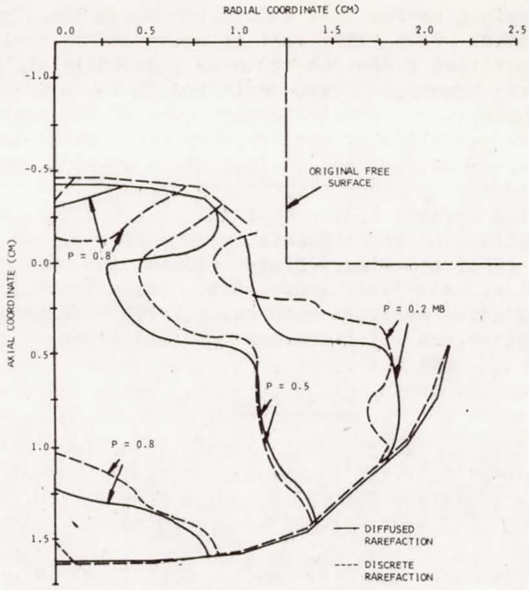

Figure 8 Pressure fields. V_o = 7.6 km/sec, t = 1.55 μsec, d_o = 2.5 cm

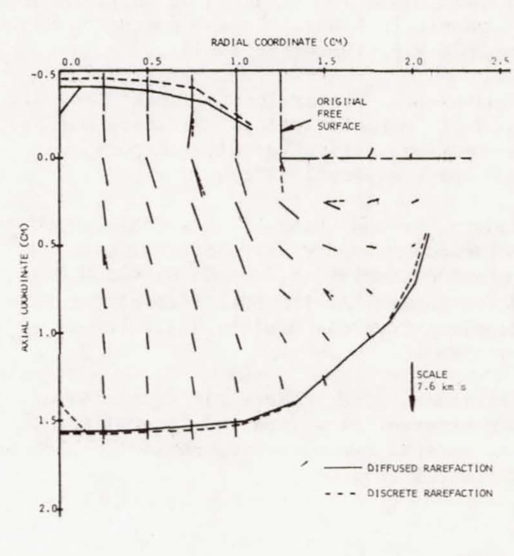

Figure 9 Velocity vectors. V_o = 7.6 km/sec, t = 1.50 μsec, d_o = 2.5 cm

Concluding Remarks

It may be surmised from the calculated results using the method of characteristics that, if the rarefaction is not considered as a discrete discontinuity, the pressures for the initial stages of an axially symmetric hypervelocity impact may be quite different from their actual values before the rarefaction is reflected from the axis of symmetry. This is particularly true for the pressure distribution at the axis of symmetry. After the reflection of the rarefaction wave, however, the effect of numerical "diffusion" introduced by not treating the rarefaction front as a discrete discontinuity diminishes. This means that if the pressure fields and shock fronts are desired at a time after the rarefaction wave has been reflected from the axis of symmetry, an approximate procedure of the method of characteristics by not treating the rarefaction as discrete may be used. Since the computing time required for hypervelocity impact calculations using the method of characteristics with discrete rarefaction and shock fronts is very large, this procedure of allowing diffused rarefaction can be useful for relatively long impact time calculations or spallation analyses with relatively thick target plates (compared with the projectile diameter).

References

[1]Johnson, W. E., "OIL: A Continuous Two-Dimensional Eulerian Hydrodynamic Code," General Atomics Division, General Dynamics Corporation, Report No. 55-80-Revised (January 1965).

[2]Riney, T. D., "Theoretical Hypervelocity Impact Calculations Using the PICWICK Code," General Electric Space Sciences Laboratory Report, No. R64SD13 (February 1964).

[3]Bjork, R., Brooks, N. and Papette, R., "A Numerical Technique for Solution of Multidimensional Hydrodynamic Problems," Rand Corporation Report, No. R.M. 2628 P.R. (December 1963).

[4]Madden, R., "Hypervelocity Impact Analysis by the Method of Characteristics," National Aeronautics and Space Administration Technical Report, No. NASA TR-R-298 (January 1969).

[5]Madden, R. and Chang, T. S., "Axially Symmetric Hypervelocity Impact Calculations Using the Method of Characteristics," North Carolina State University, Report No. TSC-68-1 (February 1968). Also, American Physical Society Bulletin, II13(5), 821 (May 1968).

[6]Tillotson, J. H., "Metallic Equations of State for Hypervelocity Impact," General Atomic Division, General Dynamics Corporation, Report No. GA-3216 (July 1962).

Reprinted from

[redacted]

PERGAMON PRESS
OXFORD NEW YORK LONDON PARIS

Int. J. Engng Sci., 1972, Vol. 10, pp. 353–367. Pergamon Press. Printed in Great Britain

N75-15329

NONLINEAR WAVES IN A RATE-SENSITIVE, ELASTOPLASTIC MATERIAL

E. E. BURNISTON
Department of Mathematics, North Carolina State University, Raleigh, North Carolina, U.S.A.

and

T. S. CHANG†
Center for Space Research, Massachusetts Institute of Technology, Cambridge, Massachusetts, U.S.A.

(Communicated by A. C. ERINGEN)

Abstract—Two classes of closed form solutions of one-dimensional, nonlinear waves in a rate-sensitive, elastoplastic material are reported. One class of these solutions is self-similar and the other class consists of constant speed propagations. Applications of these solutions to unsteady motions behind propagating discontinuities are also considered.

1. INTRODUCTION

THE PURPOSE of this paper is to discuss two interesting classes of closed form solutions of one-dimensional, unsteady motion of a rate-sensitive, elastoplastic material. One class of these solutions is self-similar and is deduced from the invariant theorems of continuous groups of transformations. This class of unsteady motion is governed by a single, first-order, nonlinear, ordinary differential equation of the Riccati type and closed form solutions in terms of elementary functions are obtained under special circumstances. If the material in consideration possesses the additional property of instantaneous linear elasticity [1] under 'high rate' of straining, it may be demonstrated that one of these self-similar solutions can be used to describe the dispersed nonlinear wave motion behind a propagating shockfront into an initially quiescent region.

The second class of solutions is obtained by searching for one-dimensional wave motions with constant speeds of propagation. These solutions are expressible as simple quadratures and closed form expressions can be obtained for specific constitutive relations. Such solutions represent non-characteristic propagations, i.e. they are not propagations of weak discontinuities of arbitrary wave forms. It may be demonstrated, using the Poincaré–Bendixon theorem, that these solutions, in general, are not periodic. Assuming a sub-elastic, constant-speed, propagating discontinuity preceded by an elastic precurser with an unloading, relaxation zone, or a constant stress region, the nonlinear wave solution with a constant propagation speed equal to that of the discontinuity can be used to describe the 'unsteady'‡ motion behind the discontinuity.

One-dimensional rectilinear motion, in the strict sense, involves not just one spatial coordinate but also only one component of stress, strain, and particle velocity. For such a type of motion, only a one-dimensional stress–strain or constitutive relation is required. Various rate-sensitive, constitutive equations have been proposed in the

†Permanent address: North Carolina State University.

‡Such an 'unsteady' motion, of course, becomes essentially steady for a moving observer following the propagating discontinuity.

literature and a comprehensive review of this subject can be found in Cristescu [2]. The solutions described in this paper are obtained based on a model first proposed by Sokolovskii [3, 4]. This model cannot, in general, be used to describe the structure or generation of shock waves [5, 6]. In applying the solutions given in this paper to the unsteady motions behind propagating shock layers or relaxation zones, additional material properties may have to be assumed within these shock or relaxation regions.

2. MATHEMATICAL FORMULATION

One-dimensional motion may be described by a scalar deformation field,

$$\bar{x} = \bar{x}(\bar{X}, \bar{t}), \tag{2.1}$$

where $\bar{x}$ is the instantaneous position coordinate at time $\bar{t}$ of a generic particle whose position coordinate at $\bar{t} = 0$ was $\bar{X}$. The Lagrangian equation of motion and kinematic compatibility condition for rectilinear, one-dimensional motion are†

$$\rho \partial u / \partial \bar{t} = \partial \bar{\sigma} / \partial \bar{X}, \tag{2.2}$$

$$\partial \epsilon / \partial \bar{t} = \partial u / \partial \bar{X}, \tag{2.3}$$

where $\bar{\sigma}$ is the longitudinal stress, and

$$u = \partial \bar{x} / \partial \bar{t}, \tag{2.4}$$

$$\epsilon = \partial \bar{x} / \partial \bar{X} - 1. \tag{2.5}$$

are the particle velocity and linear Lagrangian strain, respectively. The material is assumed to be initially unstressed and unstrained with a constant density ρ.

In this analysis, the material under consideration will be assumed to follow the special constitutive relation for a rate-sensitive, elastoplastic material generalized from a model suggested by Sokolovskii [3, 4],

$$\partial \epsilon / \partial \bar{t} = \partial u / \partial \bar{X} = E^{-1} \partial \bar{\sigma} / \partial \bar{t} + \gamma f(\bar{\sigma}/\sigma_0 - 1) 1_+ (\bar{\sigma}/\sigma_0 - 1), \tag{2.6}$$

where $f(\cdot)$ is a dimensionless C^1 function with $f(\eta) > 0$ for $\eta > 0$, $1_+(\cdot)$ is the Heaviside function, E is the modulus of elasticity which is assumed to be a constant, σ_0 is the static yield stress, and γ is a material constant. Thus, the material is assumed to have an elastic range with a constant modulus. If the strain rate is held constant, Equation (2.6) may be integrated by simple quadrature‡. Typical stress–strain curves for $\partial \epsilon / \partial \bar{t} =$ constant are displayed in Fig. 1. It is seen that the dynamic yield stress is rate-sensitive and there are no strain-hardening effects. Equation (2.6) includes the well-known models suggested by Cowper and Symonds [8], and Perzyna [9], as special cases. It is a special form of a more general constitutive equation suggested by Malvern [10].

Equations (2.2) and (2.6) are the basic equations describing the functions, $u(\bar{X}, \bar{t})$, $\bar{\sigma}(\bar{X}, \bar{t})$, [and $\epsilon(\bar{X}, \bar{t})$], characterizing the one-dimensional motions to be considered in this paper. These equations may be combined into one single, second-order, nonlinear,

†See e.g. Courant and Friedrichs [7].

‡The authors are grateful to Professor A. C. Eringen for suggesting this.

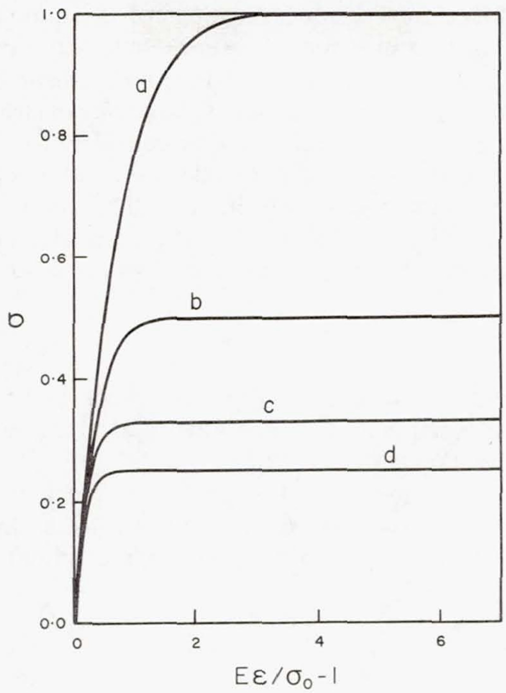

Fig. 1. Typical stress–strain curves for constant strain rates. (a) $\sqrt{\gamma}/k = 1$, (b) $\sqrt{\gamma}/k = 2$, (c) $\sqrt{\gamma}/k = 3$, (d) $\sqrt{\gamma}/k = 4$, $k = \partial\epsilon/\partial t$.

hyperbolic, partial differential equation of the evolution type in dimensionless form as follows:

$$\beta(\partial^2\sigma/\partial x^2 - \partial^2\sigma/\partial t^2) = [1_+(\sigma)\mathrm{d}f(\sigma)/\mathrm{d}\sigma + \delta(\sigma)f(0)]\partial\sigma/\partial t, \tag{2.7}$$

where

$$\sigma(x,t) \equiv \bar{\sigma}/\sigma_0 - 1, \tag{2.8}$$

is the dimensionless overstress,

$$x \equiv \alpha\bar{X}, \tag{2.9}$$

$$t \equiv \alpha c\bar{t}, \tag{2.10}$$

$$c \equiv \sqrt{E/\rho}, \tag{2.11}$$

$$\alpha \equiv \beta\gamma\sqrt{\rho E/\sigma_0}, \tag{2.12}$$

$\delta(\cdot)$ is the Dirac delta functional, and $\beta > 0$ is a dimensionless constant included here in the definition of α for convenience.

Materials described by the constitutive relation given in (2.6) probably cannot support shock layers or explain the generation of shockfronts. If a shock layer is dissipative, then generalized viscoelastic theories and constitutive relations such as those considered by Varley and Rogers[6], Coleman and Gurtin[11], Dunwoody and Dunwoody [12] and Pipkin [5], or further generalizations of these models, should be used to describe it. For propagation in a rod, the shock layer may be dispersive due to lateral deformation† instead of due to any dissipative mechanism. Such a shock transition may be described in terms of a low frequency, large rate of straining expansion of a three-dimensional deformation field similar to that considered by Parker and Varley [13]. In applying one of the self-similar motions described in this paper to a nonlinear wave motion behind a propagating shockfront, it will be assumed that the rate of straining in the shock layer is high enough to allow the material to exhibit instantaneous linear elasticity‡ [1]. Thus, across such a shock layer, it will be assumed that

$$[\overline{\sigma}] = E[\epsilon], \tag{2.13}$$

where $[\chi]$ denotes the jump in value of χ across the shock layer, and the value of E will be assumed to be a constant and have the same value as the modulus of the elastic range of the constitutive relation given by (2.6).

From the Lagrangian equation of motion (2.2) and the kinematic compatibility condition (2.3), two additional jump conditions relating $[u]$, and $[\epsilon]$, can be deduced formally following a technique suggested by Courant and Friedrichs [7]. The results are:

$$\rho U[u] + [\overline{\sigma}] = 0, \tag{2.14}$$

$$U[\epsilon] + [u] = 0, \tag{2.15}$$

where U is the propagation speed of the shockfront. Equations (2.14) and (2.15) can also be deduced from physical arguments directly. The jump conditions, (2.13)–(2.15), indicate that the speed of propagation of a shock layer of a material exhibiting instantaneous elasticity is

$$|U| = \sqrt{E/\rho}, \tag{2.16}$$

which is, in fact, the same as the elastic speed of propagation of small disturbances.

In applying the constant speed solutions to the 'unsteady' motion behind a propagating discontinuity which moves at a constant sub-elastic speed, it will be assumed that there is an elastic precurser and an unloading, relaxation zone, or a constant stress region, ahead of the discontinuity. The details of the unsteady motion of a relaxation zone ahead of such a discontinuity may be very complicated and will not be considered in this paper.

3. A CLASS OF SELF-SIMILAR SOLUTIONS

Cowper and Symonds [8] proposed, in 1957, a power law,

$$f(\sigma) = \sigma^{\delta}, \tag{3.1}$$

†The authors are indebted to Professor E. Varley for a discussion pertaining to this point.

‡The range of rate of straining within which materials exhibit instantaneous elasticity varies from one material to another. There is usually an upper (and lower) cutoff point in rate of straining above (and below) which a material may have to be considered viscoelastic. The authors are indebted to Professor R. S. Rivlin for pointing this out to them.

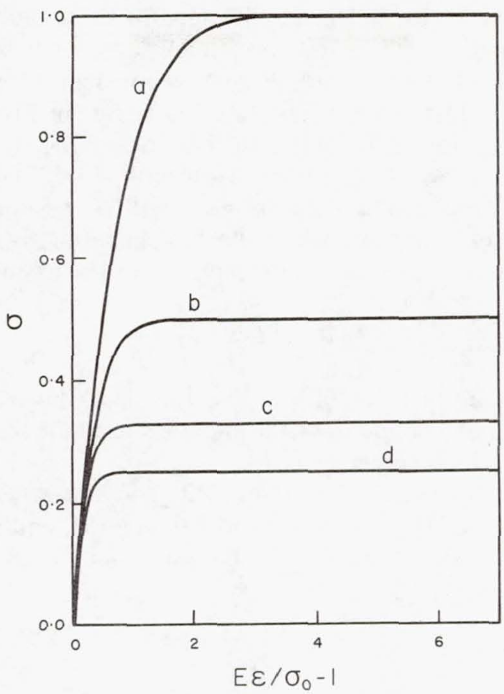

Fig. 1. Typical stress–strain curves for constant strain rates. (a) $\sqrt{\gamma}/k = 1$, (b) $\sqrt{\gamma}/k = 2$, (c) $\sqrt{\gamma}/k = 3$, (d) $\sqrt{\gamma}/k = 4$, $k = \partial\epsilon/\partial t$.

hyperbolic, partial differential equation of the evolution type in dimensionless form as follows:

$$\beta(\partial^2\sigma/\partial x^2 - \partial^2\sigma/\partial t^2) = [1_+(\sigma)\mathrm{d}f(\sigma)/\mathrm{d}\sigma + \delta(\sigma)f(0)]\partial\sigma/\partial t, \tag{2.7}$$

where

$$\sigma(x,t) \equiv \bar{\sigma}/\sigma_0 - 1, \tag{2.8}$$

is the dimensionless overstress,

$$x \equiv \alpha\bar{X}, \tag{2.9}$$

$$t \equiv \alpha c\bar{t}, \tag{2.10}$$

$$c \equiv \sqrt{E/\rho}, \tag{2.11}$$

$$\alpha \equiv \beta\gamma\sqrt{\rho E/\sigma_0}, \tag{2.12}$$

$\delta(\cdot)$ is the Dirac delta functional, and $\beta > 0$ is a dimensionless constant included here in the definition of α for convenience.

Materials described by the constitutive relation given in (2.6) probably cannot support shock layers or explain the generation of shockfronts. If a shock layer is dissipative, then generalized viscoelastic theories and constitutive relations such as those considered by Varley and Rogers[6], Coleman and Gurtin[11], Dunwoody and Dunwoody [12] and Pipkin [5], or further generalizations of these models, should be used to describe it. For propagation in a rod, the shock layer may be dispersive due to lateral deformation† instead of due to any dissipative mechanism. Such a shock transition may be described in terms of a low frequency, large rate of straining expansion of a three-dimensional deformation field similar to that considered by Parker and Varley [13]. In applying one of the self-similar motions described in this paper to a nonlinear wave motion behind a propagating shockfront, it will be assumed that the rate of straining in the shock layer is high enough to allow the material to exhibit instantaneous linear elasticity‡ [1]. Thus, across such a shock layer, it will be assumed that

$$[\bar{\sigma}] = E[\epsilon], \tag{2.13}$$

where $[\chi]$ denotes the jump in value of χ across the shock layer, and the value of E will be assumed to be a constant and have the same value as the modulus of the elastic range of the constitutive relation given by (2.6).

From the Lagrangian equation of motion (2.2) and the kinematic compatibility condition (2.3), two additional jump conditions relating $[u]$, and $[\epsilon]$, can be deduced formally following a technique suggested by Courant and Friedrichs [7]. The results are:

$$\rho U[u] + [\bar{\sigma}] = 0, \tag{2.14}$$

$$U[\epsilon] + [u] = 0, \tag{2.15}$$

where U is the propagation speed of the shockfront. Equations (2.14) and (2.15) can also be deduced from physical arguments directly. The jump conditions, (2.13)–(2.15), indicate that the speed of propagation of a shock layer of a material exhibiting instantaneous elasticity is

$$|U| = \sqrt{E/\rho}, \tag{2.16}$$

which is, in fact, the same as the elastic speed of propagation of small disturbances.

In applying the constant speed solutions to the 'unsteady' motion behind a propagating discontinuity which moves at a constant sub-elastic speed, it will be assumed that there is an elastic precurser and an unloading, relaxation zone, or a constant stress region, ahead of the discontinuity. The details of the unsteady motion of a relaxation zone ahead of such a discontinuity may be very complicated and will not be considered in this paper.

3. A CLASS OF SELF-SIMILAR SOLUTIONS

Cowper and Symonds [8] proposed, in 1957, a power law,

$$f(\sigma) = \sigma^{\delta}, \tag{3.1}$$

†The authors are indebted to Professor E. Varley for a discussion pertaining to this point.

‡The range of rate of straining within which materials exhibit instantaneous elasticity varies from one material to another. There is usually an upper (and lower) cutoff point in rate of straining above (and below) which a material may have to be considered viscoelastic. The authors are indebted to Professor R. S. Rivlin for pointing this out to them.

where $\delta > 0$ is a dimensionless material constant, to describe the rate-sensitivity of perfectly plastic materials. This law seems to be quite adequate in approximating the dynamic responses of certain metallic alloys[14, 15] under moderately high rates of straining. The material constants, γ and δ, for such a material may be determined by explosive ring-tests as suggested by Perrone[16]. Recent investigators[17–21] have applied this model to impulsively loaded beams, rods, and plates. The class of self-similar solutions described in this paper is based on the constitutive relation (2.6) and the special form of $f(\sigma)$ given by (3.1). Under these constitutive assumptions, equation (2.7) may be expressed as follows:

$$\phi(\sigma_{xx}, \sigma_{tt}, \sigma_t, \sigma; x, t) = 0, \tag{3.2}$$

where

$$\phi \equiv \sigma_{xx} - \sigma_{tt} - \sigma^{\delta-1}\sigma_t 1_+(\sigma), \tag{3.3}$$

and subscripts denote partial differentiation. The constant β which appeared in the definition of α in (2.12) has been replaced by the material constant δ.

Consider a one-parameter continuous group of transformations defined by

$$(X, T, \Sigma) = (bx, b^m t, b^n \sigma), \tag{3.4}$$

$$(\Sigma_{XX}, \Sigma_{TT}, \Sigma_T) = (b^{n-2}\sigma_{xx}, b^{n-2m}\sigma_{tt}, b^{n-m}\sigma_t), \tag{3.5}$$

where b is the parameter, and m,n are constants. It can be shown that for the special case of $m = 1, n = 1/(1-\delta)$,

$$\phi(\sigma_{xx}, \sigma_{tt}, \sigma_t, \sigma; x, t) = b^{(1-2\delta)/(1-\delta)}\phi(\Sigma_{XX}, \Sigma_{TT}, \Sigma_T, \Sigma; X, T), \tag{3.6}$$

where it is assumed that $\delta \neq 1$. For $\delta = 1$, equation (3.2) is linear and the analytical solution has been discussed in detail by Malvern[10]. Thus, ϕ is a constant conformal invariant under the group defined by equations (3.4) and (3.5) with $m = 1$, and $n = 1/(1-\delta)$. According to a theorem proven by Morgan[22], the solution to equation (3.2) may be expressed in terms of a function $F(\xi)$ of an absolute invariant ξ of the transformation group defined by

$$(X, T) = (bx, bt). \tag{3.7}$$

The function $F(\xi)$ is an absolute invariant of the transformation group defined by

$$(X, T, \Sigma) = (bx, bt, b^{1/(1-\delta)}\sigma). \tag{3.8}$$

It will be straightforward to verify that

$$\xi = t/x, \tag{3.9}$$

$$F(\xi) = x^{1/(\delta-1)}\sigma(x, t), \tag{3.10}$$

are absolute invariants of the groups defined by equations (3.7) and (3.8), respectively.

Thus, there exists a class of self-similar solutions to equation (3.2) of the form

$$\sigma = x^{1/(1-\delta)}F(\xi), \tag{3.11}$$

where ξ is given by (3.9).

Substituting equation (3.11) into equation (3.2) and using equation (3.3), a non-linear, second-order ordinary differential equation results. For $\sigma > 0$, this equation is expressible as follows:

$$(\xi^2-1)F''-\{[2\delta/(1-\delta)]\xi+F^{\delta-1}\}F'+[\delta/(1-\delta)^2]F=0, \tag{3.12}$$

where prime denotes differentiation.

For the special case of $\delta=2$, $\xi > 0$, equation (3.12) is immediately integrable to the following Riccati equation:

$$2(\xi^2-1)F'+4\xi F-F^2=4K, \tag{3.13}$$

where K is an arbitrary constant. This equation may be converted into a linear, second-order, ordinary differential equation by the following transformation:

$$(\xi^2-1)^r V(z) = \mathrm{Exp}\left[-\frac{1}{2}\int^{\xi}\frac{F(\xi')}{\xi'^2-1}\,\mathrm{d}\xi'\right], \tag{3.14}$$

$$2z=\xi+1. \tag{3.15}$$

The result is:

$$z(1-z)V''+2(1+r)(1-2z)V'-(2r-K)V=0, \tag{3.16}$$

where r satisfies the quadratic equation,

$$4r^2+4r+K=0. \tag{3.17}$$

Equation (3.16) has three regular singular points at $z=0$, 1, and ∞. The solutions to this equation are expressible in terms of hypergeometric functions. For $\xi > 1$, the appropriate general solution to (3.16) is, in the usual notation,

$$V(z) = Cz^{-2r-3}{}_2F_1[2r+3,2,4;1/z], \tag{3.18}$$

where C is an arbitrary constant. Thus, from equation (3.14), the corresponding expression for $F(\xi)$ is

$$F(\xi) = 6(\xi-1)-4r+2(2r+3)\,\frac{(\xi-1){}_2F_1[2r+4,3,5;2/(\xi+1)]}{(\xi+1){}_2F_1[2r+3,2,4;2/(\xi+1)]}. \tag{3.19}$$

The expression (3.19) for $F(\xi)$ assumes some particularly simple forms in terms of elementary functions for special values of K. As examples, typical expressions for $F(\xi)$ and $\sigma(x,t)$ for two different values of K are listed below:

$K = 0$, (i.e. $r = 0$, or -1)

$$F(\xi) = 8\{2\xi + (\xi^2 - 1) \ln [(\xi - 1)/(\xi + 1)] + A_1(\xi^2 - 1)\}^{-1}. \quad (3.20)$$

$$\sigma(x, t) = 8x\{2xt + (t^2 - x^2) \ln [(t - x)/(t + x)] + A_1(t^2 - x^2)\}^{-1}. \quad (3.21)$$

$K = -3$, (i.e. $r = 1/2$ or $-3/2$)

$$F(\xi) = 6(1 + A_2\xi + \xi^2)/(A_2 + 3\xi - \xi^2), \quad (3.22)$$

$$\sigma(x, t) = 6(x^2 + A_2xt + t^2)/(A_2x^3 + 3x^2t - t^3). \quad (3.23)$$

In these expressions, A_1 and A_2 are arbitrary constants.

It is interesting to note that the solution given by (3.21) is invariant under the translation defined by $(x', t') = (x + a, t + a)$, where a is an arbitrary constant. This property will be utilized in Section 5 to derive a closed form solution of a self-similar, unsteady, dispersed, nonlinear wave motion behind a constant 'elastic-speed' shockfront propagating into an initially quiescent region.

4. NONLINEAR WAVES WITH CONSTANT SPEEDS

Equation (2.7) is a nonlinear, hyperbolic differential equation of the evolution type. The characteristic speeds related to this equation are given by,

$$\mathrm{D}_{\pm}\bar{X}/\mathrm{D}t = \pm c, \quad (4.1)$$

or,

$$\mathrm{D}_{\pm}x/\mathrm{D}t = \pm 1, \quad (4.2)$$

where $\mathrm{D}_{\pm}(\cdot)/\mathrm{D}\bar{t}$ and $\mathrm{D}_{\pm}(\cdot)/\mathrm{D}t$ denote differentiation along the characteristics.

Due to the presence of the evolution or dissipative term, $[1_{+}(\sigma)\mathrm{d}f(\sigma)/\mathrm{d}\sigma + \delta(\sigma)f(0)]\cdot \partial\sigma/\partial t$, in equation (2.7), it is expected that, in the plastic range, the material can also support dissipative, dispersive waves in addition to the characteristic propagations of discontinuities given by equation (4.1) or (4.2). To demonstrate the existence of non-characteristic propagations, a class of constant speed solutions to equation (2.7) is considered in this section. This class of solutions is obtained by searching for expressions of the form:

$$\sigma(x, t) = g(s), \quad (4.3)$$

where

$$s \equiv \bar{c}\bar{t} - x, \quad (4.4)$$

and $\bar{c}$ = constant determines the speed of propagation.

Substituting equation (4.3) into equation (2.7), a nonlinear, second-order, ordinary differential equation results:

$$\beta(1 - \bar{c}^2)g'' = \bar{c}[1_{+}(g)f'(g) + \delta(g)f(0)]g', \quad (4.5)$$

where primes denote differentiation. This equation can be integrated once immediately to yield,

$$\beta(1-\bar{c}^2)g' = \bar{c}1_+(g)f(g)+A, \tag{4.6}$$

where A is an arbitrary constant. Actually, the fact that equation (4.5) can be integrated once in closed form is not due to the special choice of the constitutive equation, (2.6), since, by assuming solutions of constant speeds of propagation, equation (2.2) can be integrated at once without making any additional assumptions. By comparing the expression (4.6) with the basic equations, (2.2) and (2.6), it is easily demonstrated that $A = 0$. Thus,

$$\beta(1-\bar{c}^2)g' = \bar{c}1_+(g)f(g), \tag{4.7}$$

for constant speeds of propagation.

If $g < 0$, then equation (4.7) becomes

$$(1-\bar{c}^2)g' = 0. \tag{4.8}$$

Except for the trivial case of $g =$ constant, equation (4.8) requires that $\bar{c} = \pm 1$, which of course is the elastic speed of propagation. For $g > 0$, equation (4.7) requires that

$$\text{(i) } \bar{c}^2 < 1, \text{for } (g'/\bar{c}) > 0, \tag{4.9}$$

$$\text{(ii) } \bar{c}^2 > 1, \text{for } (g'/\bar{c}) < 0. \tag{4.10}$$

Thus, for the physically more meaningful case $\bar{c}^2 < 1$, the overstress may increase or decrease with s depending on whether $\bar{c} > 0$ or < 0. Equations (4.9) and (4.10) also indicate that if solutions for $g > 0$ exist, the waves represented by these solutions are not characteristic propagations.†

On setting $h = g'$, equation (4.5) for $g > 0$ may be written as

$$\frac{h'}{g'} = \frac{\bar{c}}{\beta(1-\bar{c}^2)}f'(g). \tag{4.11}$$

Since $f(g)$ is a C^1 function, equation (4.11) does not have any singular points. Thus, according to the Poincaré–Bendixon theorem, it may be concluded that equation (4.11), in general, does not possess periodic solutions.

For $g > 0$, equation (4.7) may be integrated, in general, by quadrature as follows:

$$s = [\beta(1-\bar{c}^2)/\bar{c}] \int^g f^{-1}(\zeta)\,\mathrm{d}\zeta + C', \tag{4.12}$$

where C' is an arbitrary constant.

Perzyna[9] in 1963, suggested two interesting expressions for $f(\zeta)$. In slightly generalized forms, these expressions are given as follows:

†In fact, these waves are similar to the so-called solitary waves which are constant-speed, nonlinear propagations of special wave forms. The authors are indebted to Professor G. S. S. Ludford for pointing this out to them.

$$\text{(i) } f(\zeta) = \sum_{l=0}^{L} a_l \zeta^l, \tag{4.13}$$

$$\text{(ii) } f(\zeta) = b_0 + \sum_{l=1}^{L} b_l (\operatorname{Exp} \zeta^l - 1), \tag{4.14}$$

where a_l, b_l are constants. Expression (i) or equation (4.13) includes the model $f(\zeta) = \zeta^\delta$ suggested by Cowper and Symonds [8] as a special case. For $F(\zeta) = \zeta^\delta$, and $\delta \neq 1$, equation (4.12) becomes,

$$s - s_1 = \frac{\delta(1-\bar{c}^2)}{(1-\delta)\bar{c}} (g^{1-\delta} - g_1^{1-\delta}), \tag{4.15}$$

where $g_1 = g(s_1)$, s_1 is a constant, and β has been chosen as δ.

Another simple result is obtained for the constitutive relation (ii) or equation (4.14) with $L = 1$. The integrated expression is

$$s - s_1 = \frac{(1-\bar{c}^2)}{\bar{c}} \left[(g_1 - g) + \ln\left(\frac{e^g - 1}{e^{g_1} - 1}\right) \right], \tag{4.16}$$

where, again, $g_1 = g(s_1)$, s_1 is a constant, and β has been chosen as b_1.

It is of interest to note that for the constitutive relation (i), or equation (4.13), $f^{-1}(\zeta)$ may be expressed in the form:

$$f^{-1}(\zeta) = \sum_{k=1}^{m} c_k (\alpha_1 \zeta + \alpha_2)^{-k} + \sum_{p=1}^{n} (d_p \zeta + e_p)(\beta_1 \zeta^2 + 2\beta_2 \zeta + \beta_3)^{-p}, \tag{4.17}$$

where α_1, α_2, β_1, β_2, β_3, c_k, d_p, and e_p are real constants, with $\beta_2^2 < \beta_1 \beta_3$. Thus, the integral in equation (4.12) can always be evaluated in closed form in terms of elementary functions.

5. NONLINEAR WAVE MOTION BEHIND PROPAGATING DISCONTINUITIES

5.1 *Self-similar solution behind a constant-speed shockfront*

Consider a one-dimensional shockfront propagating at some speed $U (> 0)$ into an initially quiescent one-dimensional region ($x \geqslant 0$). As it had been remarked earlier, if the range of the rate of straining within the shock layer renders the material to exhibit instantaneous linear elasticity, then the shockfront will propagate at a constant speed,

$$U = \sqrt{E/\rho}, \tag{5.1}$$

where E is the instantaneous modulus of elasticity. If the value of E is chosen to be the same as the modulus of the elastic range of the constitutive equation, (2.6), then the shock speed has the same value as the characteristic speed $\mathrm{D}_+X/\mathrm{D}\bar{t}$ given by equation (4.1). Under such an assumption, the values of u and $\bar{\sigma}$ immediately behind the shock layer must satisfy the characteristic compatibility condition [10]:

$$\mathrm{d}\bar{\sigma} - \rho c \mathrm{d}u = -E\gamma f(\bar{\sigma}/\sigma_0 - 1) 1_+(\bar{\sigma}/\sigma_0 - 1)\, \mathrm{d}\bar{t}, \tag{5.2}$$

where $c = U = \sqrt{E/\rho}$.

The values of u, $\bar{\sigma}$, and ϵ, immediately behind the shock layer must also satisfy the jump conditions given by equations (2.13) to (2.15). Since u, $\bar{\sigma}=0$ in the quiescent region in front of the shock layer, equation (2.14) requires that,

$$\bar{\sigma}=-\rho U u=-\rho c u, \tag{5.3}$$

immediately behind the shock layer. Combining equations (5.2) and (5.3), the following differential equation results:

$$2\beta \mathrm{d}\sigma=-f(\sigma)1_{+}(\sigma)\,\mathrm{d}t, \tag{5.4}$$

where as before, $\sigma \equiv (\bar{\sigma}/\sigma_0-1)$ and $t \equiv \alpha c\bar{t}$ with $\alpha \equiv \beta\gamma\sqrt{\rho E}/\sigma_0$. Equation (5.4) indicates that, if $\sigma > 0$, then the overstress immediately behind the shockfront always attenuates with time along the shock.

Assuming that $\sigma > 0$ behind the shockfront, equation (5.4) can be integrated by quadrature as follows:

$$t=2\beta\int^{\sigma} f^{-1}(\zeta)\,\mathrm{d}\zeta+C'', \tag{5.5}$$

where the integral is identical to that of equation (4.12). Thus, closed-form solutions of equation (5.5) are possible for special constitutive assumptions. For $f(\zeta)=\zeta^{\delta}$ with $\delta \neq 1$, equation (5.5) becomes

$$t=[2\delta/(1-\delta)](\sigma_1^{1-\delta}-\sigma^{1-\delta}), \tag{5.6}$$

where $\sigma_1 \equiv \sigma(0)$, and β has been chosen as δ. Therefore, the overstress immediately behind the shock attenuates monotonically with time along the shockfront from $\sigma=\sigma_1$ at $t=0$ to $\sigma=0$ at $t=\infty$.

It is interesting to note that for $\delta=2$, equation (5.6) can be satisfied by one of the self-similar solutions given in Section 3:

$$8\sigma^{-1}=(x+a)[2\eta+(\eta^2-1)\{A_1+\ln[(\eta-1)/(\eta+1)]\}], \tag{5.7}$$

where $\eta=(t+a)/(x+a)$, and a, A_1 are constants. To satisfy the compatibility condition (5.6) for $\delta=2$, the constant a in (5.7) must be chosen as follows:

$$a=4/\sigma_1. \tag{5.8}$$

Therefore, the dimensionless overstress $\sigma(x,t)$ behind the shockfront is given by,

$$\sigma=8\Big/\left[(t+4/\sigma_1)\left\{2+(\eta-1/\eta)\left[A_1+\ln\left(\frac{\eta-1}{\eta+1}\right)\right]\right\}\right], \tag{5.9}$$

and the stress boundary condition at $x=0$ is,

$$\sigma(0,t)=8/[2(t+4/\sigma_1)+(2t+\sigma_1 t^2/4)\{A_1-\ln[1+8/(\sigma_1 t)]\}]. \tag{5.10}$$

The behavior of this function for various values of A_1 is shown in Fig. 2.

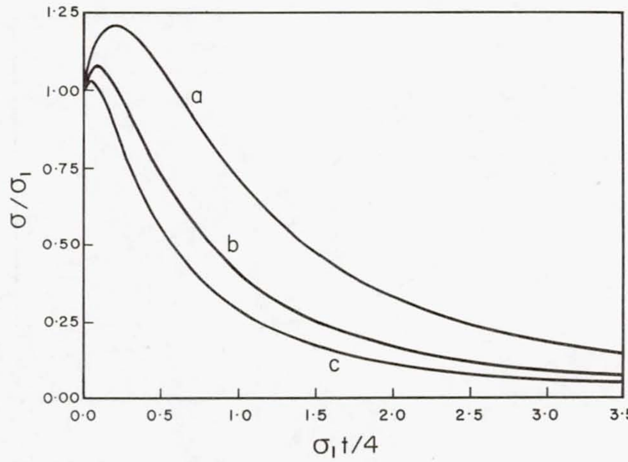

Fig. 2. Variation of σ/σ_1 with $\sigma_1 t/4$ at $\bar{X}=0$. Self-similar solution ($\delta=2$). (a) $A_1=\ln 2$, (b) $A_1=\ln 4$, (c) $A_1=\ln 8$.

In dimensional forms, the resulting expressions for $\sigma(\bar{X},\bar{t})$, $u(\bar{X},\bar{t})$, and $\epsilon(\bar{X},\bar{t})$ for this case are given as follows:

$$\sigma=\bar{\sigma}/\sigma_0-1=[4c\sigma_0/(E\gamma)](\bar{X}+ct_0)[2c(\bar{X}+ct_0)(\bar{t}+\bar{t}_0)-[c^2\bar{t}(\bar{t}+2t_0) \\ -\bar{X}(\bar{X}+2ct_0)]\{\ln[(c\bar{t}+\bar{X}+2ct_0)/(c\bar{t}-\bar{X})]+B\}]^{-1}, \tag{5.11}$$

$$u=-(\sigma_0/\rho)[\sigma(\bar{t}+t_0)/(\bar{X}+ct_0)+c^{-1}], \tag{5.12}$$

$$\epsilon=(\sigma_0/\rho)[\sigma(\bar{t}+t_0)^2/(\bar{X}+ct_0)^2+c^{-2}], \tag{5.13}$$

where

$$t_0=2\sigma_0/(\gamma\sigma_1 E), \tag{5.14}$$

and B is a constant. The behavior of the functions $u(0,\bar{t})$ and $\epsilon(0,\bar{t})$ for various values of A_1 are indicated in Figs. 3 and 4. It is of interest to note that (5.13) yields a permanent strain ϵ_p given by

$$\epsilon_p=\lim_{\bar{t}\to\infty}\epsilon=(\sigma_0/E)[(4c\sigma_0/A_1\gamma E))(\bar{X}+ct_0)^{-1}+1]. \tag{5.15}$$

Typical distributions of the permanent strain are shown in Fig. 5.

5.2. *Constant speed solution behind an elastic precurser*

Duvall[23] suggested that the one-dimensional, unsteady motion in a semi-infinite ($x \geqslant 0$), rate-sensitive, elastoplastic region generated by a continuously applied load at its boundary ($x=0$) may eventually consist of an elastic precurser propagating into an initially quiescent region, an unloading, relaxation zone, and a sub-elastic, constant-speed, nonlinear wave motion as depicted in Fig. 6. After a reasonable length of time, the elastic precurser will be far ahead of the leading wave of the constant speed region

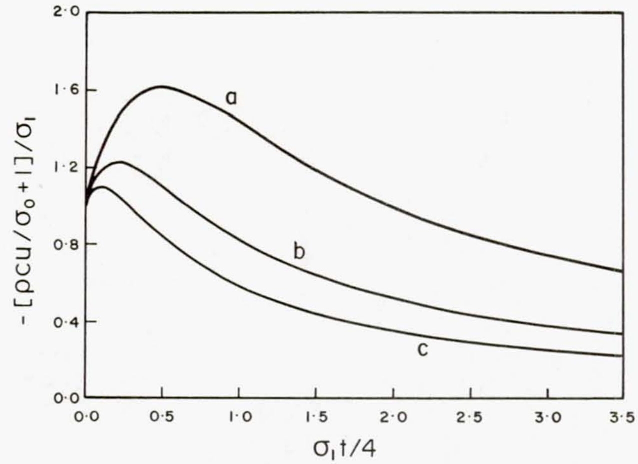

Fig. 3. Variation of $-[\rho cu/\sigma_0+1]/\sigma_1$ with $\sigma_1 t/4$ at $\bar{X}=0$. Self-similar solution ($\delta=2$). (a) $A_1=\ln 2$, (b) $A_1=\ln 4$, (c) $A_1=\ln 8$.

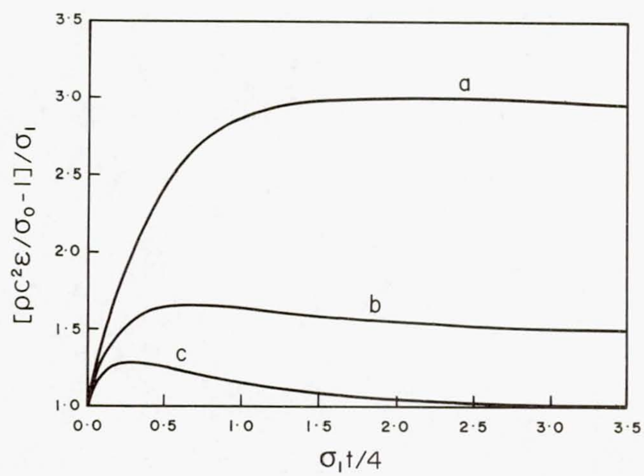

Fig. 4. Variation of $[\rho c^2\epsilon/\sigma_0-1]/\sigma_1$ with $\sigma_1 t/4$ at $\bar{X}=0$. Self-similar solution ($\delta=2$). (a) $A_i=\ln 2$, (b) $A_1=\ln 4$, (c) $A_1=\ln 8$.

and the boundary of $x=0$ will be far behind it. Relative to an observer moving with the leading wave of the constant speed region, the unsteady motion behind the leading wave becomes essentially steady.

Any of the constant-speed, nonlinear wave solutions described by equation (4.12) in section 4 with $\bar{c}<1$ may be considered as a constant-speed portion of such an 'unsteady' motion. If the overstress on the leading wave $s=s_1$ is $\sigma_1>0$, then the quadrature expression, (4.12), becomes,

$$s-s_1=[\beta(1-\bar{c}^2)/\bar{c}]\int_{\sigma_1}^{\sigma} f^{-1}(\zeta)\,d\zeta, \tag{5.16}$$

where $s\equiv\bar{c}t-x$, and $\bar{c}<1$. From equation (5.16), the stress boundary condition

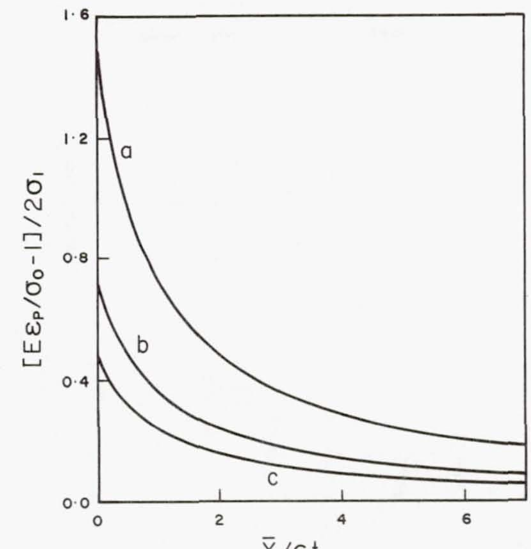

Fig. 5. Typical distributions of the permanent strain. Self-similar solution ($\delta = 2$). (a) $A_1 = \ln 2$, (b) $A_1 = \ln 4$, (c) $A_1 = \ln 8$.

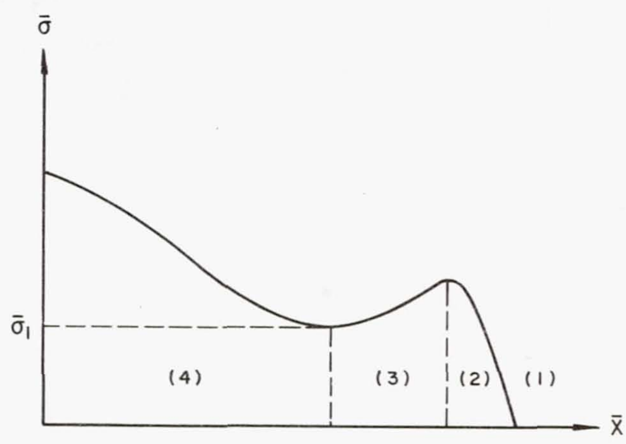

Fig. 6. Schematic representation of a nonlinear wave motion behind a relaxation zone. (1) quiescent region, (2) elastic precursor, (3) relaxation zone, (4) sub-elastic, constant speed region.

required to maintain the constant-speed motion can be evaluated in a straightforward manner.

It is of interest to note that, if the initial rate of loading of the applied stress at the boundary is not too high such that the time required to raise the stress $\bar{\sigma}$ from zero to the value of the static yield stress σ_0 is much longer than the pertinent characteristic relaxation time of the medium, then a complete description of a possible non-linear wave motion for a continuously loading boundary may be constructed exactly. Figure 7 is a schematic representation of such a motion. It consists of four solution regions

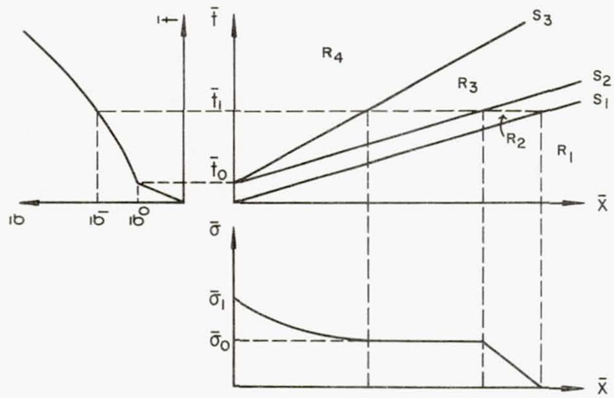

Fig. 7. Schematic representation of a possible nonlinear wave motion due to a continuously loading boundary at $\bar{X} = 0$.

separated by three discontinuities described as follows:

(1) *Solution regions*

R_1: the undisturbed region, $\overline{\sigma} = 0$

R_2: the elastic region, $\overline{\sigma} < \sigma_0$

R_3: the constant stress region, $\overline{\sigma} = \sigma_0$

R_4: the constant speed solution region, $\overline{\sigma} > \sigma_0$.

(2) *Discontinuities*

S_1: the leading elastic wave

S_2: the trailing elastic wave

S_3: the leading constant speed wave.

Such an unsteady motion may be generated by a monotonically increasing stress boundary condition. The manner in which the stress varies at the boundary in the elastic range can be quite arbitrary (so long as the rate of loading is small enough so that there will be no dynamic overstressing in the elastic precurser) and has been chosen as a linear function of $\bar{t}$ in Fig. 7 for simplicity, while the rate of stressing beyond the static yield stress must follow the expression given in equation (4.12) or the differential equation, (4.7). It is clear from equation (4.7) that nontrivial solutions in R_4 can be generated from a leading wave S_3 on which the stress is $\overline{\sigma} = 0$ only if $f(0) > 0$. The value of $f(0)$ can be arbitrarily small. Alternatively, if $f(0) = 0$ for a specific constitutive relation, a solution such as the one depicted by Fig. 7 can still be generated by viewing S_3 as a small discontinuity in the value of $\overline{\sigma}$ such that the overstress jumps across this 'plastic shock' from zero to some small constant positive value $\sigma_1 \ll 1$. The jump in σ from 0 to σ_1 at the boundary of $\bar{X} = 0$ may be viewed as the result of a very fast rate of loading r in a small interval of time $\Delta\bar{t}$ near $\bar{t} = \bar{t}_0$ such that $\lim_{\Delta\bar{t} \to 0} (r\Delta\bar{t}) = \overline{\sigma}_1 = (1+\sigma_1)\sigma_0$ and $0 < \sigma_1 \leqslant 1$. The fact that $\overline{\sigma} = \sigma_0$ in R_3 is an admissible solution can be deduced immediately from equation (2.7).

Acknowledgment—This investigation was partially supported by the Advanced Research Projects Agency of the Department of Defense and monitored by the Office of Naval Research under Contract Number N00014-68-A-0187, and partially supported by the National Aeronautics and Space Administration under Grant Number NASA-NGL34-002-084. A portion of this work was completed when one of us (T. S. C.) was visiting the Center for the Application of Mathematics, Lehigh University, and the Department of

Theoretical and Applied Mechanics, Cornell University. The authors are indebted to Professors A. C. Eringen, Y. Horie, G. S. S. Ludford, R. S. Rivlin, and E. Varley for their comments and suggestions.

REFERENCES

[1] R. S. RIVLIN, *Q. appl. Math.* **14**, 83 (1956).
[2] N. CRISTESCU, *Dynamic Plasticity*. North-Holland (1967).
[3] V. V. SOKOLOVSKII, *Dokl. Akad. Nauk SSSR* **60**, 775 (1948).
[4] V. V. SOKOLOVSKII, *Prikl. Mat. Mekh.* **12**, 261 (1948).
[5] A. C. PIPKIN, *Q. appl. Math.* **23**, 297 (1965).
[6] E. VARLEY and T. G. ROGERS, *Proc. R. Soc.* Series A **296**, 498 (1967).
[7] R. COURANT and K. O. FRIEDRICHS, *Supersonic Flow and Shock Waves*. Interscience (1948).
[8] G. R. COWPER and P. S. SYMONDS, *Technical Report No.* 28, *Contract Nonr* 562 (10). Brown University (1957).
[9] P. PERZYNA, *Archwm Mech. stosow* **15**, 113 (1963).
[10] L. E. MALVERN, *Q. appl. Math.* **8**, 405 (1951).
[11] B. D. COLEMAN and M. E. GURTIN, *Proc. IUTAM Symp. Vienna* 54, Springer-Verlag (1968).
[12] J. DUNWOODY and N. DUNWOODY, *Int. J. Engng Sci.* **3**, 417 (1965).
[13] D. F. PARKER and E. VARLEY, *Q. Jl Mech. appl. Math.* **21(3)**, 329 (1968).
[14] M. J. MANJOINE, *J. appl. Mech.* **11**, 211 (1944).
[15] E. W. PARKES, *Proc. Instn civil Engrs* **10**, 277 (1958).
[16] N. PERRONE, *Exp. Mech.* **8**, 232 (1968).
[17] S. R. BODNER and P. S. SYMONDS, *Proc. 2nd Symp. nav. struct. Mech.* 488, Pergamon Press (1960).
[18] T. C. T. TING and P. S. SYMONDS, *Proc. 4th U.S. natn. Congr. appl. Mech.* 1153 (1962).
[19] S. R. BODNER and P. S. SYMONDS, *J. appl. Mech.* **29**, 719 (1962).
[20] T. C. T. TING, *Q. appl. Math.* **21**, 133 (1963).
[21] N. PERRONE, *J. appl. Mech.* **32**, 489 (1965).
[22] A. J. A. MORGAN, *Q. J. Math.* **2**, 250 (1952).
[23] G. E. DUVALL, *Proc. IUTAM Symp. Stress Waves in Anelastic Solids* 20, Springer-Verlag (1964).

(*Received* 20 *July* 1971)

Résumé – Deux classes de solutions du type fermé d'ondes non-linéaires à une dimension, dans un matériau élasto-plastique sensible àla vitesse sont présentées. Une classe de ces solutions est auto-semblable et l'autre classe consiste en des propagations à vitesse constante. Des applications de ces solutions à des mouvements instables en arrière de la propagation de discontinuités sont également considérées.

Zusammenfassung – Zwei Klassen von Lösungen geschlossener Form von eindimensionalen, nicht-linearen Wellen in einem ratenempfindlichen elestoplastischen Stoffe werden mitgeteilt. Eine Klasse dieser Lösungen ist selbst-ähnlich und die andere Klasse besteht aus konstanten Geschwindigkeitsfortpflanzungen. Anwendungen dieser Lösungen auf unstetige Bewegungen hinter sich fortpflanzenden Diskontinuitäten werden auch untersucht.

Sommario – Si tratta di una relazione su due classi di soluzioni di forma chiusa di onde monodimensionali e non lineari in un materiale elastoplastico e sensibile al ritmo. Una classe di queste soluzioni è autosimilare e l'altra consiste in propagazioni a velocità constante. Si prendono anche in considerazione le applicazioni di queste soluzioni ai movimenti instabili dietro le discontinuità di propagazione.

Абстракт — Установлены два класса решений замкнутого вида для одномерных нелинейных волн в эластопластическим материале чувствительном к скорости. Один класс этих решений — самоподобным, а другой состоит из распространений постоянной скорости. Рассмотрены и применения эти решений к нестационарным движениям за распространяющиесь разрывы.

75-04939
N75-15329

Research Notes

Research Notes published in this Section include important research results of a preliminary nature which are of special interest to the physics of fluids and new research contributions modifying results already published in the scientific literature. Research Notes cannot exceed five printed columns in length including space allowed for title, abstract, figures, tables, and references. The abstract should have three printed lines. Authors must shorten galley proofs of Research Notes longer than five printed columns before publication.

Curved Characteristics Behind Blast Waves

O. LAPORTE
Department of Physics, University of Michigan, Ann Arbor, Michigan 48104
AND
T. S. CHANG*
Center for Space Research, Massachusetts Institute of Technology, Cambridge, Massachusetts 02139

(Received 22 December 1970; final manuscript received 6 August 1971)

Exact solutions, expressed in closed form in terms of elementary functions, are presented for the three sets of curved characteristics behind a self-similar, strong blast wave.

Blast waves are produced in gaseous media due to the sudden deposition of large amounts of energy in relatively small regions. The propagation of a point-source blast wave into an ideal gas, whose initial pressure is assumed to be negligibly low, is known to be self-similar. This property can be deduced using either dimensional arguments[1] or invariant theorems of continuous groups of transformations.[2] Closed form solutions describing the flow variables in the nonisentropic region behind such a blast wave in $n=1, 2, 3$ dimensions were obtained independently by von Neumann[3] and Sedov.[4] The reflection of strong blast waves was discussed in an earlier paper[5] by the authors.

It is known that the basic equations governing the nonisentropic flow behind a propagating blast wave admit three distinct characteristic directions given by

$$\frac{dr}{dt}=u, \qquad u\pm a, \tag{1}$$

where r is the radial distance from the point of explosion, t is the elapsed time, u is the velocity, and a is the isentropic speed of sound. The first characteristic direction coincides with the local particle velocity and the family of characteristics is, therefore, composed of particle lines. This direction corresponds to the speed of propagation of entropy disturbances. The other two characteristic directions correspond to the local speeds of propagation of pressure, density, or velocity disturbances. The purpose of this note is to report the interesting result that these three families of curved characteristics can also be represented in closed form, and remarkably, still in terms of elementary functions.

First, consider the (u) characteristics or particle lines. According to its definition and the self-similar solution of Ref. 5, it may be easily deduced that along a (u) characteristic,

$$dr/dt=(2+n)U\hat{u}y(\hat{u})/2, \tag{2}$$

where

$$U=[2K_n/(2+n)](E_0/\rho_0)^{1/(2+n)}t^{-n/(2+n)} \tag{3}$$

is the shock speed, $y(\hat{u})$ is given by Eq. (5) of Ref. 5, $\hat{u}=ut/r$, E_0 is the energy released per unit area for a planar wave, per unit length for a cylindrical wave, and the total energy released for a spherical wave, ρ_0 is the initial density, and K_n is determined by the condition of conservation of total energy.

But, from the definition of the similarity parameter and the expression for the shock radius of Ref. 5, it can be shown that, in general,

$$dr/dt=K_n(E_0/\rho_0)^{1/(2+n)}t^{-n/(2+n)}[2y/(2+n)+t\,dy/dt]. \tag{4}$$

Therefore, from Eq. (5) of Ref. 5 and Eqs. (2)–(4), it is found that,

$$d\ln t=\frac{d\ln y}{d\hat{u}}\frac{d\hat{u}}{\hat{u}-[2/(2+n)]}, \tag{5}$$

along a particle line, where,

$$\frac{d\ln y}{d\hat{u}}=\frac{(\gamma-1)\hat{u}^2/2+[\hat{u}-2/(2+n)][\hat{u}-2/\gamma(2+n)]}{\hat{u}[2/\gamma(2+n)-\hat{u}][(2-n+n\gamma)\hat{u}/2-1]}, \tag{6}$$

and γ is the adiabatic index. Thus, Eq. (5) can be integrated in terms of elementary functions. The result is

$$\hat{t}=\alpha\hat{u}(A_2-\hat{u})^{\beta_1}(\hat{u}-A_2/\gamma)^{\beta_2}(\hat{u}-A_5^{-1})^{\beta_3}, \tag{7}$$

where

$$\alpha = A_1(A_2 - A_1^{-1})^{-\beta_1}(A_1^{-1} - A_2/\gamma)^{-\beta_2}(A_1^{-1} - A_5^{-1})^{-\beta_3},$$

$$\beta_1 = (2\gamma + n - 2)[n(\gamma - 2)]^{-1}\beta_2,$$

$$\beta_2 = n\gamma(2+n)(2-\gamma)(\gamma-1)[2(2n\gamma+2\gamma-n+2) \times (2-n-2\gamma) + 2n\gamma(2-\gamma)(n\gamma+4) + 2(\gamma+1)(2+n) \times (n\gamma^2 - 2n\gamma + n + 2\gamma - 2)]^{-1},$$

$$\beta_3 = (2+n)(n\gamma^2 - 2n\gamma + n + 2\gamma - 2)[n(2-\gamma) \times (n\gamma - n + 2)]^{-1}\beta_2 - 1, \quad (8)$$

$\hat{t} = t/t_0$ is a dimensionless time normalized with respect to some convenient time scale t_0, and the A's are given by Eqs. (6) of Ref. 5.

To complete the solution for the particle lines, an expression relating $(r, t, \hat{u})$ is obtained from Eqs. (2) and (5) of Ref. 5. In dimensionless form, this expression becomes,

$$\hat{r} = (A_1\hat{u})^{-A_2}[A_3(\gamma\hat{u}/A_2 - 1)]^{A_8} \times [A_1(1 - A_5\hat{u})/(A_1 - A_5)]^{A_6 - A_9}\hat{t}^{2/(2+n)}, \quad (9)$$

where $\hat{r} = r/R(t_0)$. Equations (8) and (9) form the closed form parametric solution for the family of (u) characteristics or particle lines behind a self-similar blast wave.

For the $(u \pm a)$ characteristics, we have

$$\frac{d_\pm r}{dt} = u'f \pm \left[\frac{\gamma p' g}{\rho' h}\right]^{1/2} = [U/(\gamma+1)]\{2A_1\hat{u}y(\hat{u}) \pm [2\gamma(\gamma-1)g(\hat{u})/h(\hat{u})]^{1/2}\}, \quad (10)$$

where $g(\hat{u})$, $h(\hat{u})$, and $y(\hat{u})$ are given by Eqs. (4) and (5) of Ref. 5, and the shock speed U by Eq. (3). Combining with Eq. (4) and after considerable manipulation, it is found that

$$d\ln t = G(\hat{u})\, d\hat{u}, \quad (11)$$

where,

$$G(\hat{u}) = (d\ln y/d\hat{u})\{[\hat{u} - 2/(2+n)] \pm [\gamma(\gamma-1)(2 - 2\hat{u} - n\hat{u})/2(2\gamma\hat{u} + n\gamma\hat{u} - 2)]^{1/2}\hat{u}\}^{-1}. \quad (12)$$

The expression $d\ln y/d\hat{u}$ in $G(\hat{u})$ is known and given by Eq. (6). Therefore, $G(\hat{u})$ may be reduced to an algebraic function involving square roots of second degree polynomials of $\hat{u}$ as radicals. This means that Eq. (11) can be integrated in terms of elementary, albeit transcendental, functions. The results are

$$\ln\hat{t} = K_\pm + \ln|A_5\hat{u}/(1 - A_5\hat{u})| \pm (m/l^{1/2}) \times \sin^{-1}\{[l/(A_5^{-1} - \hat{u}) - k]/(k^2 - l)^{1/2}\}, \quad (13)$$

where,

$$k = A_5^{-1} - (\gamma+1)[\gamma(2+n)]^{-1},$$

$$l = A_5^{-2} - 2A_5^{-1}(\gamma+1)[\gamma(2+n)]^{-1} + 4[\gamma(2+n)^2]^{-1},$$

$$m = -A_5^{-1}[(\gamma-1)/2]^{1/2}. \quad (14)$$

Equation (13) and the parametric expression for $(\hat{r}, \hat{t}, \hat{u})$ given by Eq. (9) form the closed form parametric solutions for the two families of $(u \pm a)$ characteristics in the dimensionless $\hat{r}$–$\hat{t}$ plane. The constant $K_\pm$ in Eq. (13) must be evaluated for each characteristic from a set of known values of $(\hat{r}, \hat{t}, \hat{u})$.

Figure 1 displays a typical set of solution curves expressing the dimensionless time $\hat{t}$ as functions of the dimensionless distance $\hat{r}$ for $n = 3$ and $\gamma = \frac{5}{3}$. The terminating curve A is the path of the front of the blast wave. Behind A, there are three families of characteristics: (1) The solid curves are the (u) characteristics or particle lines; (2) the dashed curves are the $(u+a)$ characteristics; and (3) the dot-dashed curves are the $(u-a)$ characteristics.

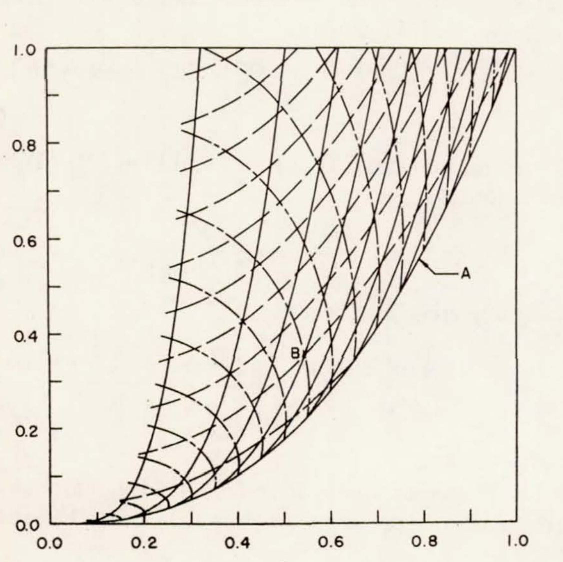

FIG. 1. Curved characteristics behind a strong blast wave for $n=3$, $\gamma=5/3$.

The authors are grateful to Mr. T. Tucker of Oak Ridge National Laboratory for computational assistance.

This research was supported in part by the Department of Defense Project Themis at Lehigh University under Contract Number DAAD05-69-C-0053 monitored by the Ballistic Research Laboratories, and by the National Aeronautics and Space Administration Grant number NASA-NGL34-002-084.

A portion of this manuscript was completed when one of us (T.S.C.) was visiting Cornell University under the auspices of the Army Research Office, Durham.

* Permanent address: North Carolina State University, Raleigh, North Carolina 27607.

[1] G. I. Taylor, Report of Civil Defense Research Committee of the Ministry of Home Security, RC-210, 12 (1941); also, Proc. Roy. Soc. (London) **A201**, 159 (1950).

[2] O. Laporte and T. S. Chang, Ballistic Research Laboratories Technical Report, CAM-110-14 (1971).

[3] J. von Neumann, *Collected Works of von Neumann*, edited by A. H. Taub (Pergamon, New York, 1963), Vol. 6, p. 219.
[4] L. I. Sedov, Prikl. Mat. Mekh. **10,** 241 (1946); also, *Similarity and Dimensional Methods in Mechanics* (Academic, New York, 1959), Chap. IV.
[5] T. S. Chang and O. Laporte, Phys. Fluids **7,** 1225 (1964).

75-04939

THE PHYSICS OF FLUIDS VOLUME 16, NUMBER 1 JANUARY 1973

Comments on "Application of singular eigenfunction expansions to the propagation of periodic disturbances in a radiating grey gas"

T. S. Chang*
Physics Department, Massachusetts Institute of Technology, Cambridge, Massachusetts 02139
and
K. H. Kim and M. N. Özişik
Departments of Engineering Mechanics and Mechanical and Aerospace Engineering, North Carolina State University, Raleigh, North Carolina 27607

(Received 5 June 1972)

Recently, we have been extending our analysis[1] of sound propagation in dissociative, radiative media to include the effects of scattering. It is of interest to note that the set of pertinent integrodifferential equations can also be solved exactly using the singular eigenfunction expansion technique. For the special case of an ideal, grey, scattering gas, our resulting integral equation for the elementary solutions (in terms of the notations of Cheng and Leonard[2]) becomes

$$\left(1-\frac{\mu}{\mathrm{Bu}\nu}\right)\Psi_\nu(\mu)=\tfrac{1}{2}\{[\bar{g}(\nu;c)]^{-1}+c\}\int_{-1}^{1}\Psi_\nu(\mu')\,d\mu', \tag{1}$$

with

$$\bar{g}(\nu;c)=\frac{[(1-c)+i\beta](\nu^2-\bar{\xi}^2)}{(\nu^2+1/\gamma)(1-c)^2},$$

and

$$\bar{\xi}^2=-\frac{(1-c)/\gamma+i\beta}{(1-c)+i\beta},$$

where c denotes the single scattering albedo which is the ratio of the scattering coefficient to the extinction coefficient.

It can be shown that Eq. (1) admits both discrete eigenvalues and a continuous spectrum. The discrete eigenvalues are determined by the dispersion relation

$$\Lambda(\nu)=1-\tfrac{1}{2}(\mathrm{Bu}\nu)\{[\bar{g}(\nu;c)]^{-1}+c\}\int_{-1}^{1}\frac{d\mu}{\mathrm{Bu}\nu-\mu}=0, \tag{2}$$

which for $c=0$ corresponds to Eq. (11) of Ref. 2. Using the argument principle we are able to show that Eq. (2) admits either two or four discrete roots in plus-minus complex pairs. In Figs. 1 and 2 we present the discrete eigenvalues of ν_0 and ν_1 for Bo (Boltzmann number) = 3.23, $\gamma=1.4$, and $c=0.2$. We note that, similar to the results of Cheng and Leonard, there exists a frequency cutoff of the second pair of roots $\pm\nu_1$ below a critical Bouguer number, $\mathrm{Bu}\cong 0.08161$.

We find that it is possible to obtain explicit expressions for the eigenroots of the transcendental equation (2). For example, to determine the explicit expressions for the four roots for $c=0$ with $\mathrm{Bu}\geq\mathrm{Bu}_1=0.1107$, we merely calculate $\Lambda(z)$ and $X(\pm z)$ at two arbitrary values of $z=z_{1,2}$ (preferably along the imaginary axis) according to Eqs. (12) and (26) of Ref. 2. Equation (34) of Ref. 2 then provides a pair of coupled polynomial equations for ν_0 and ν_1,

$$(\nu_0^2-z_i^2)(\nu_1^2-z_i^2)=\frac{\Lambda(z_i)(\xi^2-z_i^2)[1+(1/i\beta)]}{X(z_i)X(-z_i)} \quad \text{for } i=1 \text{ and } 2. \tag{3}$$

Equations (3) can be solved readily to yield the desired explicit expressions for $\pm\nu_0$ and $\pm\nu_1$. Results of some

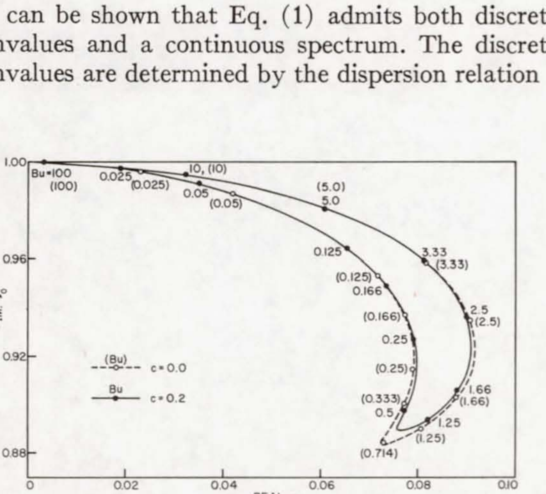

FIG. 1. The first discrete root (ν_0) of $\Lambda(\nu)=0$ for Bo=3.23, $\gamma=1.4$, and $c=0.0$, 0.2.

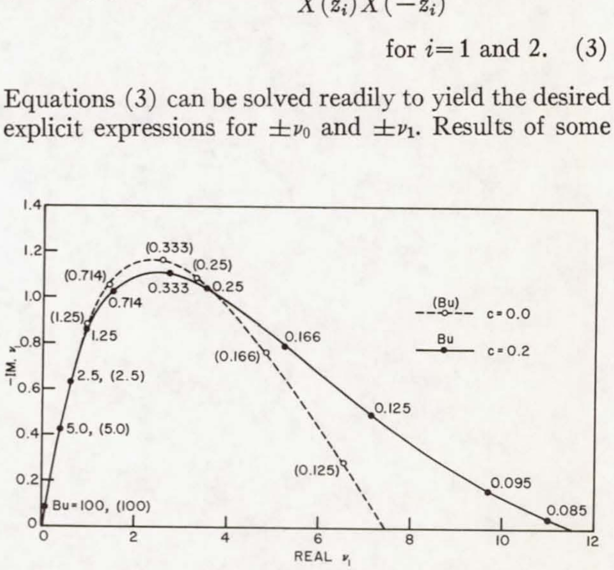

FIG. 2. Second discrete root (ν_1) of $\Lambda(\nu)=0$ for Bo=3.23, $\gamma=1.4$, and $c=0.0$, 0.2.

TABLE I. Discrete eigenvalues for $\mathrm{Bu}=1/6$, $\mathrm{Bo}=3.23$, $\gamma=1.4$, and $c=0$.

	a	b	c
$\mathrm{Re}\nu_0$	0.07738627380	0.07738629373	0.07738
$\mathrm{Im}\nu_0$	−0.9372360013	−0.9372359958	−0.9372
$\mathrm{Re}\nu_1$	4.860766870	4.860766867	4.860
$\mathrm{Im}\nu_1$	−0.7599477400	−0.7599477363	−0.7599

[a] Calculated using a bisection method where the roots are determined by simultaneous sign changes of the real and imaginary parts of $\Lambda(z)$.

[b] Calculated using the explicit expressions.

[c] Values provided by P. Cheng.

sample calculations of the discrete eigenvalues based on this method have been compared with those obtained using the more conventional numerical schemes in Table I. In general, we are able to obtain an accuracy up to eight significant figures using the explicit expressions.

The authors are indebted to Professor P. Cheng for his assistance and for providing us with the numerical values quoted in Table I.

We are grateful to Dr. E. E. Burniston and Dr. C. E. Siewert for valuable discussion and to Dr. J. T. Kriese for his help in calculating the eigenroots using the explicit scheme.

This research was supported in part by National Aeronautics and Space Administration grant NGL34-002-084 and National Science Foundation grant GU-1590.

* Permanent address: Riddick Laboratories, North Carolina State University, Raleigh, North Carolina 27607.

[1] G. K. Lea and T. S. Chang, Phys. Fluids **12**, 983 (1969).

[2] P. Cheng and A. Leonard, Phys. Fluids **14**, 906 (1971).

75-04939

Reprinted from

[redacted]

PERGAMON PRESS
OXFORD · NEW YORK

Int. J. Engng Sci., 1974, Vol. 12, pp. 441–470. Pergamon Press. Printed in Great Britain

N75-15329

ELEMENTARY SOLUTIONS OF COUPLED MODEL EQUATIONS IN THE KINETIC THEORY OF GASES

J. T. KRIESE†
Department of Nuclear Engineering, North Carolina State University, Raleigh, North Carolina 27607, U.S.A.

T. S. CHANG‡
Physics Department, Massachusetts Institute of Technology, Cambridge, Massachusetts 02139, U.S.A.

C. E. SIEWERT
Department of Nuclear Engineering, North Carolina State University, Raleigh, North Carolina 27607, U.S.A.

Abstract—The method of elementary solutions is employed to solve two coupled integrodifferential equations sufficient for determining temperature–density effects in a linearized BGK model in the kinetic theory of gases.

Full-range completeness and orthogonality theorems are proved for the developed normal modes and the infinite-medium Green's function is constructed as an illustration of the full-range formalism.

The appropriate homogeneous matrix Riemann problem is discussed, and half-range completeness and orthogonality theorems are proved for a certain subset of the normal modes. The required existence and uniqueness theorems relevant to the **H** matrix, basic to the half-range analysis, are proved, and an accurate and efficient computational method is discussed. The half-space temperature-slip problem is solved analytically, and a highly accurate value of the temperature-slip coefficient is reported.

1. INTRODUCTION

THERE EXISTS in the kinetic theory of gases a class of one-dimensional problems for which the transverse momentum and heat-transfer effects can be separated by projecting the basic kinetic equation describing the particle distribution function onto certain properly chosen directions in a Hilbert space. The resulting expression describing the heat-transfer and compressibility effects is a vector integrodifferential equation with a matrix kernel similar in form to one studied previously by Bond and Siewert[4] and Burniston and Siewert[5] in connection with the scattering of polarized light. It can be shown that such a vector integrodifferential equation admits a general solution similar to that suggested by Case[7] for scalar transport problems and applied by Cercignani[12] to kinetic equations.

We develop in this paper the elementary solutions to the vector integrodifferential equation basic to a linearized, constant collision frequency (BGK) model suggested by Bhatnagar *et al.*[3] and Welander[29]. The elementary solutions, some of which are generalized functions[14], can be shown to possess rather general full-range and half-range completeness and orthogonality properties. The expansion (or completeness) theorems are proved by reducing a system of singular integral equations to an equivalent matrix Riemann problem and subsequently making use of the theory of Mandžavidze and Hvedelidze[20] and Muskhelishvili[21] to establish the solubility of the resulting equations.

†Present Address: Bettis Atomic Power Laboratory, Westinghouse Electric Corporation, Pittsburgh, Pennsylvania 15122, U.S.A.

‡Permanent Address: Riddick Laboratories, North Carolina State University, Raleigh, North Carolina 27607, U.S.A.

As an application of our established analysis, we construct in this paper the infinite-medium Green's function useful for developing particular solutions to the basic transport equation. We also make use of the half-range expansion theorem to solve the notoriously difficult temperature slip problem considered previously [2, 19, 23, 28, 29] by approximate methods. Our solution permits an accurate computation of the 'temperature slip coefficient' which may be used to evaluate the merits of approximate techniques.

2. THE KINETIC MODEL AND LINEARIZATION

Basically, the BGK model is constructed by replacing the collision integral in the Boltzmann equation by a more tractable relaxation term; we therefore write

$$\left[\frac{\partial}{\partial \tau} + \mathbf{u} \cdot \nabla\right] f(\mathbf{y}, \mathbf{u}, \tau) = \nu[\hat{f}(\mathbf{y}, \mathbf{u}, \tau) - f(\mathbf{y}, \mathbf{u}, \tau)], \tag{2.1}$$

where $f(\mathbf{y}, \mathbf{u}, \tau)$ is the particle distribution function, $\mathbf{y}$ is the position vector, $\mathbf{u}$ is the particle velocity, τ is the time, and ν is a characteristic collision frequency. To ensure that the model conserves particles, momentum and energy, we require that

$$\int [\hat{f}(\mathbf{y}, \mathbf{u}, \tau) - f(\mathbf{y}, \mathbf{u}, \tau)]\mathbf{U}\, \mathrm{d}^3 u = \mathbf{0}, \tag{2.2}$$

where the integration is to be taken over all velocity space and $\mathbf{U}$ is a five-element vector with components 1, u_1, u_2, u_3, and u^2, the collisional invariants. Here u_α, $\alpha = 1, 2$, and 3, and u are respectively the components and magnitude of $\mathbf{u}$. The invariance requirements given by equation (2.2) can be satisfied by choosing

$$\hat{f}(\mathbf{y}, \mathbf{u}, \tau) = n(\mathbf{y}, \tau)\left[\frac{m}{2\pi k T(\mathbf{y}, \tau)}\right]^{3/2} \exp\left[-\frac{m|\mathbf{u} - \mathbf{q}(\mathbf{y}, \tau)|^2}{2kT(\mathbf{y}, \tau)}\right], \tag{2.3}$$

the local Maxwellian distribution. Here m is the particle mass and k is the Boltzmann constant. In addition

$$\begin{bmatrix} n(\mathbf{y}, \tau) \\ n(\mathbf{y}, \tau)\, \mathbf{q}(\mathbf{y}, \tau) \\ 3n(\mathbf{y}, \tau)\, kT(\mathbf{y}, \tau) \end{bmatrix} = \int f(\mathbf{y}, \mathbf{u}, \tau) \begin{bmatrix} 1 \\ \mathbf{u} \\ m|\mathbf{u} - \mathbf{q}(\mathbf{y}, \tau)|^2 \end{bmatrix} \mathrm{d}^3 u \tag{2.4}$$

defines the local number density $n(\mathbf{y}, \tau)$, the fluid velocity $\mathbf{q}(\mathbf{y}, \tau)$, and the absolute temperature $T(\mathbf{y}, \tau)$.

It is not difficult to demonstrate that the model given by equations (2.1), (2.3), and (2.4) admits an H theorem, such that

$$\frac{\partial}{\partial \tau} \int f(\mathbf{u}, \tau) \ln f(\mathbf{u}, \tau)\, \mathrm{d}^3 u \leqslant 0, \tag{2.5}$$

for spatially uniform conditions. Thus the model possesses many of the important properties of the full Boltzmann equation.

Because of equation (2.4), the model is described by a nonlinear functional equation; however, we consider circumstances for which the particle distribution function

$f(\mathbf{y}, \mathbf{u}, \tau)$ differs only slightly from an initial Maxwellian distribution $f_0(\mathbf{u})$ characterized by a set of constant initial values of the number density n_0, fluid velocity $\mathbf{q}_0$, and temperature T_0. If we now write

$$f(\mathbf{y}, \mathbf{u}, \tau) = f_0(\mathbf{u}) + f_1(\mathbf{y}, \mathbf{u}, \tau), \tag{2.6}$$

and truncate $\hat{f}(\mathbf{y}, \mathbf{u}, \tau)$ at the linear terms in a Taylor series expansion about f_0, we find that equation (2.1) can be approximated by

$$\left[\frac{\partial}{\partial t} + (\mathbf{c}+\mathbf{v}) \cdot \nabla + 1\right] \hat{h}(\mathbf{x}, \mathbf{c}, t) = \int \hat{h}(\mathbf{x}, \mathbf{c}', t) K(\mathbf{c}' : \mathbf{c}) \mathrm{e}^{-c'^2} \mathrm{d}^3 c', \tag{2.7}$$

with

$$K(\mathbf{c}' : \mathbf{c}) = \frac{1}{\pi^{3/2}}\left[1 + 2\mathbf{c} \cdot \mathbf{c}' + \frac{2}{3}\left(c^2 - \frac{3}{2}\right)\left(c'^2 - \frac{3}{2}\right)\right], \tag{2.8}$$

and where

$$\mathbf{x} = \nu\left(\frac{m}{2kT_0}\right)^{1/2} \mathbf{y}, \qquad t = \nu\tau, \tag{2.9a,b}$$

$$\mathbf{c} = \left(\frac{m}{2kT_0}\right)^{1/2} (\mathbf{u} - \mathbf{q}_0), \qquad \mathbf{v} = \left(\frac{m}{2kT_0}\right)^{1/2} \mathbf{q}_0, \tag{2.10a,b}$$

and

$$f_0(\mathbf{c}) \hat{h}(\mathbf{x}, \mathbf{c}, t) = f_1(\mathbf{x}, \mathbf{c}, t). \tag{2.11}$$

A model equation more general than equation (2.7) may be constructed, as suggested by Gross and Jackson[13] and Sirovich[27], by expanding the kernel of a linearized Boltzmann equation in an appropriately chosen complete and orthonormal set of eigenfunctions. We shall, however, restrict our attention to the linearized model described by equation (2.7).

If we now let $\phi_\alpha(\mathbf{c})$, $\alpha = 1, 2, \ldots, 5$, denote the elements of the vector

$$\boldsymbol{\phi}(\boldsymbol{c}) = \frac{1}{\pi^{3/4}} \begin{bmatrix} 1 \\ \sqrt{\tfrac{2}{3}}(c^2 - \tfrac{3}{2}) \\ \sqrt{2}\, c_2 \\ \sqrt{2}\, c_3 \\ \sqrt{2}\, c_1 \end{bmatrix}, \tag{2.12}$$

where c_1, c_2, c_3, and c are respectively the components and magnitude of $\mathbf{c}$, then equation (2.8) can be written as

$$K(\mathbf{c}' : \mathbf{c}) = \tilde{\boldsymbol{\phi}}(\mathbf{c}) \boldsymbol{\phi}(\mathbf{c}'). \tag{2.13}$$

Here the superscript tilde is used to denote the transpose operation. We note that the elements of $\boldsymbol{\phi}(\mathbf{c})$ obey the orthonormal conditions

$$(\phi_\alpha, \phi_\beta)_a = \delta_{\alpha,\beta}\,;\ \ \alpha,\beta = 1, 2, \ldots, 5, \tag{2.14}$$

in a Hilbert space (a) of the functions of $\mathbf{c}$ defined by the inner product

$$(A_1, A_2)_a = \int A_1(\mathbf{c})A_2(\mathbf{c})\, e^{-c^2}\, d^3c. \tag{2.15}$$

The elements $\phi_\alpha(\mathbf{c})$ are, of course, related to the collisional invariants which define the $\mathbf{U}$ vector in equation (2.2), and the orthogonality conditions stated in equation (2.14) are therefore direct consequences of the invariance requirements of equation (2.2).

3. THE VECTOR KINETIC EQUATION

As stated in the Introduction, we are primarily interested in steady-state gas-kinetic problems with plane symmetry. Without loss of generality, we set $\mathbf{q}_0 = \mathbf{0}$, and thus the steady-state version of equation (2.7) for

$$h(x_1, \mathbf{c}) \stackrel{\Delta}{=} \hat{h}(x_1, \mathbf{c}) - 2\pi^{-3/2}c_1(c_1, \hat{h})_a \tag{3.1}$$

becomes

$$\left[c_1\frac{\partial}{\partial x_1} + 1\right]h(x_1, \mathbf{c}) = \sum_{\alpha=1}^{4} \phi_\alpha(\mathbf{c})(\phi_\alpha,\ h)_a. \tag{3.2}$$

We now follow Cercignani[12] and consider the functions

$$\begin{aligned} g_1(c_2, c_3) &= \pi^{-1/2}, \qquad g_2(c_2, c_3) = \pi^{-1/2}(c_2^2 + c_3^2 - 1), \\ g_3(c_2, c_3) &= \left(\frac{\pi}{2}\right)^{-1/2} c_2, \quad \text{and} \quad g_4(c_2, c_3) = \left(\frac{\pi}{2}\right)^{-1/2} c_3. \end{aligned} \tag{3.3}$$

It is a straightforward matter to demonstrate that the g functions given by equations (3.3) satisfy the orthonormal conditions

$$(g_\alpha, g_\beta)_b = \delta_{\alpha,\beta},\ \alpha = 1, 2, 3, \text{and } 4, \tag{3.4}$$

in a subspace (b) of the functions of c_2 and c_3 defined by the inner product

$$(B_1, B_2)_b = \int_{-\infty}^{\infty}\int_{-\infty}^{\infty} B_1(c_2, c_3)B_2(c_2, c_3)e^{-(c_2^2+c_3^2)}\, dc_2 dc_3. \tag{3.5}$$

We now span the Hilbert space (b) by the subspace (c) characterized by the g_α's and a subspace (d), the orthogonal complement to (c); subsequently we expand $h(x_1, \mathbf{c})$ of equation (3.2) in the manner

$$h(x_1, \mathbf{c}) = \sum_{\alpha=1}^{4} \Psi_\alpha(x_1, c_1)g_\alpha(c_2, c_3) + \Psi_5(x_1, \mathbf{c}), \tag{3.6}$$

where $\Psi_5(x_1, \mathbf{c})$ is the component of $h(x_1, \mathbf{c})$ belonging to the subspace (d). Such an expansion yields the interesting property that the inner products $(\Psi_\alpha, \phi_\alpha)_a$, $\alpha = 1, 2, 3$, and 4, are simply related to the perturbations of the number density, the temperature, and the transverse components of the fluid velocity, respectively.

Substituting equation (3.6) into equation (3.2) and projecting each term onto the appropriate directions of g_α in the Hilbert space (b), we obtain

$$\left[\mu\frac{\partial}{\partial x}+1\right]\hat{\mathbf{\Psi}}(x,\mu)=\frac{1}{\sqrt{\pi}}\mathbf{J}(\mu)\int_{-\infty}^{\infty}\tilde{\mathbf{J}}(\mu')\hat{\mathbf{\Psi}}(x,\mu')\,\mathrm{e}^{-\mu'^2}\,\mathrm{d}\mu', \tag{3.7}$$

where $\hat{\mathbf{\Psi}}(x, \mu)$ is a four-element vector with components $\Psi_\alpha(x, \mu)$, $\alpha = 1, 2, \ldots, 4$, and

$$\mathbf{J}(\mu)=\begin{bmatrix}\sqrt{\tfrac{2}{3}}(\mu^2-\tfrac{1}{2}) & 1 & 0 & 0\\ \sqrt{\tfrac{2}{3}} & 0 & 0 & 0\\ 0 & 0 & 1 & 0\\ 0 & 0 & 0 & 1\end{bmatrix}. \tag{3.8}$$

For convenience, we have changed the variables x_1 and c_1 to x and μ. We note that the two functions $\Psi_1(x, \mu)$ and $\Psi_2(x, \mu)$, characterizing the perturbations of the number density and temperature respectively, are described by a set of two coupled integrodifferential equations. These two equations are, of course, uncoupled from the functions $\Psi_3(x, \mu)$ and $\Psi_4(x, \mu)$ which describe the perturbations of the transverse momenta.

4. ELEMENTARY SOLUTIONS OF THE TWO-VECTOR TRANSPORT EQUATION RELEVANT TO TEMPERATURE-DENSITY EFFECTS

We are interested in the steady-state, gas-kinetic effects of temperature-density variations in plane-parallel media. According to equation (3.7), the relevant coupled equations are

$$\mu\frac{\partial}{\partial x}\mathbf{\Psi}(x,\mu)+\mathbf{\Psi}(x,\mu)=\frac{1}{\sqrt{\pi}}\mathbf{Q}(\mu)\int_{-\infty}^{\infty}\tilde{\mathbf{Q}}(\mu')\mathbf{\Psi}(x,\mu')\mathrm{e}^{-\mu'^2}\,\mathrm{d}\mu', \tag{4.1}$$

where $\tilde{\mathbf{Q}}(\mu)$ is the transpose of

$$\mathbf{Q}(\mu)=\begin{bmatrix}\sqrt{\tfrac{2}{3}}(\mu^2-\tfrac{1}{2}) & 1\\ \sqrt{\tfrac{2}{3}} & 0\end{bmatrix}, \tag{4.2}$$

and $\Psi_1(x, \mu)$ and $\Psi_2(x, \mu)$, which are sufficient to determine the temperature–density effects, are respectively the upper and lower entries in the two-vector $\mathbf{\Psi}(x, \mu)$. We should like to note that equation (4.1) is quite similar to the equation of transfer used in a related study [4, 5] of the scattering of polarized light.

Following Case [7] who introduced the method of normal modes in regard to one-speed neutron-transport theory, we search for elementary solutions to equation (4.1) of the form

$$\mathbf{\Psi}_\xi(x,\mu)=\mathbf{F}(\xi,\mu)\mathrm{e}^{-x/\xi}, \tag{4.3}$$

where ξ and $\mathbf{F}(\xi, \mu)$ are the eigenvalues and eigenvectors to be determined. From equation (4.1), we obtain

$$(\xi - \mu)\mathbf{F}(\xi, \mu) = \frac{1}{\sqrt{\pi}}\xi\mathbf{Q}(\mu)\mathbf{M}(\xi) \tag{4.4}$$

where the normalization vector $\mathbf{M}(\xi)$ is given by

$$\mathbf{M}(\xi) = \int_{-\infty}^{\infty} \tilde{\mathbf{Q}}(\mu)\mathbf{F}(\xi, \mu)\mathrm{e}^{-\mu^2}\,\mathrm{d}\mu. \tag{4.5}$$

Equation (4.4) admits both discrete eigenvalues and a continuous spectrum. We consider first the discrete spectrum: $\xi = \eta_i$, $Im\ \eta_i \neq 0$, and solve equation (4.4) to obtain

$$\mathbf{F}(\eta_i, \mu) = \frac{1}{\sqrt{\pi}}\frac{\eta_i}{\eta_i - \mu}\mathbf{Q}(\mu)\mathbf{M}(\eta_i), \tag{4.6}$$

where η_i are the zeros (in the complex plane cut along the entire real axis) of the dispersion function

$$\Lambda(z) = \det \mathbf{\Lambda}(z). \tag{4.7}$$

Here the dispersion matrix is

$$\mathbf{\Lambda}(z) = \mathbf{I} + z\int_{-\infty}^{\infty} \mathbf{\Psi}(\mu)\frac{\mathrm{d}\mu}{\mu - z}, \tag{4.8}$$

with $\mathbf{I}$ denoting the unit matrix and the characteristic matrix given by

$$\mathbf{\Psi}(\mu) = \frac{1}{\sqrt{\pi}}\tilde{\mathbf{Q}}(\mu)\mathbf{Q}(\mu)\mathrm{e}^{-\mu^2}. \tag{4.9}$$

Further, $\mathbf{M}(\eta_i)$ is a null vector of $\mathbf{\Lambda}(\eta_i)$ such that

$$\mathbf{\Lambda}(\eta_i)\mathbf{M}(\eta_i) = \mathbf{0}. \tag{4.10}$$

The argument principle [10] may be used to show that $\Lambda(z)$ has no zeros in the finite cut plane; however, since $\Lambda(z) \sim (a/z^4) + \ldots$, for $|z|$ tending to infinity, we may deduce four 'discrete' solutions to equation (4.1). In the limit $|z| \to \infty$, we obtain from equations (4.6) and (4.10)

$$\mathbf{F}_1(\mu) = \mathbf{Q}(\mu)\begin{bmatrix}1\\0\end{bmatrix} = \sqrt{\frac{2}{3}}\begin{bmatrix}\mu^2 - \frac{1}{2}\\1\end{bmatrix}, \text{ and } \mathbf{F}_2(\mu) = \mathbf{Q}(\mu)\begin{bmatrix}0\\1\end{bmatrix} = \begin{bmatrix}1\\0\end{bmatrix}. \tag{4.11}$$

To construct the other two solutions requires a technique discussed by Case and Zweifel [8] to split the degeneracy at infinity. The resulting solutions are

$$\mathbf{\Psi}_3(x, \mu) = (\mu - x)\sqrt{\frac{2}{3}}\begin{bmatrix}\mu^2 - \frac{1}{2}\\1\end{bmatrix}, \text{ and } \mathbf{\Psi}_4(x, \mu) = (\mu - x)\begin{bmatrix}1\\0\end{bmatrix}. \tag{4.12}$$

It should be noted that equations (4.11) are solutions to equation (4.1) and to equation (4.4) in the limit $|\xi|\to\infty$; whereas, equations (4.12) are solutions only to equation (4.1).

We now consider the continuous spectrum: $\xi=\eta$, with $Im\ \eta=0$, and the solutions to equation (4.4) are

$$\mathbf{F}(\eta,\mu)=\frac{1}{\sqrt{\pi}}\left[\eta Pv\left(\frac{1}{\eta-\mu}\right)+\lambda^*(\eta)\delta(\eta-\mu)\right]\mathbf{Q}(\mu)\mathbf{M}(\eta), \tag{4.13}$$

where $Pv(1/x)$ denotes the Cauchy principal-value distribution, and $\delta(x)$ represents the Dirac delta distribution. Pre-multiplying equation (4.13) by $\tilde{\mathbf{Q}}(\mu)\,\mathrm{e}^{-\mu^2}$ and integrating over all μ, we find

$$[\boldsymbol{\lambda}(\eta)-\lambda^*(\eta)\boldsymbol{\Psi}(\eta)]\mathbf{M}(\eta)=\mathbf{0}, \tag{4.14}$$

where

$$\boldsymbol{\lambda}(\eta)=\mathbf{I}+\eta P\int_{-\infty}^{\infty}\boldsymbol{\Psi}(\mu)\frac{\mathrm{d}\mu}{\mu-\eta}; \tag{4.15}$$

and hence from

$$\det[\boldsymbol{\lambda}(\eta)-\lambda^*(\eta)\boldsymbol{\Psi}(\eta)]=0, \tag{4.16}$$

we obtain a quadratic equation for the function $\lambda^*(\eta)$. In general there are two solutions which we label $\lambda_1^*(\eta)$ and $\lambda_2^*(\eta)$, and thus we write the two-fold degenerate continuum solutions as

$$\mathbf{F}_\alpha(\eta,\mu)=\frac{1}{\sqrt{\pi}}\left[\eta Pv\left(\frac{1}{\eta-\mu}\right)+\lambda_\alpha^*(\eta)\delta(\eta-\mu)\right]\mathbf{Q}(\mu)\mathbf{M}_\alpha(\eta),\ \alpha=1\text{ or }2,\ \eta\in(-\infty,\infty), \tag{4.17}$$

where the vectors $\mathbf{M}_\alpha(\eta)$ are to be determined by the corresponding $\lambda_\alpha^*(\eta)$, through equation (4.14).

Having established the elementary solutions, we write our general solution to equation (4.1) as

$$\boldsymbol{\Psi}(x,\mu)=\sum_{\alpha=1}^{2}A_\alpha\mathbf{F}_\alpha(\mu)+\sum_{\alpha=3}^{4}A_\alpha\boldsymbol{\Psi}_\alpha(x,\mu)+\sum_{\alpha=1}^{2}\int_{-\infty}^{\infty}A_\alpha(\eta)\mathbf{F}_\alpha(\eta,\mu)\mathrm{e}^{-x/\eta}\,\mathrm{d}\eta, \tag{4.18}$$

where the expansion coefficients A_α and $A_\alpha(\eta)$ are to be determined once the boundary conditions of a particular problem are specified. Although in general the integral terms in equation (4.18) may diverge for $x\neq 0$, this will not be the case when the specific problems of sections 7 and 13 are considered.

5. A FULL-RANGE EXPANSION THEOREM

To ensure that the normal modes developed in the previous sections are sufficiently general for full-range, $\mu\in(-\infty,\infty)$, boundary-value problems, we should now like to prove a basic result.

Theorem 1. *The functions* $\mathbf{F}_1(\mu)$, $\mathbf{F}_2(\mu)$, $\mathbf{F}_3(\mu)=\boldsymbol{\Psi}_3(0,\mu)$, $\boldsymbol{F}_4(\mu)=\boldsymbol{\Psi}_4(0,\mu)$, *and* $\mathbf{F}_\alpha(\eta,\mu)$, $\alpha=1$ and 2, $\eta\in(-\infty,\infty)$, *form a complete basis set for the expansion of an* *arbitrary two-vector* $\mathbf{I}(\mu)$, *which is Hölder continuous on any open interval of the real axis and, for sufficiently large* $|\mu|$, satisfies

$$|I_\alpha(\mu)| \exp(-|\mu|) < \infty, \alpha = 1 \text{ or } 2,$$

in the sense that

$$\mathbf{I}(\mu) = \sum_{\alpha=1}^{4} A_\alpha \mathbf{F}_\alpha(\mu) + \sum_{\alpha=1}^{2} \int_{-\infty}^{\infty} A_\alpha(\eta)\mathbf{F}_\alpha(\eta, \mu)\, \mathrm{d}\eta, \mu \in (-\infty, \infty). \tag{5.1}$$

To prove the theorem, we shall construct an analytical solution to the above coupled singular integral equations. For the sake of brevity, we write

$$\hat{\mathbf{I}}(\mu) = \mathbf{I}(\mu) - \sum_{\alpha=1}^{4} A_\alpha \mathbf{F}_\alpha(\mu), \tag{5.2}$$

introduce the (2×2) matrix

$$\mathbf{G}(\eta, \mu) = [\mathbf{F}_1(\eta, \mu) \quad \mathbf{F}_2(\eta, \mu)], \tag{5.3}$$

let $\mathbf{A}(\eta)$ denote a vector with elements $A_\alpha(\eta)$, $\alpha = 1$ and 2, and thus write equation (5.1) as

$$\hat{\mathbf{I}}(\mu) = \int_{-\infty}^{\infty} \mathbf{G}(\eta, \mu)\mathbf{A}(\eta)\, \mathrm{d}\eta, \mu \in (-\infty, \infty). \tag{5.4}$$

Pre-multiplying equation (4.13) by $\tilde{\mathbf{Q}}(\mu)\, \mathrm{e}^{-\mu^2}$ and invoking equation (4.14), we obtain

$$\tilde{\mathbf{Q}}(\mu)\mathbf{G}(\eta, \mu)\, \mathrm{e}^{-\mu^2} = \left[\eta Pv\left(\frac{1}{\eta - \mu}\right)\mathbf{\Psi}(\mu) + \delta(\eta - \mu)\boldsymbol{\lambda}(\eta)\right]\mathbf{V}(\eta), \tag{5.5}$$

where

$$\mathbf{V}(\eta) = [\mathbf{M}_1(\eta) \quad \mathbf{M}_2(\eta)] \tag{5.6}$$

is the (2×2) normalization matrix. We now pre-multiply equation (5.4) by $\tilde{\mathbf{Q}}(\mu)\, \mathrm{e}^{-\mu^2}$, make use of equation (5.5), and integrate the δ term to obtain

$$\tilde{\mathbf{Q}}(\mu)\hat{\mathbf{I}}(\mu)\mathrm{e}^{-\mu^2} = \boldsymbol{\lambda}(\mu)\mathbf{B}(\mu) + \mathbf{\Psi}(\mu)P\int_{-\infty}^{\infty} \eta\mathbf{B}(\eta)\frac{\mathrm{d}\eta}{\eta - \mu}, \tag{5.7}$$

where $\mathbf{B}(\eta) = \mathbf{V}(\eta)\mathbf{A}(\eta)$. Equation (5.7) may now be solved explicitly by using the theory of Muskhelishvili [21]. To convert equation (5.7) to a special form of a matrix Riemann problem, we introduce the sectionally holomorphic matrix

$$\mathbf{N}(z) = \frac{1}{2\pi i}\int_{-\infty}^{\infty} \eta\mathbf{B}(\eta)\frac{\mathrm{d}\eta}{\eta - z}. \tag{5.8}$$

The boundary values of $\mathbf{N}(z)$ as z approaches the real line from above (+) and below

(−) follow from the Plemelj formulae[21]:

$$\pi i[\mathbf{N}^+(\mu)+\mathbf{N}^-(\mu)] = P\int_{-\infty}^{\infty} \eta\mathbf{B}(\eta)\frac{\mathrm{d}\eta}{\eta-\mu} \tag{5.9a}$$

and

$$\mathbf{N}^+(\mu)-\mathbf{N}^-(\mu) = \mu\mathbf{B}(\mu). \tag{5.9b}$$

In a similar manner, the boundary values of the dispersion matrix follow from equation (4.8):

$$\mathbf{\Lambda}^+(\mu)+\mathbf{\Lambda}^-(\mu) = 2\boldsymbol{\lambda}(\mu), \tag{5.10a}$$

and

$$\mathbf{\Lambda}^+(\mu)-\mathbf{\Lambda}^-(\mu) = 2\pi i\mu\mathbf{\Psi}(\mu). \tag{5.10b}$$

Equations (5.9) and (5.10) may now be used in equation (5.7) to yield

$$\mu\tilde{\mathbf{Q}}(\mu)\hat{\mathbf{I}}(\mu)\mathrm{e}^{-\mu^2} = \mathbf{\Lambda}^+(\mu)\mathbf{N}^+(\mu)-\mathbf{\Lambda}^-(\mu)\mathbf{N}^-(\mu), \tag{5.11}$$

which can be solved to give

$$\mathbf{N}(z) = \mathbf{\Lambda}^{-1}(z)\frac{1}{2\pi i}\int_{-\infty}^{\infty} \mu\tilde{\mathbf{Q}}(\mu)\hat{\mathbf{I}}(\mu)\mathrm{e}^{-\mu^2}\frac{\mathrm{d}\mu}{\mu-z}. \tag{5.12}$$

We note that for large $|z|$,

$$\mathbf{\Lambda}(z) \sim -\frac{1}{z^2}\begin{bmatrix} \frac{7}{6} & \frac{1}{\sqrt{6}} \\ \frac{1}{\sqrt{6}} & \frac{1}{2} \end{bmatrix}, \text{ as } |z|\to\infty, \tag{5.13}$$

and

$$\mathbf{\Lambda}^{-1}(z) \sim -\frac{12}{5}z^2\begin{bmatrix} \frac{1}{2} & \frac{-1}{\sqrt{6}} \\ \frac{-1}{\sqrt{6}} & \frac{7}{6} \end{bmatrix}, \text{ as } |z|\to\infty, \tag{5.14}$$

and therefore if the $\mathbf{N}(z)$ as given by equation (5.12) is to vanish when $|z|$ tends to infinity, as equation (5.8) prescribes, we must impose on the vector $\hat{\mathbf{I}}(\mu)$ the four constraints

$$\int_{-\infty}^{\infty} \mu^\alpha\tilde{\mathbf{Q}}(\mu)\hat{\mathbf{I}}(\mu)\mathrm{e}^{-\mu^2}\,\mathrm{d}\mu = \mathbf{0}, \quad \alpha = 1 \text{ and } 2. \tag{5.15}$$

Recalling equation (5.2) for $\hat{\mathbf{I}}(\mu)$, we observe that equation (5.15) will be inherently satisfied if we specify the expansion coefficients A_α, $\alpha = 1, 2, 3$, and 4, to be

$$\begin{bmatrix} A_1 \\ A_2 \\ A_3 \\ A_4 \end{bmatrix} = \frac{12}{5\sqrt{6\pi}} \begin{bmatrix} -\frac{3}{2}I_{12} + I_{14} + I_{22} \\ \frac{8}{\sqrt{6}}I_{12} - \sqrt{\frac{2}{3}}I_{14} - \sqrt{\frac{2}{3}}I_{22} \\ -\frac{3}{2}I_{11} + I_{13} + I_{21} \\ \frac{8}{\sqrt{6}}I_{11} - \sqrt{\frac{2}{3}}I_{13} - \sqrt{\frac{2}{3}}I_{21} \end{bmatrix}, \tag{5.16}$$

where

$$I_{\alpha\beta} \stackrel{\Delta}{=} \int_{-\infty}^{\infty} \mu^\beta I_\alpha(\mu) \mathrm{e}^{-\mu^2} \mathrm{d}\mu, \quad \alpha = 1 \text{ or } 2; \beta = 1, 2, 3 \text{ or } 4, \tag{5.17}$$

and $I_1(\mu)$ and $I_2(\mu)$ are respectively the upper and lower entries of $\mathbf{I}(\mu)$. Theorem 1 is therefore established.

Although we could pursue equations (5.9b) and (5.12) to obtain explicit results for the continuum coefficients $A_\alpha(\eta)$, $\alpha = 1$ or 2, we prefer to summarize the final expressions in terms of the formalism of the full-range orthogonality relations given in the next section.

6. ORTHOGONALITY RELATIONS AND EXPLICIT SOLUTIONS

We should first like to state the general orthogonality relation relevant to all solutions including the special distributions, $\mathbf{F}(\xi, \mu)$, of the separated equation (4.4).

Theorem 2. All eigenvectors $\mathbf{F}(\xi, \mu)$ *which are solutions of equation* (4.4) *are orthogonal on the full range,* $\mu \in (-\infty, \infty)$, *in the sense that*

$$\int_{-\infty}^{\infty} \tilde{\mathbf{F}}(\xi', \mu)\mathbf{F}(\xi, \mu)\mathrm{e}^{-\mu^2} \mu \, \mathrm{d}\mu = 0, \quad \xi' \neq \xi. \tag{6.1}$$

To prove the theorem, equation (4.4) is first pre-multiplied by $\tilde{\mathbf{F}}(\xi', \mu)\mathrm{e}^{-\mu^2}/\xi$, the transpose of equation (4.4) with ξ changed to ξ' is post-multiplied by $\mathbf{F}(\xi, \mu)\mathrm{e}^{-\mu^2}/\xi'$, and the two resulting equations are then integrated over all μ and subtracted one from the other to yield

$$\left(\frac{1}{\xi} - \frac{1}{\xi'}\right) \int_{-\infty}^{\infty} \tilde{\mathbf{F}}(\xi', \mu)\mathbf{F}(\xi, \mu)\mathrm{e}^{-\mu^2} \mu \, \mathrm{d}\mu = 0, \tag{6.2}$$

which establishes equation (6.1). Though equation (6.2) is a general statement of full-range orthogonality, it is clear that several additional relations are required here. First of all, since $\mathbf{F}_1(\mu)$ and $\mathbf{F}_2(\mu)$ are both associated with $\xi \to \infty$, equation (6.2) does not ensure that they will be mutually orthogonal in the sense of equation (6.1). In addition, the vectors $\mathbf{F}_3(\mu)$ and $\mathbf{F}_4(\mu)$, being derived from the solutions of equation (4.1), rather than equation (4.4), are not included in Theorem 2. However, it can be easily shown that $\mathbf{F}_1(\mu)$ and $\mathbf{F}_2(\mu)$ are mutually orthogonal, and, in fact, self-orthogonal; the same is true for $\mathbf{F}_3(\mu)$ and $\mathbf{F}_4(\mu)$. In addition, $\mathbf{F}_3(\mu)$ and $\mathbf{F}_4(\mu)$ are orthogonal to the continuum solutions $\mathbf{F}_1(\eta, \mu)$ and $\mathbf{F}_2(\eta, \mu)$. We note that $\mathbf{F}_1(\mu)$ and $\mathbf{F}_2(\mu)$ are not orthogonal to $\mathbf{F}_3(\mu)$ and $\mathbf{F}_4(\mu)$; however, suitably defined adjoint vectors for these special cases can be developed by employing a Schmidt-type procedure.

Considering first the normalization integrals related to the solutions given by equation (4.13), we find

$$\int_{-\infty}^{\infty} \tilde{\mathbf{F}}_\alpha(\eta', \mu)\mathbf{F}_\beta(\eta, \mu)\mathrm{e}^{-\mu^2}\,\mu\,\mathrm{d}\mu = S(\eta)\delta(\eta-\eta')\delta_{\alpha,\beta}\,;\ \alpha,\beta = 1, 2, \tag{6.3}$$

where

$$S(\eta) = \frac{\eta}{\sqrt{\pi}}[\pi^2\eta^2 + \lambda^*_\alpha(\eta)\lambda^*_\beta(\eta)]\tilde{\mathbf{M}}_\alpha(\eta)\boldsymbol{\Psi}(\eta)\mathbf{M}_\beta(\eta). \tag{6.4}$$

The Kronecker $\delta_{\alpha,\beta}$ appearing in equation (6.3) should be noted since it ensures that the degenerate continuum solutions given by equation (4.13) are orthogonal even for $\eta' = \eta$. To establish equation (6.3) requires the use of the Poincaré-Bertrand formula [21] and

$$[\lambda^*_\alpha(\eta) - \lambda^*_\beta(\eta)]\tilde{\mathbf{M}}_\alpha(\eta)\boldsymbol{\Psi}(\eta)\mathbf{M}_\beta(\eta) = 0, \tag{6.5}$$

a relation which can be deduced from equation (4.14).

Though the representations of the two continuum solutions given by equation (4.13) were convenient for proving the full-range expansion theorem, we choose to make use of more explicit forms for actual applications. We note that equation (4.16) is quadratic in $\lambda^*(\eta)$, and thus the two solutions will in general involve radicals. To avoid the cumbersome nature of the ensuing solutions, we prefer the linear combinations

$$\boldsymbol{\Phi}_\alpha(\eta, \mu) = T_{\alpha 1}(\eta)\mathbf{F}_1(\eta, \mu) + T_{\alpha 2}(\eta)\mathbf{F}_2(\eta, \mu), \quad \alpha = 1 \text{ and } 2, \tag{6.6}$$

which, for judicious choices of $T_{\alpha\beta}(\eta)$, enable us to deduce the more tractable solutions

$$\boldsymbol{\Phi}_1(\eta, \mu) = \begin{bmatrix} \dfrac{1}{\sqrt{\pi}}\eta\left(\mu^2 - \dfrac{1}{2}\right)Pv\left(\dfrac{1}{\eta-\mu}\right)\mathrm{e}^{-\eta^2} + \lambda_1(\eta)\delta(\eta-\mu) \\ \dfrac{1}{\sqrt{\pi}}\eta Pv\left(\dfrac{1}{\eta-\mu}\right)\mathrm{e}^{-\eta^2} + \left[\dfrac{1}{2} + \lambda_0(\eta)\right]\delta(\eta-\mu) \end{bmatrix} \tag{6.7a}$$

and

$$\boldsymbol{\Phi}_2(\eta, \mu) = \begin{bmatrix} \dfrac{1}{\sqrt{\pi}}\eta Pv\left(\dfrac{1}{\eta-\mu}\right)\mathrm{e}^{-\eta^2} + \lambda_0(\eta)\delta(\eta-\mu) \\ \dfrac{1}{2}\delta(\eta-\mu) \end{bmatrix}, \tag{6.7b}$$

where

$$\lambda_0(\eta) = 1 + \frac{1}{\sqrt{\pi}}\eta P\int_{-\infty}^{\infty} \mathrm{e}^{-\mu^2}\frac{\mathrm{d}\mu}{\mu-\eta}, \tag{6.8a}$$

or

$$\lambda_0(\eta) = 1 - 2\eta \mathrm{e}^{-\eta^2} \int_0^\eta \mathrm{e}^{\mu^2}\,\mathrm{d}\mu, \tag{6.8b}$$

and

$$\lambda_1(\eta) = \tfrac{1}{2} + (\eta^2 - \tfrac{1}{2})\lambda_0(\eta). \tag{6.9}$$

We note that equations (6.7) are not mutually orthogonal for $\eta' = \eta$; however, a Schmidt-type procedure may be used here as well. Since our final adjoint vectors follow in a manner analogous to that reported by Siewert and Zweifel[26], we shall simply summarize our conclusions below. For the case of the degenerate continuum modes, we find that the procedure discussed in reference [26] can be used to establish the required adjoint vectors. To unify our notation, we also define

$$\boldsymbol{\Phi}_\alpha(\mu) \stackrel{\Delta}{=} \mathbf{F}_\alpha(\mu), \quad \alpha = 1, 2, 3 \text{ and } 4. \tag{6.10}$$

The *orthonormal* full-range adjoint set is given by:

$$\mathbf{X}_1(\mu) = \frac{1}{5\sqrt{\pi}}[6\boldsymbol{\Phi}_3(\mu) - 2\sqrt{6}\boldsymbol{\Phi}_4(\mu)], \tag{6.11a}$$

$$\mathbf{X}_2(\mu) = \frac{1}{5\sqrt{\pi}}[-2\sqrt{6}\boldsymbol{\Phi}_3(\mu) + 14\boldsymbol{\Phi}_4(\mu)], \tag{6.11b}$$

$$\mathbf{X}_3(\mu) = \frac{1}{5\sqrt{\pi}}[6\boldsymbol{\Phi}_1(\mu) - 2\sqrt{6}\boldsymbol{\Phi}_2(\mu)], \tag{6.11c}$$

$$\mathbf{X}_4(\mu) = \frac{1}{5\sqrt{\pi}}[-2\sqrt{6}\boldsymbol{\Phi}_1(\mu) + 14\boldsymbol{\Phi}_2(\mu)], \tag{6.11d}$$

$$\mathbf{X}_1(\eta, \mu) = \frac{1}{N(\eta)}[N_{22}(\eta)\boldsymbol{\Phi}_1(\eta, \mu) - N_{12}(\eta)\boldsymbol{\Phi}_2(\eta, \mu)], \tag{6.11e}$$

and

$$\mathbf{X}_2(\eta, \mu) = \frac{1}{N(\eta)}[N_{11}(\eta)\boldsymbol{\Phi}_2(\eta, \mu) - N_{12}(\eta)\boldsymbol{\Phi}_1(\eta, \mu)], \tag{6.11f}$$

where

$$N_{11}(\eta) = [\lambda_0(\eta) + \tfrac{1}{2}]^2 + \lambda_1^2(\eta) + \pi\eta^2[(\eta^2 - \tfrac{1}{2})^2 + 1]\,\mathrm{e}^{-2\eta^2},$$

$$N_{12}(\eta) = \lambda_0(\eta)\lambda_1(\eta) + \tfrac{1}{2}\lambda_0(\eta) + \tfrac{1}{4} + \pi\eta^2(\eta^2 - \tfrac{1}{2})\,\mathrm{e}^{-2\eta^2},$$

$$N_{22}(\eta) = \lambda_0^2(\eta) + \tfrac{1}{4} + \pi\eta^2\,\mathrm{e}^{-2\eta^2},$$

and

$$N(\eta) = \tfrac{9}{4}\eta\,\mathrm{e}^{-\eta^2}\Lambda^+(\eta)\Lambda^-(\eta). \tag{6.12}$$

The required orthogonality relations among the full-range basis and adjoint sets are:

$$\int_{-\infty}^{\infty} \tilde{\mathbf{X}}_\alpha(\mu)\boldsymbol{\Phi}_\beta(\mu)\,\mathrm{e}^{-\mu^2}\,\mu\,\mathrm{d}\mu = \delta_{\alpha,\beta}\,;\ \alpha,\beta = 1, 2, 3, \text{ or } 4, \tag{6.13a}$$

$$\int_{-\infty}^{\infty} \tilde{\mathbf{X}}_\alpha(\mu)\boldsymbol{\Phi}_\beta(\eta, \mu)\,\mathrm{e}^{-\mu^2}\,\mu\,\mathrm{d}\mu = 0;\ \alpha = 1, 2, 3, \text{ or } 4, \beta = 1 \text{ or } 2, \tag{6.13b}$$

$$\int_{-\infty}^{\infty} \tilde{\mathbf{X}}_\alpha(\eta', \mu)\boldsymbol{\Phi}_\beta(\eta, \mu)\,\mathrm{e}^{-\mu^2}\,\mu\,\mathrm{d}\mu = \delta(\eta - \eta')\delta_{\alpha,\beta}\,;\ \alpha,\beta = 1 \text{ or } 2, \tag{6.13c}$$

$$\int_{-\infty}^{\infty} \tilde{\mathbf{X}}_\alpha(\eta', \mu)\boldsymbol{\Phi}_\beta(\mu)\,\mathrm{e}^{-\mu^2}\,\mu\,\mathrm{d}\mu = 0;\ \alpha = 1 \text{ or } 2,\ \beta = 1, 2, 3, \text{ or } 4. \tag{6.13d}$$

With the formalism thus established, we note that all expansion coefficients in equations of the form

$$\mathbf{I}(\mu) = \sum_{\alpha=1}^{4} A_\alpha \boldsymbol{\Phi}_\alpha(\mu) + \sum_{\alpha=1}^{2} \int_{-\infty}^{\infty} A_\alpha(\eta)\boldsymbol{\Phi}_\alpha(\eta, \mu)\,\mathrm{d}\eta,\ \mu \in (-\infty, \infty), \tag{6.14}$$

may be expressed immediately in terms of inner products:

$$A_\alpha = \int_{-\infty}^{\infty} \tilde{\mathbf{X}}_\alpha(\mu)\mathbf{I}(\mu)\,\mathrm{e}^{-\mu^2}\,\mu\,\mathrm{d}\mu,\ \alpha = 1, 2, 3 \text{ and } 4, \tag{6.15}$$

and

$$A_\alpha(\eta) = \int_{-\infty}^{\infty} \tilde{\mathbf{X}}_\alpha(\eta, \mu)\mathbf{I}(\mu)\,\mathrm{e}^{-\mu^2}\,\mu\,\mathrm{d}\mu,\ \alpha = 1 \text{ and } 2. \tag{6.16}$$

7. THE INFINITE-MEDIUM GREEN'S FUNCTION

In order to illustrate the use of the elementary solutions of equation (4.1) and the relevant orthogonality relations, we should now like to develop the infinite-medium Green's function. Here we seek a solution to

$$\mu \frac{\partial}{\partial x} \boldsymbol{\Psi}(x, \mu) + \boldsymbol{\Psi}(x, \mu) = \frac{1}{\sqrt{\pi}}\mathbf{Q}(\mu) \int_{-\infty}^{\infty} \tilde{\mathbf{Q}}(\mu')\boldsymbol{\Psi}(x, \mu')\,\mathrm{e}^{-\mu'^2}\,\mathrm{d}\mu' + \mathbf{S}(x_0, \mu_1, \mu_2; x, \mu), \tag{7.1}$$

where

$$\mathbf{S}(x_0, \mu_1, \mu_2; x, \mu) = \delta(x - x_0)\begin{bmatrix} \rho_1\ \delta(\mu - \mu_1) \\ \rho_2\ \delta(\mu - \mu_2) \end{bmatrix}. \tag{7.2}$$

Clearly, since the kinetic equation conserves particles, kinetic energy, and momentum, there will exist no bounded (at infinity) solution to equation (7.1); however, the Green's function we develop may be used in the classical manner to construct particular solutions to equation (7.1) for arbitrary inhomogeneous source terms for semi-infinite or finite media. As discussed by Case and Zweifel [8], we neglect the inhomogeneous term in equation (7.1) and require the solution to the resulting homogeneous equation to satisfy the 'jump' boundary condition

$$\mu[\boldsymbol{\Psi}(x_0, \mu_1, \mu_2; x_0^+, \mu) - \boldsymbol{\Psi}(x_0, \mu_1, \mu_2; x_0^-, \mu)] = \begin{bmatrix} \rho_1\, \delta(\mu - \mu_1) \\ \rho_2\, \delta(\mu - \mu_2) \end{bmatrix}, \quad \mu \in (-\infty, \infty), \tag{7.3}$$

where the argument list has been extended to include the parameters x_0, μ_1, and μ_2. We therefore write the desired solution as

$$\boldsymbol{\Psi}(x_0, \mu_1, \mu_2; x, \mu) = \sum_{\alpha=1}^{2} A_\alpha \boldsymbol{\Phi}_\alpha(\mu) + \sum_{\alpha=1}^{2} \int_0^\infty A_\alpha(\eta) \boldsymbol{\Phi}_\alpha(\eta, \mu)\, \mathrm{e}^{-(x-x_0)/\eta}\, \mathrm{d}\eta, \tag{7.4a}$$

for $x > x_0$,

and

$$\boldsymbol{\Psi}(x_0, \mu_1, \mu_2; x, \mu) = -\sum_{\alpha=3}^{4} A_\alpha \boldsymbol{\Psi}_\alpha(x - x_0, \mu) - \sum_{\alpha=1}^{2} \int_{-\infty}^{0} A_\alpha(\eta) \boldsymbol{\Phi}_\alpha(\eta, \mu)\, \mathrm{e}^{-(x-x_0)/\eta}\, \mathrm{d}\eta$$

for $x < x_0$. (7.4b)

Substitution of equations (7.4) into equation (7.3) yields the full-range expansion

$$\begin{bmatrix} \rho_1\, \delta(\mu - \mu_1) \\ \rho_2\, \delta(\mu - \mu_2) \end{bmatrix} = \mu \left\{ \sum_{\alpha=1}^{4} A_\alpha \boldsymbol{\Phi}_\alpha(\mu) + \sum_{\alpha=1}^{2} \int_{-\infty}^{\infty} A_\alpha(\eta) \boldsymbol{\Phi}_\alpha(\eta, \mu)\, \mathrm{d}\eta \right\}, \ \mu \in (-\infty, \infty). \tag{7.5}$$

Though the left-hand side of equation (7.5) certainly is not a Hölder function, Case and Zweifel [8] have concluded that expansion theorems similar to our Theorem 1 remain valid formally even for this type of delta distribution. We therefore pre-multiply equation (7.5) by $\tilde{\mathbf{X}}_\alpha(\mu)\, \mathrm{e}^{-\mu^2}$, $\alpha = 1, 2, 3$, or 4 and $\tilde{\mathbf{X}}_\alpha(\eta', \mu)\, \mathrm{e}^{-\mu^2}$, $\alpha = 1$ or 2, and integrate over all μ to find, after invoking equation (6.13),

$$A_\alpha = \rho_1 X_{\alpha 1}(\mu_1)\, \mathrm{e}^{-\mu_1^2} + \rho_2 X_{\alpha 2}(\mu_2)\, \mathrm{e}^{-\mu_2^2}, \ \alpha = 1, 2, 3, \text{and } 4, \tag{7.6a}$$

and

$$A_\alpha(\eta) = \rho_1 X_{\alpha 1}(\eta, \mu_1)\, \mathrm{e}^{-\mu_1^2} + \rho_2 X_{\alpha 2}(\eta, \mu_2)\, \mathrm{e}^{-\mu_2^2}, \ \alpha = 1 \text{ and } 2, \tag{7.6b}$$

where the subscripts 1 and 2 are used to denote the upper and lower elements of the $\mathbf{X}$ vectors. Since all expansion coefficients required in equations (7.4) are given by equations (7.6), the infinite-medium Green's function is established.

8. A HALF-RANGE EXPANSION THEOREM

Having developed in sections 5 and 6 the necessary completeness and orthogonality properties of our normal modes, we should now like to discuss the analysis required for the considerably more interesting problems defined by half-range, $\mu \in (0, \infty)$, boundary conditions. The following theorem states the very important half-range expansion properties basic to a certain subset of our derived elementary solutions.

Theorem 3. *The functions* $\mathbf{F}_1(\mu)$, $\mathbf{F}_2(\mu)$ *and* $\mathbf{F}_\alpha(\eta, \mu)$, $\alpha = 1$ *and* 2, $\eta \in (0, \infty)$, *form a complete basis set for the expansion of an arbitrary two-vector* $\mathbf{I}(\mu)$ *which is Hölder* *continuous on any open interval of the positive real axis and, for sufficiently large* $|\mu|$, satisfies

$$|\mathrm{I}_\alpha(\mu)| \exp(-|\mu|) < \infty, \alpha = 1 \text{ or } 2,$$

in the sense that

$$\mathbf{I}(\mu) = \sum_{\alpha=1}^{2} A_\alpha \mathbf{F}_\alpha(\mu) + \sum_{\alpha=1}^{2} \int_0^\infty A_\alpha(\eta)\mathbf{F}_\alpha(\eta, \mu)\, \mathrm{d}\eta,\ \mu \in (0, \infty). \tag{8.1}$$

To prove this theorem, we premultiply equation (8.1) by $\mathrm{e}^{-\mu^2}\,\tilde{\mathbf{Q}}(\mu)$, integrate the δ term and use equations (4.13) and (4.14) to obtain

$$\tilde{\mathbf{Q}}(\mu)\hat{\mathbf{I}}(\mu)\,\mathrm{e}^{-\mu^2} = \boldsymbol{\lambda}(\mu)\mathbf{B}(\mu) + \boldsymbol{\Psi}(\mu)P\int_0^\infty \eta\mathbf{B}(\eta)\frac{\mathrm{d}\eta}{\eta-\mu},\ \mu \in (0, \infty), \tag{8.2}$$

where

$$\hat{\mathbf{I}}(\mu) = \mathbf{I}(\mu) - \sum_{\alpha=1}^{2} A_\alpha \mathbf{F}_\alpha(\mu) \tag{8.3}$$

and

$$\mathbf{B}(\eta) = \mathbf{V}(\eta)\mathbf{A}(\eta). \tag{8.4}$$

In addition, $\mathbf{V}(\eta)$ is given by equation (5.6) and the unknown $\mathbf{A}(\eta)$ has elements $A_1(\eta)$ and $A_2(\eta)$. In a manner similar to that used to prove Theorem 1, we now introduce

$$\mathbf{N}(z) = \frac{1}{2\pi i}\int_0^\infty \eta\mathbf{B}(\eta)\frac{\mathrm{d}\eta}{\eta - z}. \tag{8.5}$$

The $\mathbf{N}$ matrix is clearly analytic in the complex plane cut along the positive real axis. Further, the Plemelj formulae[21] can be used, with equation (8.5), to show that the boundary values of $\mathbf{N}(z)$ satisfy

$$\pi i[\mathbf{N}^+(\mu) + \mathbf{N}^-(\mu)] = P\int_0^\infty \eta\mathbf{B}(\eta)\frac{\mathrm{d}\eta}{\eta-\mu} \tag{8.6a}$$

and

$$\mathbf{N}^+(\mu) - \mathbf{N}^-(\mu) = \mu\mathbf{B}(\mu). \tag{8.6b}$$

Equations (8.6) can now be used, along with equations (5.10), to express equation (8.2) in the form

$$\mu\tilde{\mathbf{Q}}(\mu)\hat{\mathbf{I}}(\mu)\,\mathrm{e}^{-\mu^2} = \boldsymbol{\Lambda}^+(\mu)\mathbf{N}^+(\mu) - \boldsymbol{\Lambda}^-(\mu)\mathbf{N}^-(\mu),\ \mu \in (0, \infty). \tag{8.7}$$

If we now let $\tilde{\mathbf{X}}(z)$ denote a canonical (non-singular in the finite plane) solution to the homogeneous Riemann problem defined by

$$\tilde{\mathbf{X}}^+(\mu) = \mathbf{G}(\mu)\tilde{\mathbf{X}}^-(\mu),\ \mu \in (0, \infty), \tag{8.8a}$$

where

$$\mathbf{G}(\mu) = \mathbf{\Lambda}^{+}(\mu)[\mathbf{\Lambda}^{-}(\mu)]^{-1}, \tag{8.8b}$$

then equation (8.7) can be solved immediately to yield

$$\mathbf{N}(z) = \mathbf{X}^{-1}(z)\left[\frac{1}{2\pi i}\int_0^\infty \mathbf{\Gamma}(\mu)\tilde{\mathbf{Q}}(\mu)\hat{\mathbf{I}}(\mu)\,\mathrm{e}^{-\mu^2}\frac{\mathrm{d}\mu}{\mu - z} + \mathbf{P}(z)\right]. \tag{8.9}$$

Here, $\mathbf{P}(z)$ is a matrix of polynomials, and

$$\mathbf{\Gamma}(\mu) = \mu\mathbf{X}^{+}(\mu)[\mathbf{\Lambda}^{+}(\mu)]^{-1}. \tag{8.10}$$

Since the $\mathbf{G}$ matrix given by equation (8.8b) is continuous for $\mu \in [0, \infty)$, $\mathbf{G}(0) = \mathbf{I}$ and $\mathbf{G}(\mu) \to \mathbf{I}$ as $\mu \to \infty$, the analysis of Mandžavidze and Hvedelidze[20] can be used, after an elementary transformation of variables, to ensure the existence of a canonical solution to the Riemann problem defined by equation (8.8a). In section 9 we argue that the partial indices κ_1 and κ_2 associated with our canonical solution $\tilde{\mathbf{X}}(z)$ are

$$\kappa_1 = \kappa_2 = 1, \tag{8.11}$$

and thus if we allow our canonical matrix $\tilde{\mathbf{X}}(z)$ to be of normal form at infinity[21], we may write

$$\lim_{z\to\infty} z\,\mathbf{X}(z) = \mathbf{\Delta}, \tag{8.12}$$

where $\mathbf{\Delta}$ is nonsingular and bounded.

From the defining equation (8.5), we observe that $z\,\mathbf{N}(z)$ must be bounded as $|z| \to \infty$, and thus from equation (8.9) we conclude that

$$\lim_{|z|\to\infty} z\mathbf{\Delta}^{-1}\left[\frac{-1}{2\pi i}\int_0^\infty \mathbf{\Gamma}(\mu)\tilde{\mathbf{Q}}(\mu)\hat{\mathbf{I}}(\mu)\,\mathrm{e}^{-\mu^2}\,\mathrm{d}\mu + z\mathbf{P}(z)\right] < \infty; \tag{8.13}$$

we must therefore set $\mathbf{P}(z) = \mathbf{0}$ and, in addition, require that

$$\int_0^\infty \mathbf{\Gamma}(\mu)\tilde{\mathbf{Q}}(\mu)\hat{\mathbf{I}}(\mu)\,\mathrm{e}^{-\mu^2}\,\mathrm{d}\mu = \mathbf{0}. \tag{8.14}$$

Equation (8.14) is, of course, not satisfied by all $\hat{\mathbf{I}}(\mu)$, but recalling equation (8.3), we conclude that choosing the discrete expansion coefficients to be solutions of

$$\int_0^\infty \mathbf{\Gamma}(\mu)\mathbf{\Psi}(\mu)\,\mathrm{d}\mu\begin{bmatrix}A_1\\A_2\end{bmatrix} = \frac{1}{\sqrt{\pi}}\int_0^\infty \mathbf{\Gamma}(\mu)\tilde{\mathbf{Q}}(\mu)\mathbf{I}(\mu)\,\mathrm{e}^{-\mu^2}\,\mathrm{d}\mu \tag{8.15}$$

renders equation (8.1) valid for all appropriate $\mathbf{I}(\mu)$. The matrix in equation (8.15) whose inverse is required to obtain A_1 and A_2 can be shown to be non-singular by making use of a Cauchy integral representation of $\mathbf{X}(z)$. The theorem is therefore proved.

Though, as for the full-range case, we could pursue this completeness proof to construct the continuum expansion coefficients $\mathbf{A}(\eta)$, $\eta \in (0, \infty)$, we find it more convenient to express the final results in terms of half-range orthogonality relations.

9. A PROOF REGARDING THE PARTIAL INDICES OF THE RIEMANN PROBLEM

The proof of the half-range expansion theorem given in section 8 is based on the proposition that the partial indices κ_1 and κ_2 are both non-negative. In fact, equation (8.13) is valid only if the partial indices are given by $\kappa_1 = \kappa_2 = 1$. In this section we develop the required proof that $\kappa_1 = \kappa_2 = 1$.

We consider then the homogeneous matrix Riemann problem defined by

$$\boldsymbol{\Phi}^+(\mu) = \mathbf{G}(\mu)\boldsymbol{\Phi}^-(\mu),\ \mu \in [0, \infty), \tag{9.1}$$

where

$$\mathbf{G}(\mu) = \boldsymbol{\Lambda}^+(\mu)[\boldsymbol{\Lambda}^-(\mu)]^{-1},\ \mu \in [0, \infty). \tag{9.2}$$

Here we seek a matrix $\boldsymbol{\Phi}(z)$ analytic in the plane cut along the positive real axis, non-singular in the finite plane, and with boundary values $\boldsymbol{\Phi}^\pm(\mu)$ which satisfy equation (9.1).

Since $\mathbf{G}(0) = \mathbf{I}$ and $\mathbf{G}(\mu) \to \mathbf{I}$ in the limit as $\mu \to \infty$, we can define $\mathbf{G}(\mu) = \mathbf{I}$ on the entire negative real axis and thus consider equation (9.1) for $\mu \in (-\infty, \infty)$. To make use of the results developed by Mandžavidze and Hvedelidze[20], valid for closed contours, we make the change of variables

$$\zeta = \frac{i - z}{i + z} \tag{9.3}$$

which maps the upper half of the z plane into the interior of the unit circle in the ζ-plane. We note that the positive (negative) real axis maps into $|\zeta| = 1$, $Im\ \zeta > (<)\ 0$. The existence of a solution to the Riemann problem in the ζ plane follows from the theory of Mandžavidze and Hvedelidze[20], since the resulting $\mathbf{G}$ matrix is continuous on the unit circle, and $\boldsymbol{\Phi}(z)$, the canonical solution in the z-plane, is the image of the solution in the ζ plane postmultiplied by an appropriate matrix of rational functions.

It can be demonstrated[5] that the $\boldsymbol{\Lambda}$ matrix can be factored as

$$\boldsymbol{\Lambda}(z) = \boldsymbol{\Phi}(z)\mathcal{P}(z)\tilde{\boldsymbol{\Phi}}(-z) \tag{9.4}$$

where $\boldsymbol{\Phi}(z)$ is any canonical solution (of ordered normal form at infinity) to equation (9.1) and $\mathcal{P}(z)$ is a matrix of polynomials, which depends on the particular choice for $\boldsymbol{\Phi}(z)$.

The fact that $\overline{\mathbf{G}(\mu)} = [\mathbf{G}(\mu)]^{-1}$, where the bar indicates the complex conjugate, enables us to extend the results of Siewert and Burniston's[25] Theorem II to the Riemann problem defined by equation (9.1):

Theorem 4. *There exists at least one canonical matrix $\boldsymbol{\Phi}_1(z)$ of ordered normal form at infinity for the Riemann problem defined by equation* (9.1) *such that $\overline{\boldsymbol{\Phi}_1(\bar{z})} = \boldsymbol{\Phi}_1(z)$.*

Since the proof of Theorem 4 follows very closely one previously reported[25], it will not be given here.

If we use $\boldsymbol{\Phi}_1(z)$ in the factorization of $\boldsymbol{\Lambda}(z)$, the resulting polynomial matrix $\mathcal{P}(z)$ is such that $\mathcal{P}(z)=\tilde{\mathcal{P}}(-z)$ and $\mathcal{P}(z)=\overline{\mathcal{P}(\bar{z})}$, since $\boldsymbol{\Lambda}(z)=\tilde{\boldsymbol{\Lambda}}(z)=\boldsymbol{\Lambda}(-z)$ and $\boldsymbol{\Lambda}(z)=\overline{\boldsymbol{\Lambda}(\bar{z})}$.

By definition[21], a canonical solution of ordered normal form at infinity is such that

$$\lim_{|z|\to\infty}\boldsymbol{\Phi}_1(z)\begin{bmatrix} z^{\kappa_1} & 0 \\ 0 & z^{\kappa_2}\end{bmatrix}=\mathbf{K},\ \det\mathbf{K}\neq 0, \tag{9.5}$$

where κ_1 and $\kappa_2 \geq \kappa_1$ are the partial indices. Furthermore the sum of κ_1 and κ_2 must yield the total index κ, which in the manner of Muskelishvili[21] can be computed directly once the $\mathbf{G}$ matrix and the appropriate contour are specified. For this problem, we find

$$\kappa_1+\kappa_2=\kappa=2. \tag{9.6}$$

If we now evaluate equation (9.4), for $\boldsymbol{\Phi}(z)=\boldsymbol{\Phi}_1(z)$ at $z=0$, we obtain

$$\mathcal{P}(0)=\boldsymbol{\Phi}_1^{-1}(0)\tilde{\boldsymbol{\Phi}}_1^{-1}(0), \tag{9.7}$$

and since $\boldsymbol{\Phi}_1(0)$ is real (recall that $\boldsymbol{\Phi}_1(z)=\overline{\boldsymbol{\Phi}_1(\bar{z})}$), we conclude from equation (9.7) that $\mathcal{P}_{11}(0)\neq 0$ and $\mathcal{P}_{22}(0)\neq 0$. Again from equation (9.4), for $\boldsymbol{\Phi}(z)=\boldsymbol{\Phi}_1(z)$, we can write, after using equation (5.13),

$$\mathcal{P}(z)\to-\frac{1}{z^2}\begin{bmatrix} z^{\kappa_1} & 0 \\ 0 & z^{\kappa_2}\end{bmatrix}\mathrm{K}^{-1}\begin{bmatrix} \frac{7}{6} & \frac{\sqrt{6}}{6} \\ \frac{\sqrt{6}}{6} & \frac{1}{2}\end{bmatrix}\tilde{\mathrm{K}}^{-1}\begin{bmatrix} (-z)^{\kappa_1} & 0 \\ 0 & (-z)^{\kappa_2}\end{bmatrix}, \tag{9.8}$$

$$\text{as } |z|\to\infty,$$

from which it follows, since $\mathbf{K}$ is real, that

$$\kappa_1=\kappa_2=1. \tag{9.9}$$

It is clear, since $\boldsymbol{\Phi}_1(z)$ is a canonical solution of ordered normal form at infinity, and since $\kappa_1=\kappa_2=1$, that

$$\boldsymbol{\Phi}_0(z)\overset{\Delta}{=}\boldsymbol{\Phi}_1(z)\mathbf{K}^{-1}\sqrt{2}\begin{bmatrix} \sqrt{\frac{5}{12}} & \frac{\sqrt{6}}{6} \\ 0 & \frac{1}{2}\end{bmatrix} \tag{9.10}$$

is also a canonical solution of ordered normal form at infinity and is such that $\boldsymbol{\Phi}_0(z)=\overline{\boldsymbol{\Phi}_0(\bar{z})}$. In view of equations (9.8) and (9.10), we can therefore write equation (9.4) as

$$\boldsymbol{\Lambda}(z)=\boldsymbol{\Phi}_0(z)\tilde{\boldsymbol{\Phi}}_0(-z), \tag{9.11}$$

where

$$\boldsymbol{\Phi}_0(0)\tilde{\boldsymbol{\Phi}}_0(0)=\mathbf{I} \tag{9.12a}$$

and

$$\lim_{|z|\to\infty} z\boldsymbol{\Phi}_0(z) = \sqrt{2}\begin{bmatrix} \sqrt{\frac{5}{12}} & \frac{\sqrt{6}}{6} \\ 0 & \frac{1}{2} \end{bmatrix}. \tag{9.12b}$$

We note that Cercignani [11] has reported a factorization in the spirit of our equation (9.11). We have been unable, however, to justify some of Cercignani's results [11; pp. 84–85] since, for example, upon 'taking' determinants of his equation (311) we find an inconsistency in the number of poles on the two sides of the equality sign. We have found that the extension of scalar results to the case of matrix Riemann problems, in general, does not follow immediately [6].

10. HALF-RANGE ORTHOGONALITY AND NORMALIZATION INTEGRALS

The half-range orthogonality relations developed by Kuščer, McCormick, and Summerfield [18] for the elementary solutions of the one-speed neutron-transport equation have proved to be useful for establishing concisely the solutions to a scalar singular integral equation somewhat analogous to equation (8.1). We should thus like to prove, in a manner similar to that reported by Siewert [24] for an equation of transfer basic to the scattering of polarized light, the following theorem concerning the half-range orthogonality properties of a subset of our developed normal modes.

Theorem 5. *The eigenvectors* $\mathbf{F}_1(\mu)$, $\mathbf{F}_2(\mu)$, $\mathbf{F}_1(\eta, \mu)$, *and* $\mathbf{F}_2(\eta, \mu)$, $\eta \in (0, \infty)$, *are orthogonal to the related set* $\mathbf{G}_1(\mu)$, $\mathbf{G}_2(\mu)$, $\mathbf{G}_1(\eta, \mu)$ *and* $\mathbf{G}_2(\eta, \mu)$, $\eta \in (0, \infty)$, *on the half-range*, $\mu \in (0, \infty)$, *in the sense that*

$$\int_0^\infty \tilde{\mathbf{G}}(\xi', \mu)\mathbf{F}(\xi, \mu)\, e^{-\mu^2}\, \mu\, d\mu = 0,\ \xi \neq \xi';\ \xi, \xi' = \infty \text{ or } \in (0, \infty). \tag{10.1}$$

Here $\mathbf{F}(\xi, \mu)$, $\xi = \infty$ or $\in (0, \infty)$, denotes any of the eigenvectors $\mathbf{F}_1(\mu)$, $\mathbf{F}_2(\mu)$, for $\xi = \infty$, or $\mathbf{F}_1(\eta, \mu)$, $\mathbf{F}_2(\eta, \mu)$, for $\eta \in (0, \infty)$. In a similar manner, $\mathbf{G}(\xi, \mu)$, represents either

$$\mathbf{G}_\alpha(\mu) = \mathbf{Q}(\mu)\mathbf{H}(\mu)\mathbf{H}_1^{-1}\mathbf{Q}^{-1}(\mu)\mathbf{F}_\alpha(\mu),\ \alpha = 1 \text{ or } 2, \tag{10.2a}$$

or

$$\mathbf{G}_\alpha(\eta, \mu) = \mathbf{Q}(\mu)\mathbf{H}(\mu)\mathbf{H}^{-1}(\eta)\mathbf{Q}^{-1}(\mu)\mathbf{F}_\alpha(\eta, \mu),\ \eta \in (0, \infty),\ \alpha = 1 \text{ or } 2. \tag{10.2b}$$

In addition

$$\tilde{\mathbf{H}}_1 = \int_0^\infty \tilde{\mathbf{H}}(\mu)\boldsymbol{\Psi}(\mu)\, \mu\, d\mu \tag{10.3}$$

and $\mathbf{H}(\mu)$ is the $\mathbf{H}$ matrix basic to our half-range analysis. In section 11 we prove the existence of a unique solution to the system of singular integral equations

$$\tilde{\mathbf{H}}(\mu)\boldsymbol{\lambda}(\mu) = \mathbf{I} + \mu P\int_0^\infty \tilde{\mathbf{H}}(\eta)\boldsymbol{\Psi}(\eta)\frac{d\eta}{\eta - \mu},\ \mu \in (0, \infty), \tag{10.4a}$$

plus the constraint

$$\int_0^\infty \tilde{\mathbf{H}}(\mu)\boldsymbol{\Psi}(\mu)\,\mathrm{d}\mu = \mathbf{I}, \tag{10.4b}$$

which we take to specify $\mathbf{H}(\mu)$. As shall be shown, $\mathbf{H}(\mu)$ can be expressed in terms of $\boldsymbol{\Phi}_0(z)$, our canonical solution, of ordered normal form at infinity, of the matrix Riemann problem defined by equation (9.1); that is

$$\mathbf{H}(\mu) = \tilde{\boldsymbol{\Phi}}_0^{-1}(-\mu)\tilde{\boldsymbol{\Phi}}_0(0), \tag{10.5}$$

which can be extended to the complex plane cut along the negative real axis to yield a factorization of $\boldsymbol{\Lambda}(z)$:

$$\boldsymbol{\Lambda}(z) = \tilde{\mathbf{H}}^{-1}(z)\mathbf{H}^{-1}(-z). \tag{10.6}$$

To establish our Theorem 5, we first pre-multiply equation (4.4) by $\tilde{\mathbf{G}}(\xi', \mu)\,\mathrm{e}^{-\mu^2}/\xi$, we then post-multiply the transpose of equation (4.4), having changed ξ to ξ', by $\tilde{\mathbf{Q}}^{-1}(\mu)\tilde{\mathbf{H}}^{-1}(\xi')\tilde{\mathbf{H}}(\mu)\tilde{\mathbf{Q}}(\mu)\mathbf{F}(\xi, \mu)\exp(-\mu^2)/\xi'$, integrate the two resulting equations over μ from 0 to ∞ and subtract the two equations, one from the other, to obtain

$$\left(\frac{1}{\xi}-\frac{1}{\xi'}\right)\int_0^\infty \tilde{\mathbf{G}}(\xi', \mu)\mathbf{F}(\xi, \mu)\,\mathrm{e}^{-\mu^2}\,\mu\,\mathrm{d}\mu = \frac{1}{\sqrt{\pi}}[K_1(\xi', \xi) - K_2(\xi', \xi)],\ \xi \text{ and } \xi' > 0. \tag{10.7}$$

Here

$$K_1(\xi', \xi) = \tilde{\mathbf{M}}(\xi')\tilde{\mathbf{H}}^{-1}(\xi')\int_0^\infty \tilde{\mathbf{H}}(\mu)\tilde{\mathbf{Q}}(\mu)\mathbf{F}(\xi, \mu)\,\mathrm{e}^{-\mu^2}\,\mathrm{d}\mu \tag{10.8}$$

and

$$K_2(\xi', \xi) = \int_0^\infty \tilde{\mathbf{F}}(\xi', \mu)\tilde{\mathbf{Q}}^{-1}(\mu)\tilde{\mathbf{H}}^{-1}(\xi')\tilde{\mathbf{H}}(\mu)\tilde{\mathbf{Q}}(\mu)\mathbf{Q}(\mu)\,\mathrm{e}^{-\mu^2}\,\mathrm{d}\mu\,\mathbf{M}(\xi). \tag{10.9}$$

If now, in the manner similar to that previously reported[24], we make use of equations (4.5), (4.11), (4.13), (4.14) and (10.4) to evaluate equations (10.8) and (10.9) for all appropriate ξ and ξ', we find

$$K_1(\xi', \xi) = K_2(\xi', \xi);\ \xi' \in (0, \infty),\ \xi = \infty \text{ or } \in (0, \infty), \tag{10.10}$$

and from equation (10.7) we obtain

$$\left(\frac{1}{\xi}-\frac{1}{\xi'}\right)\int_0^\infty \tilde{\mathbf{G}}(\xi', \mu)\mathbf{F}(\xi, \mu)\,\mathrm{e}^{-\mu^2}\,\mu\,\mathrm{d}\mu = 0;\ \xi, \xi' > 0, \tag{10.11}$$

which proves the theorem. We have only established equation (10.11) formally for $\xi' \neq \infty$. However, considering that case separately, we do find that $\mathbf{G}_\alpha(\mu)$, $\alpha = 1$ or 2, is orthogonal to $\mathrm{F}(\xi, \mu)$ in the sense of Theorem 5. Of course, since $\mathbf{F}_1(\mu)$ and $\mathbf{F}_2(\mu)$ both correspond to the eigenvalue $\xi = \infty$, equation (10.1) does not ensure that the inner product, in the sense of Theorem 5, of $\mathbf{G}_1(\mu)$ with $\mathbf{F}_2(\mu)$ and $\mathbf{G}_2(\mu)$ with $\mathbf{F}_1(\mu)$ is zero.

However, for this special case we have carried out the algebra prescribed by equation (10.1) to show explicitly that

$$\int_0^\infty \tilde{\mathbf{G}}_\alpha(\mu)\mathbf{F}_\beta(\mu)\,\mathrm{e}^{-\mu^2}\,\mu\,\mathrm{d}\mu = 0,\ \alpha \neq \beta, \tag{10.12}$$

so that all of the half-range eigenvectors are orthogonal in the manner of Theorem 5.

Having established the required half-range orthogonality results, we should now like to consider again the normalized solutions given by equation (6.7) in order to present our half-range normalization integrals in a form analogous to that used for the full-range theory. We consider then the half-range adjoint set

$$\mathbf{\Theta}_\alpha(\mu) = \frac{1}{\sqrt{\pi}}\mathbf{Q}(\mu)\mathbf{H}(\mu)\mathbf{H}_1^{-1}\mathbf{Q}^{-1}(\mu)\boldsymbol{\Phi}_\alpha(\mu),\ \alpha = 1 \text{ and } 2, \tag{10.13a}$$

and

$$\mathbf{\Theta}_\alpha(\eta,\mu) = \mathbf{Q}(\mu)\mathbf{H}(\mu)\mathbf{H}^{-1}(\eta)\mathbf{Q}^{-1}(\mu)\mathbf{X}_\alpha(\eta,\mu),\ \eta \in (0,\infty),\ \alpha = 1 \text{ and } 2, \tag{10.13b}$$

where the vectors $\mathbf{X}_\alpha(\eta,\mu)$, $\alpha = 1$ and 2, are given by equations (6.11e) and (6.11f); we can therefore summarize our results in the manner

$$\int_0^\infty \tilde{\mathbf{\Theta}}_\alpha(\mu)\boldsymbol{\Phi}_\beta(\mu)\,\mathrm{e}^{-\mu^2}\,\mu\,\mathrm{d}\mu = \delta_{\alpha,\beta};\ \alpha,\beta = 1 \text{ or } 2, \tag{10.14a}$$

$$\int_0^\infty \tilde{\mathbf{\Theta}}_\alpha(\mu)\boldsymbol{\Phi}_\beta(\eta,\mu)\,\mathrm{e}^{-\mu^2}\,\mu\,\mathrm{d}\mu = 0,\ \eta \in (0,\infty);\ \alpha,\beta = 1 \text{ or } 2, \tag{10.14b}$$

$$\int_0^\infty \tilde{\mathbf{\Theta}}_\alpha(\eta',\mu)\boldsymbol{\Phi}_\beta(\eta,\mu)\,\mathrm{e}^{-\mu^2}\,\mu\,\mathrm{d}\mu = \delta_{\alpha,\beta}\delta(\eta-\eta');\ \eta,\eta' \in (0,\infty),\ \alpha,\beta = 1 \text{ or } 2, \tag{10.14c}$$

and

$$\int_0^\infty \tilde{\mathbf{\Theta}}_\alpha(\eta,\mu)\boldsymbol{\Phi}_\beta(\mu)\,\mathrm{e}^{-\mu^2}\,\mu\,\mathrm{d}\mu = 0;\ \eta \in (0,\infty),\ \alpha,\beta = 1 \text{ or } 2. \tag{10.14d}$$

With the half-range formalism thus established, we note that the solutions for all expansion coefficients in equations of the form

$$\mathbf{I}(\mu) = \sum_{\alpha=1}^{2} A_\alpha \mathbf{F}_\alpha(\mu) + \sum_{\alpha=1}^{2}\int_0^\infty A_\alpha(\eta)\mathbf{F}_\alpha(\eta,\mu)\,\mathrm{d}\eta,\ \mu \in (0,\infty), \tag{10.15}$$

can be expressed concisely as

$$A_\alpha = \int_0^\infty \tilde{\mathbf{\Theta}}_\alpha(\mu)\mathbf{I}(\mu)\,\mathrm{e}^{-\mu^2}\,\mu\,\mathrm{d}\mu,\ \alpha = 1 \text{ and } 2, \tag{10.16a}$$

and

$$A_\alpha(\eta) = \int_0^\infty \tilde{\mathbf{\Theta}}_\alpha(\eta,\mu)\mathbf{I}(\mu)\,\mathrm{e}^{-\mu^2}\,\mu\,\mathrm{d}\mu,\ \alpha = 1 \text{ and } 2. \tag{10.16b}$$

We note that a set of integrals of the form

$$T(\xi', \xi) = \int_0^\infty \tilde{\mathbf{\Theta}}(\xi', \mu)\boldsymbol{\Phi}(-\xi, \mu)\, e^{-\mu^2}\, \mu\, d\mu,\ \xi \text{ and } \xi' > 0, \tag{10.17}$$

has been evaluated and is listed elsewhere [16].

11. EXISTENCE AND UNIQUENESS OF THE H MATRIX

We first wish to prove

Theorem 6. *The equations*

$$\tilde{\mathbf{H}}(\mu)\boldsymbol{\lambda}(\mu) = \mathbf{I} + \mu P \int_0^\infty \tilde{\mathbf{H}}(\eta)\boldsymbol{\Psi}(\eta)\frac{d\eta}{\eta - \mu},\ \mu \in (0, \infty), \tag{11.1a}$$

and

$$\int_0^\infty \tilde{\mathbf{H}}(\mu)\boldsymbol{\Psi}(\mu)\, d\mu = \mathbf{I} \tag{11.1b}$$

possess a unique solution in the class of functions continuous on every open interval of the positive real axis.

Though for the sake of brevity we do not give an explicit derivation of equations (11.1), we note that the **H** matrix specified by equations (11.1) is sufficient for establishing the half-range orthogonality theorem.

To prove Theorem VI we make use of the equivalence of the given singular-integral equations to a certain matrix version of the Riemann problem. In the manner of Muskhelishvili [21], we introduce the matrix

$$\mathbf{N}(z) = \frac{1}{2\pi i}\int_0^\infty \tilde{\mathbf{H}}(\eta)\boldsymbol{\Psi}(\eta)\frac{d\eta}{\eta - z} \tag{11.2}$$

which is analytic in the plane cut along the real axis and vanishes at least as fast as $1/z$ as $|z|$ tends to infinity. The Plemelj formulae [21] can be used with equation (11.2) to yield

$$\pi i[\mathbf{N}^+(\mu) + \mathbf{N}^-(\mu)] = P\int_0^\infty \tilde{\mathbf{H}}(\eta)\boldsymbol{\Psi}(\eta)\frac{d\eta}{\eta - \mu},\ \mu \in (0, \infty), \tag{11.3}$$

and

$$\mathbf{N}^+(\mu) - \mathbf{N}^-(\mu) = \tilde{\mathbf{H}}(\mu)\boldsymbol{\Psi}(\mu),\ \mu \in (0, \infty). \tag{11.4}$$

If we make use of equations (5.10), (11.3) and (11.4) then equation (11.1a) can be cast in the equivalent form of an inhomogeneous Riemann problem:

$$\tilde{\mathbf{N}}^+(\mu) = \mathbf{G}(\mu)\tilde{\mathbf{N}}^-(\mu) + \boldsymbol{\Psi}(\mu)[\boldsymbol{\Lambda}^-(\mu)]^{-1},\ \mu \in (0, \infty), \tag{11.5}$$

where

$$\mathbf{G}(\mu) = \boldsymbol{\Lambda}^+(\mu)[\boldsymbol{\Lambda}^-(\mu)]^{-1}. \tag{11.6}$$

The solution to equation (11.5) can be written as

$$\tilde{\mathbf{N}}(z) = \frac{1}{2\pi i}\boldsymbol{\Phi}(z)\left[\int_0^\infty \mathbf{K}(\eta)\frac{d\eta}{\eta - z} + \hat{\mathbf{P}}(z)\right] \tag{11.7}$$

where $\hat{\mathbf{P}}(z)$ is a matrix of polynomials,

$$\mathbf{K}(\mu) = [\boldsymbol{\Phi}^+(\mu)]^{-1}\boldsymbol{\Psi}(\mu)[\boldsymbol{\Lambda}^-(\mu)]^{-1}, \tag{11.8}$$

and $\boldsymbol{\Phi}(z)$ is any canonical solution (of ordered normal form at infinity) to the homogeneous Riemann problem defined by equation (9.1). In order that equation (11.7) have behavior as $|z|$ approaches infinity consistent with equation (11.2), we must take $\hat{\mathbf{P}}(z)$ to be a constant matrix.

Following closely Siewert and Burniston's [25] work on the scattering of polarized light, we can now use the constraint to specify uniquely the constant $\hat{\mathbf{P}}(z)$ in equation (11.7). It thus follows that equation (11.7) along with equations (9.11) and (11.4) yields the result

$$\mathbf{H}(\mu) = \tilde{\boldsymbol{\Phi}}_0^{-1}(-\mu)\tilde{\boldsymbol{\Phi}}_0(0),\ \mu \in (0, \infty), \tag{11.9}$$

where $\boldsymbol{\Phi}_0(z)$ is the canonical solution (of ordered normal form at infinity) used in equation (9.11). We note from equation (11.9), since $\boldsymbol{\Phi}_0(z) = \overline{\boldsymbol{\Phi}_0(\bar{z})}$, that $\mathbf{H}(\mu)$ is real for $\mu \in (0, \infty)$. Further, equation (11.9) can be used to extend the definition of $\mathbf{H}(\mu)$ to the complex plane:

$$\mathbf{H}(z) = \tilde{\boldsymbol{\Phi}}_0^{-1}(-z)\tilde{\boldsymbol{\Phi}}_0(0), \tag{11.10}$$

so that the $\boldsymbol{\Lambda}$ matrix can now be factored as

$$\boldsymbol{\Lambda}(z) = \tilde{\mathbf{H}}^{-1}(-z)\mathbf{H}^{-1}(z).$$

We note that equations (5.10), (9.11) and (11.10) can be used in the Cauchy integral representation

$$\boldsymbol{\Phi}_0(z) = \frac{1}{2\pi i}\int_0^\infty [\boldsymbol{\Phi}_0^+(\mu) - \boldsymbol{\Phi}_0^-(\mu)]\frac{d\mu}{\mu - z} \tag{11.11}$$

to obtain

$$\mathbf{H}(z) = \mathbf{I} + z\mathbf{H}(z)\int_0^\infty \tilde{\mathbf{H}}(\eta)\boldsymbol{\Psi}(\eta)\frac{d\eta}{\eta + z} \tag{11.12}$$

or

$$\mathbf{H}(\mu) = \mathbf{I} + \mu\mathbf{H}(\mu)\int_0^\infty \tilde{\mathbf{H}}(\eta)\boldsymbol{\Psi}(\eta)\frac{d\eta}{\eta + \mu},\ \mu \in [0, \infty). \tag{11.13}$$

Since we have established the existence of a unique solution to equations (11.1) and developed equation (11.13) specifically to be used, along with equation (11.1b), as the basis for our procedure for computing the **H** matrix, it follows that we require proof of

Theorem 7. *The equations*

$$\mathbf{H}(\mu)=\mathbf{I}+\mu\mathbf{H}(\mu)\int_0^\infty \tilde{\mathbf{H}}(\eta)\boldsymbol{\Psi}(\eta)\frac{\mathrm{d}\eta}{\eta+\mu},\ \mu\in[0,\infty), \tag{11.14a}$$

and

$$\int_0^\infty \tilde{\mathbf{H}}(\mu)\boldsymbol{\Psi}(\mu)\,\mathrm{d}\mu=\mathbf{I} \tag{11.14b}$$

possess a unique solution in the class of functions continuous on every open interval of the positive real axis.

We have shown that equations (11.1) possess a unique solution; thus we need only show that any solution of equation (11.14a) is also a solution of equation (11.1a). We first write equation (11.14a) as

$$\mathbf{H}(\mu)\left[\mathbf{I}-\mu\int_0^\infty \tilde{\mathbf{H}}(\eta)\boldsymbol{\Psi}(\eta)\frac{\mathrm{d}\eta}{\eta+\mu}\right]=\mathbf{I} \tag{11.15a}$$

or, alternatively,

$$\left[\mathbf{I}-\mu\int_0^\infty \tilde{\mathbf{H}}(\eta)\boldsymbol{\Psi}(\eta)\frac{\mathrm{d}\eta}{\eta+\mu}\right]\mathbf{H}(\mu)=\mathbf{I}. \tag{11.15b}$$

If the transpose of equation (11.15b) is post-multiplied by

$$\mathbf{I}+\mu P\int_0^\infty \tilde{\mathbf{H}}(\eta)\boldsymbol{\Psi}(\eta)\frac{\mathrm{d}\eta}{\eta-\mu}$$

then, after making use of some partial-fraction analysis and equations (4.15) and (11.15), we obtain

$$\tilde{\mathbf{H}}(\mu)\boldsymbol{\lambda}(\mu)=\mathbf{I}+\mu P\int_0^\infty \tilde{\mathbf{H}}(\eta)\boldsymbol{\Psi}(\eta)\frac{\mathrm{d}\eta}{\eta-\mu},\ \mu\in(0,\infty), \tag{11.16}$$

which proves Theorem 7.

12. AN EXPEDIENT METHOD FOR COMPUTING THE H MATRIX

It is clear from the previous sections of this paper that the **H** matrix is the basic quantity required in the solutions of problems defined in terms of equation (4.18) and specified by half-range, $\mu\in(0,\infty)$, boundary conditions. It is also apparent from the analysis of section 11 that the basic proofs regarding the existence and uniqueness of the **H** matrix have been established; however, to demonstrate the utility of our analysis, we must now establish a procedure by which we can compute the **H** matrix accurately and efficiently.

As we have discussed, the **H** matrix is uniquely specified by the nonlinear equation

$$\mathbf{H}(\mu) = \mathbf{I} + \mu \mathbf{H}(\mu) \int_0^\infty \tilde{\mathbf{H}}(\eta)\mathbf{\Psi}(\eta)\frac{d\eta}{\eta + \mu}, \ \mu \in [0, \infty), \tag{12.1a}$$

and the constraint

$$\int_0^\infty \tilde{\mathbf{H}}(\mu)\mathbf{\Psi}(\mu)\, d\mu = \mathbf{I}. \tag{12.1b}$$

Rather than seek a numerical solution to equation (12.1a) which must also satisfy equation (12.1b), we prefer [15, 22] first to write

$$\mathbf{H}(\mu) = (1 + \mu)\mathbf{L}(\mu), \ \mu \in [0, \infty). \tag{12.2}$$

If we now substitute equation (12.2) into equation (12.1a), perform some elementary partial-fraction analysis, and make use of the constraint, equation (12.1b), then we find that $\mathbf{L}(\mu)$ must satisfy

$$\mathbf{L}(\mu) = \mathbf{I} + \mu \mathbf{L}(\mu) \int_0^\infty (1 - \eta^2)\tilde{\mathbf{L}}(\eta)\mathbf{\Psi}(\eta)\frac{d\eta}{\eta + \mu}, \ \mu \in [0, \infty), \tag{12.3a}$$

and

$$\int_0^\infty \tilde{\mathbf{L}}(\mu)\mathbf{\Psi}(\mu)(1 + \mu)\, d\mu = \mathbf{I}. \tag{12.3b}$$

It follows from Theorem 7 that equations (12.3) have a unique solution. We regard equations (12.3) as the basic equations to be solved numerically because an iterative procedure based on these equations has proven to converge faster than a similar iterative solution of equations (12.1).

For calculational convenience, we now prefer to make in equations (12.3) the change of variable

$$t = \frac{\mu}{1 + \mu} \tag{12.4}$$

and thus to write

$$\mathbf{L}_*(t) = \mathbf{I} + t\mathbf{L}_*(t) \int_0^1 \frac{1 - 2s}{(1 - s)^3}\tilde{\mathbf{L}}_*(s)\mathbf{\Psi}_*(s)\frac{ds}{t(1 - s) + s(1 - t)}, \ t \in [0, 1), \tag{12.5}$$

where we have introduced the notation $g_*(t) = g[t/(1 - t)]$. We have found that equation (12.5) can be solved quite effectively by iteration.

The computations were performed in double-precision arithmetic on an IBM 370/165 computer, and we used an improved Gaussian-quadrature [17] representation of the integration process. The iterative procedure was terminated when successive calculations of $\mathbf{L}_*(t)$ differed by no more than 10^{-15}.

To substantiate confidence in our computations, several "checks" were incorporated in the calculation. As expected $\mathbf{L}_*(t)$ satisfied

$$\mathbf{I} - \int_0^1 \tilde{\mathbf{L}}_*(t)\mathbf{\Psi}_*(t)\frac{dt}{(1 - t)^3} = \mathbf{0}, \tag{12.6}$$

an identity corresponding to the constraint, equation (12.1b), to thirteen significant figures. The equation in terms of $\mathbf{L}_*(t)$ corresponding to the identity[16]

$$2\int_0^\infty \mathbf{\Psi}(\mu)\,\mu^2 \mathrm{d}\mu - \int_0^\infty \mathbf{\Psi}(\mu)\mathbf{H}(\mu)\,\mu\,\mathrm{d}\mu \int_0^\infty \tilde{\mathbf{H}}(\mu)\mathbf{\Psi}(\mu)\,\mu\,\mathrm{d}\mu = \mathbf{0} \tag{12.7}$$

was also verified to thirteen significant figures.

The analytical solution[16]

$$H(z) = \det \mathbf{H}(z) = \sqrt{\frac{12}{5}} z^2 \exp\left\{-\frac{1}{\pi}\int_0^\infty \arg \Lambda^+(\mu)\frac{\mathrm{d}\mu}{\mu + z}\right\}, \tag{12.8}$$

where $\arg \Lambda^+(0) = -2\pi$, can be shown to satisfy

$$H(\mu) = 1 + \mu H(\mu)\int_0^\infty f(\eta)H(\eta)\frac{\mathrm{d}\eta}{\eta+\mu},\ \mu \in [0, \infty), \tag{12.9}$$

where

$$f(\eta) = \frac{1}{3}\frac{1}{\sqrt{\pi}}\mathrm{e}^{-\eta^2}\left[\frac{11}{2} - \eta^2 - 8\eta\,\mathrm{e}^{-\eta^2}\int_0^\eta \mathrm{e}^{t^2}\,\mathrm{d}t\right]. \tag{12.10}$$

Rather than solve equation (12.9) and the appropriate constraint for $H(\mu)$ we prefer to write

$$H(\mu) = (1+\mu)^2 L(\mu),\ \mu \in [0, \infty). \tag{12.11}$$

If we substitute equation (12.11) into equation (12.9), perform some partial-fraction analysis and make use of two identities[16] for $H(\mu)$ then we find that (after an appropriate change of variables) $L_*(t) = \det \mathbf{L}_*(t)$ must satisfy

$$\frac{1}{L_*(t)} = 1 - t\int_0^1 \frac{(1-2s)^2}{(1-s)^5} f_*(s)L_*(s)\frac{\mathrm{d}s}{s(1-t)+t(1-s)},\ t \in [0, 1). \tag{12.12}$$

We have compared $L_*(t)$ as computed from equation (12.5) to a direct solution of equation (12.12) and the appropriate constraint to find agreement to nine significant figures.

Finally the number of quadrature points used to represent the integration process was increased to suggest that the numerical values of the $\mathbf{L}_*$ matrix given in the accompanying Table (1) were insensitive to further refinements in the quadrature scheme.

13. AN APPLICATION OF THE THEORY: THE TEMPERATURE SLIP PROBLEM

We consider the effect of a body surface on the behavior of the particle distribution function of a rarefied gaseous medium. It is known that, in the absence of boundaries, the particle distribution function in a gas with slowly varying physical parameters obeys the Chapman–Enskog equations (and therefore the macroscopic variables obey the

Table 1. The $\mathbf{L}_*$ matrix

t	$L_{*11}(t)$	$L_{*12}(t)$	$L_{*21}(t)$	$L_{*22}(t)$
0·0	1·0	0·0	0·0	1·0
0·05	1·05781	−0·0409718	−0·0406202	1·08988
0·10	1·08842	−0·0702992	−0·0691920	1·14897
0·15	1·10976	−0·0960791	−0·0939297	1·19824
0·20	1·12527	−0·119749	−0·116314	1·24158
0·25	1·13648	−0·141931	−0·136989	1·28073
0·30	1·14424	−0·162963	−0·156307	1·31664
0·35	1·14909	−0·183053	−0·174483	1·34992
0·40	1·15139	−0·202341	−0·191658	1·38097
0·45	1·15138	−0·220921	−0·207929	1·41009
0·50	1·14926	−0·238862	−0·223361	1·43748
0·55	1·14514	−0·256214	−0·238000	1·46333
0·60	1·13912	−0·273011	−0·251873	1·48774
0·65	1·13125	−0·298278	−0·264997	1·51082
0·70	1·12157	−0·305030	−0·277373	1·53265
0·75	1·11008	−0·320274	−0·288995	1·55328
0·80	1·09678	−0·335010	−0·299844	1·57276
0·85	1·08162	−0·349228	−0·309887	1·59111
0·90	1·06454	−0·362913	−0·319081	1·60835
0·95	1·04545	−0·376036	−0·327361	1·62449
0·99	1·02864	−0·386105	−0·333271	1·63660

Navier–Stokes equations). Near the body surface, the behavior of the gas is described by a rarefied Knudsen layer in which the collisional effects are only of secondary importance. It is natural to ask how the outer Chapman–Enskog (or Navier–Stokes) region can be matched consistently with the inner Knudsen layer. Saying it differently, we ask what are the velocity and temperature slip boundary conditions at a body surface for the Navier–Stokes equations due to the presence of the Knudsen layer adjacent to the body surface.

To understand the asymptotic behavior of the Knudsen layer, we may stretch locally the coordinate normal to the body surface such that the gas-kinetic motion in the Knudsen layer reduces to a locally defined half-space problem and the kinetic equation takes on a one-dimensional character in the form studied in this paper.

Since the asymptotic boundary condition of the Knudsen layer is given by the Chapman–Enskog equations, the asymptotic form of the particle distribution function is nearly Maxwellian. If we also assume that the effect of the body surface is to re-emit molecules described by a suitably chosen Maxwellian distribution and that the macroscopic variables do not vary appreciably throughout the Knudsen layer, a linearization scheme for the one-dimensional kinetic equation in the sense described in sections 2 and 3 is justified. Based on the constant collision frequency BGK model, the pertinent linearized kinetic equation for the Knudsen layer is that given by equation (3.7). The velocity-slip (or Kramers problem) for this equation for a diffusely reflecting wall has been solved exactly by Cercignani [9] and an accurate velocity-slip coefficient has been calculated, [1]. Although approximate analyses of the associated temperature slip problem have been reported by a number of authors [2, 19, 23, 28, 29], an accurate calculation of the temperature-slip coefficient has not been previously reported. Since the temperature-density effects for the problem for a diffusely reflecting wall are uncoupled from the transverse momentum effects, we will show that an accurate determination of the temperature slip coefficient for steady gas-kinetic motion may be effected by using the method of elementary solutions and the half-range expansion theorem developed in this paper for the vector integrodifferential equation (4.1).

It is straightforward to demonstrate that the heat flux in the normal direction in the Knudsen layer is a constant and since the Chapman–Enskog solution relates the heat flux linearly to the temperature gradient, to match the Chapman–Enskog region and the Knudsen layer it is only necessary to consider an asymptotic boundary condition with a constant temperature gradient. It is interesting to note that such an asymptotic boundary condition, as far as the temperature-density effects are concerned, can be satisfied by taking the asymptotic perturbation distribution function to be

$$h_{asy}(x, \mathbf{c}) = \begin{bmatrix} 1 \\ c_2^2 + c_3^2 - 1 \end{bmatrix}^T \left[\sum_{\alpha=1}^{2} A_\alpha \boldsymbol{\Phi}_\alpha(\mu) + \sum_{\beta=3}^{4} A_\beta \boldsymbol{\Psi}_\beta(x, \mu) \right], \tag{13.1}$$

where the $\boldsymbol{\Phi}'_\alpha$s and $\boldsymbol{\Psi}'_\beta$s are the discrete solutions to equation (4.1), and c_2, c_3 are the components of the dimensionless particle velocity in the transverse directions. Since the Chapman–Enskog theory requires the medium to obey the perfect gas law and the pressure in the Knudsen layer far from the wall is a specified constant, we deduce from the definitions

$$n_{asy}(x) \triangleq \pi^{-3/2} \int h_{asy}(x, \mathbf{c})\, \mathrm{e}^{-c^2}\, \mathrm{d}^3 c, \tag{13.2}$$

and

$$T_{asy}(x) \triangleq \tfrac{2}{3}\pi^{-3/2} \int h_{asy}(x, \mathbf{c})(c^2 - \tfrac{3}{2})\, \mathrm{e}^{-c^2}\, \mathrm{d}^3 c, \tag{13.3}$$

the requirements

$$A_2 = -\sqrt{\tfrac{2}{3}}A_1 \text{ and } A_4 = -\sqrt{\tfrac{2}{3}}A_3. \tag{13.4}$$

For an asymptotic temperature gradient of unity, it is clear that the temperature slip coefficient ξ defined by $T_{asy}(0) = \xi(\mathrm{d}/\mathrm{d}x)T_{asy}(x)|_{x=0}$ will be given by $\xi = \epsilon' l_t$, [19], where

$$\epsilon' = \sqrt{\tfrac{2}{3}}A_1, \tag{13.5}$$

$l_t = (4/5)(\mathcal{K}/nk)(m/2kT)^{1/2}$ is a mean free path, and $\mathcal{K}$ is the thermal conductivity.

For a diffusely reflecting wall, the boundary condition at $x = 0$ requires

$$\begin{bmatrix} B \\ 0 \end{bmatrix} = \sum_{\alpha=1}^{4} A_\alpha \boldsymbol{\Phi}_\alpha(\mu) + \sum_{\alpha=1}^{2} \int_0^\infty A_\alpha(\eta)\boldsymbol{\Phi}_\alpha(\eta, \mu)\, \mathrm{d}\eta,\ \mu \in (0, \infty). \tag{13.6}$$

The unknown constant B is related to the density of the gas near the wall and need not be specified for temperature-slip coefficient calculations. We make use of equation (13.4) and the specified asymptotic temperature gradient to write equation (13.6) as

$$\sqrt{\tfrac{3}{2}}\boldsymbol{\Phi}_3(\mu) - \boldsymbol{\Phi}_4(\mu) = A_1\boldsymbol{\Phi}_1(\mu) + (A_2 - B)\boldsymbol{\Phi}_2(\mu) + \sum_{\alpha=1}^{2} \int_0^\infty A_\alpha(\eta)\boldsymbol{\Phi}_\alpha(\eta, \mu)\, \mathrm{d}\eta. \tag{13.7}$$

Theorem 3 and equation (10.16a) enable us to solve equation (13.7) for A_1:

$$A_1 = \int_0^\infty \tilde{\Theta}_1(\mu)[\sqrt{\tfrac{3}{2}}\Phi_3(\mu) - \Phi_4(\mu)]\, e^{-\mu^2}\, \mu\, d\mu. \tag{13.8}$$

It is clear from the definition of $\Theta_1(\mu)$ that A_1 may be expressed in terms of appropriate moments of the **H** matrix discussed in section 11. The numerical procedure used to evaluate integrals involving the **H** matrix was given in section 12. We find

$$\epsilon' = \tfrac{5}{8}\pi^{1/2}(1{\cdot}17597). \tag{13.9}$$

This compares with the variational result of $\epsilon' = \frac{5}{8}\pi^{1/2}(1{\cdot}1621)$, [2, 19, 23], Wang Chang and Uhlenbeck's result of $\epsilon' = \frac{5}{8}\pi^{1/2}(1{\cdot}150)$, [28], and Welander's value of $\epsilon' = \frac{5}{8}\pi^{1/2}$ $(1{\cdot}173)$, [29]. We believe our result to be accurate to the number of significant figures quoted.

Acknowledgement—The authors are grateful to Professor E. E. BURNISTON for many valuable discussions during the course of this investigation. This research was supported in part by NSF grants GK-11935 and GU-1590, and NASA grant NGL34–002–084, and the Triangle Universities Consortium on Air Pollution (comprising Duke University, North Carolina State University and the University of North Carolina at Chapel Hill), which is funded by the Office of Manpower Development of the U.S. Environmental Protection Agency.

REFERENCES

[1] S. ALBERTONI, C. CERCIGNANI and L. GOTUSSO, *Phys. Fluids* **6**, 993 (1963).
[2] P. BASSANINI, C. CERCIGNANI and C. D. PAGANI, *Int. J. Heat Mass Transfer* **10**, 447 (1967).
[3] P. L. BHATNAGAR, E. P. GROSS and M. KROOK, *Phys. Rev.* **94**, 511 (1954).
[4] G. R. BOND and C. E. SIEWERT, *Astrophys. J.* **164**, 97 (1971).
[5] E. E. BURNISTON and C. E. SIEWERT, *J. Math Phys.* **11**, 3416 (1970).
[6] E. E. BURNISTON, C. E. SIEWERT, P. SILVENNOINEN and P. F. ZWEIFEL, *Nucl. Sci. Engng* **45**, 331 (1971).
[7] K. M. CASE, *Ann. Phys.* **9**, 1 (1960).
[8] K. M. CASE and P. F. ZWEIFEL, *Linear Transport Theory.* Addison–Wesley (1967).
[9] C. CERCIGNANI, *J. Math. Analysis Applic.* **10**, 568 (1965).
[10] R. V. CHURCHILL, *Complex Variables and Applications* McGraw-Hill (1960).
[11] C. CERCIGNANI, *Elementary solutions of linearized kinetic models and boundary value problems in the kinetic theory of gases.* Brown Univ. Report (1965).
[12] C. CERCIGNANI, *Mathematical Methods in Kinetic Theory.* Plenum (1969).
[13] E. P. GROSS and E. A. JACKSON, *Physics Fluids* **2**, 432 (1959).
[14] I. M. GELFAND and G. E. SHILOV, *Generalized Functions.* Academic (1964).
[15] J. T. KRIESE and C. E. SIEWERT, *Astrophys. J.* **164**, 389 (1971).
[16] J. T. KRIESE, Ph.D. Thesis, North Carolina State University (1972).
[17] A. S. KRONROD, *Nodes and Weights of Quadrature Formulas.* Consultants Bureau (1965).
[18] I. KUSCER, N. J. McCORMICK and G. C. SUMMERFIELD, *Ann. Phys.* **30**, 411 (1964).
[19] S. K. LOYALKA and J. H. FERZIGER, *Physics Fluids* **11**, 1668 (1968).
[20] G. F. MANDŽAVIDZE and B. V. HVEDELIDZE, *Dokl. Akad. Nauk SSSR* **123**, 791 (1958).
[21] N. I. MUSKHELISHVILI, *Singular Integral Equations.* Noordhoff (1953).
[22] S. PAHOR, *Nucl. Sci. Engng.* **31**, 110 (1968).
[23] S. F. SHEN, *Rarefied Gas Dynamics,* (Edited by C. L. BAUNDIN). Academic Press (1967).
[24] C. E. SIEWERT, *J. Quant. Spectrosc. Radiat. Transfer* **12**, 683 (1972).
[25] C. E. SIEWERT and E. E. BURNISTON, *Astrophys. J.* **174**, 629 (1972).
[26] C. E. SIEWERT and P. F. ZWEIFEL, *Ann. Phys.* **36**, 61 (1966).
[27] L. SIROVICH, *Phys. Fluids* **5**, 908 (1962).
[28] C. S. WANG CHANG and G. E. UHLENBECK, University of Michigan Engineering Research Institute Project Report M999 (1954).
[29] P. WELANDER, *Ark. Fy.* **7**, 507 (1954).

(*Received* 8 *June* 1972)

Résumé—La méthode des solutions élémentaires est employée pour résoudre deux équations integro-différentielles couplées pour la détermination des effets du rapport température-densité, dans un modèle BGK linéarisé dans la théorie cinétique des gaz. L'état complet de tout le domaine et les théorèmes d'orthogonalité sont démontrés pour les modes normaux développés et la fonction de Green pour un milieu infini est établie comme illustration du formalisme sur tout le domaine.

Le problème de Riemen approprié à une matrice homogène est étudiée et l'état complet de tout le domaine et les théorèmes d'orthogonalité sont démontrés pour un certain sous-système des modes normaux. Les théorèmes nécessaires d'existence et d'unicité concernant la matrice H, fondamentale pour l'analyse du domaine complet, sont démontrés et une méthode de calcul précise et efficace est présentée. Le problème du glissement de température d'un demiespace est résolu analytiquement et une valeur très précise du coefficient de glissement de température est donnée.

Zusammenfassung—Das Verfahren elementarer Lösungen wird verwendet, um zwei gekuppelte Integrodifferentialgleichungen zu lösen, die genügen, um die Temperatur-Dichtewirkungen in einem linearisierten BGK-Modell in der kinetischen Theorie von Gasen zu bestimmen.

Vollbereichs-Vollständigkeits- und Orthogonalitätstheoreme werden für die entwickelten Normalformen bewiesen und Green's Funktion des unendlichen Stoffes wird als eine Illustration des Vollbereichsformalismus konstruiert.

Das entsprechende Riemann'sche Problem einer homogenen Matrix wird besprochen und Halbbereichs-Vollständigkeits- und Orthogonalitätstheoreme werden für eine bestimmte Untergruppe der Normalformen bewiesen. Die für die $\underline{H}$-Matrix belangreichen erforderlichen Existenz- und Eindeutigkeitstheoreme, grundlegend für die Halbbereichs-Analyse, werden bewiesen, und eine genaue und wirksame Berechnungsmethode wird besprochen. Das Temperaturgleitproblem des Halbraumes wird analytisch gelöst und ein sehr genauer Wert des Temperaturgleitkoeffizienten wird berichtet.

Sommario—Il metodo delle soluzioni elementari viene usato per risolvere due equazioni integrodifferenziali accoppiate, sufficienti a determinare gli effetti della densità di temperatura in un modello BGK linearizzato nella teoria cinetica dei gas.

Vengono dimostrati i teoremi della completezza e dell'ortogonalità su tutta la gamma per i modi normali sviluppati e, per illustrare il formalismo sull'intera gamma, viene costruita la funzione di Green per un mezzo infinito.

Viene discusso il problema di Riemann per una matrice omogenea appropriata e, per un certo sottoassieme dei modi normali, vengono dimostrati i problemi di completezza e ortogonalità per la semigamma. Vengono dimostrati i necessari teoremi di esistenza e unicità relativi alla matrice $\underline{H}$, fondamentali per l'analisi della semigamma, e viene discusso un metodo di calcolo accurato ed efficiente. Il problema temperatura/scorrimento del semispazio viene risolto analiticamente e viene dato un valore molto accurato del coefficiente temperatura/scorrimento.

Абстракт — Применен метод элементарных решений для решения двух интегро-дифференциальных уравнений достаточных для определения эффектов температуры и плотности в линеаризованной модели (BGK) в кинетической теории газов. Даны доказательства теорем об общей полноте и ортогональности для развиваемых нормальных режимов, построена функция Грина для бесконечной среды в качестве иллюстрации общего формализма. Обсуждена соответствующая римановская проблема однородной матрицы, даны доказательства теорем о половинной полноте и ортогональности для определенной подсистемы нормальных режимов. Доказаны искомые теоремы о существовании и единственности относительно матрицы H, лежащие в основе анализа половинной полноты, а также обсужден точный рациональный метод вычисления. Аналитически решена проблема полупространственного скольжения и температуры, сообщено высокоточное значение коэффициента скольжения и температуры.

75-04939

N75-15329

Tricritical points in multicomponent fluid mixtures*

Alex Hankey†
Stanford Linear Accelerator Center, Stanford University, Stanford, California 94305

T. S. Chang‡ and H. E. Stanley§
Department of Physics, Massachusetts Institute of Technology, Cambridge, Massachusetts 02139
(Received 2 July 1973)

In view of experimental considerations, we give a model-independent argument that the novel tricritical points in multicomponent fluid mixtures, where three phases simultaneously become critical, are points on the boundary of a *single two-dimensional surface of critical points*. This result is corroborated by the Landau model suggested by Griffiths. The relationship between these tricritical points and the complex "higher-order" critical points proposed to exist in certain magnetic systems is elucidated.

I. INTRODUCTION

In 1970 Griffiths[1] proposed the concept of a tricritical point as being the point of intersection of three lines of critical points in a phase diagram using intensive thermodynamic variables. He further suggested, as examples, metamagnets,[2] He^3-He^4 mixtures,[3] and ammonium chloride.[4] There has also been considerable speculation[1,5] that similar points might exist and might be found in the phase diagrams of complex fluid mixtures. That such points have already been proposed and, indeed, that they had been investigated prior to 1970 has recently been pointed out by Widom and Griffiths.[6-8] A full and very complete discussion of experimental evidence for these points has been given in Refs. 6–8, and we refer the reader to these papers for details.

A different way in which critical points more complex than tricritical points can occur has been shown to involve intersecting lines of tricritical points, and a classification of critical points has been introduced to differentiate these points from tricritical points or ordinary critical points.[5] The question has been raised[6,8] as to how the new points discovered in fluids are related to such a classification.

Properties of the phase diagram[9] were the basis of the approach we suggested previously.[5,10] In particular, we emphasized the importance of the connectivity properties of different spaces of critical points and tricritical points. Accordingly it is the connectivity of the different critical points of multicomponent fluid mixtures in the space of truly intensive or "field" variables that we emphasize here.

II. DEMONSTRATION THAT ALL CRITICAL POINTS FORM A SINGLE CONNECTED SURFACE

The basic idea is to consider a system where three distinct phases can be in equilibrium. These might be three liquids or two liquids and a vapor phase. On changing the thermodynamic variables (temperature, pressure, chemical potentials of different components) one pair of phases will become critical, in the presence of the third. In a binary system the point where this occurs is the end point of a line of critical points which bounds the surface of points where the two phases coexist. There are no degrees of freedom and such a point is unique in the phase diagram.[7]

In a ternary, quaternary, or more complicated system this point has one or more degrees of freedom. Thus a line of "critical end points" is possible. Such a line is the boundary of a surface of critical points where two phases are critical.

In the particular systems of interest it is possible, by varying physical conditions, to make a different pair of the three phases become critical in the presence of the third, thus producing a second line of critical end points.

Finally, by achieving exactly the correct physical conditions it is possible for all three phases to become critical simultaneously. In a ternary system such a point is unique; there are zero degrees of freedom. Here, only this and similarly simple cases are considered.

Experimentally there is the following arrangement. A tube containing a three-component mixture with a three-phase system is cooled to observe the appearance of successive phases. We will call these phases α, β, and γ, where for purposes of argument $\rho_\alpha < \rho_\beta < \rho_\gamma$. The ratio of the various components is varied until the second meniscus appears via a critical mode. This could be the lower meniscus in which case phases γ and β become critical at a lower temperature. If pressure, temperature, and one other intensive parameter are allowed to vary, a phase diagram of the type shown in Fig. 1(a) will be observed. At the point P, the phases γ and β become critical in the presence of a third phase α. If pressure is increased, the lightest phase α will disappear and a line of critical points between phases γ and β will develop. For increasing temperatures above P, there will be a line of critical points bounding the surface of coexistence points which separates the region of light phase α from the region of the heavier phase $\gamma\beta$.

By varying the ratios of components appropriately, it is possible, in the physical systems of interest, to make the upper meniscus, separating phase β from phase α, appear second on cooling. The corresponding phase diagram is shown in Fig. 1(c). Again there is a special point P' which is the end point of a line of critical points for phases β and α, and which is also the end point of the line of points where three phases coexist. If the temperature is increased above P' then the coexistence surface separating phase γ from the combined phases $\beta\alpha$ will terminate in a line of critical points.

If the transition to the phase diagram of Fig. 1(c) happens by a continuous variation from Fig. 1(a) then there must be a situation where both menisci become critical simultaneously.

The corresponding phase diagram is shown in Fig. 1(b). It may be seen that the point P of Fig. 1(a) has migrated along the coexistence surface to the point P_t on the boundary. At the point P_t all three lines of critical points, a ($\gamma\beta$ critical), b ($\gamma\alpha$ critical), and c ($\beta\alpha$ critical) meet.

The purpose of constructing Figs. 1(a)–1(c) is to consider the behavior of the critical surface in the immediate neighborhood of the tricritical point P_t, and the figures should therefore be understood to represent the phase diagram close to P_t and not far away from the tricritical point. Also, since our primary interest is the connectivity of the surface of critical points, and not its specific shape, we do not have to choose the variables precisely, since the connectedness would remain unchanged even if different variables were chosen. [Similar remarks apply to Figs. 2(a) and 2(b) in what follows.]

We can now demonstrate that the lines of critical points a, b, c in Figs. 1(a)–1(c) form a single continuous surface of critical points bounded by the line of critical end points P-P_t-P'. Consider a

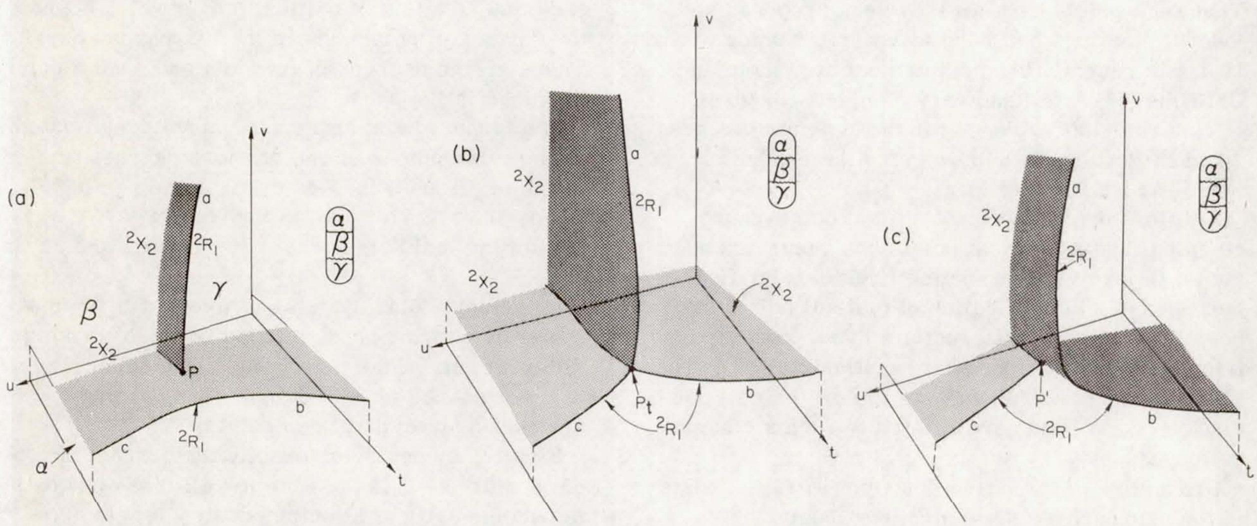

FIG. 1. Three-dimensional subspaces of the full four-dimensional space of field variables of a three-component system (or of five dimensions for four components). The variable t may be thought of as the temperature, the variable v as the pressure, and the third variable u as a suitable combination of chemical potentials. We use the notation of Ref. 5 to indicate lines and surfaces of critical points in the diagram. Lines of critical points are indicated $^2R_1$ (order 2, dimension 1). Coexistence surfaces are indicated by $^2X_2$ (two phases and dimension 2). (a) Section containing a point P where the two heavier phases γ, β are critical in the presence of the lightest α, as represented by the schematic tube showing the $\gamma\beta$ meniscus critical and the $\beta\alpha$ meniscus stable. (b) Section through the point P_t where all three phases become critical simultaneously, the $\gamma\beta$ and $\beta\alpha$ menisci are simultaneously critical in the schematic tube. (c) Section containing a point P' where the lighter phases β, α are critical in the presence of the heaviest γ, as shown in the schematic representation.

point on line a in Fig. 1(a); move continuously through Figs. 1(b) to 1(c). Now move along the line a-b to a point at the "b" end, and now move along continuously through Figs. 1(b) to 1(a). Still being on line b, we can move along the line b-c to the "c" end. Now move continuously through Figs. 1(b) to 1(c) and our assertion is demonstrated. We have not passed through the point P_t and so the lines a, b, c form sections of a single continuous surface of critical points bounded by lines of critical end points $P - P_t - P'$.

The fact that there is only a single surface of critical points is also corroborated by the model of Griffiths[8] (see his Fig. 3). This fact is in strong contrast to the metamagnet where it is not possible to go from a point on the wing boundaries to a point on the physical critical line without passing through a tricritical point[1,10] and the spaces of critical points are distinct and separate.

It will be plausible to conjecture that since all the critical points form a single surface, the critical-point exponents are the same at all critical points except the tricritical point itself. In contrast, for a metamagnet no reasons have been presented for why the critical-point exponents should be the same along all three of the critical lines meeting at the tricritical point. However, it has been suggested[11] that for most tricritical points the existence of a hidden variable linking the wing boundaries to the physical critical line (the variable called a_3 by Griffiths[8]) might force the equality of exponents.

III. MODEL SURFACE OF CRITICAL POINTS

The phase diagrams of Figs. 1(a)–1(c) were three dimensional and so parametrizing them with an extra field variable introduces a fourth dimension to the phase diagram. The connectivity, and other properties, of the surface of critical points formed by the critical lines a, b, c of Fig. 1, are most easily studied in a three-dimensional subspace of the full phase diagram which contains the whole critical surface. The shape of the critical surface in such a subspace may be determined as follows.

Consider the critical lines as they appear on the paper in Figs. 1(a)–1(c) and consider how these lines would form a smooth surface in three dimensions if the extra parameter were used to plot the height of the paper, with Fig. 1(c) above 1(b) above 1(a). By this combined projection and motion we generate a single connected surface of critical points with a boundary formed by the line of points P-P_t-P'.

A surface, which is topologically equivalent to the surface of critical points thus obtained, is shown in Figs. 2(a) and 2(b). Fig. 2(a) is a contour map of the surface, and the heights h of the contours are given by the hyperbolae $xy = h$. The boundary of the surface P-P_t-P' is represented by the parabola $y = -cx^2$ in the lower half of Fig. 2(a). The topological equivalence of the surface of Fig. 2(a) to the surface of critical points may be seen as follows.

Consider a section of Fig. 2(a) at constant height h. If $h > 0$ there are two hyperbolae, one in the upper right quadrant and one which terminates on the portion of the parabola labeled P in the lower left. This is a representation of Fig. 1(a) for which there are two critical lines, one labeled (a) terminating at P and another labeled (b-c).

If $h < 0$ there are again two hyperbolae, one in the upper left quadrant which corresponds to the line of critical points (a, b) of Fig. 1(c), and one

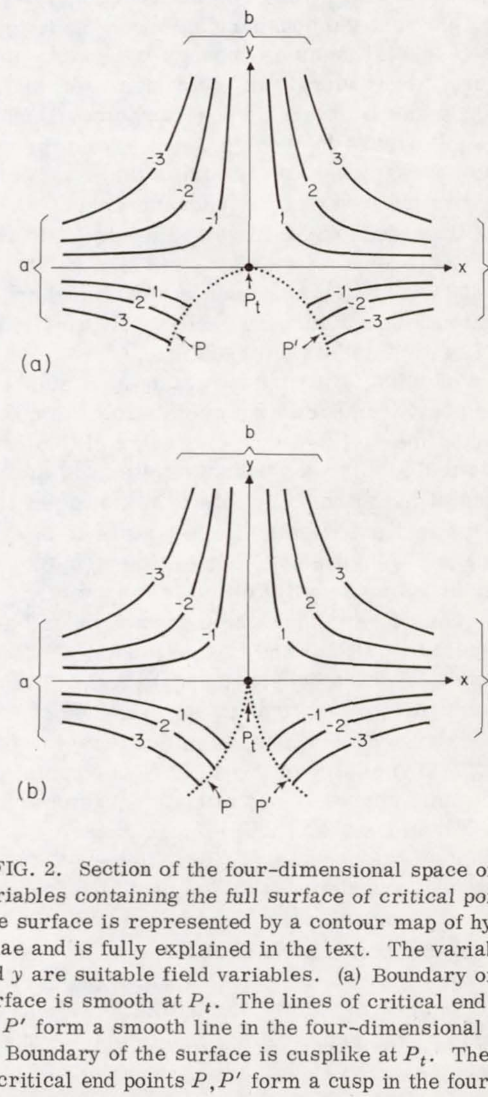

FIG. 2. Section of the four-dimensional space of field variables containing the full surface of critical points. The surface is represented by a contour map of hyperbolae and is fully explained in the text. The variables x and y are suitable field variables. (a) Boundary of the surface is smooth at P_t. The lines of critical end points P, P' form a smooth line in the four-dimensional space. (b) Boundary of the surface is cusplike at P_t. The lines of critical end points P, P' form a cusp in the four-dimensional space.

in the lower right quadrant of Fig. 2 which corresponds to the critical line c terminating at P in Fig. 1(c).

When $h=0$ the hyperbolae degenerate into the three axes, for $x<0$, $y>0$, and $x>0$ corresponding to the lines a, b, c of Fig. 1(b) which terminate at P_t.

Accordingly, in Fig. 2, the ends of the hyperbolae are labeled a, b, c according to the parts of the critical lines in Fig. 1 to which they correspond.

The complete topological correspondence between the sections of the surface in Fig. 2 and the critical lines of Fig. 1 is therefore clear. The points P, P_t, P' are a line forming a boundary of the surface of critical points, and the point P_t, which is the tricritical point, corresponds to a saddle point of the surface in the projective space of Fig. 2.

It may seem that a very special space has been chosen, and that the boundary has been made to go in a very special fashion—through the saddle point. However, this is merely in accordance with the following general physical requirements: (i) Only one point P occurs in each phase diagram; therefore the boundary *has* to pass from the lower left quadrant to the lower right quadrant without passing through the upper two quadrants; (ii) Critical lines only split or end at a point like P. Thus the point P *has* to pass through the origin where the section would otherwise necessarily give four lines of critical points intersecting.

This analysis of the critical points as a single surface provides another viewpoint from which to understand the fact that only two pairs of the three possible pairs of phases became critical in the presence of the third. The simplest viewpoint is that of the test tube itself. If the phases α, β, γ are ordered in increasing density, then (α, β) can be critical (same density) in the presence of γ, and $(\beta\gamma)$ can be critical in the presence of α, but $(\alpha\gamma)$ cannot be critical and of equal density without the phase β having a density equal to both. Thus the possibility $(\alpha\gamma)$ critical in the presence of β is eliminated. Widom[7] has related this fact to the geometric asymmetry of the solid figure containing three distinct phases α, β, γ at constant temperature less than the tricritical temperature.

In terms of the phase diagrams in spaces of truly intensive variables (Widom used densities, or extensive variables), the existence of two lines of critical end points instead of three has a very simple topological interpretation: the boundary of a single surface is locally divided into *two* separate parts by the removal of a single point. Thus the tricritical point P_t divides the boundary of the surface of critical points into two lines of critical end points but *cannot* divide it into three different lines of critical end points.

IV. SPECIAL DIRECTIONS

It was shown by Griffiths[8] that in his model there are four variables of scaling, each with different exponents at the special point. From a purely phenomenological point of view one can define four different directions at the special point P_t in the same spirit as Griffiths and Wheeler.[9] From Fig. 2 it may be seen that these directions are (i) the limiting "strong" direction for the surface of critical points, (ii) the limiting "weak" direction for the surface of critical points, (iii) the tangent to the line of critical end points at the tricritical point, and (iv) the limiting second direction parametrizing the surface of critical points. These correspond to the variables called a_1, a_2, a_4, and a_3, respectively, by Griffiths.[8]

V. TRANSLATION TO COMPOSITION VARIABLES

The variables over which the experimentalist has easy control are unfortunately not the intensive field variables like the chemical potentials, but only the densities. In these variables the phase diagrams have been discussed by Widom.[7] It has been pointed out by Griffiths[8] that the precise composition of the tricritical point P_t probably does not coincide with the composition of the regions of coexistence of three phases at temperatures smaller than the temperature at P_t.

Such behavior has probably been observed in the system carbon-dioxide-methanol-water because when a constant volume specimen (i.e., a sealed tube) of precisely the correct composition is increased in temperature, one does not observe the simultaneous disappearance of two menisci. Instead[12] one meniscus disappears critically and simultaneously a second appears critically. This remarkable behavior does not change any of our geometric conclusions, because it can be interpreted as follows: the constant volume, constant composition path does not follow the line of points where three phases coexist in Fig. 1(b), but rather it passes from one coexistence surface (γ, β) to another (α, β) directly through the point P_t.

VI. RELATIONSHIP TO OTHER COMPLEX SYSTEMS

In previous work[5,10] we have given several examples of complex magnetic systems and we have attempted to systematically classify all the coexistence and critical points in such systems. For points where several phases coexist without being critical this is relatively simple, since the appropriate quantities are the number of coexisting phases and the dimensionality of the space. These are related to the total number of thermodynamic intensive variables by the phase rule.[5]

For critical points, it can be argued that every phase that becomes critical after the first two implies the loss of an extra degree of freedom in addition to the one lost because of coexistence.[7] Hence if there is a system with n thermodynamic variables possessing a point where p phases are in coexistence, of which q are critical (altogether rather than in two separate groups q_1 and q_2, although the generalization to such cases is simple). The dimensionality of the space on which this occurs will be given by

$$d=n-(p-1)-m, \tag{1}$$

where $m=\max(q-1,0)$ since the case $q=1$ is not meaningful and $m=0$ if $q=0$. As a special case if all p of the phases are critical we obtain $d=n+2-2p$.

While this equation holds for fluids, it is violated by the original tricritical points, for which $n=p=3$, $d=0$ and also by certain magnetic models[10] which contain highly symmetric points where lines of tricritical points intersect, and $n=p=4$ and $d=0$. Before giving the equation which correctly describes both fluids and the complex magnetic systems let us contrast the two ways of classifying more complicated critical points that have been proposed.

For fluids Widom[7] has proposed that the important quantity is the number of phases becoming critical, and that this number should be used as the order of the critical points.

For complex magnetic systems we have proposed an apparently different scheme which is based on the original proposal for tricritical points[1] where three different lines of critical points intersected. Accordingly we gave examples of systems where different lines of tricritical points intersected, and gave the points of intersection an order different from (one larger than) that of tricritical points. Because of the symmetry of the various systems we investigated, there were no lines of critical end points, i.e., points where one or more phases coexist with others that are critical. Consequently the number of variables n needed to obtain a point where four phases are simultaneously critical was reduced from six to four.

For tricritical points in fluids, it is possible to artificially reduce the number of variables and eliminate the lines of critical end points from the phase diagram. For example, Fig. 1(b) is an illustration of this since it is a three-dimensional section of the four-dimensional field space with all lines of critical points ending at the tricritical point. Similarly the $h=0$ section of Fig. 2 produces the same result. Griffiths[8] has shown how a similar phase diagram can be obtained by taking the section $a_3=0$ of his four-dimensional phase diagram with variables a_1, a_2, a_3, a_4.

Let us now return to the case of the intersecting lines of tricritical points in the variable interaction metamagnet. It has been shown[10] that the point of intersection (the point of order 4) is a point where four phases become simultaneously critical. Thus in this case the definition of order suggested by us coincides with the definition suggested by Widom.[7] This fact may be generalized, because the only reason there should be more than one line of tricritical points is because there are more than three phases available. The different lines of tricritical points will intersect at points where more than three phases become simultaneously critical.

To obtain a version of Eq. (1) which is satisfied by all the cases considered so far, it is necessary to consider the number of variables which possess nonzero scaling power at the point under consideration. It is important to note that this number may be less than the number of significant directions picked out by the phase diagram. For example, on an ordinary line of critical points three directions are determined, but only two (the strong and weak) are associated with variables which scale. Alternatively, on the line of critical end points P, P_t, P', all four of the directions (i)–(iv) are defined but only (i) and (ii) are associated with variables which scale (except at P_t where all four enter the scaling equation). The implications of the simple Landau model[8] are that for fluids the number of scaling directions $s=2(q-1)$. Another quantity that is important is the number of phases which are in equilibrium but which are not critical, $x=p-q$. In terms of the variables s and x, Eq. (1) may be rewritten as[13]

$$s+x+d=n. \tag{2}$$

It will be seen that this equation also holds for the old tricritical points, and the intersection of lines of tricritical points. It is satisfied by construction from (1) by all the points in generalizations of Widom's scheme for which the order is given by $\Theta \equiv q = \frac{1}{2}s+1$ and by all the points in our scheme[5] for which the order is given by $\Theta = s$. These two possibilities express, respectively, the maximum and minimum number of scaling variables at a point where Θ phases became critical, $\Theta \leq s \leq 2(\Theta-1)$. For $\Theta=2$ there is only one possibility, $s=2$; for $\Theta=3$ there are two cases, $s=3,4$; and for $\Theta>3$ there are many possibilities.

Thus we have proposed[5] a minimal scheme for complex critical points whereas Widom and Griffiths have proposed a maximal scheme.

In conclusion it should be reiterated that while the definition of order for critical points suggested in Ref. 5 does not appear to be applicable to fluids, it is consistent with the definition in terms of the number of phases becoming critical.[7]

ACKNOWLEDGMENT

We would like to thank Professor B. Widom and Professor R. B. Griffiths for drawing our attention to the references cited in the Soviet literature in this manuscript and for stimulating conversations. Also thanks are due to R. B. G. for comments on a previous version of this paper.

---

*Supported in part by the U.S. Atomic Energy Commission, the National Science Foundation, the National Aeronautics and Space Administration, the Office of Naval Research, and the Air Force Office of Scientific Research.

†Lindemann Fellow.

‡Permanent address: Riddick Laboratories, North Carolina State University, Raleigh, N. C. 27607.

§Address to whom requests for reprints should be sent.

[1]R. B. Griffiths, Phys. Rev. Lett. 24, 715 (1970).

[2]V. A. Schmidt and S. A. Friedberg, Phys. Rev. B 1, 2250 (1970); F. Harbus and H. E. Stanley, Phys. Rev. Lett. 29, 58 (1972); Phys. Rev. B 8, 1141 (1973) and B 8, 1156 (1973).

[3]G. Goellner and H. Meyer, Phys. Rev. Lett. 26, 1543 (1971).

[4]C. W. Garland and B. B. Weiner, Phys. Rev. B 3, 1634 (1971).

[5](a) T. S. Chang, A. Hankey, and H. E. Stanley, Phys. Rev. B 8, 346 (1973); (b) A. Hankey, T. S. Chang, and H. E. Stanley, Phys. Rev. B 8, 1178 (1973). Preliminary accounts of this work are given by A. Hankey, T. S. Chang, and H. E. Stanley, AIP Conf. Proc. 10, 889 (1972).

[6]B. Widom and R. B. Griffiths, Phys. Rev. A 8, 2173 (1973).

[7]B. Widom, J. Phys. Chem. 77, 2196 (1973).

[8]R. B. Griffiths, Cornell University Material Science Center Report No. 1995 (unpublished).

[9]R. B. Griffiths and J. C. Wheeler, Phys. Rev. A 2, 1047 (1970).

[10]F. Harbus, A. Hankey, H. E. Stanley, and T. S. Chang, Phys. Rev. B 8, 2273 (1973).

[11]R. B. Griffiths (private communication).

[12]G. D. Efremova and A. V. Shvarts, Russ. J. of Phys. Chem. 43, 968 (1969).

[13]We are much indebted to J. Nicoll for discussions leading to this equation. A more complete account will be given in a separate paper.

75 - 04939
N75-15329

PHYSICAL REVIEW B VOLUME 8, NUMBER 1 1 JULY 1973

Generalized Scaling Hypothesis in Multicomponent Systems. I. Classification of Critical Points by Order and Scaling at Tricritical Points*

T. S. Chang,† Alex Hankey,‡ and H. Eugene Stanley§
Department of Physics, Massachusetts Institute of Technology, Cambridge, Massachusetts 02139
(Received 10 October 1972; revised manuscript received 29 January 1973)

The goal of this work is to provide an analysis of spaces of critical points for multicomponent systems. First, we propose the geometric concept of order $\mathcal{O}$ for critical points; we distinguish it from a previous definition of a "multicritical" point. Specifically, we may define the intersection of spaces of critical points of order $\mathcal{O}$ to be a space of critical points of order $(\mathcal{O}+1)$. Ordinary critical points are defined to be of order $\mathcal{O}=2$, so that the tricritical points introduced by Griffiths are of order $\mathcal{O}=3$. We discuss more general examples of critical spaces of order $\mathcal{O}=3$ which are known for a wide variety of systems; we also propose several examples of models of magnetic systems showing critical points of order $\mathcal{O}=4$—i.e., systems having *intersecting lines of tricritical points.* The analysis of critical and coexistence spaces also provides a new form of the Gibbs phase rule suitable for complex magnetic models. Next we define—for the critical points of order $\mathcal{O}$ of which examples have been given—special directions in terms of which to make a scaling hypothesis. We give the hypothesis for simple systems and then for tricritical points, and then, in a subsequent paper, part II, the special directions are used to make a scaling hypothesis at spaces of critical points of any order. Certain predictions (e.g., scaling laws and "single-power" scaling functions) follow in a simple and straightforward fashion. We consider the scaling hypothesis at a critical space of order $\mathcal{O}$ in terms of a group of transformations. We can define a set of invariants of the group. It is possible, for $\mathcal{O}\geq 3$, to make a *second* scaling hypothesis for the space of order $\mathcal{O}-1$ using certain of these invariants as *independent* variables. This is advantageous because certain "double-power" scaling functions then follow directly; these predict that for $\mathcal{O}=3$, experimental data collapse from a *volume* onto a *line*. This prediction is to be contrasted with ordinary scaling functions, which predict that data collapse by only a single dimension (e.g., from a volume onto a surface or from a surface onto a line).

I. INTRODUCTION: THE ORDER OF A CRITICAL POINT

The purpose of this work is (i) to propose the concept of the "order" of a critical point, (ii) to give examples of critical points of orders three and four, and (iii) to present a form of the scaling hypothesis for spaces of *arbitrary* order. The work is divided into two parts. In this paper (I), we focus upon concrete examples illustrating critical points and scaling at critical points of order three, while in a subsequent paper[1] (II), we consider scaling for spaces of arbitrary order. Firstly, we must develop the concept of the order of a critical point, and that is the task of this section.

The scaling hypothesis was originally formulated for the critical point of a simple magnet and a simple fluid.[2-4] These systems each have two purely intensive variables [(H, T) and (P, T), respectively]. Such variables we call *fields*, adopting the terminology of Griffiths and Wheeler.[5]

A very wide variety of physical systems whose critical phenomena are under active study have more than two field variables; two common examples are antiferromagnets and binary mixtures. In such systems, one can have lines (or, in general, spaces of dimension larger than one) of critical points. Recently, special attention has come to focus on those systems for which *three* lines of critical points intersect, and the point of intersection has been called a *tricritical point* by Griffiths.[6]

The scaling hypothesis has recently been extended[7] to treat some (but not all) aspects of this novel type of "critical point". In this work we present a comprehensive scaling treatment of general multicomponent systems. First we give a detailed treatment of tricritical points. Our approach is then generalized to more complex situations.

One example of a more complex situation is a system for which *four* lines of critical points intersect; in a natural extension of Griffiths's terminology, Nagle and Bonner[8] have called such points tetracritical points. We show here that, in the particular case studied by those authors, *the tetracritical point is qualitatively the same as a tricritical point* in the sense that the formulation of the scaling hypothesis there is the same as at tricritical points.

Qualitatively different points ("spaces")[9] can be achieved in systems with more than three field variables; a more general scaling hypothesis is needed and correspondingly more predictions are obtained. These are discussed in detail in Paper II.

Two simple examples of systems with more than three field variables are provided by He^3-He^4 and ammonium chloride, and both these systems show *lines* of tricritical points.

Liquid He^3-He^4 mixtures have thermodynamic variables $[P, T, \mu_4 - \mu_3, \eta]$, where P denotes pressure, T denotes temperature, μ_4 and μ_3 are the chemical potentials of He^4 and He^3, respectively, and η is a variable conjugate to the superfluid density. The "λ line" in the P-T plane becomes a two-dimensional surface of singularities with increasing mole fraction of He^3. This surface terminates at a line of special points,[10(a)] which is in fact a line of tricritical points.

Ammonium chloride possesses an order-disorder transition for which the transition temperature increases with increasing pressure, and changes from first order to second order at a tricritical point. If one replaces some of the hydrogen by deuterium in the ammonium group,[10(b)] then the position of the tricritical point (and the whole line of order-disorder transitions) changes. The variables are thus $(P, T, \mu_H - \mu_D, \eta)$, where η is a variable conjugate to the order parameter.

In a system of sufficient complexity, several lines of tricritical points can occur. A point of intersection of lines of tricritical points is qualitatively different from a point where lines of ordinary critical points intersect. This should be clear from the topology of the situation: At a line of tricritical points, surfaces of critical points meet, while at a point where lines of tricritical points intersect, several surfaces of critical points (bounded on each side by the tricritical lines) converge on the point.

To distinguish such points—and in general spaces of such points—we will refer to them as critical points of higher order, and we will associate a number with each order as follows. We define ordinary critical points to be of order $\mathcal{O} = 2$; then a critical point (or space of points) of order $\mathcal{O}+1$ ($\mathcal{O} \geq 2$) is defined to be a special point where lines (or spaces) of points of order $\mathcal{O}$ intersect. Thus a tricritical point is of order $\mathcal{O}=3$ and a point of intersection of lines of tricritical points is of order $\mathcal{O}=4$.

Griffiths and Wheeler[5] reasoned that the dimensionality of a space of ordinary critical points (of order $\mathcal{O}=2$) is $(n-2)$. In the systems we consider below the dimensionality, d, of a space of critical points of order $\mathcal{O}$ is always one less than the dimensionality of the spaces of critical points of order $(\mathcal{O}-1)$ which intersect at it. Therefore, we find the value of d for arbitrary $\mathcal{O}$ by induction from $\mathcal{O}=2$ to be, in these cases,

$$d = n - \mathcal{O}, \tag{1.1}$$

where n is the total number of field (and fieldlike)[11] variables available.

Critical points of complex thermodynamic systems can also be analyzed by making the scaling hypothesis from the outset. The significant quantity is then the number of relevant scaling variables. Using the renormalization group, it has been suggested[12] how more than two relevant scaling variables can occur, but the geometry of the phase diagram was not considered at all. In most of the examples known to the authors, the number of significant scaling directions is equal to the order. This may not always be true for more complex systems [e.g., fluid mixtures, for which Eq. (1.1) may need modification, becoming $d \leq n - \mathcal{O}$].

A specific example which demonstrates the importance of distinguishing the order of a critical point from the number of critical lines meeting there is the tetracritical point. This is a point of order $\mathcal{O}=3$ with true field variables (H, H_2, T), where H and H_2 are direct and staggered (i.e., wavelength 2 lattice sites) magnetic fields. When a fieldlike variable $\tilde{\mathcal{R}}$ (the ratio of short- to long-range-interaction strengths) is also included, (i.e., $n=4$), Eq. (1.1) indicates that the system has a line of critical points of order $\mathcal{O}=3$. This is verified in the analysis of Sec. III, where it is shown that in this model there are three surfaces of critical points of order $\mathcal{O}=2$, meeting at the line of points of order $\mathcal{O}=3$. The tetracritical point is simply a point on a smooth line of tricritical points; the "tetracritical point" arises because we have chosen a section of the four-dimensional $(H, H_2, T, \tilde{\mathcal{R}})$ space that is tangent to the line of tricritical points, rather than a section which intersects it.

First we give, in Sec. II, examples of systems exhibiting spaces of critical points of order $\mathcal{O} \geq 3$, and explain a convenient notation for the phase diagrams of such systems. This leads to an equation equivalent to the Gibbs phase rule.

In Sec. III we explicitly demonstrate the importance of distinguishing between the order of a critical point and the number of lines meeting at a critical point—the former leads to an essential increase in complexity, while the latter does not. To do this, we compare several one-dimensional Ising models with long-range interactions, all of which are exactly soluble.

Special directions at spaces of order $\mathcal{O}$ are defined in Sec. IV; these are analogous to the strong and weak directions defined by Griffiths and Wheeler.[5] A way of deriving these directions for tricritical points using the renormalization group approach has been pointed out by Riedel and Wegner.[12(c)]

To make the formulation of a scaling hypothesis easier to follow, we give an account in Sec. V of the scaling hypothesis using generalized homogeneous functions and equations invariant under a one-parameter continuous group of transformations at points of order 2.

In Sec. VI we give a full account of the scaling hypothesis at tricritical points and we include an account of a space of invariant variables as a very useful way to derive "double-power" scaling functions and to plot "crossover surfaces". These predictions have not yet been tested experimentally.

We present the scaling hypothesis at a critical point of arbitrary order in Paper II. The hypothesis is framed as a sequence of operations to be repeated as the hypothesis is formed successively at critical points of decreasing order. The proposed sequence is illustrated by detailed consideration of a system of Ising planes with a variable interplanar interaction.

II. SYSTEMS EXHIBITING CRITICAL POINTS OF ORDER HIGHER THAN TWO: NOTATION FOR SUCH POINTS

Critical points more complex than ordinary $\mathcal{O}=2$ critical points have been found in many experimental and theoretical systems. Without doubt, the systems exhibiting the richest possibilities are multicomponent fluid mixtures; however, specific examples of critical points of order three or more in these systems have yet to be found.

Systems on which experiments have been analyzed are liquid helium,[10(a)] ammonium chloride,[10(b)] metamagnets,[13] and anisotropic antiferromagnets.[14] In addition, one-dimensional magnetic models provide a rich opportunity for theoretical and numerical investigations. Liquid helium[10(a)] and NH_4Cl[10(b)] provide excellent examples where there exist lines of tricritical points—as discussed in Sec. I. In metamagnets,[13] lines of tricritical points can be generated by introducing transverse fields, and also by introducing a parameter into the Hamiltonian which changes the strength of the interaction. Decreasing the latter causes the tricritical points to converge to a point on the temperature axis; this point is a critical point of order 4 and is treated in more detail below.

An anisotropic antiferromagnet,[14] which exhibits a spin-flop transition, contains a point in its phase diagram where two lines of ordinary critical points intersect a line of first-order transitions. This special point has an order of at least 3, but whether it is 3 or more has yet to be determined.

To be able to discuss phenomena in phase diagrams of any complexity easily, we introduce a notation for spaces of points where several phases coexist and for critical points of arbitrary order $\mathcal{O}$. Critical spaces are denoted by an abbreviation of the notation CRS of Griffiths and Wheeler[5]; the order of the space will be given a preceding superscript and the dimensionality a subscript, and hence a critical space of order $\mathcal{O}$ and dimensionality d is written as ${}^{\mathcal{O}}R_d$. The relation between $\mathcal{O}$, d, and the total number n of field (or fieldlike) variables, in general, is given by Eq. (1.1), $\mathcal{O}=n-d$.

Coexistence spaces are designated by an abbreviation of the Griffiths-Wheeler notation CXS but now the number of coexisting phases is given by the preceding superscript; hence the general space of dimension d where p phases coexist is written as ${}^{p}X_d$. The equation analogous to Eq. (1.1) is

$$p=n-d+1\,. \tag{2.1}$$

The dimension d of the CXS may be interpreted as the number of "degrees of freedom", f, and for a chemical system n is one greater than the number of components c. Thus (2.1) is similar to the usual statement of the Gibbs phase rule, $p\geq c-f+2$, but it is in a form valid for all the systems considered in this work. The Gibbs phase rule contains an inequality because it refers to any phase diagram, even those in a restricted space of fields. For example, the ${}^{2}X_2$ in the H-T plane of a simple nearest-neighbor antiferromagnet (with field variables H, H_2, and T) satisfies Eq. (2.1) as an equality providing all three fields are considered, but as an inequality if only T and H are considered. Consideration of other models[8,15] leads us to conclude that Eq. (2.1) is satisfied as an equality (for $T>0$) if and only if a sufficient set of conjugate fields (i.e., conjugate to every possible phase of the system) has been introduced. Thus Eq. (2.1) can be used as a criterion for whether enough conjugate fields have been considered or not. It is noteworthy that Eqs. (1.1) and (2.1) depend only on topologically significant quantities like the dimension of a subspace in the phase diagram, and should therefore be understood as topological statements.

To illustrate the notation and to provide a good example of a system with a phase diagram exhibiting critical spaces of orders 2, 3, and 4, we consider the $d=3$ Ising model with variable interaction strength $\mathcal{R}J$ between planes of constant z:

$$\mathcal{H}=-\sum_{x,y,z} S_{x,y,z}\,[J(S_{x+1,y,z}+S_{x,y+1,z}) +\mathcal{R}JS_{x,y,z+1}+H+(-1)^{z}H_2\,]\,. \tag{2.2}$$

Here the symbol $S_{x,y,z}$ is the value of the spin on lattice site with coordinates (x, y, z). The variable $\mathcal{R}$ allows for a variation in the strength of interaction in the z direction. The phase diagram of this model is four dimensional, with fields H, H_2, T, and the fieldlike variable $\mathcal{R}$. For $\mathcal{R}>0$, we have a three-dimensional Ising model with "lattice anisotropy," which tends as $\mathcal{R}\to 0$ to the two-dimensional Ising model. The invariance of the Hamiltonian under the transformation $S_{x,y,z}\to(-1)^{z}S_{x,y,z}$, $\mathcal{R}\to-\mathcal{R}$, $H\to H_2$, and $H_2\to H$ relates the phase diagram for $\mathcal{R}<0$ to that for $\mathcal{R}>0$.

For $\mathcal{R}<0$, Eq. (2.2) describes a metamagnet. The phase diagram of this system is well known and shown in Fig. 1. As $|\mathcal{R}|$ is decreased, the values of T_t and T_N decrease (unpublished results

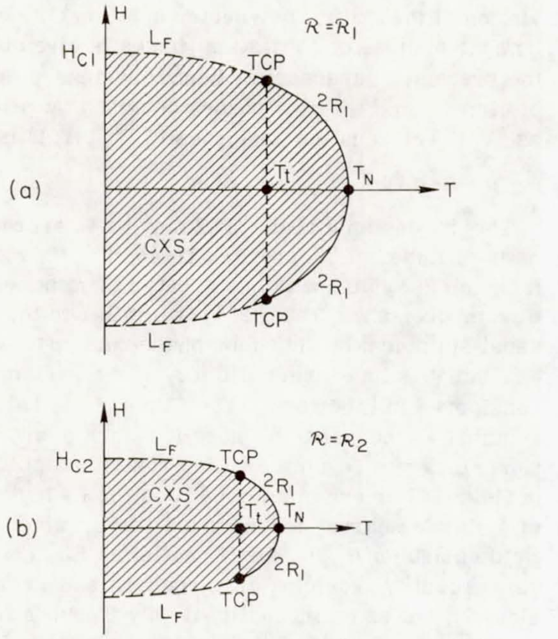

FIG. 1. (a) Phase diagram for $\mathcal{R}=\mathcal{R}_1<0$, in the (H, T) plane $(H'=0)$. The $^2R_1$ terminates at a pair of tricritical points ($^3R_0$) shown as TCP. The $^2X_2$ separating the antiferromagnetic phases A^+A^- is bounded below the tricritical temperature T_t by the lines of first-order transitions L_F, which terminate at a magnetic field value H_{C1}. (b) The same for $\mathcal{R}_2<0$, where $|\mathcal{R}_2|<|\mathcal{R}_1|$. Note that $H_{C2}<H_{C1}$ and that both T_t and T_N have decreased. See also, F. Harbus *et al.*, Ref. 1.

of F. Harbus). This is shown in the Fig. 1(b) as compared to Fig. 1(a).

As $|\mathcal{R}|\to 0$, the behavior of $T_N(\mathcal{R})$ is described by the well-known crossover exponent and symmetry between $\mathcal{R}<0$ and $\mathcal{R}>0$ mentioned above shows that in the plane $H=H_2=0$ there is a reflection symmetry about $\mathcal{R}=0$.

From these considerations we obtain Fig. 2, which is a three-dimensional phase diagram in the $H_2=0$ plane. For $\mathcal{R}<0$ and constant, there is a phase diagram like Fig. 1, and for $\mathcal{R}>0$ the ordinary crossover behavior holds.

The two tricritical points in Fig. 1 become lines of critical points of order 3, $^3R_1$, in Fig. 2. The symmetry of the Hamiltonian shows that there are two additional $^3R_1$ for $\mathcal{R}>0$ at nonzero H_2. The symmetry of the Hamiltonian forces these four lines (tricritical lines) to converge upon a point lying on the temperature axis—a critical point of order 4. On the temperature axis below the $^4R_0$ four phases are in coexistence: it is a $^4X_1$.

The validity of Eqs. (1.1) and (2.1) may be verified and it can also be seen that in this system a $^pX_{d+1}$ is bounded for increasing T by a $^{\mathcal{O}}R_d$, where $\mathcal{O}=p$. A CXS which in the full phase diagram is a $^pX_{d+1}$ is, when considered in the zero-temperature plane, only a ^pX_d. In the model considered in this section, therefore, a coexistence hypersurface which in the $T=0$ phase diagram is a ^pX_d evolves as the temperature increases into an $^{\mathcal{O}}R_d$, with $\mathcal{O}=p$. In other words, the space of critical points of order $\mathcal{O}$ is the upper bound (as temperature increases) of a space of points where $\mathcal{O}$ phases coexist.

This is a very significant point and can be understood by examples, and from the following consideration. In a phase diagram, a space where three phases coexist is necessarily a place of intersection of spaces where two phases coexist. The spaces where two phases coexist are bounded from above by spaces of critical points of order two. Therefore, the upper bound of the space where three phases coexist is either the boundary of one critical space of order 2 or the intersection of all three critical spaces of order 2. Because of the symmetry properties holding in the present model, and

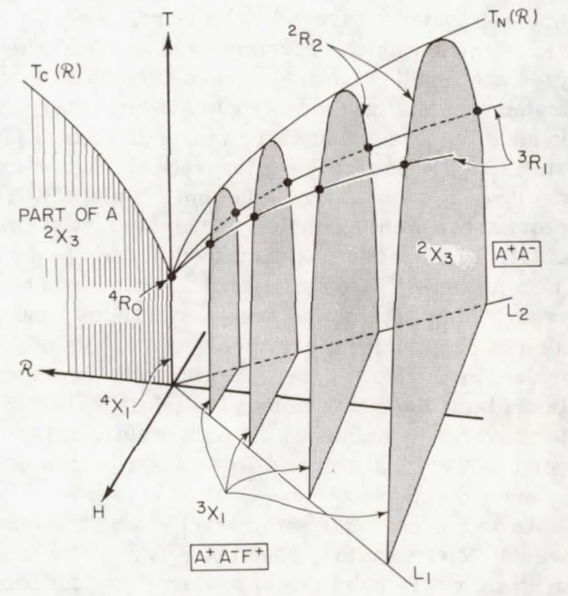

FIG. 2. Phase diagram in the $H_2=0$ hyperplane for Ising model with variable interplanar interaction. For $\mathcal{R}<0$ the $\mathcal{R}=$const sections are similar to Fig. 1. These sections are schematically shaded. As $\mathcal{R}$ varies continuously the ^pX_d and $^{\mathcal{O}}R_d$ of Fig. 1 become $^pX_{d+1}$ and $^{\mathcal{O}}R_{d+1}$. Thus the $^2X_2$ of Fig. 1 becomes the interior of the "mountain"; this is a $^2X_3$ separating phases A^+, A^-. The lines L_F where three phases coexist become surfaces of the mountain ($^3X_2$) below the line of tricritical points $^3R_1$ corresponding to TCP of Fig. 1. The $^2R_1$ of Fig. 1 becomes a $^2R_2$, the top of the "mountain" in Fig. 2. The T axis becomes a line of special points where all four phases A^+, A^- and the ferromagnetic F^+ and F^- all coexist; it is a $^4X_0$. The $^3R_1$ meet at the T axis at the end of this line; at a $^4R_0$. The region $\mathcal{R}>0$ appears simpler because it corresponds to the $(H=0)$ section of $\mathcal{R}<0$, and the rest of the mountain occurs at $H_2\neq 0$. See also, F. Harbus *et al.*, Ref. 1.

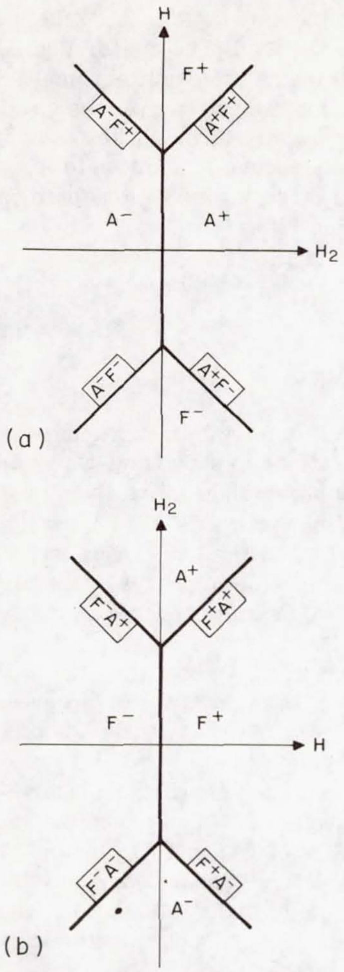

FIG. 3. The phase diagram at $T=0$ of an Ising (a) antiferromagnet and (b) ferromagnet. The phases with spins parallel are indicated by $F^{\pm}$ and with spins antiparallel by $A^{\pm}$. The lines indicate where the various phases are in equilibrium.

also because it is an Ising model, the latter condition holds. An entirely analogous argument can be constructed for critical points of order 4 or more.

It is therefore possible, for Ising models, to make predictions about the relationships between ${}^{\Theta}R_d$ in the full phase diagram, by considering the relationships between the ${}^{p}X_d$ in the $T=0$ phase diagram. We will make extensive use of this method in Sec. III.

III. SPACES OF TRICRITICAL POINTS IN ONE-DIMENSIONAL MODELS

There has been much work recently on one-dimensional Ising models possessing a long-range interaction.[8,15] The effect of this interaction is to shift the critical temperature from the value $T=0$ to a nonzero temperature, thereby enabling the critical points to obey scaling laws.

The purpose of this section is to display two models for which critical points of order $\Theta=4$ occur; these are both Ising models with long-range interactions.[16]

Models exhibiting a critical point of order 4 also possess a line of points where four phases coexist, as explained at the end of Sec. II. Therefore, a simple method of deciding whether a particular model can possess a critical point of order 4 is to analyze the $T=0$ hyperplane of the phase diagram and see if points where four phases coexist continue to have four distinct phases in equilibrium as T is increased. Cases where this does and does not happen are discussed below.

Before analyzing a case where there is a long-range interaction, let us consider the $T=0$ phase diagram of a one-dimensional Ising antiferromagnet with only nearest-neighbor interactions.

Hamiltonians

The Hamiltonian is given by

$$\mathcal{H}_{\mathrm{SR}} = -J_{\mathrm{SR}} \sum_{i=1}^{N-1} s_i s_{i+1} - H \sum_{i=1}^{N} s_i - H_2 \sum_{i=1}^{N} (-)^{i+1} s_i , \tag{3.1}$$

where J_{SR} is the nearest-neighbor (nn) interaction strength and $s_i=\pm 1$ are the Ising spins situated at site i of the chain. When $J_{\mathrm{SR}}>0$ the interaction is ferromagnetic and when $J_{\mathrm{SR}}<0$ the interaction is antiferromagnetic. H is the magnetic field and H_2 is the staggered magnetic field of wavelength 2 lattice sites. The phase diagram will appear as in Fig. 3(a). Here the four phases $F^{\pm}$, $A^{\pm}$ are defined in Table I: F means ferromagnetic and A means antiferromagnetic. The $T=0$ "critical point" of the

TABLE I. Definitions, energies, and equations of Figs. 3 and 5. Here $\tilde{\mathfrak{R}} \equiv J_{\mathrm{SR}}/J_{\mathrm{LR}}$; $h \equiv H/J_{\mathrm{LR}}$; $h_2 \equiv H_2/J_{\mathrm{LR}}$. Star means not shown in Fig. 5.

Configuration	Name	Field	Energy
↑ ↑	F^+	H	$E_F=-J_{\mathrm{LR}}-J_{\mathrm{SR}}-H$
↓ ↓	F^-		
↑ ↓	A^+	H_2	$E_2=+J_{\mathrm{SR}}-H_2$
↓ ↑	A^-		

Surface	Equation	Line	Equation
$[F^+,F^-]$	$H=0$	L_1	$h_2=1+2\tilde{\mathfrak{R}}$; $h=0$
			$\tilde{\mathfrak{R}}>-\frac{1}{2}$
$[A^+,A^-]$	$H_2=0$	L_2	$h_2=1-2\tilde{\mathfrak{R}}$; $h=0$
$[F^+,A^+]^*$	$h-h_2+1+2\tilde{\mathfrak{R}}=0$	L_3	$h=-1-2\tilde{\mathfrak{R}}$; $h_2=0$
			$\tilde{\mathfrak{R}}<-\frac{1}{2}$
$[F^-,A^-]^*$	$h-h_2-1+2\tilde{\mathfrak{R}}=0$	L_4	$h=-1+2\tilde{\mathfrak{R}}$; $h_2=0$
$[F^+,A^-]^*$	$h+h_2+1+2\tilde{\mathfrak{R}}=0$		
$[F^-,A^+]^*$	$h+h_2-1-2\tilde{\mathfrak{R}}=0$		

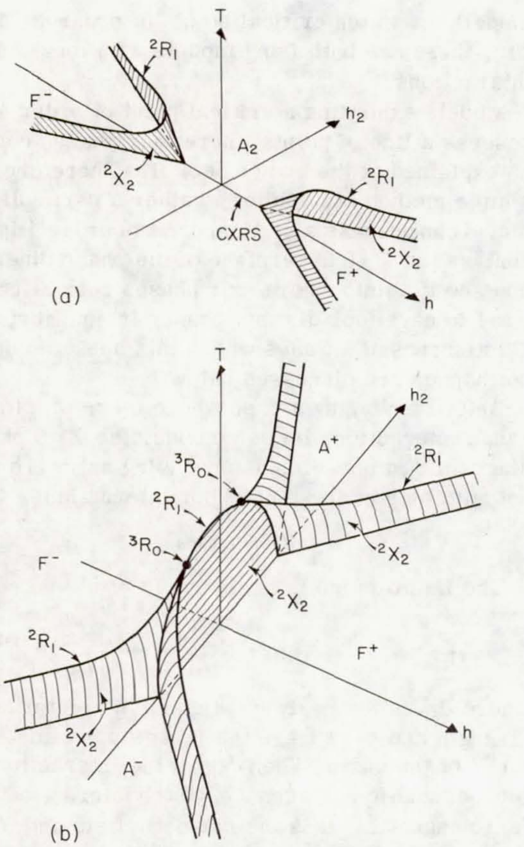

FIG. 4. (a) The extension of Fig. 3(a) into the space with $T>0$ when a weak long-range interaction is included. Note that the $T=0$ plane corresponds to Fig. 3(a), and that the $[A^+, A^-]$ phase boundary only separates phases at $T=0$. The other lines in Fig. 3(a) develop normally, giving coexistence surfaces ($^2X_2$) ending in critical lines $^2R_1$. (b) The phase diagram of the same model but without the antiferromagnetic interaction ($J_{SR}=0$ or $J_{SR}>0$). Now all lines in the $T=0$ plane become coexistence surfaces $^2X_2$. The points of interaction become $^3X_1$ (lines where three phases coexist) and there terminate at two $^3R_0$ (tricritical points).

Ising antiferromagnet becomes a *line* of critical points for nonzero values of magnetic field. This line bifurcates at points where it is energetically more favorable[17] for the system to order ferromagnetically (i.e., with all spins parallel).

Normal scaling laws do not apply to one-dimensional Ising models with short-range interactions, as these display essential singularities at the $T=0$ critical point. Thus the lines in Fig. 3(a) are lines of both critical points and coexistence points. These lines do not have very much in common with either the conventional critical points ^2R_d or the conventional coexistence surfaces ^pX_d that divide up the field space at finite values of temperature. A suitable nomenclature for the lines of Fig. 3(a) might be "coexistence-critical surfaces" and we will denote them by CXRS. A CXRS is necessarily confined to the $T=0$ plane as for Fig. 3(a). Thus we see that the nn Ising antiferromagnet contains five CXRS lines where two phases coexist and two CXRS points where three phases coexist.

Then we introduce in addition to $\mathcal{H}_{SR}$ of Eq. (3.1), a long-range interaction, defined by the Hamiltonian

$$\mathcal{H}_{LR} = -\sum_{i=1}^{N}\sum_{r} J(r) s_i s_{i+r}, \tag{3.2a}$$

where

$$J(r) = \lim_{\gamma\to 0} a\gamma e^{-\gamma|r|}, \tag{3.2b}$$

the phases $F^\pm$ are stabilized at nonzero temperature and continue to show long-range order for $T>0$. The phase diagram is given in Fig. 4(a). The CXRS [on the H axis of Fig. 3(a)] is not stabilized at $T>0$ by the long-range interaction; the two antiferromagnetic phases $A^\pm$ coexisting at the CXRS at $T=0$, simply become a single disordered phase for $T>0$.

There are two $^2X_2$ separating the ordered (ferromagnetic) phase from the disordered phase at higher temperatures. These $^2X_2$ end in $^2R_1$ (lines of critical points).

If the dominating nearest-neighbor interactions are ferromagnetic, $J_{SR}>0$, then the situation depicted in Figs. 3(b) and 4(b) results. The two points where three phases coexist at $T=0$ become the end points of two $^3X_1$ lines where three phases coexist. Each $^3X_1$ line terminates at a $^3R_0$ (a tricritical point).

If sufficient care is taken to decide whether a space in the $T=0$ hyperplane is a CXRS or a CXS, then the nature of the extension of the space and its subspaces into $T>0$ can be easily ascertained. The rules exemplified from Figs. 3 and 4 are the following: (i) Two phases which can only be distinguished by a staggered magnetic field coexist on a CXRS. (ii) Such staggered phases give only one phase for $T>0$. (iii) A line where one phase which maintains order for $T>0$ coexists with any other phase is *always* a CXS. (iv) A point where a CXRS meets a CXS has no special properties. It is simply a point on a CXS.

Using these rules we can analyze the model of Nagle and Bonner[8] which includes a long-range interaction, a variable short-range interaction, and the two fields of Fig. 3.[18] A point where four critical lines meet, a tetracritical point, is known for this model. We will show here that this point is a critical point of order 3. Since a variant of this model, which we discuss below, shows a critical point of order 4, it is worth treating the Nagle-Bonner model in some detail first.

Figure 5 depicts the surfaces of coexistence of the four phases in the $T=0$ plane. Definitions and

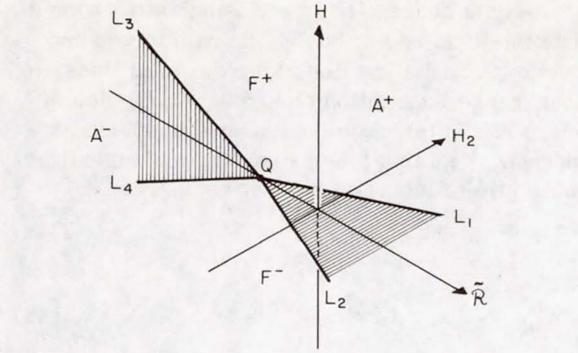

FIG. 5. $T=0$ hyperplane for an Ising model with competing long- and short-range interactions. Here $\tilde{\mathfrak{R}} \equiv J_{SR}/J_{LR}$ and H_2 is a staggered magnetic field of wavelength 2 lattice sites. The lines L_1, L_2 are in the $(H_2, \tilde{\mathfrak{R}})$ plane, and the lines L_3, L_4 are in the $(H, \tilde{\mathfrak{R}})$ plane. The surfaces $[A^-F^+]$, $[A^+F^-]$, $[F^+,A^+]$, $[F^-,A^-]$ have been omitted. The surface $[A^+,A^-]$ is a CXRS, Fig. 3(a) is an (H_2, H) plane for $\tilde{\mathfrak{R}}<\tilde{\mathfrak{R}}_Q$, while Fig. 3(b) is for $\tilde{\mathfrak{R}}>\tilde{\mathfrak{R}}_Q$.

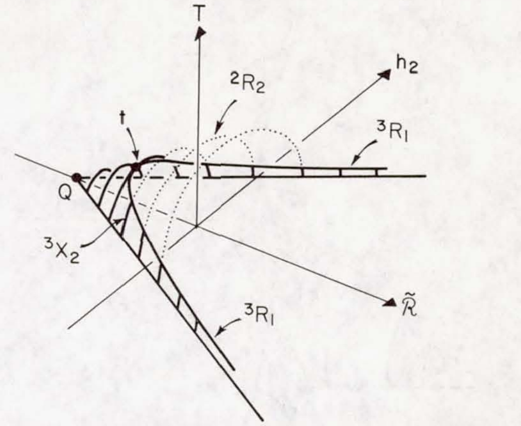

FIG. 6. $H=0$ hyperplane of the model of Fig. 5. The lines L_1, L_2 extend into $T>0$. The lines where three phases coexist in Fig. 4(b) have become a single surface, denoted here by $^3X_2$. This terminates at a *line* of tricritical points $^3R_1$; the $^3R_1$ also bounds a surface of ordinary critical points $^2R_2$. The point t where the $^3R_1$ intersects the plane $h_2=0$ is the location of the tetracritical point (Ref. 8). The $\tilde{\mathfrak{R}}=0$ section of this figure corresponds to the $H=0$ section of Fig. 4(b). Note that at t a surface $\tilde{\mathfrak{R}}=\text{const}$ is parallel to the $^3R_1$.

equations are given in Table I. For clarity four surfaces are omitted; e.g., those that separate the phases $[F^+A^+]$, $[F^-A^-]$, $[F^+A^-]$, and $[F^-A^+]$. As may be seen there are four lines where three phases coexist and a point Q where all four phases coexist. The surface $[A^+A^-]$ bounded by the lines L_3, L_4, is a CXRS since for constant values of $\tilde{\mathfrak{R}}$ less than x_Q, the phase diagrams are the same as Figs. 3(a) and 4(a). Here

$$\tilde{\mathfrak{R}} \equiv J_{SR}/J_{LR}\,, \tag{3.3}$$

where J_{LR} is the "equivalent neighbor" long-range parameter.[8]

For $T \neq 0$, the two $^2X_2$ surfaces $[A^+F^+]$ and $[A^-F^-]$ of Fig. 5 end in a single surface of critical points, and the same is true for the $[A^-F^+]$, $[A^+F^-]$ surfaces; this is shown in Fig. 4(a).

The point Q of Fig. 5, where four phases coexist,

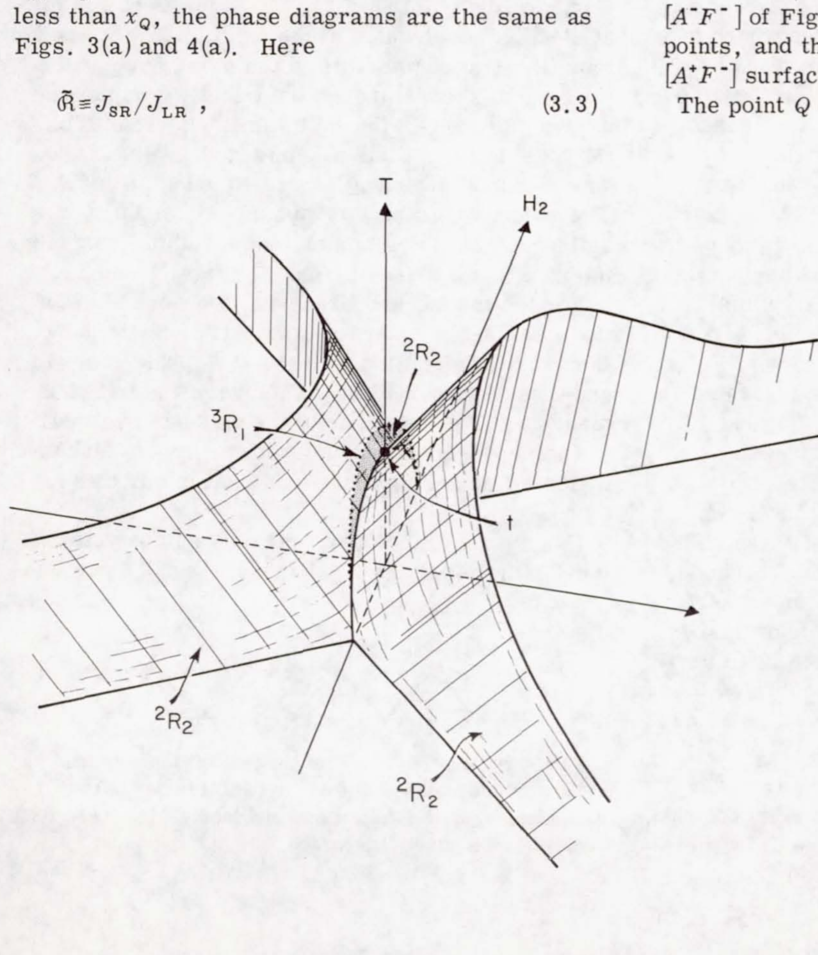

FIG. 7. Ray projection of the four-dimensional space, from Q onto $\tilde{\mathfrak{R}}=0$ showing the topology of the surfaces of critical points. The $\tilde{\mathfrak{R}}$ axis in Figs. 5 and 6 has become a combination of $\tilde{\mathfrak{R}}$ and h. The curved $^2R_2$ surfaces are the ends of those surfaces which end on L_3 and L_4 of Fig. 5. The $^2R_1$ of Figs. 4(a) and 4(b) are lines in this surface. The flat $^2R_2$ shown in the (T, H_2) plane is the surface $^2R_2$ of Fig. 6.

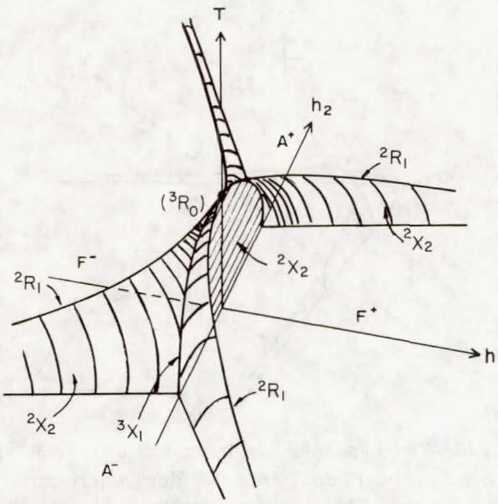

FIG. 8. Plot of the $^2X_2$ and the four lines of critical points meeting at the tetracritical point t. The value of the interaction strength ratio $\tilde{\mathcal{R}} \equiv J_{SR}/J_{LR}$ is equal to its appropriate value $\tilde{\mathcal{R}}_c = 0$.

is seen (Fig. 6) to be only a special point on a $^3X_2$ and Q does *not* give rise to a $^4X_1$ on increasing the temperature. To see this (in the full phase diagram) it is necessary to consider Figs. 4(b) and 5–7. First, in Fig. 4(b), the phase diagram of the system is shown at constant $\tilde{\mathcal{R}} > 0$. The relationship of this figure to Fig. 5 can be understood by looking at the $T = 0$ plane of Fig. 4(b). The lines where two phases coexist are lines on the appropriate surfaces of Fig. 5, and points where lines in the $T = 0$ plane of Fig. 4(b) meet are points on the lines L_1, L_2. Therefore Fig. 4(b) shows that the lines L_1, L_2 do give rise to coexistence surfaces and are lines on $^3X_2$, as shown in Fig. 6. The line of points where three phases coexist ($^3X_1$) in Fig. 5 has become a surface ($^3X_2$) in Fig. 6, and this surface is terminated by a single line of tricritical points, $^3R_1$. Figure 6 shows that the point Q is just a point on a $^3X_2$, and does not generate a $^4X_1$.

The three surfaces of critical points generated by the lines of critical points in Figs. 4(a) and 4(b) are shown schematically in Fig. 7. It can be seen that the two $^3R_0$ (tricritical points) of Fig. 4(b) form a continuous line (a $^3R_1$) bounding three $^2R_2$ (surfaces of critical points). The point t was called a tetracritical point by Nagle and Bonner[8] because, for $\tilde{\mathcal{R}} = \tilde{\mathcal{R}}_c$, *four* lines of critical points meet there (see Fig. 8). However, Figs. 6 and 7 show that t is an indistinguishable point on a smooth line of tricritical points of order 3; this is corroborated by the fact[8] that the exponents at t are the same as at the other tricritical points.

To produce a model where the point Q is stable at higher temperatures demands only a slight change in the structure of the interactions. We draw the linear-chain nearest-neighbor Ising antiferromagnet in the form shown in Fig. 9, with the nn antiferromagnetic interaction along the solid lines, and a long-range interaction along each of the dotted lines. The latter stabilizes each sublattice independently, enabling the system to adopt an antiferromagnetic ordering at nonzero temperature:

$$\mathcal{H}_i = \mathcal{H}_{SR} + \mathcal{H}^0_{LR} + \mathcal{H}^E_{LR}, \tag{3.4a}$$

where

$$\mathcal{H}^{0,E}_{LR} = -\sum_i \sum_r J(2r) s_i s_{i+2r}. \tag{3.4b}$$

Here odd-numbered spins are on the top lattice of Fig. 9 and $\mathcal{H}^0$ has all i odd. Even numbered spins are on the lower lattice and $\mathcal{H}^E$ has all i even; $J(2r)$ is defined by Eq. (3.2b). The point Q is now at the origin and stable for $T > 0$, and we are able to have four $^3X_2$; these are generated by the lines L_1, L_2, L_3, L_4 (of Fig. 5) meeting at the $^4X_1$, generated by Q. The $^3X_2$ should end in a $^3R_1$ (as in Fig. 6) but unlike the system of Fig. 6, the $^3R_1$ all terminate at a $^4R_0$.

This Hamiltonian has an important discrete symmetry which will necessarily be reflected by the phase diagram of the solution of the model. It is given by the operation $s_i \to (-)^i s_i$, $H \to H_2$, $H_2 \to H$, $J_{SR} \to -J_{SR}$. Therefore,

$$G(H, H_2, T; +J_{SR}) = G(H_2, H, T; -J_{SR}).$$

Further, the point Q in Fig. 5 (which is now stable at $T > 0$) is now located at the origin. There are now four $^3R_1$; two of which lie in the $H_2 = 0$ hyperplane for $\tilde{\mathcal{R}} < 0$ and these are symmetrically complemented by two more $^3R_1$ in the $H = 0$ for $\tilde{\mathcal{R}} > 0$. These four $^3R_1$ meet at the T-axis at some finite value of T. This point at which all four $^3R_1$ meet is a $^4R_0$. The phase diagram for this model is the same as that for the Ising model with variable interplanar interaction discussed in Sec. II (Figs. 1 and 2).

For the model just discussed, we were able to make use of the extensive analysis of Nagle and Bonner in conjunction with the $T = 0$ phase diagram, and thus we deduced the structure of the full phase diagram. The existence of the discrete symmetry and the consequent analogy with the model discussed in Sec. II makes us more confident in our conclusions.

For the next model, we use only an analysis of the $T = 0$ phase diagram and we make the extrapola-

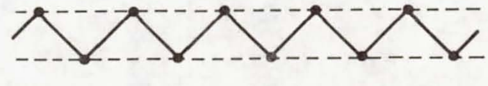

FIG. 9. Modified one-dimensional lattice exhibiting a critical point of order $\mathcal{O} = 4$. The solid lines represent antiferromagnetic interactions and the dashed lines, long-range (ferromagnetic) interactions.

TABLE II. Definitions of spin orderings of phases and fields for an Ising model with two staggered fields.

Spin configuration				Name	Conjugate field
↑	↑	↑	↑	F^+	H
↓	↓	↓	↓	F^-	
↑	↓	↑	↓	A_2^+	H_2
↓	↑	↓	↑	A_2^-	
↑	↑	↓	↓	A_4^+	H_4
↓	↓	↑	↑	A_4^-	
↑	↑	↑	↓	M_a^+	$\frac{1}{2}[H_2+H_4 \pm H]$
↑	↓	↓	↓	M_a^-	
↑	↑	↓	↑	M_b^+	$\frac{1}{2}[-H_2+H_4 \pm H]$
↓	↑	↓	↓	M_b^-	
↑	↓	↑	↑	M_c^+	$\frac{1}{2}[H_2-H_4 \pm H]$
↓	↓	↑	↓	M_c^-	
↓	↑	↑	↑	M_d^+	$\frac{1}{2}[-H_2-H_4 \pm H]$
↓	↓	↓	↑	M_d^-	

tions explained at the end of Sec. II. Our knowledge of the extensive occurrence of tricritical points in certain Ising models gives us a reasonable basis from which to predict the existence of a critical point of order 4.

This second model for which an exact solution is fairly readily obtainable[16] is a model with a second staggered magnetic field. It turns out that the analysis for an exact solution is simplest if the staggered field, "H_4," is of wavelength four lattice sites.[19] The Hamiltonian will therefore be given by

$$\mathcal{H}=\mathcal{H}_{\mathrm{SR}}+\mathcal{H}_{\mathrm{LR}}-H_4 \sum_{i=1}^{N} u_i s_i \,, \tag{3.5}$$

where the number $u_i=+1$ for $i=4n+1$, $4n+2$ and $u_i=-1$ for $i=4n-1$, $4n$. We define the names of the various phases in Table II and also the phase of H_4 relative to H_2. We give the energies of the phases at $T=0$ in Table III. The phase adopted at $T=0$ is that of lowest energy, and so the problem of finding the phase diagram at $T=0$ is simple. The phases coexist at points where the energies of two different phases are equal, and the most important equalities are given in Table IV(a).

An extended analysis[16] shows that the significant values of $\tilde{\mathcal{R}}$ are -1, $-\frac{1}{2}$, and 0, and a sequence of phase diagrams can be drawn in the space of variables H, H_2, H_4 for values of $\tilde{\mathcal{R}}$ greater than, equal to, and less than these numbers. A representative

TABLE III. Energies of various phases at $T=0$ for an Ising model with two staggered fields. Here the long-range energy is given by J_{LR} and the nearest neighbor by J_{SR}. Only the phase + is shown; to get the value of E_{X^-}, reverse the sign of the conjugate field.

Phase	Energy per spin
F^+	$E_F=-J_{\mathrm{LR}}-J_{\mathrm{SR}}-H$
A_2^+	$E_2=+J_{\mathrm{SR}}-H_2$
A_4^+	$E_4=-H_4$
M_a^+	$E_a=-\frac{1}{2}J_{\mathrm{LR}}-\frac{1}{2}[+H_2+H_4+H]$
M_b^+	$E_b=-\frac{1}{2}J_{\mathrm{LR}}-\frac{1}{2}[-H_2+H_4+H]$
M_c^+	$E_c=-\frac{1}{2}J_{\mathrm{LR}}-\frac{1}{2}[+H_2-H_4+H]$
M_d^+	$E_d=-\frac{1}{2}J_{\mathrm{LR}}-\frac{1}{2}[-H_2-H_4+H]$

TABLE IV. (a) Equations of planes and lines in Fig. 10 for an Ising model with two staggered fields. Here we have divided all energies through by J_{LR} and defined $h_i=H_i/J_{\mathrm{LR}}$, $\tilde{\mathcal{R}}\equiv J_{\mathrm{SR}}/J_{\mathrm{LR}}$. In Fig. 10, $\tilde{\mathcal{R}}$ is positive, e.g., $\frac{1}{2}$ or ∞. Star means that the plane was omitted from Fig. 10. Double star indicates that this is only a line: (b) Equations of lines in Fig. 10.

(a)

Phase boundary	Equation	Region
$[F^+,F^-]$	$h=0$	
$[M_a^+,M_a^-]$	$h=0$	
$[F^+,M_a^+]^*$	$h_2+h_4-1-2\tilde{\mathcal{R}}=h$	$h, h_2, h_4>0$
$[F^+,M_b^+]^*$	$h_2-h_4+1+2\tilde{\mathcal{R}}=-h$	$h, h_4>0,\ h_2<0$
$[F^+,A_4^+]$	$h_4-1-\tilde{\mathcal{R}}=h$	$h_4>0,\ h>0$
$[A_4^+,M_a^+]$	$h_4-h_2-1=h$	$h, h_4>0,\ h_2>0$
$[A_4^+,M_b^+]$	$h_4+h_2-1=h$	$h, h_4>0,\ h_2<0$
$[F^+,A_2^+]^{**}$	$h_2-1-2\tilde{\mathcal{R}}=h$	$h, h_2>0;\ h_4=0$
$[A_2^+,M_a^+]$	$h_2-h_4-1-2\tilde{\mathcal{R}}=h$	$h, h_2, h_4>0$

(b)

Line	Intersection	Equation
$[4: F^+F^-M_a^+M_a^-]$	$[F^+,F^-]\,[M_a^+,M_a^-]$	$h_2+h_4=1+2\tilde{\mathcal{R}}$
	$[F^+,M_a^+],\ [F^-,M_a^-]$	$h=0$
$[3: F^+F^-A_4^+]$	$[F^+,F^-]\,[F^+,A_4^+]$	$h_4=1+\tilde{\mathcal{R}}$
	$[F^-,A_4^+]^*$	$h=0$
$[3: F^+M_a^+A_4^+]$	$[F^+,A_4^+]\,[A_4^+,M_a^+]$	$h_4-h=1+\tilde{\mathcal{R}}$
	$[F^+,M_a^+]^*$	$h_2=\tilde{\mathcal{R}}$
$[3: F^+M_b^+A_4^+]$	$[F^+A_4^+]\,[A_4^+,M_b^+]$	$h_4-h=1+\tilde{\mathcal{R}}$
	$[F^+,M_b^+]^*$	$h_2=-\tilde{\mathcal{R}}$
$[4: F^+M_a^+M_c^+A_2^+]$	$[F^+,M_a^+]^*[F^+M_c^+]^*$	$h_2-h=1+2\tilde{\mathcal{R}}$
	$[M_a^+,A_2^+]\,[M_c^+,A_2^+]$	$h_4=0$
$[3: M_a^+, M_a^-, A_4^+]$	$[M_a^+,M_a^-]\,[M_a^+,A_4^+]$	$h_4-h_2=1$
	$[M_a^-,A_4^+]^*$	$h=0$
$[3: M_a^+, M_a^-, A_2^+]$	$[M_a^+,M_a^-],\ [M_a^+,A_2^+]$	$h_2-h_4=1+2\tilde{\mathcal{R}}$
	$[M_a^+,A_2^-]$	$h=0$

diagram is shown in Fig. 10 for which the equations of the lines are given in Table IV(b). Some of the surfaces and lines of Fig. 10 are labeled and the reader can discover the labels for the rest by reference to Tables IV(a) and IV(b).

There are several important points about this model: firstly, the "mixed" phases $M_a^{\pm}$ are distinguished at $T=0$ as $M_a^{+}\cdots M_d^{+}$ but above absolute zero there are only phases M^{+} and M^{-}. The phases $M^{\pm}$ are stable for $T>0$ because they contain a long-range contribution to their energy; thus all the lines and surfaces on Fig. 10 will survive at $T>0$ because they separate phases stabilized by the long-range interaction from phases ($A_2^{\pm}$, $A_4^{\pm}$) stable only at $T=0$.

There are several points where many phases coexist. In particular, at the point P_2 the phases $F^{\pm}$, $M_a^{\pm}$, and A_4^{+} coexist. The lines where three or more phases coexist which meet at P_2 are all stable at $T>0$ and so should end in tricritical points. Thus P_2 will give rise to a line of points where five phases coexist; this line ends at a critical point of order 4. Other points in Fig. 10 (viz., P_1) are much more complex in structure and will not be discussed here. The object of introducing the model given by Eq. (3.5) was to show a critical point of order four and this, at least, we have done.

In this section we have shown that it is reasonably easy to find model systems which are soluble and which show critical points of order 4 or more. The analysis of the two models suggested was omitted for the sake of brevity, and will be given in future work.[16]

IV. SPECIAL DIRECTIONS AT CRITICAL SPACES OF ORDER Θ: A SET OF "CANONICAL DIRECTIONS"

In order to properly formulate the scaling hypothesis for multicomponent systems, it is important to choose the proper independent variables. It is this problem that is treated in the present section. We shall argue that the considerations that Griffiths and Wheeler[5] applied to their discussion of second-order critical spaces (${}^2R_d$) can be extended to spaces of higher order in a natural and straightforward fashion.

A ${}^2X_d$ is, by definition, a hypersurface where two phases coexist; it necessarily divides the total space of n field variables locally into two regions and is therefore of dimension $d=n-1$, where n is the total number of truly intensive or "field" variables.[5] A ${}^2R_d$ (a simple second-order critical space) is the boundary of a ${}^2X_{n-1}$ and is therefore of dimension $d=n-2$.

At a ${}^2R_{n-2}$ there are $n-2$ directions parametrizing the critical space. The two remaining directions are of significance for the generalized scaling hypothesis. Directions not locally parallel to the ${}^2X_{n-1}$ (coexistence surface) we call strong directions, and directions locally parallel to the ${}^2X_{n-1}$ but not in the ${}^2R_{n-2}$ we call weak directions. The strong and weak directions will be called directions of type 1 and 2, respectively; this terminology is useful in Sec. VI and in Paper II, where the appropriate generalization to critical spaces of order larger than 2 is made. Examples are given in Figs. 11 and 12.

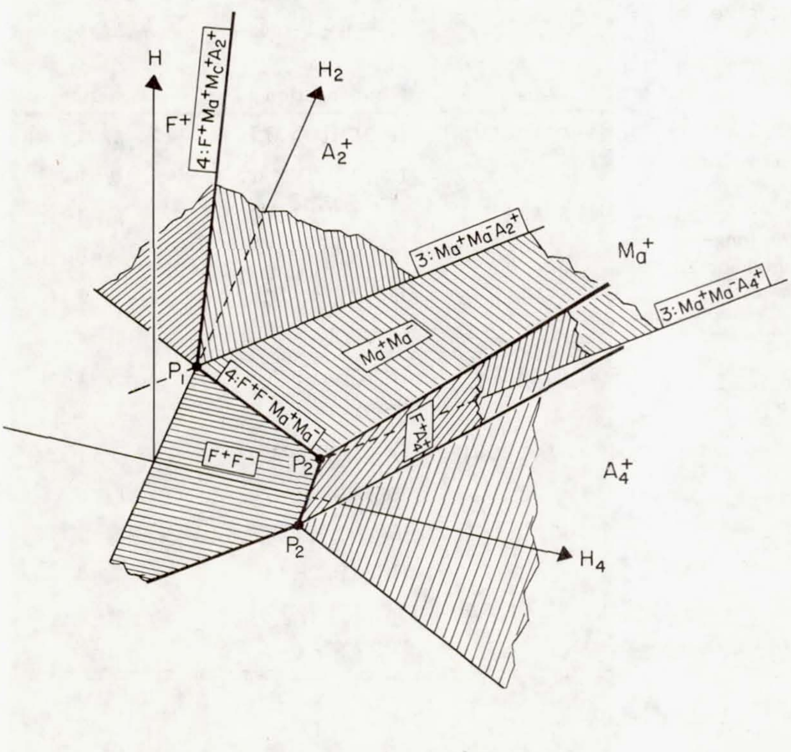

FIG. 10. Coexistence surfaces in the $T=0$ phase for a system with a long-range interaction, a nn interaction, magnetic field h, and staggered magnetic fields h_2, h_4 of wavelengths 2 and 4. Here the short-range interaction is also ferromagnetic. The surfaces are labeled by the phases in coexistence. The surface $[F^+, M_a^+]$ is omitted. The lines are labeled by the three or four phases in coexistence there. At the point P_2, five phases coexist; at P_1, seven phases coexist. The phases F and M are stable above $T=0$.

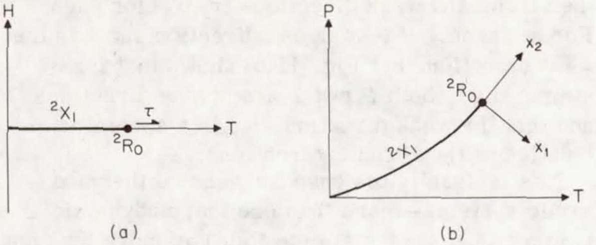

FIG. 11. (a) Phase transition for a ferromagnetic system. The coexistence surface ${}^2X_1$ ends at a critical point ${}^2R_0$. The strong direction H and weak direction τ are defined at the ${}^2R_0$. (b) Phase transition for a simple fluid. The coexistence surface ${}^2X_1$ ends at a critical point ${}^2R_0$. The strong direction x_1 and weak direction x_2 are indicated; both P and T directions are strong.

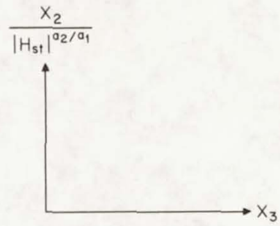

FIG. 13. Invariant space for an antiferromagnet. (x_3 is merely a parameter.)

Next, we introduce the concept of a direction of type 3. In the examples discussed, the critical spaces of order 3 have a dimension of $d = n-3$. If one approaches a particular tricritical point along a line of critical points of order 2, then in addition to the two directions singled out by the ${}^2R_1$ (and its associated ${}^2X_2$), there is a third direction of significance for scaling. This direction, which we call a direction of type 3, is a direction tangent to the line of critical points (Figs. 12 and 14). This concept is easily generalized to $n>3$ for the case mentioned above, for which the dimension d of the space of critical points of order three is indeed given by $d=n-3$. In this case directions of type 3 are those directions which are neither strong nor weak for a particular ${}^2R_{n-2}$ bounded by the ${}^3R_{n-3}$, nor are they locally tangent to the space of critical points of third order.

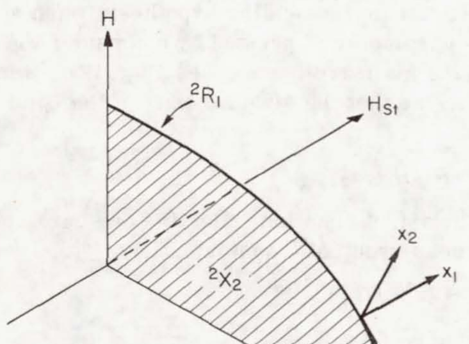

FIG. 12. Phase transition for an antiferromagnet. The coexistence surface ${}^2X_2$ lies in the H, T plane and the line of critical points ${}^2R_1$ bounds it. The strong direction is everywhere H_{st}, the staggered magnetic field. The weak direction may be either H or T, *except* at the Néel point where it can only be T. The independent direction x_0 lies in the ${}^2R_1$.

In the similar cases where Eq. (1.1) holds as an equality, one can generalize the above concepts to define directions of types 1, 2, ..., Θ, and these are important in applying the scaling hypothesis to critical spaces of order Θ. Specifically, since a critical point of order Θ is, by definition, a particular point on a "line" of critical points of order $\Theta-1$, the generalization follows by analogy with the case treated above. The directions of types 1 through Θ are of great importance because they are used as the independent variables of the Gibbs function when the scaling hypothesis is made. Accordingly, they will be referred to in later sections as the "principal directions of scaling."

Thus, to set up a coordinate system at a ${}^{\Theta}R_{n-\Theta}$ (a general critical space of order Θ), a set of critical spaces ${}^{j}R_{n-j}$ of orders $j=2, 3, \ldots, \Theta$ must be selected. This set of spaces must satisfy an inclusion principle: ${}^{\Theta}R_{n-\Theta} \subset {}^{i}R_{n-i} \subset {}^{j}R_{n-j}$ for $j<i<\Theta$. The directions of types 1, 2, ..., Θ are then sequentially defined. Here the inclusion symbol $\subset$ means not only that the ${}^{i}R_{n-i}$ is also part of a ${}^{j}R_{n-j}$ (for $i>j$) but also that the ${}^{i}R_{n-i}$ can be reached as a limiting point or boundary of the ${}^{j}R_{n-j}$.

The hierarchy of spaces ${}^{j}R_{n-j}$ is not unique, and the large number of choices available presents an apparent problem because many more than Θ linearly independent vector directions are definable. For the $\Theta=3$ example of Fig. 14 the ${}^3R_0$ can be approached along any of the three ${}^2R_1$, and each of these three "critical lines" (with its associated ${}^2X_2$) defines a set of directions of types 1, 2, and 3. This apparent problem is resolved by the generalized scaling hypothesis, because the shape of each critical space of order j ($j<\Theta$) near the ${}^{\Theta}R_d$ is constrained by the scaling hypothesis so that all the different directions end up mutually consistent. Accordingly, we now turn our attention to the scaling hypothesis, making it firstly in Sec. V for simple systems ($n=2$), for $n=3$ systems with a ${}^3R_0$ (tricritical point) in Sec. VI, and in Paper II for a ${}^{\Theta}R_{n-\Theta}$ (a general critical space of order Θ).[20]

V. INVARIANT THEOREMS OF ONE-PARAMETER CONTINUOUS GROUPS; APPLICATION TO THE SCALING HYPOTHESIS FOR CRITICAL SPACES OF ORDER 2

The scaling hypothesis for a simple system with two independent field variables can be made in

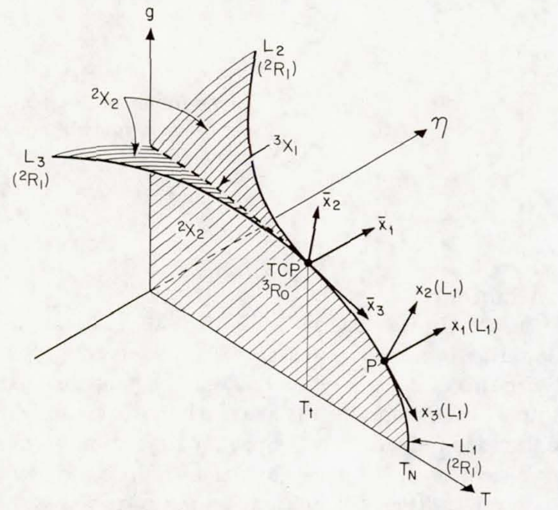

FIG. 14. Phase diagram for a metamagnet. The three $^2X_2$ end in lines of critical points $^2R_1$. These lines intersect at the tricritical point $^3R_0$. At a point P on the line L_1, a triad of strong, weak, and parallel (to L_1) directions is shown. This triad attains the limiting orientation $(\bar{x}_1, \bar{x}_2, \bar{x}_3)$ at the tricritical point $^3R_0$.

several essentially equivalent fashions. One statement is that the singular part of the Gibbs potential is asymptotically a generalized homogeneous function (GHF) of the appropriate variables.[21] For the simple magnet, this statement takes the form that there exist two numbers a_H, a_τ (called "scaling powers") such that for all positive λ,

$$G(\lambda^{a_H}H, \lambda^{a_\tau}\tau) = \lambda G(H, \tau), \quad (5.1)$$

where H is the magnetic field and $\tau \equiv T - T_c$. Using Eq. (5.1), one can express all possible thermodynamic exponents in terms of (a_H, a_τ).[21]

This form of the scaling hypothesis implies that the singular part of the Gibbs potential

$$G = F(H, \tau) \quad (5.2)$$

is an invariant equation under the "scaling" transformation defined by

$$G' \equiv \lambda G, \quad (5.3a)$$

$$H' \equiv \lambda^{a_H}H; \ \tau' \equiv \lambda^{a_\tau}\tau, \quad (5.3b)$$

such that $G' = F(H', \tau')$. The transformations defined by Eq. (5.3) form a one-parameter group[22] $\mathcal{G}_F$ and the scaling hypothesis may be restated in the following fashion: (5.2) is an invariant equation under the group of transformations $\mathcal{G}_F$ of (5.3).

For a simple magnet the thermodynamic axes are parallel to the directions used in the scaling hypothesis (5.1) (the "principal axes of scaling"). In other systems, this is not always so. In Fig. 11 we contrast the phase diagrams of a simple fluid and a simple magnet, and show the orientations of the strong and weak directions (x_1, x_2) for each. For a magnet, H is a strong direction and τ is the weak direction, but Fig. 11(b) shows that for a simple fluid, both P *and* T are strong directions and that the weak direction, x_2, is a special combination of the P and T directions.

This is usually the case for general thermodynamic systems—more than one thermodynamic axis is strong (as for the simple fluid) or more than one axis is weak (as for an antiferromagnet, see Fig. 12).

The scaling hypothesis at a $^2R_{n-2}$ for a general system can be made by choosing the strong and weak directions as the principal axes of scaling. Then the statement is that the singular part of the Gibbs function

$$G = \mathcal{F}(x_1, x_2; \ldots, x_n) \quad (5.4)$$

is an invariant equation under the one-parameter[23] continuous group of transformations $\mathcal{G}$:

$$\mathcal{G}\begin{cases} G' = \lambda G, & (5.5a) \\ x_i' = \lambda^{a_i}x_i, \quad i = 1, 2, \ldots, n, \quad [a_i = 0, \ i > 2]. & (5.5b) \end{cases}$$

Equation (5.5) is defined for all positive λ; the a_i are called scaling powers. This statement is equivalent to the scaling hypothesis

$$G(\lambda^{a_1}x_1, \lambda^{a_2}x_2; x_3 \cdots x_n) = \lambda G(x_1, x_2; \cdots x_n). \quad (5.6)$$

For future reference, we will use a superscript s to denote the subgroup generated by the transformations of the independent variables x_i $(i = 1, 2, \ldots, n)$. Thus we may generally define the full group by two equations, where the second denotes the subgroup $\mathcal{G}^s$.

To illustrate the scaling hypothesis when an inactive parameter is present, we consider the example of the antiferromagnet (see Fig. 12). Here we hypothesize that the singular part of the Gibbs potential

$$G = \mathcal{F}_A(H_{st}, x_2, x_3) \quad (5.7)$$

is an invariant equation under the one parameter continuous group of transformations $\mathcal{G}_A$:

$$\mathcal{G}_A\begin{cases} G' = \lambda G, \\ H_{st}' = \lambda^{a_1}H_{st}, \ x_2' = \lambda^{a_2}x_2, \ x_3' = x_3, \end{cases} \quad (5.8)$$

where x_2 is a weak direction, $[T - T_c(H)]$ or $[H - H_c(T)]$, and x_3 parametrizes the position of the critical point on the line of critical points. Equivalently G satisfies a GHF equation[24]

$$G(\lambda^{a_1}H_{st}, \lambda^{a_2}x_2; x_3) = \lambda G(H_{st}, x_2; x_3). \quad (5.9)$$

Here H_{st} denotes the staggered magnetic field.

Scaling functions for ferromagnets and antiferromagnets can be obtained the usual way[21] from

Eqs. (5.1) and (5.9), respectively. For example, by setting $\lambda \equiv 1/|H|^{1/a_H}$ in Eq. (5.1), we obtain[25]

$$G(1, \tau/|H|^{a_\tau/a_H}) = |H|^{-1/a_H} G(H, \tau). \qquad (5.10)$$

The function $G(H, \tau)$ can be plotted as a curve in a two-dimensional plane with coordinates specified by $G/|H|^{1/a_H}$ and $\tau/|H|^{a_\tau/a_H}$. We note that both $G/|H|^{1/a_H}$ and $\tau/|H|^{a_\tau/a_H}$ are absolute invariants of the group $\mathcal{G}_F$ defined by Eq. (5.3), i.e.,

$$G_H \equiv \frac{G'}{|H'|^{1/a_H}} = \frac{G}{|H|^{1/a_H}}, \qquad (5.11a)$$

$$\tau_H \equiv \frac{\tau'}{|H'|^{a_\tau/a_H}} = \frac{\tau}{|H|^{a_\tau/a_H}}, \qquad (5.11b)$$

where the second equalities in (5.11) follow from (5.3).

Similarly, by setting $\lambda \equiv 1/|H_{st}|^{1/a_1}$, Eq. (5.9) may be written

$$G(1, x_2/|H_{st}|^{a_2/a_1}; x_3) = |H_{st}|^{-1/a_1} G(H_{st}, x_2; x_3), \qquad (5.12)$$

and $G/|H_{st}|^{1/a_1}$, $x_2/|H_{st}|^{a_2/a_1}$, x_3 are absolute invariants of the group $\mathcal{G}_A$. In addition, the last two quantities are absolute invariants of the subgroup $\mathcal{G}_A^s$.

To derive exponents and scaling laws for the antiferromagnet, the procedures developed in Ref. 21 can be simply applied to Eq. (5.9). At points where the critical line is not parallel to the T axis, it is easily shown that

$$\beta = (1 - a_1)/a_2, \qquad (5.13a)$$

$$1/\delta = (1 - a_1)/a_1, \qquad (5.13b)$$

$$-\gamma = (1 - 2a_1)/a_2, \qquad (5.13c)$$

$$-\alpha = (1 - 2a_2)/a_2, \qquad (5.13d)$$

where the order parameter M_{st} tends to zero when the critical line is approached in a weak direction with exponent β,

$$M_{st} \propto |T - T_c(H)|^{\beta}, \qquad (5.14a)$$

and with exponent $1/\delta$ when it is approached in a strong direction

$$M_{st} \propto H_{st}^{1/\delta}. \qquad (5.14b)$$

The staggered susceptibility $\chi_{st} = \partial M_{st}/\partial H_{st}$ diverges with exponent γ,

$$\chi_{st} \propto |T - T_c(H)|^{-\gamma}, \qquad (5.14c)$$

and the specific heat at constant order parameter diverges with exponent α:

$$C_{M_{st}} \propto |T - T_c(H)|^{-\alpha}. \qquad (5.14d)$$

The last two exponents γ and α refer to weak directions of approach (in the plane $H_{st} = 0$) to the critical line.[26]

In the same way, exponents for the ordinary magnetization M, and ordinary susceptibility $\chi = \partial M/\partial H$ can be derived. It turns out on using Eq. (5.13d) that

$$M - M_c(H) \propto |T - T_c(H)|^{(1-\alpha)}, \qquad (5.15a)$$

$$\chi \propto |T - T_c(H)|^{-\alpha}. \qquad (5.15b)$$

From Eqs. (5.13a)–(5.13d) the usual scaling law equalities can be derived by eliminating the scaling powers a_1 and a_2:

$$\alpha + 2\beta + \gamma = 2, \quad \beta(\delta - 1) = \gamma, \quad \beta(\delta + 1) = 2 - \alpha.$$

These results are also obtainable from two simple group invariant theorems which we shall find particularly useful in making the scaling hypothesis for critical subspaces of higher order.

Theorem 1. Consider a one-parameter continuous group of transformations:

$$\mathcal{G}\begin{cases} x_0' = f(\lambda | x_0), & (5.16a) \\ x_i' = f_i(\lambda | x_1, x_2, \ldots, x_n), \quad i = 1, 2, \ldots n. & (5.16b) \end{cases}$$

There exist n functionally independent absolute invariants of the x_i ($i = 0, 1, \ldots, n$). This theorem is proved in Appendix A.

For our applications, we shall choose the invariants, denoted by y_i ($i = 0, 1, \ldots, n-1$), such that, for $i = 0$,

$$\frac{\partial y_0}{\partial x_0} \neq 0, \qquad (5.17a)$$

and for $i > 0$,

$$(y_1, y_2, \ldots, y_{n-1}) \qquad (5.17b)$$

are the $n - 1$ functionally independent absolute invariants of the subgroup $\mathcal{G}^s$.

For the simple ferromagnet, $G/|H|^{1/a_H}$ is an absolute invariant under $\mathcal{G}_F$ [see Eq. (5.3)] and $\tau/|H|^{a_\tau/a_H}$ is the functionally independent absolute invariant of (H, τ) under the transformation $\mathcal{G}_F^s$. For the antiferromagnet, $G/|H_{st}|^{1/a_1}$ is an absolute invariant under $\mathcal{G}_A$, and $(x_2/|H_{st}|^{a_2/a_1}, x_3)$ are the *two* functionally independent absolute invariants under $\mathcal{G}_A^s$.

Theorem 2. If

$$x_0 = X_0(x_1, x_2, \ldots, x_n) \qquad (5.18)$$

is an invariant equation under $\mathcal{G}$ defined by (5.16) (i.e., if X_0 is a GHF), then it can be expressed as

$$y_0 = Y_0(y_1, y_2, \ldots, y_{n-1}), \qquad (5.19)$$

where the y_i ($i = 0, 1, \ldots, n-1$) form a set of functionally independent absolute invariants of $\mathcal{G}$ given by (5.16), and satisfying (5.17).

The proof of this theorem is given in Appendix B. Equations (5.10) and (5.12) are simple applications of these theorems. The usefulness of theorems 1 and 2 will be apparent in Sec. VI.

VI. SCALING HYPOTHESIS FOR TRICRITICAL POINTS

Before making the scaling hypothesis and examining its consequences for a critical space of arbitrary order $\mathcal{O}$, we will make it for the special case of a ${}^3R_0$ (tricritical point) for which there are three fields available ($n=3$). This will clarify both notation and concepts, and make passage to the general case more painless.

As was shown in Sec. IV, it is possible at a critical point to select strong and weak directions (directions of types 1 and 2). These we call x_1 and x_2 as before. In a space of total dimension three, the critical subspaces terminating at a ${}^3R_0$ are all ${}^2R_1$. At a point on a ${}^2R_1$ we may select a direction tangent to the line. Thus as one approaches the ${}^3R_0$ along a given ${}^2R_1$, the directions of types 1, 2, and 3 are uniquely defined (see Fig. 14).

Since three critical lines meet at a ${}^3R_0$, three "rival" coordinate systems exist at the point ${}^3R_0$. A scaling hypothesis cannot be made at the tricritical point unless a unique coordinate system can be defined, and this represents an apparent obstacle.

The solution of this problem is somewhat subtle, and the full details have been given in a previous paper.[7(b)] The basic idea is that a scaling hypothesis at the ${}^3R_0$ determines the general shape of a line of critical points near the ${}^3R_0$; thus a scaling hypothesis made in a coordinate system defined by one line will restrict the shapes of the other two lines meeting it (at the tricritical point).

The coordinate systems defined with reference to the other two lines are consistent in the sense that we could have selected any line first to make the scaling hypothesis and we would have obtained the same final result.

To set up a coordinate system in which to make a scaling hypothesis at the ${}^3R_0$, we choose a point P on one of the critical lines (say L_1) and we set up a triad of directions $x_i(L_1)$. Two of these directions are of types 1 and 2, while the third is tangent to the ${}^2R_1$. The coordinate system at the tricritical point is now defined to be

$$\bar{x}_i \equiv \lim_{P \to {}^3R_0} x_i(P) \tag{6.1}$$

(see Fig. 14). The direction $\bar{x}_3$ is of type 3. The bars are used in order that the present notation be consistent with that of Ref. 7(b).

We now introduce a scaling parameter λ ($\lambda > 0$) and make the scaling hypothesis that the singular part of the Gibbs potential is a GHF, i.e.,

$$G(\lambda^{\bar{a}_1}\bar{x}_1, \lambda^{\bar{a}_2}\bar{x}_2, \lambda^{\bar{a}_3}\bar{x}_3) = \lambda G(\bar{x}_1, \bar{x}_2, \bar{x}_3), \tag{6.2}$$

where $(\bar{a}_1, \bar{a}_2, \bar{a}_3)$ are the "tricritical scaling powers". Equation (6.2) is equivalent to the statement that $G = \mathfrak{F}(\bar{x}_1, \bar{x}_2, \bar{x}_3)$ is an invariant equation under the one-parameter continuous group of transformations

$$\mathcal{G}_3 \begin{cases} G' \equiv \lambda G, & (6.3\text{a}) \\ \bar{x}_i' \equiv \lambda^{\bar{a}_i} \bar{x}_i, \quad i = 1, 2, 3. & (6.3\text{b}) \end{cases}$$

According to theorem 1 of Sec. V, the hypothesized invariance property of (6.1) under $\mathcal{G}_3$ implies that there exists a basis set of functionally independent absolute invariants of $\mathcal{G}_3$. We adopt a canonical form for the invariants y_i by scaling $\bar{x}_i$ with respect to the tangent variable—here $\bar{x}_3$—as follows:

$$y_0 \equiv \frac{\bar{x}_0}{\bar{x}_3^{1/\bar{a}_3}}, \quad y_1 \equiv \frac{\bar{x}_1}{\bar{x}_3^{\bar{a}_1/\bar{a}_3}}, \quad y_2 \equiv \frac{\bar{x}_2}{\bar{x}_3^{\bar{a}_2/\bar{a}_3}}, \tag{6.4}$$

with $\bar{x}_0 \equiv G$. Thus, theorem 2 of Sec. V states that $G(\bar{x}_1, \bar{x}_2, \bar{x}_3)$ may be expressed as[27]

$$y_0 = F_2(y_1, y_2). \tag{6.5}$$

Since the variables y_1 and y_2 forms a basis set of functionally independent absolute invariants of the scaling field variables $\bar{x}_1$, $\bar{x}_2$, and $\bar{x}_3$ of the group of transformations $\mathcal{G}_3^s$, any point (k_1, k_2) in the two-dimensional space (y_1, y_2) gives rise to an invariant curve of points in the three-dimensional space $(\bar{x}_1, \bar{x}_2, \bar{x}_3)$. That is, the point given by

$$y_i = k_i, \quad i = 1, 2 \tag{6.6}$$

corresponds to a line in the x_i space that may be conveniently parametrized by

$$(\bar{x}_1, \bar{x}_2, \bar{x}_3) = (k_1\lambda^{\bar{a}_1}, k_2\lambda^{\bar{a}_2}, \lambda^{\bar{a}_3}), \tag{6.7}$$

where λ is an arbitrary parameter (see Fig. 15). In particular the lines of critical points L_j converging on the tricritical point can be expressed in the form of Eq. (6.7), since according to the scaling hypothesis (6.2) they must be invariant under the group of symmetries $\mathcal{G}_3$ of (6.3).

Previously[7(b)] we have derived Eq. (6.7) directly from Eq. (6.2) and demonstrated that if the scaling powers $\bar{a}_i$ are all different, the curves parametrized by Eq. (6.7) end up parallel to the axis $\bar{x}_i$ corresponding to the minimum $\bar{a}_i$ (unless $k_i = 0$). Although the direction of type 3 defined for one line is not necessarily parallel to the direction of type 3 defined for another line, it will at least be parallel to *some* member of the triad defined for that other line. Thus all choices of scaling directions will be mutually consistent![7(b),28]

Along a critical line ${}^2R_1$, the conventional scaling hypothesis is normally stated in terms of a GHF equation of the form

$$G(\mu^{a_1}x_1, \mu^{a_2}x_2; x_3) = \mu G(x_1, x_2; x_3), \tag{6.8}$$

where x_3 is a parameter and does not scale. Near the ${}^3R_0$, however, the shape of the critical line is determined by Eq. (6.7). A ${}^2R_1$ near the ${}^3R_0$ maps into a point (k_1, k_2) in the $y_1 - y_2$ plane given by Eq. (6.6). Furthermore, the value of $y_0 \equiv \bar{x}_0 / \bar{x}_3^{1/\bar{a}_3}$

$= G/\bar{x}_3^{1/\bar{a}_3}$ changes only if y_1 and/or y_2 changes. It is therefore more proper to make a precise scaling hypothesis about the critical line ${}^2R_1$ near the ${}^3R_0$ making use of the variables (y_1, y_2).

If we adopt the strong requirement that a point in one phase remains in that phase under the scale transformation $\mathcal{G}_3$, the CXS surfaces become lines in the y_1-y_2 plane. Hence, it is possible to choose the principal directions of scaling for the ${}^2R_{n-2}$ as linear combinations of the variables y_1, y_2.

Because the scaled variables must be zero at the critical line we consider the variables

$$\hat{y}_1 \equiv y_1 - k_1, \tag{6.9a}$$

$$\hat{y}_2 \equiv y_2 - k_2. \tag{6.9b}$$

For the line L_1 of Fig. 15, $k_1 = 0$, the coordinate y_1, is everywhere strong and $(y_2 + k)$ is weak. For L_2 and L_3, the weak direction is parallel to the CXS mapped in the $y_1 - y_2$ plane, and both $\hat{y}_1$, $\hat{y}_2$ are strong directions unless the wings end up parallel to one axis.

We therefore define linear combinations of the variables $(y_i - k_i)$, which give the weak and strong directions (they are of necessity also absolute invariants of the group $\mathcal{G}_3$):

$$\tilde{y}_i \equiv \sum_{j=1}^{2} \tilde{R}_{ij}(y_j - k_j), \tag{6.10a}$$

where $\tilde{R}_{ij}$ is a "rotation matrix". Defining

$$\tilde{y}_0 \equiv y_0, \tag{6.10b}$$

we hypothesize that along a ${}^2R_1$ near the ${}^3R_0$, $\tilde{y}_0$ is a GHF of $(\tilde{y}_1, \tilde{y}_2)$,

$$\tilde{y}_0(\mu^{a_1}\tilde{y}_1, \mu^{a_2}\tilde{y}_2) = \mu\tilde{y}_0(\tilde{y}_1, \tilde{y}_2), \tag{6.11}$$

i.e., $\tilde{y}_0 = \mathfrak{F}_2(\tilde{y}_1, \tilde{y}_2)$ is an invariant equation under a group $\mathcal{G}_2$ defined by

$$\mathcal{G}_2 \begin{cases} \tilde{y}_0' = \mu\tilde{y}_0, & (6.12\text{a}) \\ \tilde{y}_i' = \mu^{a_i}\tilde{y}_i, \quad i = 1, 2. & (6.12\text{b}) \end{cases}$$

In general, the group $\mathcal{G}_2$ will be different (having different a_i) for *each* critical line at the tricritical point, and will only be valid within a certain region close to the critical line. The different groups $\mathcal{G}_2$ for the different lines L_i do not have regions of overlap and there is therefore no conflict.

We can now form absolute invariants of $\mathcal{G}_2$. Scaling with respect to the weak direction we obtain

$$z_0 \equiv \frac{\tilde{y}_0}{\tilde{y}_2^{1/a_2}}, \quad z_1 \equiv \frac{\tilde{y}_1}{\tilde{y}_2^{a_1/a_2}}. \tag{6.13}$$

Theorem 2 of Sec. V states that under the hypothesis (6.11), $\tilde{y}_0(\tilde{y}_1, \tilde{y}_2)$ may be expressed as[27]

$$z_0 = \mathfrak{F}_1(z_1). \tag{6.14}$$

The simplest example of this is for the line L_1 of Fig. 15. Here the variables of scaling are

$$\hat{y}_1 = \bar{x}_1 / \bar{x}_3^{\bar{a}_1/\bar{a}_3}, \tag{6.15a}$$

$$\hat{y}_2 = (\bar{x}_2 / \bar{x}_3^{\bar{a}_2/\bar{a}_3} + k), \tag{6.15b}$$

where k is defined in Fig. 15. Rotation is not necessary and $\tilde{R}_{ij} \equiv \delta_{ij}$. Hence on using (6.13) and (6.15), Eq. (6.14) can be written in the "double-power law" form[27]

$$\frac{G}{\bar{x}_3^{1/\bar{a}_3}(\bar{x}_2/\bar{x}_3^{\bar{a}_2/\bar{a}_3} + k)^{1/a_2}} = \mathfrak{F}_1\left[\frac{\bar{x}_1}{\bar{x}_3^{\bar{a}_1/\bar{a}_3}(\bar{x}_2/\bar{x}_3^{\bar{a}_2/\bar{a}_3} + k)^{a_1/a_2}}\right]. \tag{6.16}$$

For a simple system with $n = 2$, scaling functions predict data collapsing for functions of two variables from a surface onto a line. For $n = 3$ and functions of three variables, data collapse from a volume onto a surface. However, the double-power scaling function of Eq. (6.16) predicts that data will collapse from a volume onto a line. Clearly this happens only within the region of validity of both groups of transformations $\mathcal{G}_2$ and $\mathcal{G}_3$.

The region of influence of $\mathcal{G}_2$ in the neighborhood of the tricritical point ${}^3R_0$ should also be controlled by the group $\mathcal{G}_3$. This means that the region of influence of $\mathcal{G}_2$ should be bounded by a surface which scales toward the ${}^3R_0$. In Fig. 15, where a line which scales is represented by a point, a surface which scales will be represented by a line. We therefore plot the surfaces bounding the region of influence of the group $\mathcal{G}_2$ (of transformations about a ${}^2R_1$, L_i) as a line surrounding the point in the y_1-y_2 plane, representing the particular line L_i.

In terms of the variables y_1, y_2 such a line will be represented by the equation

$$f(y_1, y_2) = 0 \tag{6.17a}$$

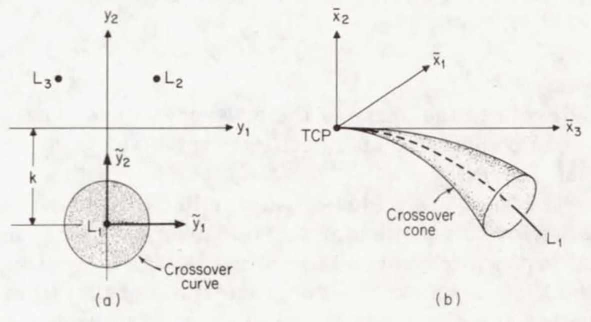

FIG. 15. (a) Plot of the invariants (y_1, y_2) for the group $\mathcal{G}_3$ of transformations about the tricritical point. The strong and weak directions for the line L_1 are y_1 and y_2. The circle around L_1 is a possible shape for the crossover region. (b) The principal points of interest of Fig. 15(a) in the full space $(\bar{x}_1, \bar{x}_2, \bar{x}_3)$. The point labeled L_1 has become a line and the circle surrounding it has become a cone.

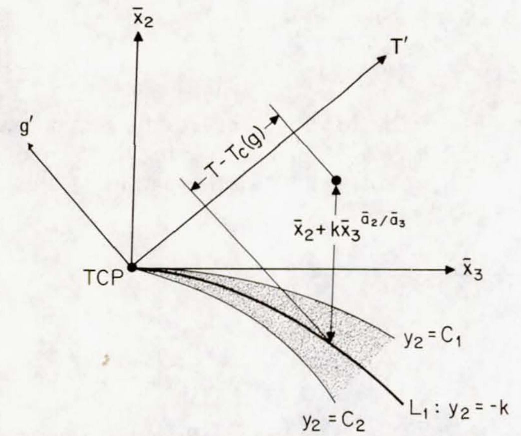

FIG. 16. Figure 15(b) sliced in the $\bar{x}_2$, $\bar{x}_3$ plane. The cone has become the two lines labeled $y_2 = C_1$, C_2 [see Fig. 15(a)]. These are generally referred to as crossover lines: $(T', g') = (T - T_t, g - g_t)$.

or

$$f(\bar{x}_1 / |\bar{x}_3|^{\bar{a}_1/\bar{a}_3}, \bar{x}_2 / |\bar{x}_3|^{\bar{a}_2/\bar{a}_3}) = 0 . \qquad (6.17b)$$

The area bounded by this curve (6.17) maps into a conical volume surrounding the critical line L_1 (Fig. 15). Scaling will not tell us the actual shape of the curve in the $y_1 - y_2$ plane but it does limit the shape in the $(\bar{x}_1, \bar{x}_2, \bar{x}_3)$ space, since all points in the y_1-y_2 plane give rise to curves approaching the tricritical point along a particular direction—the axis corresponding to the minimum $\bar{a}_i$.

In the plane $\bar{x}_1 = 0$, Eq. (6.16) requires[29] that

$$G \propto \bar{x}_3^{1/\bar{a}_3} (\bar{x}_2 / \bar{x}_3^{\bar{a}_2/\bar{a}_3} + k)^{1/a_2} , \qquad (6.18)$$

and the conical surface of Eq. (6.17) becomes the two "crossover lines"

$$\bar{x}_2 = C_{1,2} \bar{x}_3^{\bar{a}_2/\bar{a}_3} , \qquad (6.19)$$

as shown in Fig. 16. The crossover exponent φ,[7(a)] given by

$$\varphi \equiv \bar{a}_3 / \bar{a}_2 , \qquad (6.20)$$

determines the shape of the crossover lines, and it can be determined directly from the shape of the line L_1 ($^2R_1$).

The lines are called crossover lines, because the behavior of a particular function crosses over from an exponent characteristic of the $^3R_0$ far away from the line, to an exponent characteristic of the $^2R_1$ at points close to the $^2R_1$. It is important to realize that the group $\mathcal{G}_3$ does not cease to be valid, and the crossover does not refer to changing from one group to another. The group $\mathcal{G}_3$ is everywhere valid, and the crossover merely marks the limits of validity of $\mathcal{G}_2$. This principle will be extended in Paper II and the groups $\mathcal{G}_j$ will control crossovers (or boundaries for the regions of validity) of $\mathcal{G}_i$ where $j > i$.

Finally, a few remarks should be made about the exponents and the directions of approach to the tricritical point. Equation (6.18) shows that if $\bar{x}_2 / |\bar{x}_3|^{\bar{a}_2/\bar{a}_3}$ is a constant the exponent for G is $1/\bar{a}_3$. For a function f with a tricritical-point (TCP) scaling power $\bar{a}_f$, and a critical-line scaling power a_f, the equation analogous to Eq. (6.18) predicts exponents $\bar{a}_f/\bar{a}_3$ and a_f/a_2. For example, for the staggered susceptibility $\chi_{st} \equiv \partial^2 G / \partial H_{st}^2$, from (6.16),

$$\chi_{st} \propto \bar{x}_3^{(1-2\bar{a}_1)/\bar{a}_3} (\bar{x}_2 / \bar{x}_3^{\bar{a}_2/\bar{a}_3} + k)^{(1-2a_1)/a_2} , \qquad (6.21)$$

and $\bar{a}_f = 1 - 2\bar{a}_1$ and $a_f = 1 - 2a_1$ for this case. Thus for all the exponents considered below the numerators can be appropriately be replaced by $\bar{a}_f$ or a_f.

If the $^3R_0$ is approaches along a direction not asymptotically parallel to the $\bar{x}_3$ axis (i.e., outside the crossover lines), G scales with a power $1/\bar{a}_2$.

If the $^2R_1$ is approached along a line of constant $\bar{x}_3$, in the plane $\bar{x}_1 = 0$ Eq. (6.18) shows that G has an exponent $1/a_2$. This is expected, of course, since G has an exponent $1/a_2$ for any point (i.e., fixed x_3) on the line $^2R_1$ even when the point is far away from the $^3R_0$ [see Eq. (6.8)].

In Sec. V, exponents were demonstrated in terms of the scaling powers a_i [Eqs. (5.13)] and the same can be done here for the $^2R_1$ (exponents in terms of a_i) and the $^3R_0$ (exponents in terms of the $\bar{a}_i$) separately. The only new exponents, which will be derived, are exponents for the directions of approach to the $^3R_0$ along y_2 = constant and these give exponents of the form

$$f \sim |x_3|^{\bar{a}_f/\bar{a}_3} . \qquad (6.22)$$

These can be related to exponents of approach along directions of type 2 by relations of the form

$$\bar{a}_f / \bar{a}_3 = (\bar{a}_f / \bar{a}_2) / \varphi . \qquad (6.23)$$

These are new predictions of scaling specific to tricritical points [the others are analogous to Eq. (5.13)].[7(c)]

Finally, we emphasize the importance of expressing the scaling relations in terms of invariants. For example, Eq. (6.21) may be written in the alternative "mixed-exponent form"

$$\chi_{st} \propto C(\bar{x}_2 + k\bar{x}_3^{1/\varphi})^{-\gamma} , \qquad (6.24)$$

where

$$C \propto \bar{x}_3^{(\gamma - \bar{\gamma})/\varphi} , \qquad (6.25)$$

with

$$-\gamma = \frac{1 - 2a_1}{a_2} , \qquad -\bar{\gamma} = \frac{1 - 2\bar{a}_1}{\bar{a}_2} . \qquad (6.26)$$

Expressions (6.24) and (6.25) appear more complicated than they actually are. The exponents are actually not mixed when expressed in the invariant from as shown in Eq. (6.21).

ACKNOWLEDGMENTS

We wish to thank F. Harbus, R. B. Griffiths, J. C. Wheeler, and E. K. Riedel for stimulating discussions.

APPENDIX A: PROOF OF THEOREM 1

Theorem 1. Consider a one-parameter continuous group of transformations

$$\mathcal{G}: \quad x_i' = f_i(\lambda \,|\, x_0, x_1, \ldots, x_n), \tag{A1}$$

where $i = 0, 1, \ldots, n$. There exist n functionally independent absolute invariants of the x_i $(i = 0, 1, \ldots, n)$.

Proof of theorem 1. Consider a function $F(x_0', x_1', \ldots, x_n')$. Assume the derivatives of f_i with respect to λ exist. We expand $F(x_0', x_1', \ldots, x_n')$ in a Maclaurin series

$$F(x_0', x_1', \ldots, x_n') = f + f'(\delta\lambda) + \frac{f''}{2!}(\delta\lambda)^2 + \cdots, \tag{A2}$$

where

$$\begin{aligned} f &= F(x_0, x_1, \ldots, x_n), \\ f' &= \left(\frac{dF}{d\lambda}\right)_{\lambda=\lambda_0} = VF(x_0, x_1, \ldots, x_n), \\ f'' &= \left(\frac{d^2F}{d\lambda^2}\right)_{\lambda=\lambda_0} = V^2F(x_0, x_1, \ldots, x_n), \\ &\vdots \end{aligned} \tag{A3}$$

with λ_0 the value of λ corresponding to the identical transformation and

$$V \equiv \sum_{i=0}^{n} \xi_i \left(\frac{\partial}{\partial x_i}\right), \tag{A4}$$

$$\xi_i \equiv \left(\frac{\partial f_i}{\partial \lambda}\right). \tag{A5}$$

If, therefore, $F(x_0, x_1, \ldots, x_n)$ is an absolute invariant of the group $\mathcal{G}$, then

$$F(x_0', x_1', \ldots, x_n') = F(x_0, x_1, \ldots, x_n). \tag{A6}$$

The necessary and sufficient condition for $F = \text{const}$ is that

$$VF = \sum_{i=0}^{n} \xi_i \left(\frac{\partial F}{\partial x_i}\right) = 0. \tag{A7}$$

Thus, F is a solution of the partial differential equation (A7) and consequently, $F(x_0, x_1, \ldots, x_n) = \text{const}$ is a solution of the system of the equivalent ordinary differential equations

$$\frac{dx_0}{\xi_0} = \frac{dx_1}{\xi_1} = \cdots = \frac{dx_n}{\xi_n}. \tag{A8}$$

These equations admit n independent solutions (first integrals)[30,31] and theorem 1 is proved.

APPENDIX B: PROOF OF THEOREM 2

Theorem 2. If the equation

$$x_0 = X_0(x_1, x_2, \ldots, x_n) \tag{B1}$$

is invariant under

$$\mathcal{G}\begin{cases} x_0 = f(\lambda \,|\, x_0), \\ x_i' = f_i(\lambda \,|\, x_1, x_2, \ldots, x_n), \end{cases} \tag{B2}$$

then it can be expressed as

$$y_0 = Y_0(y_1, y_2, \ldots, y_{n-1}), \tag{B3}$$

where $(y_0, y_1, \ldots, y_{n-1})$ form a set of functionally independent absolute invariants under $\mathcal{G}$, with

$$\frac{\partial y_0}{\partial x_0} \neq 0,$$

and $(y_1, y_2, \ldots, y_{n-1})$, the $n-1$ functionally independent absolute invariants of $\mathcal{G}^s$.

By hypothesis, y_0 is an absolute invariant of $(x_0; x_1, \ldots, x_n)$ of $\mathcal{G}$. Thus, (B3) implies that the invariant equation (B1) may be written

$$y_0(x_0; x_1, x_2, \ldots, x_n) = Y_0(y_1, y_2, \ldots, y_{n-1}). \tag{B4}$$

Since $(y_1, y_2, \ldots, y_{n-1})$ form a basis set of functionally independent absolute invariants of $(x_1, x_2, \ldots, x_n)$ of $\mathcal{G}^s$, (B4) is equivalent to the statement that x_0 is expressible as an implicit function of $(x_1, x_2, \ldots, x_n)$:

$$y_0(x_0; x_1, x_2, \ldots, x_n) = g(x_1, x_2, \ldots, x_n), \tag{B5}$$

where g is an absolute invariant of $(x_1, x_2, \ldots, x_n)$ under $\mathcal{G}^s$.

Before we launch into the proof of the theorem, we give a proof of the following lemma.[32]

Lemma. A necessary and sufficient condition for x_0, implicitly defined by (B5), as a function of $(x_1, x_2, \ldots, x_n)$, to be the same function as x_0' of $(x_1', x_2', \ldots, x_n')$ implicitly defined by

$$y_0(x_0', x_1', x_2', \ldots, x_n') = g'(x_1', x_2', \ldots, x_n') \tag{B6}$$

is that g is an absolute invariant of $(x_1, x_2, \ldots, x_n)$ under $\mathcal{G}^s$.

Proof of lemma. Since y_0 is an absolute invariant of $\mathcal{G}$, we have

$$y_0(x_0; x_1, x_2, \ldots, x_n) = y_0(x_0'; x_1', x_2', \ldots, x_n'). \tag{B7}$$

Since we require $x_0(x_1, x_2, \ldots, x_n)$ to be exactly the same function as $x_0'(x_1', x_2', \ldots, x_n')$, (B5)–(B7) require that

$$\begin{aligned} g(x_1, x_2, \ldots, x_n) &= g'(x_1', x_2', \ldots, x_n') \\ &= g(x_1', x_2', \ldots, x_n'). \end{aligned} \tag{B8}$$

This is the necessity proof.

We now demonstrate (B8) is sufficient to ensure (B5) and (B6) admit an invariant solution such that

$x_0(x_1, x_2, \ldots, x_n)$ is exactly the same function as $x_0'(x_1', x_2', \ldots, x_n')$. Inverting (B5) and (B6), we obtain

$$x_0(x_1, x_2, \ldots, x_n) = h(g; x_1, x_2, \ldots, x_n),$$
$$x_0'(x_1', x_2', \ldots, x_n') = h'(g'; x_1, x_2, \ldots, x_n), \tag{B9}$$

in some neighborhood of the $(x_1, x_2, \ldots, x_n)$ and $(x_1', x_2', \ldots, x_n')$ spaces, respectively. It is obvious that $h(g; x_1, x_2, \ldots, x_n)$ is exactly the same function as $h'(g_1'; x_1', x_2', \ldots, x_n')$. But, by hypothesis, $g(x_1, x_2, \ldots, x_n)$ is exactly the same function as $g'(x_1', x_2', \ldots, x_n')$. Therefore, $x_0(x_1, x_2, \ldots, x_n)$ is exactly the same function as $x_0'(x_1', x_2', \ldots x_n')$.

Proof of theorem 2. Using the lemma and the fact that $g(x_1, x_2, \ldots, x_n)$ in (B5) is an absolute invariant of $(x_1, x_2, \ldots, x_n)$ under $\mathcal{G}^s$, we immediately verify the statement of theorem 2.

APPENDIX C: PROOF OF THEOREM 3

Theorem 3. Consider a one-parameter continuous group of transformations $\mathcal{G}$:

$$\mathcal{G}\begin{cases} x_0' = \lambda x_0, \\ x_i' = f_i(\lambda) x_i, \quad i = 1, 2, \ldots, n. \end{cases} \tag{C1}$$

If

$$x_0 = F(x_1, x_2, \ldots, x_n) \tag{C2}$$

is an invariant equation under $\mathcal{G}$, the most general form for $f_i(\lambda)$ is λ^{a_i}, where a_i are constants.

Proof of theorem 3. We transform (C2) by means of (C1) for two successive values of $\lambda = \lambda_1, \lambda_2$,

$$\lambda_1\lambda_2 x_0 = F[f_1(\lambda_1)f_1(\lambda_2)x_1,\ f_2(\lambda_1)f_2(\lambda_2)x_2,\ \ldots,\ f_n(\lambda_1)f_n(\lambda_2)x_n], \tag{C3}$$

and again for the value of $\lambda = \lambda_1\lambda_2$,

$$\lambda_1\lambda_2 x_0 = F[f_1(\lambda_1\lambda_2)x_1,\ f_2(\lambda_1\lambda_2)x_2,\ \ldots,\ f_n(\lambda_1\lambda_2)x_n]. \tag{C4}$$

These results are to hold for all values of x_i. Setting $x_2 = x_3 = \cdots = x_n = 0$, we have from (C3) and (C4)

$$F[f_1(\lambda_1)f_1(\lambda_2)x_1, 0, \ldots, 0] = F[f_1(\lambda_1\lambda_2)x_1, 0, \ldots, 0]. \tag{C5}$$

Therefore,

$$f_1(\lambda_1)f_1(\lambda_2) = f_1(\lambda_1\lambda_2). \tag{C6}$$

The solution[33] of the functional equation for $f_1(\lambda)$ for $\lambda > 0$ is

$$f_1(\lambda) = \lambda^{a_1}, \tag{C7}$$

where a_1 is a constant. This process may be repeated for each $f_1(\lambda)$, $i = 1, 2, \ldots, n$. Thus, theorem 3 is proved.

---

*Work forms a part of a Ph.D. thesis to be submitted to the Physics Department of MIT by A. Hankey. Preliminary reports of aspects of this work appear in T. S. Chang, A. Hankey, and H. E. Stanley, AIP Conf. Proc. **10**, 880 (1973).

†Supported by NSF Grant No. GU-1590 and NASA Grant No. NGL 34-002-084. Permanent address: Riddick Laboratories, North Carolina State University, Raleigh, N.C. 27607.

‡Supported by a Research Assistantship from the Laboratory for Nuclear Science, MIT Lindemann Fellow. Present address: SLAC, Stanford, Calif.

§Supported by NSF, ONR. and AFOSR

[1] A. Hankey, T. S. Chang, and H. E. Stanley, Phys. Rev. B (to be published), hereafter referred to as II. See also, F. Harbus, A. Hankey, H. E. Stanley, and T. S. Chang, Phys. Rev. B (to be published).

[2] (a) B. Widom, J. Chem. Phys. **43**, 3892 (1965); (b) C. Domb and D. L. Hunter, Proc. Phys. Soc. Lond. **86**, 1147 (1965); (c) L. P. Kadanoff, Physics (N.Y.) **2**, 263 (1966); (d) R. B. Griffiths, Phys. Rev. **158**, 176 (1967).

[3] E. K. Riedel and F. Wegner, Z. Phys. **225**, 195 (1969).

[4] E. K. Riedel and F. Wegner, Phys. Rev. Lett. **24**, 730 (1970).

[5] R. B. Griffiths and J. C. Wheeler, Phys. Rev. A **2**, 1047 (1970).

[6] R. B. Griffiths, Phys. Rev. Lett. **24**, 715 (1970).

[7] (a) E. K. Riedel, Phys. Rev. Lett. **28**, 675 (1972); (b) A. Hankey, H. E. Stanley, and T. S. Chang, Phys. Rev. Lett. **29**, 278 (1972). (c) See also, R. B. Griffiths, Phys. Rev. B 7, 545 (1973).

[8] J. F. Nagle, Phys. Rev. A **2**, 2124 (1970); J. F. Nagle and J. C. Bonner, J. Chem. Phys. **54**, 729 (1971); J. C. Bonner and J. F. Nagle, J. Appl. Phys. **42**, 1280 (1971).

[9] We will use the word "spaces" to mean subspaces of the total space of field or fieldlike variables. Fieldlike refers to variables which occur as parameters in the Hamiltonian and which are *not* discontinuous across coexistence surfaces.

[10] (a) E. H. Graf, D. M. Lee, and J. D. Reppy, Phys. Rev. Lett. **19**, 417 (1967). These authors only treat the tricritical point at the lowest pressure. See also, G. Goellner and H. Meyer, Phys. Rev. Lett. **26**, 1543 (1971); and G. Goellner, Ph.D. thesis (Duke University, 1972) (unpublished). (b) W. B. Yelon (private communication); see also, C. W. Garland and B. B. Weiner, Phys. Rev. B 3, 1634 (1971).

[11] Parameters in a Hamiltonian which can be varied have similar properties to field variables with respect to the geometry of the surfaces. These are used in Sec. III.

[12] (a) F. J. Wegner, Phys. Rev. B **5**, 4529 (1972); (b) Phys. Rev. B **6**, 1891 (1972); (c) E. K. Riedel and F. J. Wegner, Phys. Rev. Lett. **29**, 349 (1972).

[13] I. S. Jacobs and P. E. Lawrence, Phys. Rev. **164**, 866 (1967); V. A. Schmidt and S. A. Friedberg, Phys. Rev. B **1**, 2250 (1970); B. E. Keen, D. P. Landau, B. Schneider, and W. P. Wolf, J. Appl. Phys. **37**, 1120 (1966); W. B. Yelon and R. J. Birgeneau, Phys. Rev. B **5**, 2615 (1972); F. Harbus and H. E. Stanley, Phys. Rev. Lett. **29**, 58 (1972); Phys. Rev. B (to be published).

[14] For an elementary account of anisotropic antiferromagnets, including a brief discussion of the spin-flop transition, see, e.g., D. H. Martin, *Magnetism in Solids* (MIT Press, Cambridge, Mass., 1967), pp. 261–263. The implications of scaling here are touched on in A. Hankey, Ph.D. thesis (MIT, 1973)(unpublished).

[15] W. K. Theuman and J. S. Hoye, J. Chem. Phys. **55**, 4159 (1971); see also P. C. Hemmer and G. Stell, Phys. Rev. Lett. **24**, 1284 (1970); and G. Stell and P. C. Hemmer, J. Chem. Phys. **56**, 2474 (1972); A. Hankey, Ref. 14.

[16] A more complete account of these models will be given else-

where; a preliminary account appears in A. Hankey, T. S. Chang, and H. E. Stanley, AIP Conf. Proc. **10**, 899 (1973).

[17]This point occurs when $2mH = 2J_{SR}$, where $2m = 1$, in the remainder of this work and J_{SR} is the nearest-neighbor exchange energy [cf. Eq. (3.1)].

[18]The inclusion of a competing long-range interaction makes it possible to define a fourth variable, which is fieldlike, although it is strictly not a field. This variable is the ratio of interaction strengths in the Hamiltonians. In the figures, it is denoted by $\bar{\mathfrak{R}} \equiv J_{SR}/J_{LR}$. This variable is "fieldlike" because the CXS and CRS in the space including $\bar{\mathfrak{R}}$ have the same properties as in spaces of fields.

[19]An exact analysis of an Ising model with several staggered fields requires consideration of a regularly repeating block of spins. The length of the block will be equal to the lowest common multiple of the wavelengths of the various staggered fields. If staggered fields of wavelengths 2 and 3 had been chosen, there would be six spins in a block, but with wavelengths 2 and 4, there are only four spins per block. The analysis for a block of n spins proceeds by multiplying together n transfer matrices and so H_2 and H_4 give the smallest number of matrices to multiply.

[20]Our ideas of using the invariant theorems of continous groups of transformations for multicomponent scaling were first presented at the MIT Summer School on Critical Phenomena in 1971 (unpublished). Recently, important advances have been made by Wilson, Fisher, Wegner, Riedel and others in generating the scaling exponents using the linearized renormalization group equations. It was shown that the scaling fields may be deduced from the relevant operator densities. The number of references to work utilizing the renormalization group now exceeds 100, and the reader is urged to consult K. G. Wilson, Phys. Reports (to be published) or *Cooperative Phenomena Near Phase Transitions: A Bibliography with Selected Readings*, edited by H. E. Stanley (MIT Press, Cambridge, Mass., 1973).

[21]This form of the scaling hypothesis has been treated in detail by A. Hankey and H. E. Stanley [Phys. Rev. B **6**, 3515 (1972)]. It is a more complete discussion of the statements of the hypothesis previously used by Riedel and Wegner (Refs. 3 and 4) and also by Kadanoff (Ref. 2c). For a complete set of references, see *Cooperative Phenomena near Phase Transitions: A Bibliography with Selected Readings*, edited by H. E. Stanley (MIT Press, Cambridge, Mass., 1973).

[22]The elements of the group are parametrized by the single parameter λ. Thus the group is a one-parameter group.

[23]A more-general linear transformation will be $x_i = f_i(\lambda)x_i$. Because of the associativity property of groups, it can be shown that $f_i(\lambda) = \lambda^{a_i}$ [Appendix C]. If some of the x_i do not scale and serve only as "inactive parameters" in Eq. (5.6), the corresponding scaling powers are equal to zero.

[24]We could, of course, replace H_{st} by x_1 in Eq. (5.9), but we emphasize that (cf. Fig. 12) the only thermodynamic field axis which is a strong direction is H_{st}. Thus while the direction $H_{st} + \epsilon(H - H_c)$ or $H_{st} + \epsilon(T - T_c)$ are both strong and $\partial/\partial H_{st}$ is the same as $\partial/\partial x_1$, $\partial/\partial T$, and $\partial/\partial H$ are only equivalent to differentiating with respect to x_2.

[25]Here we will formulate the scaling hypothesis only for the Gibbs function, because the scaling equation analogous to (5.1) for other functions can be obtained by appropriate differentation with respect to its independent variables. Scaling functions for physcially more interesting functions like M and χ can then be obtained by the same method used here for G.

[26]Equations (5.14) can all be written in terms of $|H - H_c(T)|$ except at the Néel point, where the line of critical points is parallel to the H axis.

[27]Occasionally, it turns out to be appropriate to scale with respect to a variable which is not tangent—see, e.g., Paper II. This is also true when all the ${}^2R_1$ do not end up parallel and the tangent variable for one line is *not* the tangent variable for another line. We emphasize that scaled equations may change their values or functional forms when the scaling variables change signs.

[28]"Mutually consistent" means that if one chooses two different sets of axes for scaling, one set $(\bar{x}_1, \bar{x}_2, \bar{x}_3)$ with reference to a line L and the second $(\bar{x}_1', \bar{x}_2', \bar{x}_3')$ with repsect to L', then the second set is none other than a permutation of the first set.

[29]Our expression differs from that given in Ref. 7 [Eq. (8)], where the constant k is not present. The constant k is needed to ensure the divergence property of χ_{st} (and other second derivatives of G) along the critical line.

[30]L. P. Eisenhart, *Continuous Groups of Transformations* (Princeton U. P., Princeton, N.J., 1933).

[31]L. S. Pontryagin, *Ordinary Differential Equations* (Addison-Wesley, Reading, Mass., 1962).

[32]A. J. A. Morgan, Q. J. Math. **2**, 250 (1952).

[33]J. Aczèl, *Lectures on Functional Equations and their Applications* (Academic, New York, 1966).

PHYSICAL REVIEW B VOLUME 7, NUMBER 9 1 MAY 1973

Double-Power Scaling Functions near Tricritical Points*

T. S. Chang,† Alex Hankey,‡ and H. Eugene Stanley
Physics Department, Massachusetts Institute of Technology, Cambridge, Massachusetts 02139
(Received 11 September 1972)

We introduce invariants of the scaling equation about the tricritical point. Using these invariants, a modified version of the scaling hypothesis about the three critical lines meeting at the tricritical point is presented. From it we demonstrate that the thermodynamic equation of state near a tricritical point and near a critical line may be expressed as double-power scaling functions. These imply that experimental data should collapse from a *volume* onto a *line* (i.e., by two dimensions). This behavior is in contrast to ordinary "single-power" scaling functions, which predict data collapsing from a volume onto a surface or from a surface onto a line (i.e., by one dimension).

I. INTRODUCTION

There have been recent experimental measurements[1] near tricritical points[2] (TCPs) in metamagnets, NH_4Cl, and ^3He-^4He mixtures.[1] These data have been partially interpreted recently in terms of scaling arguments in which one makes not one but two scaling hypotheses.[3-5] Riedel and Wegner[6] were perhaps the first authors to note that in regions for which two scaling hypotheses are simultaneously valid, double-power-law behavior of certain functions results. In this work we present a *variation* of scaling for tricritical points, utilizing generalized homogeneous functions[7] (GHF's) of invariants of the scaling equation about the tricritical point. We obtain, in regions near a critical line and a tricritical point, double-power scaling functions which permit data to collapse from a volume onto a line, in contrast to the behavior of single-power scaling functions, which permit data to collapse by only one dimension (e.g., from a surface onto a line, or a volume onto a surface).

Before we can proceed to make the scaling hypothesis for a TCP, it will be necessary to determine the relevant directions for scaling.[3] The three thermodynamic fields (T, temperature; η, ordering field; and g, nonordering field) near a TCP are believed to constitute an affine space in which directions may be defined by parallelism only. A TCP is a point of intersection of three critical lines in this three-dimensional affine space (cf. Fig. 1). At each point P on a critical line, three different types of directions can be established. The first direction, $x_1(P)$, is a direction not locally parallel to the coexistence surface. The second, $x_2(P)$, is locally parallel to the coexistence surface but not parallel to the critical line. These are the "strong" and "weak" directions of Griffiths and Wheeler.[8] The third direction, $x_3(P)$, is locally parallel to the critical line.

As the point P moves toward the TCP, these directions attain limiting orientations. Since there are three critical lines terminating at a TCP, three "rival" sets of directions of this type exist at the TCP. It has been shown[4] that if scaling holds at a TCP, these three sets of directions are equivalent. Thus, we choose the relevant directions for scaling at a TCP as $\bar{x}_i \equiv \lim(P\rightarrow \mathrm{TCP})x_i(P)$, where P is a point on the critical line L_1 (see Fig. 1).[9]

II. SCALING HYPOTHESIS FOR TCP

Having ascertained the relevant scaling directions $\bar{x}_i$ for TCP, we now introduce a scaling parameter λ (> 0) and make the homogeneity hypothesis[3-7] that the singular part of the Gibbs potential is asymptotically a GHF,

$$G(\lambda^{\bar{a}_1}\bar{x}_1,\ \lambda^{\bar{a}_2}\bar{x}_2,\ \lambda^{\bar{a}_3}\bar{x}_3) = \lambda G(\bar{x}_1,\ \bar{x}_2,\ \bar{x}_3)\ , \tag{1}$$

where $\bar{a}_i$ are the scaling powers. Equation (1) is *equivalent* to the statement that

$$G = F_3\ (\bar{x}_1,\ \bar{x}_2,\ \bar{x}_3) \tag{2}$$

is an invariant equation under the one-parameter (λ) group ($\mathcal{G}_3$) of transformations

$$G' = \lambda G,\quad \bar{x}_i' = \lambda^{\bar{a}_i}\bar{x}_i,\quad (i = 1,\ 2,\ 3)\ . \tag{3}$$

In other words, under the transformations, Eq. (2) becomes $G' = F_3(\bar{x}_1',\ \bar{x}_2',\ \bar{x}_3')$.

The group $\mathcal{G}_3$ admits a basis set of three ($i = 0$, 1, 2) functionally independent absolute invariants, $y_i(G', \bar{x}_1', \bar{x}_2', \bar{x}_3') = y_i(G, \bar{x}_1, \bar{x}_2, \bar{x}_3)$, such that all

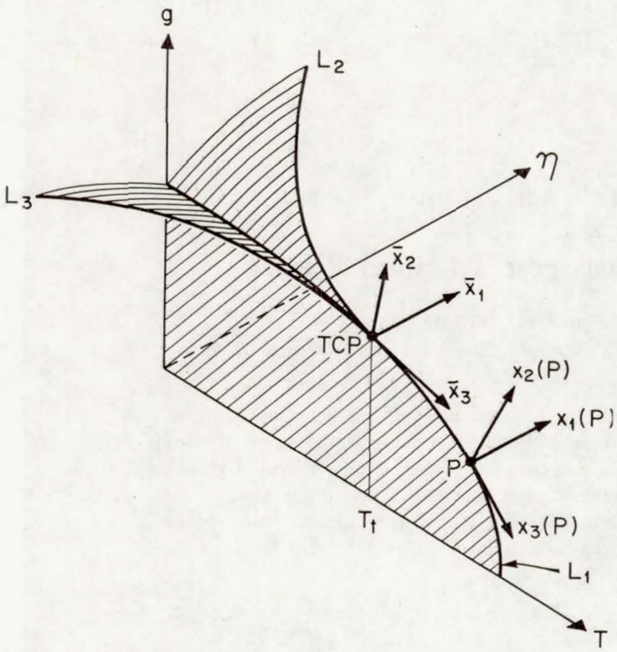

FIG. 1. Schematic phase diagram showing a TCP (at $T=T_t$). Shaded areas are coexistence surfaces. At a point P on L_1, a triad of directions $x_i(P)$ are shown. This triad becomes $\bar{x}_i$ at TCP.

other absolute invariants are expressible in terms of these. One such basis set is

$$y_0 \equiv G/\bar{x}_3^{1/\bar{a}_3}, \quad y_1 \equiv \bar{x}_1/\bar{x}_3^{\bar{a}_1/\bar{a}_3}, \quad y_2 \equiv \bar{x}_2/\bar{x}_3^{\bar{a}_2/\bar{a}_3} \quad . \tag{4}$$

The scaling hypothesis, Eq. (1), requires Eq. (2) to be expressible in terms of the basis set as a "single-power" scaling function,

$$y_0 = \bar{F}_2(y_1, \; y_2) \, , \tag{5}$$

which states that G (and other thermodynamic functions), when appropriately scaled, are functions of the invariants $(y_1, \; y_2)$ alone. This result allows data near a TCP to collapse from a *volume* onto a *surface*.

We remark that, using Eq. (1), it is possible to determine all exponent relations and "single-power" scaling laws for a TCP.[3–5]

III. GEOMETRY OF SURFACES AND CURVES NEAR TCP

Since the quantities y_1 and y_2 defined in Eqs. (4) form a basis set of functionally independent absolute invariants of $\bar{x}_i$ under the group of transformations $\bar{x}_i' = \lambda^{\bar{a}_i} \bar{x}_i$, *points* in the invariant $(y_1, \; y_2)$ plane give rise to invariant *curves* in the $(\bar{x}_1, \; \bar{x}_2, \; \bar{x}_3)$ space. We have seen that the scaling hypothesis requires scaled thermodynamic functions near a TCP to depend on y_1 and y_2 only. This implies that each of the three critical *lines* near the TCP can be expressed as a *point* $y_i = k_i$ in the (y_1, y_2) plane, where k_i are constants.

Usually, for systems exhibiting a TCP, one of the critical lines is a planar curve lying entirely in the (g, T) plane (e.g., L_1 of Fig. 1). Since $\bar{x}_1 = 0$, Eq. (4) implies that L_1 is given by $(y_1, \; y_2) = (0, \; -k)$ in the invariant plane.

Near L_1, it is expected that the symmetry property of the critical line will also influence the asymptotic form of the thermodynamic functions. The region of influence is bounded by some "crossover" curve, $f_x(y_1, \; y_2) = 0$ [Fig. 2(a)], or

$$f_x(x_1/x_3^{\bar{a}_1/\bar{a}_3}, \; \bar{x}_2/\bar{x}_3^{\bar{a}_2/\bar{a}_3}) = 0, \tag{6}$$

which is a conical surface surrounding L_1 in the $(\bar{x}_1, \; \bar{x}_2, \; \bar{x}_3)$ space [Fig. 2(b)]. Scaling cannot tell us the *actual* shape of the curve in the $(y_1, \; y_2)$ plane,[10] but it does limit the shape of the conical "crossover" surface in the $(\bar{x}_1, \; \bar{x}_2, \; \bar{x}_3)$ space, since all points in the $(y_1, \; y_2)$ plane give rise to curves approaching the TCP along the $\bar{x}_3$ axis (corresponding to the minimum $\bar{a}_i$).[11]

IV. DOUBLE-POWER SCALING FUNCTIONS FOR L_1

We now proceed to deduce the restriction on the asymptotic form of the thermodynamic functions near a TCP adjacent to the critical line L_1.[12] Along L_1, the conventional scaling hypothesis is

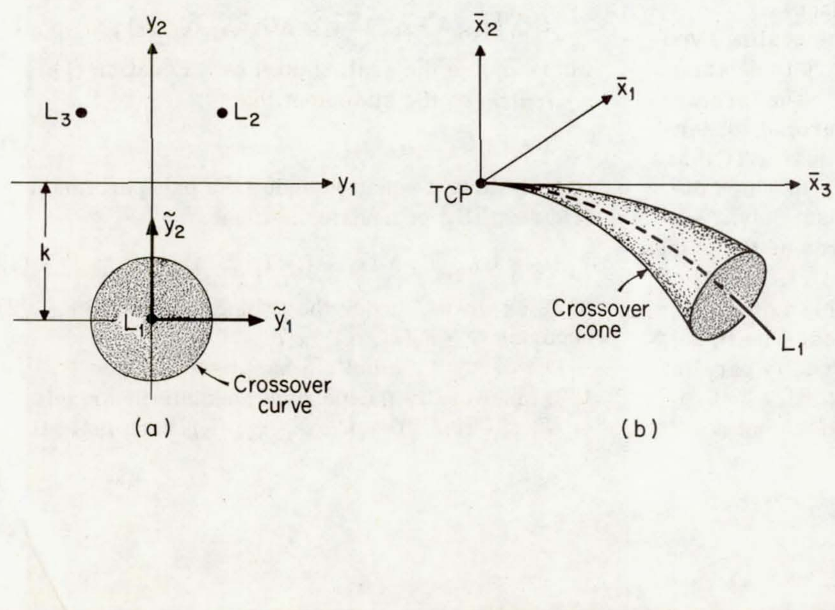

FIG. 2. (a) Invariant $(y_1, \; y_2)$ plane. The strong and weak directions for L_1 are y_1 and y_2, and the crossover curve is shown (Ref. 8). (b) Principal points of interest of (a) in the $(\bar{x}_1, \; \bar{x}_2, \; \bar{x}_3)$ space.

normally stated in terms of a GHF equation

$$G(\mu^{a_1} x_1,\ \mu^{a_2} x_2;\ x_3) = \mu G(x_1,\ x_2;\ x_3), \tag{7}$$

where $\mu(>0)$ is an arbitrary parameter, a_1 and a_2 are the scaling powers for L_1, and x_3 is an "inactive" variable which does not scale. Near the TCP, by Eq. (5) the value of $y_0 \equiv G/\bar{x}_3^{1/\bar{a}_3}$ changes only if the values y_1 and/or y_2 change. It is much better therefore to make a scaling hypothesis about L_1 near the TCP using y_1 and y_2.[13]

Since the coexistence surface bounded by L_1 maps into the vertical axis of the $(y_1,\ y_2)$ plane, the direction y_1 is strong and y_2 is weak. Thus, we deduce that the proper scaling variables for L_1 (near the TCP) are

$$\tilde{y}_1 \equiv y_1, \quad \tilde{y}_2 \equiv y_2 + k; \tag{8}$$

these vanish at the line $(y_1,\ y_2) = (0,\ -k)$.

We now hypothesize that along L_1 near the TCP, $\tilde{y}_0 \equiv y_0$ is a GHF of $(\tilde{y}_1,\ \tilde{y}_2)$:

$$\tilde{y}_0(\mu^{a_1}\tilde{y}_1,\ \mu^{a_2}\tilde{y}_2) = \mu\tilde{y}_0(\tilde{y}_1,\ \tilde{y}_2). \tag{9}$$

In other words, instead of (7) we postulate that

$$\tilde{y}_0 = F_2(\tilde{y}_1,\ \tilde{y}_2) \tag{10}$$

is an invariant equation under the group $(\mathcal{G}_2)$ of transformations $(\tilde{y}_0' = \mu\tilde{y}_0, \tilde{y}_1' = \mu^{a_1}\tilde{y}_1$, and $\tilde{y}_2' = \mu^{a_2}\tilde{y}_2)$.

By the same reasoning used for the derivation of Eq. (5), we see that (9) requires that (10) may be written in the form

$$z_0 = F_1(z_1)\ , \tag{11}$$

where $z_0 \equiv \tilde{y}_0/\tilde{y}_2^{1/a_2}$ and $z_1 \equiv \tilde{y}_1/\tilde{y}_2^{a_1/a_2}$ form a set of functionally independent absolute invariants of $\mathcal{G}_2$ and therefore of the variables $G,\ \bar{x}_1,\ \bar{x}_2,\ \bar{x}_3$ under the direct-product group $\mathcal{G}_2 \otimes \mathcal{G}_3$.

Reexpressing Eq. (11) in terms of the original variables $G,\ x_1,\ x_2$, and x_3 we obtain the "double-power" form[14]

$$\frac{G}{\bar{x}_3^{1/\bar{a}_3}(\bar{x}_2/\bar{x}_3^{\bar{a}_2/\bar{a}_3} + k)^{1/a_2}} = F_1\left(\frac{\bar{x}_1}{\bar{x}_3^{\bar{a}_1/\bar{a}_3}(\bar{x}_2/\bar{x}_3^{\bar{a}_2/\bar{a}_3} + k)^{a_1/a_2}}\right). \tag{12}$$

Equation (12) predicts that near the TCP *and* L_1, data will collapse from a *volume* onto a *line*. Clearly, this happens only within the crossover cone of Eq. (6) [cf. Fig. 2(b)].

In the plane $\bar{x}_1 = 0$ [i.e., the $(g,\ T)$ plane], Eq. (12) requires[15]

$$G \sim \bar{x}_3^{1/\bar{a}_3}(\bar{x}_2/\bar{x}_3^{\bar{a}_2/\bar{a}_3} + k)^{1/a_2}\ , \tag{13}$$

and the conical surface of Eq. (6) becomes two crossover lines (cf. Fig. 3) $\bar{x}_2 = C_i\bar{x}_3^{\bar{a}_2/\bar{a}_3}$ or $y_2 = C_i$, where $i = 1,\ 2$. The crossover exponent $\varphi \equiv \bar{a}_3/\bar{a}_2$, which determines the shape of the crossover lines, can be obtained directly from the shape of L_1.[3]

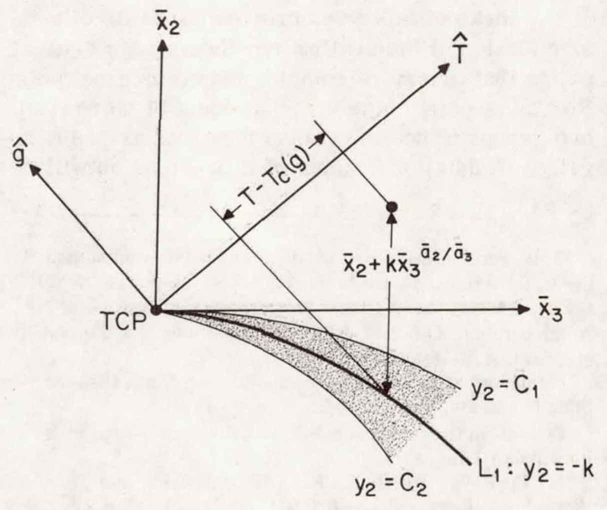

FIG. 3. Figure 2(b) sliced in the $\bar{x}_1 = 0$ plane. The crossover lines are labeled $y_2 = C_1,\ C_2$. The projection of $\bar{x}_2 + k\bar{x}_3^{\bar{a}_2/\bar{a}_3}$ along the T axis is $T - T_c(g)$, and $(\hat{T},\ \hat{g}) \equiv (T - T_t,\ g - g_t)$.

V. EXTENSIONS AND CONCLUDING REMARKS

The entire discussion in this paper may be extended to the scaling of any thermodynamic function f. For example, for the staggered susceptibility $\chi_{st} \equiv \partial^2 G/\partial\eta^2 \propto \partial^2 G/\partial\bar{x}_1^2$ (or $\partial^2 G/\partial x_1^2$) and the direct susceptibility $\chi \equiv \partial^2 G/\partial g^2 \propto \partial^2 G/\partial\bar{x}_2^2$ (or $\partial^2 G/\partial x_2^2$) of a metamagnet, the expression analogous to Eq. (13) is

$$f_i = \bar{x}_3^{(1-2\bar{a}_i)/\bar{a}_3}\ (\bar{x}_2/\bar{x}_3^{\bar{a}_2/\bar{a}_3} + k)^{(1-2a_i)/a_2}\ , \tag{14}$$

where $f_1 \equiv \chi_{st}$ and $f_2 \equiv \chi$. We note that Eq. (13) has the appropriate divergence properties at the critical line *and* at the TCP.

Finally, we make a few remarks about the exponents and directions of approach toward the TCP and L_1. Using the experimentally accessible function χ_{st} as an example, we note that if we approach the TCP along a curve $\bar{x}_2/\bar{x}_3^{\bar{a}_2/\bar{a}_3} = \text{const}$, the scaling exponent is $-\bar{\gamma}_{st}\varphi^{-1} = (1 - 2\bar{a}_1)/\bar{a}_3$. If we approach the critical line L_1 along a line $\bar{x}_3 = \text{const}$, the scaling exponent is $-\gamma_{st} = (1 - 2a_1)/a_2$ as expected. On the other hand, if the TCP is approached along a path outside the crossover lines, χ_{st} scales with an exponent $-\bar{\gamma}_{st} = (1 - 2\bar{a}_1)/\bar{a}_2$. Similar remarks may be made with respect to the three-dimensional "double-power" scaling functions of Eq. (12).

Equation (14) may be cast in "mixed-exponent" forms; e.g., $\chi_{st} \sim C[T - T_c(g)]^{-\gamma_{st}}$, in which $\bar{x}_2 + k\bar{x}_3^{\bar{a}_2/\bar{a}_3}$ has been replaced by its projection along the T axis (Fig. 3), and $C \sim \bar{x}_3^{(\gamma_{st} - \bar{\gamma}_{st})/\varphi}$ is the asymptotic amplitude. Depending on the relative magnitudes of γ_{st} and $\bar{\gamma}_{st}$, the asymptotic amplitude may diverge, vanish, or stay constant as the TCP is approached within the crossover cone.

The ideas of this work provide the basis of a formulation of the scaling hypothesis near critical points that are more complex than tricritical points. For these points, the direct product of more than two groups of scaling transformations arises naturally. A detailed account of this extension will be published elsewhere.

ACKNOWLEDGMENTS

The authors wish to thank F. Harbus, R. B. Griffiths, E. K. Riedel, and J. C. Wheeler for stimulating discussions.

---

*This work forms a portion of a Ph.D. thesis submitted to the MIT Physics Dept. by A. Hankey. Work supported by National Science Foundation, National Aeronautics and Space Administration, Office of Naval Research, and Air Force Office of Scientific Research.

†Permanent address: Riddick Laboratories, North Carolina State University, Raleigh, N. C.

‡Present address: SLAC, Stanford, Calif. Supported by a Lindemann Fellowship.

[1](a) D. P. Landau, B. E. Keen, B. Schneider, and W. P. Wolf, Phys. Rev. B **3**, 2310 (1971); (b) C. W. Garland and B. B. Weiner, Phys. Rev. B **3**, 1634 (1971); (c) E. H. Graf, D. M. Lee, and J. D. Reppy, Phys. Rev. Lett. **19**, 417 (1967); (d) R. J. Birgeneau (private communication). For additional references to the vast experimental literature, see *Cooperative Phenomena near Phase Transitions,* edited by H. E. Stanley (MIT Press, Cambridge, Mass., 1973).

[2]R. B. Griffiths, Phys. Rev. Lett. **24**, 715 (1970).

[3]E. K. Riedel, Phys. Rev. Lett. **28**, 675 (1972).

[4]A. Hankey, H. E. Stanley, and T. S. Chang, Phys. Rev. Lett. **29**, 278 (1972).

[5]R. B. Griffiths, Phys. Rev. B **7**, 545 (1973).

[6]E. K. Riedel and F. Wegner, (a) Z. Phys. **225**, 195 (1969); (b) Phys. Rev. Lett. **24**, 730 (1970).

[7]A. Hankey and H. E. Stanley, Phys. Rev. B **6**, 3515 (1972). See also H. E. Stanley, *Introduction to Phase Transitions and Critical Phenomena* (Oxford U.P., London and New York, 1971), Chap. 11. (1972). See also, H. E. Stanley, *Introduction to Phase Transitions and Critical Phenomena* (Oxford U. P., London, 1971), Chap. 11.

[8]R. B. Griffiths and J. C. Wheeler, Phys. Rev. A **2**, 1047 (1970).

[9]In general, the $\overline{x}_j$ may be nonorthogonal, but in this work we need consider only rectilinear orthogonal coordinates.

[10]Although the crossover curve may be of any form, it is shown for convenience as a circle in Fig. 2(a).

[11]In this paper, we assume $a_1 \neq a_2 \neq a_3$. (See Ref. 4 for discussion of other cases.)

[12]The scaling ideas for $L_{2,3}$ are similar. However, it will be necessary to rotate the invariant axis to determine the strong and weak directions.

[13]This assumption is equivalent to the scaling assertion of Ref. 6, that the extended homogeneity relation (1) must encompass the relation (7) asymptotically close to the critical line.

[14]Equation (12) is similar to that found in Ref. 6(b) for dynamic scaling in anisotropic magnetic systems. We emphasize that scaled equations may change their values or functional forms when the scaling variables change signs.

[15]Equation (13) is essentially equivalent to Eq. (8) of Ref. 3, provided the variable μ_1 is interpreted as the critical line scaling field.